

# J Duct Acoustics

This chapter deals with sound propagation in ducts. It begins with hard and smooth ducts in which viscous and thermal losses at the walls are taken into account; this is important in narrow ducts (capillaries). The rest of the chapter deals with lined ducts of different cross sections and different linings. Sometimes the duct is assumed to be infinitely long; sometimes it has a finite length but is still long enough to neglect reflections from the duct exit at the duct entrance. This assumption makes the contents of this chapter different from those of ➤ Ch. K “Acoustic Mufflers”, where the reflections at both ends of duct sections play a dominant role. A section at the end of this chapter will discuss the influence of flow on sound attenuation in lined ducts in an approximation which is precise enough for most technical applications. A more sophisticated discussion of the influence of flow will be given in ➤ Ch. N “Flow Acoustics”.

## J.1 Flat Capillary with Isothermal Boundaries

---

► See also: Mechel, Vol. II, Ch. 10 (1995)

For the fundamental relations and notations used see ➤ Sect. B.1

The duct has a width of  $2h$ ;  $x$  is the axial co-ordinate and  $y$  the transversal co-ordinate normal to the walls; the duct is infinite in the  $z$  direction (its dimension in this direction is much larger than that in the  $y$  direction). The co-ordinate origin is placed in the middle of the height.

The specific heat and the heat conduction of the wall material are assumed to be much higher than those of air; therefore the isothermal boundary condition holds; the acoustic temperature fluctuation of the walls is zero.

The scalar potentials  $\Phi_{\rho,\alpha}$  for the density wave (index  $\rho$ ) and the temperature wave (index  $\alpha$ ), as well as for the vector wave potential  $\Psi_v$  of the viscosity wave (index  $v$ ), are formulated with a common axial propagation constant  $\Gamma$  as:

$$\Phi_{\rho,\alpha}(x, y) = A_{\rho,\alpha} e^{-\Gamma x} \cos(\epsilon_{\rho,\alpha} y), \quad (1)$$

$$\Psi_v(x, y) = A_v e^{-\Gamma x} \sin(\epsilon_v y).$$

The wave equations for the three types of waves then give the following secular equations:

$$\epsilon_{\rho,\alpha,v}^2 = \Gamma^2 + k_{\rho,\alpha,v}^2. \quad (2)$$

The wave number definitions used are:

$$k_0^2 = \left( \frac{\omega}{c_0} \right)^2; \quad k_v^2 = -j \frac{\omega}{v}; \quad k_{\alpha 0}^2 = -j \frac{\kappa \omega}{\alpha} = \kappa \Pr \cdot k_v^2. \quad (3)$$

The boundary conditions at the walls lead to a system of equations (in matrix form) for the following amplitudes:

$$\begin{pmatrix} \Gamma h \cos(\epsilon_\rho h) & \Gamma h \cos(\epsilon_\alpha h) & \epsilon_v h \cos(\epsilon_v h) \\ \epsilon_\rho h \sin(\epsilon_\rho h) & \epsilon_\alpha h \sin(\epsilon_\alpha h) & \Gamma h \sin(\epsilon_v h) \\ \Theta_\rho \cos(\epsilon_\rho h) & \Theta_\alpha \cos(\epsilon_\alpha h) & 0 \end{pmatrix} \cdot \begin{pmatrix} A_\rho \\ A_\alpha \\ A_v \end{pmatrix} = \begin{pmatrix} 0 \\ 0 \\ 0 \end{pmatrix}. \quad (4)$$

See [Sect. B.1](#) for  $\Theta_\rho$ ,  $\Theta_\alpha$ . For the existence of a non-trivial solution the determinant must be zero:

$$(\Gamma h)^2 \left( \frac{\Theta_\rho}{\Theta_\alpha} - 1 \right) \frac{\tan(\epsilon_v h)}{\epsilon_v h} + \epsilon_\rho h \cdot \tan(\epsilon_\rho h) - \frac{\Theta_\rho}{\Theta_\alpha} \epsilon_\alpha h \cdot \tan(\epsilon_\alpha h) = 0. \quad (5)$$

This is the exact characteristic equation for  $\Gamma$ . A good explicit approximation to the solution is under the condition  $|\epsilon_\rho h| \ll 1$ :

$$\left( \frac{\Gamma}{k_0} \right)^2 \approx - \frac{1 + (\kappa - 1) \frac{\tan(k_{\alpha 0} h)}{k_{\alpha 0} h}}{1 - \frac{\tan(k_v h)}{k_v h}}. \quad (6)$$

The characteristic axial wave impedance  $Z$  is (with the same degree of approximation):

$$\frac{Z}{Z_0} = \frac{\langle p(x, y) \rangle_y}{Z_0 \langle v_x(x, y) \rangle_y} \approx j \frac{k_0}{\Gamma} \frac{\frac{\tan(\epsilon_\rho h)}{\epsilon_\rho h}}{\frac{\tan(\epsilon_\rho h)}{\epsilon_\rho h} - \frac{\tan(k_v h)}{k_v h}} \quad (7)$$

or, with some transformations:

$$\frac{\Gamma}{k_0} = j \sqrt{\left[ 1 + (\kappa - 1) \frac{\tan(k_{\alpha 0} h)}{k_{\alpha 0} h} \right] / \left[ 1 - \frac{\tan(k_v h)}{k_v h} \right]}, \quad (8)$$

$$\frac{Z}{Z_0} = \frac{1}{\sqrt{\left[ 1 + (\kappa - 1) \frac{\tan(k_{\alpha 0} h)}{k_{\alpha 0} h} \right] \cdot \left[ 1 - \frac{\tan(k_v h)}{k_v h} \right]}}. \quad (9)$$

The amplitude ratios are as follows:

$$\frac{A_\alpha}{A_\rho} = - \frac{\Theta_\rho}{\Theta_\alpha} \frac{\cos(\epsilon_\rho h)}{\cos(\epsilon_\alpha h)}; \quad \frac{A_v}{A_\rho} = \left( \frac{\Theta_\rho}{\Theta_\alpha} - 1 \right) \frac{\Gamma h}{\epsilon_v h} \frac{\cos(\epsilon_\rho h)}{\cos(\epsilon_v h)}. \quad (10)$$

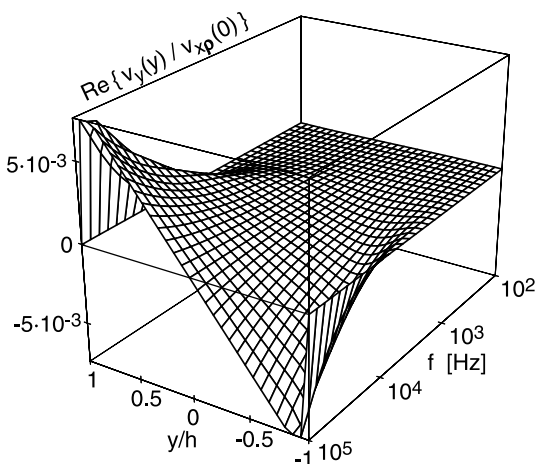
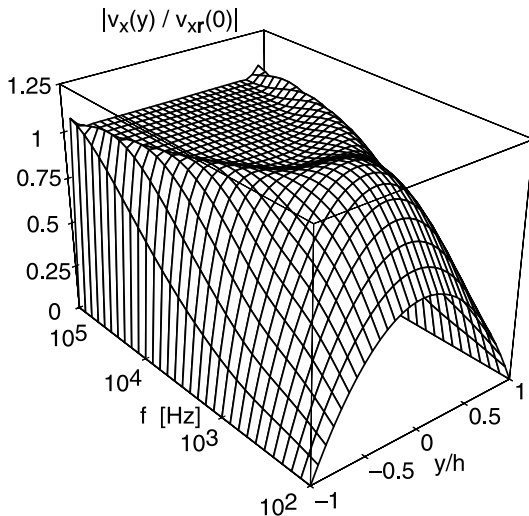
The axial particle velocity profile (relative to the axial velocity of the density wave in the centre) is:

$$\begin{aligned} \frac{v_x(x, y)}{v_{x\rho}(x, 0)} &= \cos(\epsilon_\rho h) \cdot \left[ \frac{\cos(\epsilon_\rho y)}{\cos(\epsilon_\rho h)} - \frac{\Theta_\rho}{\Theta_\alpha} \frac{\cos(\epsilon_\alpha y)}{\cos(\epsilon_\alpha h)} + \left( \frac{\Theta_\rho}{\Theta_\alpha} - 1 \right) \frac{\cos(\epsilon_v y)}{\cos(\epsilon_v h)} \right] \\ &\approx 1 - \frac{\Theta_\rho}{\Theta_\alpha} \frac{\cos(k_{\alpha 0} y)}{\cos(k_{\alpha 0} h)} + \left( \frac{\Theta_\rho}{\Theta_\alpha} - 1 \right) \frac{\cos(k_v y)}{\cos(k_v h)} \approx 1 - \frac{\cos(k_v y)}{\cos(k_v h)}. \end{aligned} \quad (11)$$

The transversal particle velocity profile (relative to the axial velocity of the density wave in the centre) is:

$$\begin{aligned} \frac{v_y(x, y)}{v_{xp}(x, 0)} &= \frac{\epsilon_\rho h}{\Gamma h} \sin(\epsilon_\rho y) \\ &\quad - \frac{\epsilon_\alpha h}{\Gamma h} \frac{\Theta_\rho}{\Theta_\alpha} \frac{\cos(\epsilon_\rho h)}{\cos(\epsilon_\alpha h)} \sin(\epsilon_\alpha y) + \frac{\Gamma h}{\epsilon_v h} \left( \frac{\Theta_\rho}{\Theta_\alpha} - 1 \right) \frac{\cos(\epsilon_\rho h)}{\cos(\epsilon_v h)} \sin(\epsilon_v y) \quad (12) \\ &\approx \frac{k_0 h}{\Gamma / k_0} \left[ \frac{y}{h} \left( 1 + \left( \frac{\Gamma}{k_0} \right)^2 \right) + \frac{\kappa - 1}{k_{\alpha 0} h} \frac{\sin(k_{\alpha 0} y)}{\cos(k_{\alpha 0} h)} - \left( \frac{\Gamma}{k_0} \right)^2 \frac{1}{k_v h} \frac{\sin(k_v y)}{\cos(k_v h)} \right]. \end{aligned}$$

Example of particle velocity profiles (with  $2 h = 4 \times 10^{-4}$  m):



## J.2 Flat Capillary with Adiabatic Boundaries

---

► See also: Mechel, Vol. II, Ch. 10 (1995)

For the fundamental relations and notations used see ➤ Sect. B.1.

No heat exchange takes place between the medium in the capillary and the walls.

The field formulation and secular equations are the same as in ➤ Sect. J.1. The boundary conditions are

$$\begin{pmatrix} \Gamma h \cos(\epsilon_\rho h) & \Gamma h \cos(\epsilon_\alpha h) & \epsilon_v h \cos(\epsilon_v h) \\ \epsilon_\rho h \sin(\epsilon_\rho h) & \epsilon_\alpha h \sin(\epsilon_\alpha h) & \Gamma h \sin(\epsilon_v h) \\ \Theta_\rho \epsilon_\rho h \sin(\epsilon_\rho h) & \Theta_\alpha \epsilon_\alpha h \sin(\epsilon_\alpha h) & 0 \end{pmatrix} \cdot \begin{pmatrix} A_\rho \\ A_\alpha \\ A_v \end{pmatrix} = \begin{pmatrix} 0 \\ 0 \\ 0 \end{pmatrix}. \quad (1)$$

The characteristic equation from  $\det = 0$  becomes:

$$\begin{aligned} (\Gamma h)^2 \frac{\tan(\epsilon_v h)}{\epsilon_v h} \left[ \frac{\Theta_\rho}{\Theta_\alpha} \epsilon_\rho h \tan(\epsilon_\rho h) - \epsilon_\alpha h \tan(\epsilon_\alpha h) \right] \\ - \left( \frac{\Theta_\rho}{\Theta_\alpha} - 1 \right) \cdot \epsilon_\rho h \tan(\epsilon_\rho h) \cdot \epsilon_\alpha h \tan(\epsilon_\alpha h) = 0. \end{aligned} \quad (2)$$

Approximate solutions for the propagation constant  $\Gamma$  are as follows:

$$\left( \frac{\Gamma}{k_0} \right)^2 \approx \frac{-1}{1 + \frac{1}{\frac{\Theta_\rho}{\Theta_\alpha} - 1} \frac{\tan k_v h}{k_v h}} \approx \frac{-1}{1 - \frac{1}{1 + (\kappa - 1) \frac{(k_0 h)^2}{(k_{\alpha 0} h)^2}} \frac{\tan k_v h}{k_v h}} \approx \frac{-1}{1 - \frac{\tan k_v h}{k_v h}}. \quad (3)$$

An approximate solution for the wave impedance  $Z_i$  is:

$$\frac{Z_i}{\rho_0 c_0} \approx \frac{j}{\Gamma/k_0} \frac{1}{1 - \frac{\tan(k_v h)}{k_v h}} \approx -\frac{j}{\Gamma/k_0} (\Gamma/k_0)^2 \approx -j \frac{\Gamma}{k_0}. \quad (4)$$

With adiabatic boundary conditions, the normalised wave impedance is approximately the rotated normalised propagation constant.

The amplitude ratios of the component waves are:

$$\frac{A_\alpha}{A_\rho} = -\frac{\Theta_\rho}{\Theta_\alpha} \frac{\epsilon_\rho h \sin(\epsilon_\rho h)}{\epsilon_\alpha h \sin(\epsilon_\alpha h)}; \quad \frac{A_v}{A_\rho} = \frac{\Gamma h}{\epsilon_v h} \frac{\cos(\epsilon_\rho h)}{\cos(\epsilon_v h)} \cdot \left[ \frac{\Theta_\rho}{\Theta_\alpha} \frac{\epsilon_\rho h \tan(\epsilon_\rho h)}{\epsilon_\alpha h \tan(\epsilon_\alpha h)} - 1 \right]. \quad (5)$$

## J.3 Circular Capillary with Isothermal Boundary

---

► See also: Mechel, Vol. II, Ch. 10 (1995)

For the fundamental relations and notations used see ➤ Sect. B.1.

Capillaries have a radius of  $a$ . The temperature at the wall is constant.

The formulation of the scalar potentials  $\Phi_{\rho,\alpha}$  for the density wave (index  $\rho$ ) and the temperature wave (index  $\alpha$ ), as well as for the vector wave potential  $\Psi_v$  of the viscosity wave (index  $v$ ) with a common axial propagation constant  $\Gamma$ , is as follows:

$$\begin{aligned}\Phi_{\rho,\alpha}(r, z) &= A_{\rho,\alpha} \cdot e^{-\Gamma x} \cdot J_0(\epsilon_{\rho,\alpha} r), \\ \Psi_v(r, z) &= A_v \cdot e^{-\Gamma x} \cdot J_1(\epsilon_v r)\end{aligned}\quad (1)$$

$$\text{with Bessel functions } J_n(z). \text{ The secular equations are } \epsilon_{\rho,\alpha,v}^2 = \Gamma^2 + k_{\rho,\alpha,v}^2. \quad (2)$$

The boundary conditions at the capillary walls (in matrix form) are:

$$\begin{pmatrix} \Gamma \cdot J_0(\epsilon_\rho a) & \Gamma \cdot J_0(\epsilon_\alpha a) & \epsilon_v \cdot J_0(\epsilon_v a) \\ \epsilon_\rho \cdot J_1(\epsilon_\rho a) & \epsilon_\alpha \cdot J_1(\epsilon_\alpha a) & \Gamma \cdot J_1(\epsilon_v a) \\ \Theta_\rho \cdot J_0(\epsilon_\rho a) & \Theta_\alpha \cdot J_0(\epsilon_\alpha a) & 0 \end{pmatrix} \cdot \begin{pmatrix} A_\rho \\ A_\alpha \\ A_v \end{pmatrix} = \begin{pmatrix} 0 \\ 0 \\ 0 \end{pmatrix}. \quad (3)$$

The characteristic equation for the propagation constant  $\Gamma$  is:

$$(\Gamma a)^2 \left( \frac{\Theta_\rho}{\Theta_\alpha} - 1 \right) \frac{J_1(\epsilon_v a)}{\epsilon_v a \cdot J_0(\epsilon_v a)} + \epsilon_\rho a \frac{J_1(\epsilon_\rho a)}{J_0(\epsilon_\rho a)} - \frac{\Theta_\rho}{\Theta_\alpha} \epsilon_\alpha a \frac{J_1(\epsilon_\alpha a)}{J_0(\epsilon_\alpha a)} = 0. \quad (4)$$

An approximate solution is:

$$\begin{aligned}\left( \frac{\Gamma}{k_0} \right)^2 &\approx \frac{\frac{\Theta_\rho}{\Theta_\alpha (k_0 a)^2} \cdot k_{\alpha 0} a \frac{J_1(k_{\alpha 0} a)}{J_0(k_{\alpha 0} a)} - \frac{1}{2}}{\left( \frac{\Theta_\rho}{\Theta_\alpha} - 1 \right) \frac{J_1(k_v a)}{k_v a \cdot J_0(k_{\alpha 0} a)} + \frac{1}{2}} \\ &\approx - \frac{1 + (\kappa - 1) \cdot 2 \frac{J_1(k_{\alpha 0} a)}{k_{\alpha 0} a \cdot J_0(k_{\alpha 0} a)}}{1 - 2 \frac{J_1(k_v a)}{k_v a \cdot J_0(k_v a)}} = - \frac{1 + (\kappa - 1) \cdot J_{1,0}(k_{\alpha 0} a)}{1 - J_{1,0}(k_v a)}.\end{aligned}\quad (5)$$

$$\text{The wave impedance } Z \text{ with } J_{1,0}(x) = \frac{2 J_1(x)}{x J_0(x)} \text{ is:} \quad (6)$$

$$\begin{aligned}Z_0 &= j \frac{(k_\rho a)^2}{k_0 a \cdot \Gamma a} \frac{1 - \frac{(k_\rho a)^2}{(k_{\alpha 0} a)^2}}{1 - \kappa \frac{(k_\rho a)^2}{(k_{\alpha 0} a)^2}} \frac{J_{1,0}(\epsilon_\rho a) - \frac{\Pi_\alpha}{\Pi_\rho} \frac{\Theta_\rho}{\Theta_\alpha} J_{1,0}(\epsilon_\alpha a)}{J_{1,0}(\epsilon_\rho a) - \frac{\Theta_\rho}{\Theta_\alpha} J_{1,0}(\epsilon_\alpha a) + \left( \frac{\Theta_\rho}{\Theta_\alpha} - 1 \right) J_{1,0}(\epsilon_v a)} \\ &\approx \frac{j}{\Gamma/k_0} \frac{J_{1,0}(\epsilon_\rho a) - \left( 1 - \frac{4\kappa \text{Pr}}{3} \right) (\kappa - 1) \frac{(k_0 a)^2}{(k_{\alpha 0} a)^2} J_{1,0}(\epsilon_\alpha a)}{J_{1,0}(\epsilon_\rho a) - (\kappa - 1) \frac{(k_0 a)^2}{(k_{\alpha 0} a)^2} J_{1,0}(\epsilon_\alpha a) - \left( 1 + (\kappa - 1) \frac{(k_0 a)^2}{(k_{\alpha 0} a)^2} \right) J_{1,0}(\epsilon_v a)} \\ &\approx \frac{j}{\Gamma/k_0} \frac{J_{1,0}(\epsilon_\rho a)}{J_{1,0}(\epsilon_\rho a) - J_{1,0}(k_v a)} \approx \frac{j}{\Gamma/k_0} \frac{1}{1 - J_{1,0}(k_v a)}.\end{aligned}\quad (7)$$

The combined solutions for numerical applications are:

$$\frac{\Gamma}{k_0} = j \sqrt{\frac{1 + (\kappa - 1)J_{1,0}(k_{\alpha 0}a)}{1 - J_{1,0}(k_v a)}}, \quad (8)$$

$$\frac{Z}{Z_0} = \frac{1}{\sqrt{[1 + (\kappa - 1)J_{1,0}(k_{\alpha 0}a)] \cdot [1 - J_{1,0}(k_v a)]}}.$$

$$\text{The effective density } \rho_{\text{eff}} \text{ is: } \frac{\rho_{\text{eff}}}{\rho_0} = -j \frac{\Gamma}{k_0} \cdot \frac{Z_i}{Z_0} = \frac{1}{1 - J_{1,0}(k_v a)}. \quad (9)$$

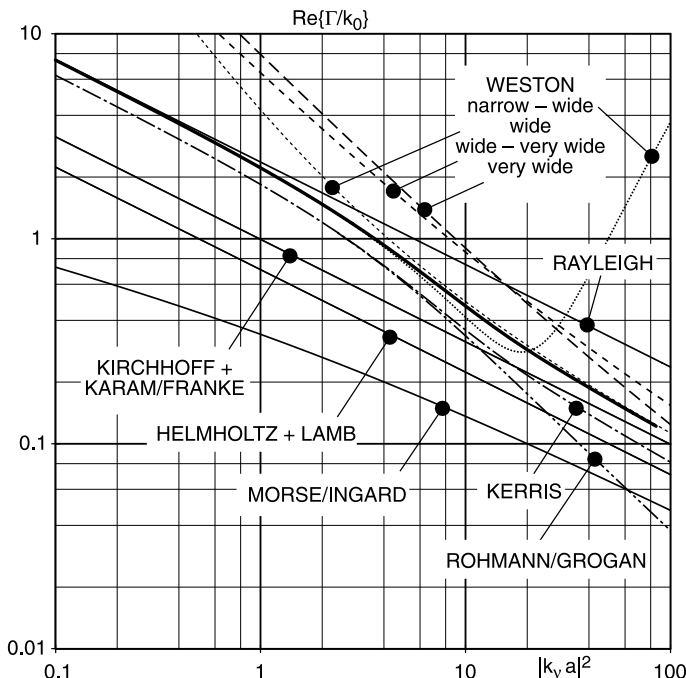
$$\text{The effective compressibility } C_{\text{eff}} \text{ is: } \frac{C_{\text{eff}}}{C_0} = -j \frac{\Gamma}{k_0} / \frac{Z_i}{Z_0} = 1 + (\kappa - 1)J_{1,0}(k_{\alpha 0}a) \quad (10)$$

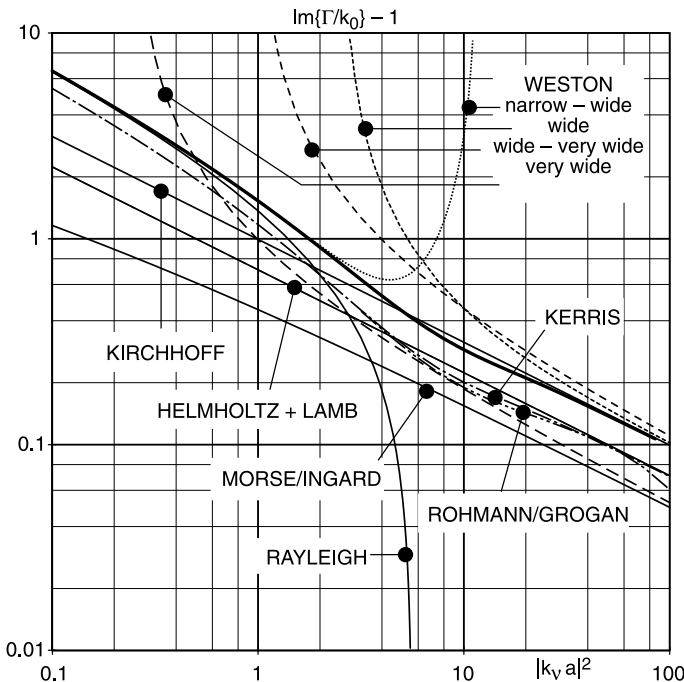
( $\rho_0, C_0$  values for air without losses).

The amplitude ratios of component waves are:

$$\frac{A_{\alpha}}{A_p} = -\frac{\Theta_p}{\Theta_{\alpha}} \frac{J_0(\epsilon_p a)}{J_0(\epsilon_{\alpha} a)}; \quad \frac{A_v}{A_p} = \left( \frac{\Theta_p}{\Theta_{\alpha}} - 1 \right) \frac{\Gamma a}{\epsilon_v a} \frac{J_0(\epsilon_p a)}{J_0(\epsilon_{\alpha} a)}. \quad (11)$$

Approximations from the literature to the components of the propagation constant  $\Gamma$  in capillaries are shown in the next diagram (for more details, see [Mechel, Vol. I-III (1989, 1995, 1998)]); the thick curve represents the solution of the exact characteristic equation. The approximation given above nearly coincides with the exact curve; it agrees with the approximation by Zwicker and Kosten (1949), although it is derived in a different way:





#### J.4 Lined Ducts, General

In general, the interior space of lined ducts is prismatic or cylindrical, and the surfaces of the lining can be assumed to lie on co-ordinate surfaces of co-ordinate systems in which the wave equation is separable. In Cartesian co-ordinates, for example, a solution of the wave equation (without flow; see later sections for flow superposition) with the axis in the x direction is:

$$p(x, y, z) = (a \cdot \cos(\varepsilon_m y) + b \cdot \sin(\varepsilon_m y)) \cdot (\alpha \cdot \cos(\eta_n z) + \beta \cdot \sin(\eta_n z)) \cdot (c \cdot e^{-\Gamma_{m,n} x} + d \cdot e^{+\Gamma_{m,n} x}) \quad (1)$$

$$\text{with the secular equation } \Gamma_{m,n}^2 = \varepsilon_m^2 + \eta_n^2 - k_0^2. \quad (2)$$

If the x axis is in the duct centre, then the first terms in parentheses (with a,  $\alpha$ ) describe symmetrical fields and the second terms (with b,  $\beta$ ) describe anti-symmetrical fields. The lateral wave numbers  $\varepsilon_m, \eta_n$  are solutions of a *characteristic equation* which follows from the boundary conditions at the lining surfaces. For locally reacting linings (see later sections for other types of linings) with surface admittances  $G_y, G_z$  on both sides of the y direction and z direction, respectively, with half-duct heights  $h_y, h_z$  in these directions, the characteristic equations for the symmetrical field components are:

$$\varepsilon_m h_y \cdot \tan(\varepsilon_m h_y) = j k_0 h_y \cdot Z_0 G_y =: j U_y, \quad (3)$$

$$\eta_n h_z \cdot \tan(\eta_n h_z) = j k_0 h_z \cdot Z_0 G_z =: j U_z.$$

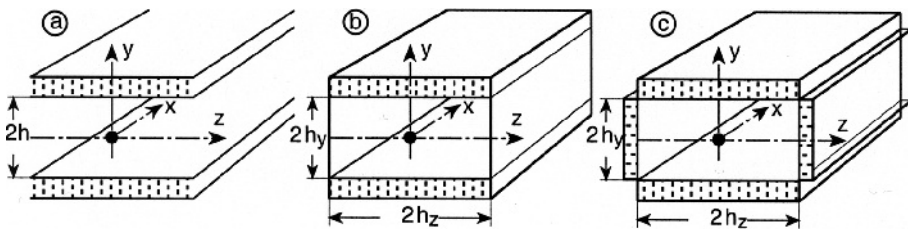
The right-hand sides, and therefore  $U_y, U_z$  are known values for given linings. The equations have an infinite number  $m, n = (0), 1, 2, \dots$  of solutions because of the

periodicity of the tan function. They are *mode solutions*. It is important that the task of finding mode solutions be the same regardless of whether the duct is two-dimensional or three-dimensional; in the latter case the same task has to be solved twice, and only in the evaluation of the axial propagation constant from

$$\Gamma_{m,n}^2 = \epsilon_m^2 + \eta_n^2 - k_0^2 \quad (4)$$

does the dimensionality become important. That is why in Cartesian co-ordinates mostly two-dimensional (*flat*) ducts are considered.

The linings on opposite sides of the duct are largely the same and the duct is *symmetrical*. If in addition the sound excitation is symmetrical, then it is sufficient to consider symmetrical modes only. (It is important in this context that the *least attenuated mode* is a symmetrical mode.)



A "standard form" of a rectangular lined duct therefore is a flat duct with a hard wall at  $y = 0$  (plane of symmetry) and a lining surface at  $y = h$ . The secular equation then becomes:

$$\Gamma_m^2 = \epsilon_m^2 - k_0^2 . \quad (5)$$

It is automatically satisfied if a *modal angle*  $\Theta_n$  is introduced by:

$$1 = (\epsilon_n/k_0)^2 - (\Gamma_n/k_0)^2 = (\epsilon_n/k_0)^2 + (\Gamma_n/jk_0)^2 = \sin^2 \Theta_n + \cos^2 \Theta_n$$

$$\sin \Theta_n = \frac{\epsilon_n}{k_0} ; \quad \cos \Theta_n = \frac{\Gamma_n}{jk_0} . \quad (6)$$

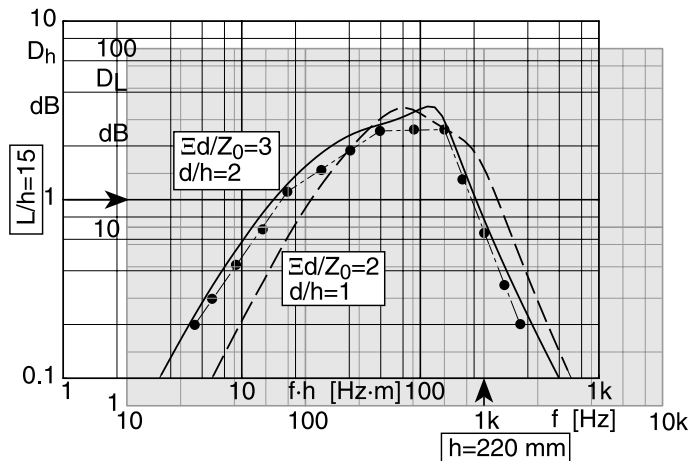
With the present choice of association, the modal angle  $\Theta_n$  is the angle which the wave vector of the plane waves includes with the x axis, which by their superposition form the trigonometric lateral mode profile:

$$\left. \begin{aligned} \cos(\epsilon_y y) \\ \sin(\epsilon_y y) \end{aligned} \right\} = \frac{1}{2} [e^{+j\epsilon_y y} \pm e^{-j\epsilon_y y}] . \quad (7)$$

The mode angles  $\Theta_n$  are defined even when they become complex quantities.

The most important target quantity of a silencer of finite length L (L sufficiently large, so that end reflections can be neglected; see later sections for end effects) is its transmission loss  $D_L = 8.68 \cdot \text{Re}\{\Gamma L\} = L/h \cdot D_h$  with  $D_h = 8.68 \cdot \text{Re}\{\Theta h\}$ .  $D_h$  is the preferred quantity for the presentation of the silencer attenuation because it follows immediately from the secular and characteristic equations and permits a better comparison between silencers with different linings.

Suppose we have a set of computed  $D_h$  curves, plotted in a double-logarithmic scale over  $f \cdot h$  [Hz · m], and a required transmission loss  $D_L$  plotted in a double-logarithmic scale over  $f$  [Hz]. Suppose also that one of the diagrams is on a transparent foil (or the diagrams are plotted in a graphics computer program which permits drawing and moving of graphs in different levels). Then select a suitable silencer with the following procedure.



The required  $D_L$  over  $f$  is plotted as points in the *shaded diagram*. The computed  $D_h$  over  $f \cdot h$  are plotted as *lines* in the other diagram. Move one of the diagrams so that the  $D_L$  values are just below a computed  $D_h$ . Read opposite to  $f = 1$  kHz the value of  $h$  in mm and opposite to  $D_h = 1$  the value of  $L/h$ . The other values needed are taken from the parameter list

The main subtask in the determination of  $D_h$  is the solution of the characteristic equation. Important tools are *Muller's procedure* for the solution of transcendent complex equations and the *continued fraction* representation of the  $\tan(z)$  and  $\cot(z)$  functions as well as of Bessel function ratios.

*Muller's procedure* for the solution of the equation  $f(z) = 0$  requires three starting values,  $z_{i-2}$ ,  $z_{i-1}$ ,  $z_i$ , and the associated function values  $f_{i-2} = f(z_{i-2})$ ,  $f_{i-1} = f(z_{i-1})$ ,  $f_i = f(z_i)$ . A new approximation of the solution is:

$$z_{i+1} = z_i + \lambda_{i+1} \cdot (z_i - z_{i-1}), \quad (8)$$

where  $\lambda_{i+1}$  is a solution of the quadratic equation:

$$\lambda_{i+1}^2 \cdot \lambda_i h_i + \lambda_{i+1} \cdot g_i + f_i \delta_i = 0 \quad (9)$$

with the abbreviations:

$$\begin{aligned}\lambda_i &= \frac{z_i - z_{i-1}}{z_{i-1} - z_{i-2}}, \\ \delta_i &= 1 + \lambda_i = \frac{z_i - z_{i-2}}{z_{i-1} - z_{i-2}}, \\ h_i &= f_{i-2}\lambda_i - f_{i-1}\delta_i + f_i, \\ g_i &= f_{i-2}\lambda_i^2 - f_{i-1}\delta_i^2 + f_i(\lambda_i + \delta_i).\end{aligned}\quad (10)$$

Therefore:

$$\lambda_{i+1} = \frac{1}{2\lambda_i h_i} \left[ -g_i \pm \sqrt{g_i^2 - 4f_i\lambda_i\delta_i h_i} \right] = \frac{-2f_i\delta_i}{g_i \pm \sqrt{g_i^2 - 4f_i\lambda_i\delta_i h_i}}. \quad (11)$$

The sign of the root is selected such that the denominator in the second form has the maximum magnitude. Special cases are:

$$\begin{aligned}\lambda_i = 0: \quad \lambda_{i+1} &= -\frac{f_i}{f_i - f_{i-1}}, \\ h_i = 0: \quad \lambda_{i+1} &= -\frac{f_i\delta_i}{g_i}, \\ g_i = 0: \quad \lambda_{i+1} &= \pm j\sqrt{\frac{f_i\delta_i}{\lambda_i h_i}}, \\ \text{radicand } = 0: \quad \lambda_{i+1} &= -\frac{g_i}{2\lambda_i h_i} = -\frac{2f_i\delta_i}{g_i}.\end{aligned}\quad (12)$$

Approximations  $z_i$  should not coincide. The iteration is terminated if either or both

$$|f(z_{i+1})| \leq \delta^2 \text{ and/or } |1 - z_i/z_{i+1}| < \delta \quad (13)$$

with a small number  $\delta$  ( $\approx 10^{-8}$ ). One can, to some degree, influence the direction of the search for a solution by the arrangement of the starters  $z_{i-2}, z_{i-1}, z_i$ .

*Continued fractions* (Cf) may be written in one of the following forms:

$$Cf = b_0 + \cfrac{a_1}{b_1 + \cfrac{a_2}{b_2 + \cfrac{a_3}{b_3 + \dots}}} = b_0 + \frac{a_1}{b_1 + \frac{a_2}{b_2 + \frac{a_3}{b_3 + \dots}}}. \quad (14)$$

The evaluation “from behind” is fast if one knows where to truncate the expansion. An evaluation in the opposite direction uses the following recursion:

$$\begin{aligned}Cf_n &= \frac{A_n}{B_n} = b_0 + \frac{a_1}{b_1 + \frac{a_2}{b_2 + \frac{a_3}{b_3 + \dots + \frac{a_n}{b_n}}}}, \\ A_{-1} &\equiv 1; \quad A_0 = b_0; \quad B_{-1} \equiv 0; \quad B_0 \equiv 1, \\ A_n &= b_n A_{n-1} + a_n A_{n-2}, \\ B_n &= b_n B_{n-1} + a_n B_{n-2}.\end{aligned}\quad (15)$$

Tests of convergence can be performed repeatedly after a certain number of steps.

## J.5 Modes in Rectangular Ducts with Locally Reacting Lining

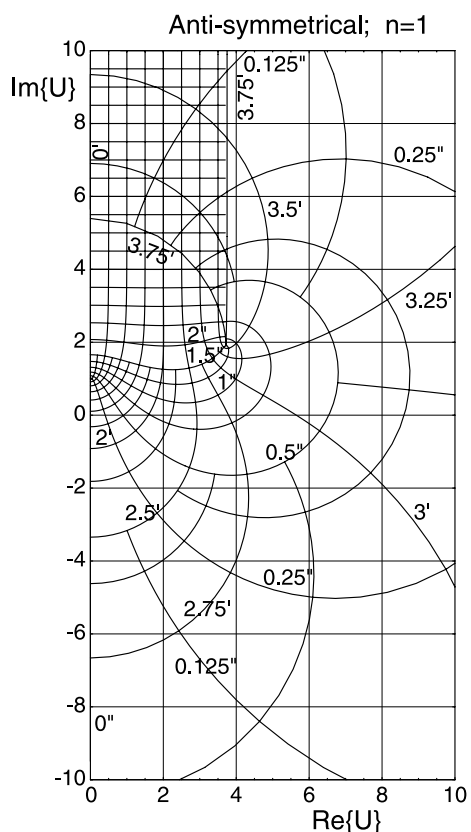
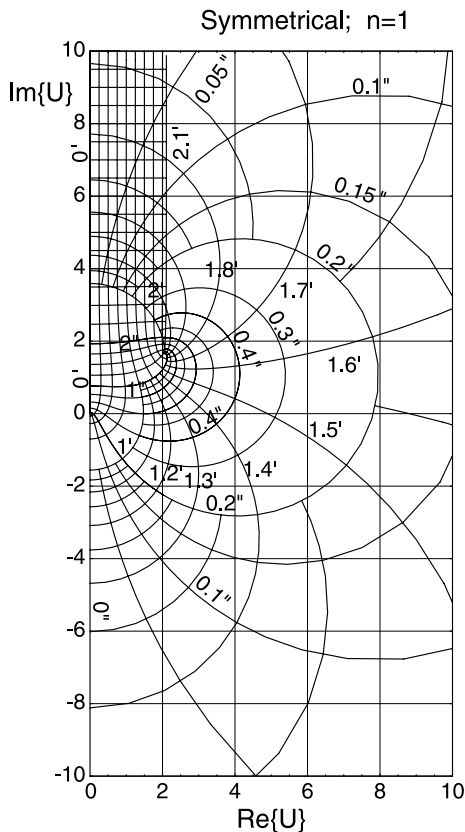
► See also: Mechel, Vol. III, Ch. 26 (1998)

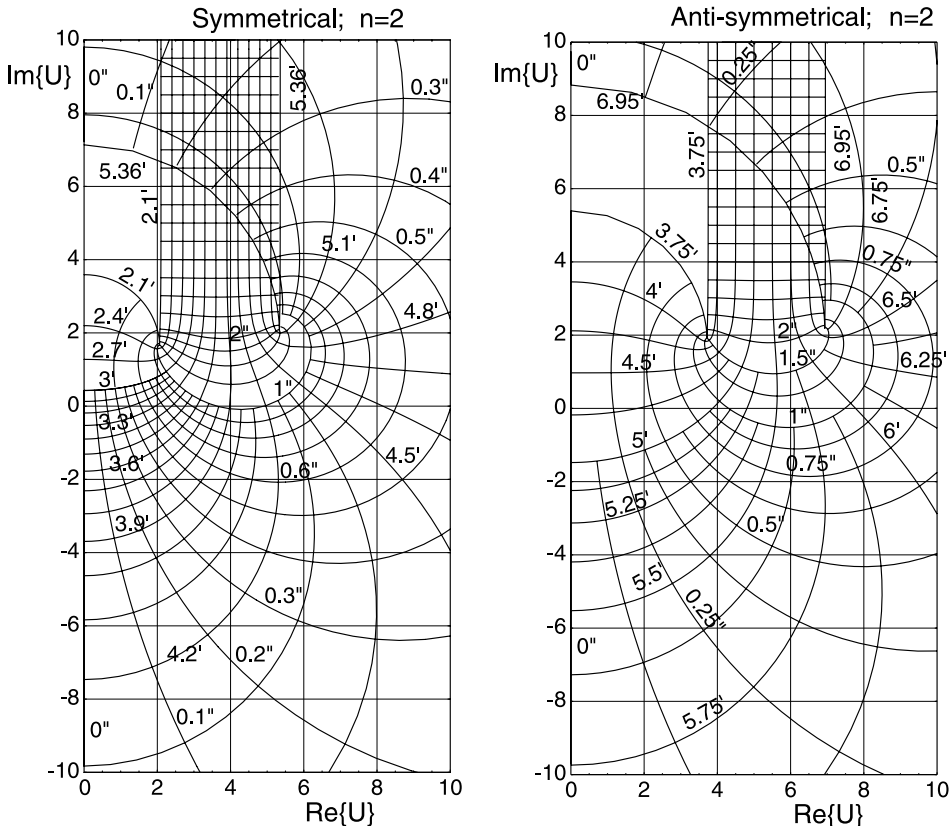
Let the axial co-ordinate  $x$  be in the centre of the duct with heights  $2h_y$  and  $2h_z$ . Let the linings on opposite walls be equal and have the surface admittances  $G_y$  and  $G_z$  on the walls normal to the  $y$  and  $z$  axes, respectively. Modes (i. e. solutions to the wave equation and of the boundary conditions) have the following form:

$$p(x, y, z) = q_y(y) \cdot q_z(z) \cdot e^{-\Gamma x} \quad (1)$$

with lateral profiles:

$$\begin{aligned} q_y(y) &= \begin{cases} \cos(\epsilon_y y) ; & \text{symmetrical mode,} \\ \sin(\epsilon_y y) ; & \text{anti-symmetrical mode;} \end{cases} \\ q_z(z) &= \begin{cases} \cos(\epsilon_z z) ; & \text{symmetrical mode,} \\ \sin(\epsilon_z z) ; & \text{anti-symmetrical mode.} \end{cases} \end{aligned} \quad (2)$$





The wave equation is satisfied if the following secular equation holds:

$$\Gamma^2 = \epsilon_y^2 + \epsilon_z^2 - k_0^2 ; \quad \operatorname{Re}\{\Gamma\} \geq 0 ; \quad \operatorname{Im}\{\Gamma\} \geq 0 \quad (3)$$

(the first sign convention has priority; the second convention holds if  $\operatorname{Re}\{\dots\} = 0$ ). The boundary conditions at the lining surfaces give the following characteristic equations:

$$\begin{aligned} \text{symmetrical modes} \quad & \epsilon_y h_y \cdot \tan(\epsilon_y h_y) = j k_0 h_y \cdot Z_0 G_y =: j U_y , \\ & \epsilon_z h_z \cdot \tan(\epsilon_z h_z) = j k_0 h_z \cdot Z_0 G_z =: j U_z ; \end{aligned} \quad (4)$$

$$\begin{aligned} \text{anti-symmetrical modes} \quad & \epsilon_y h_y \cdot \cot(\epsilon_y h_y) = -j k_0 h_y \cdot Z_0 G_y =: -j U_y , \\ & \epsilon_z h_z \cdot \cot(\epsilon_z h_z) = -j k_0 h_z \cdot Z_0 G_z =: -j U_z . \end{aligned} \quad (5)$$

$U_y$  and  $U_z$  are known quantities for a given lining. If two opposite walls are hard, e.g.  $G_z = 0$ , then:

$$\epsilon_z h_z = \begin{cases} n\pi ; & n = 0, 1, 2, \dots ; \text{ symmetrical modes} \\ (n + 1/2)\pi ; & n = 0, 1, 2, \dots ; \text{ anti-symmetrical modes} \end{cases} . \quad (6)$$

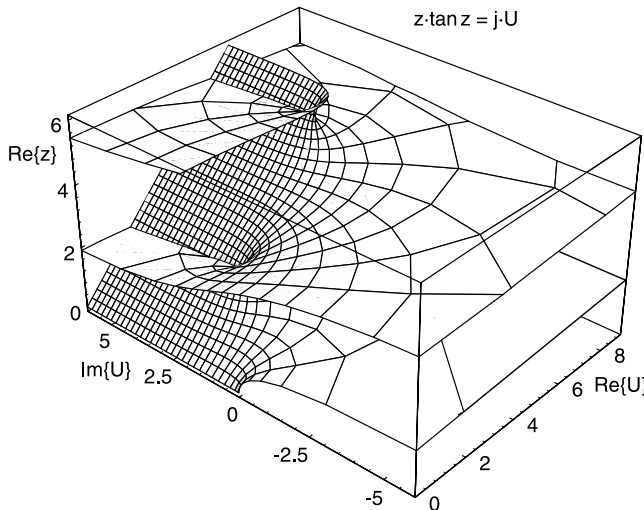
Modes in locally lined ducts are orthogonal to each other over the duct height:

$$\frac{1}{2h_y} \int_{-h_y}^{h_y} q_{\text{ym}}(y) \cdot q_{\text{yn}}(y) dy = \delta_{m,n} \cdot N_{yn} = \frac{\delta_{m,n}}{2} \left[ 1 \pm \frac{\sin(2\epsilon_m h_y)}{2\epsilon_m h_y} \right]; \quad \begin{cases} \text{symm.} \\ \text{anti-symm.} \end{cases} \quad (7)$$

with  $\delta_{m,n} = 1$  for  $m = n$  and  $\delta_{m,m} = 0$ ;  $N_{yn}$  denotes the mode norms. The characteristic equations for locally reacting linings have the form, with  $\epsilon h \rightarrow z$ :

$$z \cdot \tan z = jU; \quad \text{symm.}; \quad z / \tan z = -jU; \quad \text{anti-symm.} \quad (8)$$

with  $U$  a known (in a general complex) number with positive real part. These equations induce a transformation between  $z$  and  $U$ . If one plots for given real or imaginary parts of  $z = z' + j \cdot z''$  with a running second part being the evaluated value of  $U$  in the complex plane, then one gets a type of "Morse chart" (see diagrams at beginning of this section). If one plots the above charts over the complex  $U$  plane and introduces a third dimension  $\text{Re}\{z\}$ , one gets more instructive three-dimensional charts, for example for symmetrical modes:



Evidently there are two types of modes: one set of modes with *curved chart lines*, and a single mode with nearly *rectilinear chart lines*. The modes with *curved lines* have correspondences in a hard duct; the mode with the *rectilinear lines* is a surface wave; there is no corresponding solution in the hard duct.

## J.6 Least Attenuated Mode in Rectangular, Locally Lined Ducts

► See also: Mechel, Vol. III, Ch. 26 (1998)

Designing a silencer with the attenuation of the least attenuated mode is a "safe" design because the least attenuated mode is one of the modes to excite easily (see later section).

about excitation efficiency of modes), and for a sufficiently long silencer other possibly excited modes will have decayed at the silencer exit, so that the least attenuated mode determines the exit sound pressure level.

The least attenuated mode is among the two lowest symmetrical modes. A number of methods have been described for its evaluation. The lateral wave number  $z = \epsilon h$  is a solution of the characteristic equation

$$z \cdot \tan z = jU \quad (1)$$

$$\text{with } U = k_0 h \cdot Z_0 G. \quad (2)$$

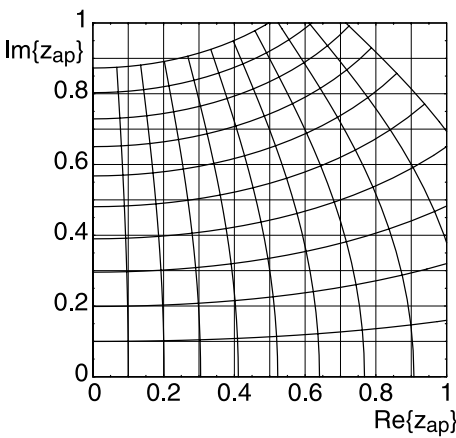
The characteristic equation is even in  $z$ , so most approximate solutions described are for  $z^2$ .

An approximate solution  $z_{ap}$  can be tested as follows: let the parts of  $z_{ex} = z'_{ex} + j \cdot z''_{ex}$  run and evaluate the associated  $U$  from the characteristic equation; then solve with this value of  $U$  for the approximation  $z_{ap}$ ; plot the lines for  $z_{ex}$  in the complex plane of  $z_{ap}$ . If the approximation is good, it reproduces (approximately) the co-ordinate grid of that plane.

#### *First approximation:*

Expand  $\tan(z)$  as a power series around  $z = 0$  and retain the first term; this gives:

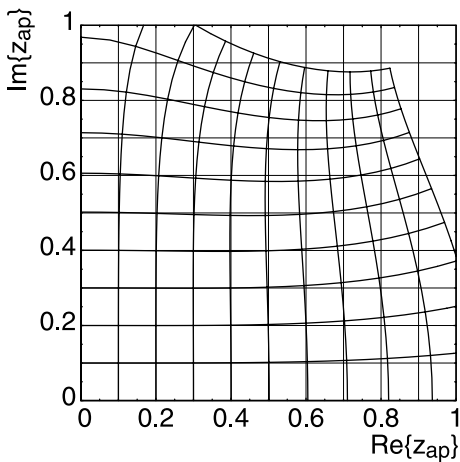
$$z^2 \approx j \cdot U. \quad (3)$$



#### *Second approximation:*

The power series expansion up to terms  $z^4$  gives the following approximation:

$$z^2 \approx 3/2 \cdot \left( -1 + \sqrt{1 + 4jU/3} \right). \quad (4)$$



*Third approximation:*

Perform first the identical transformation,

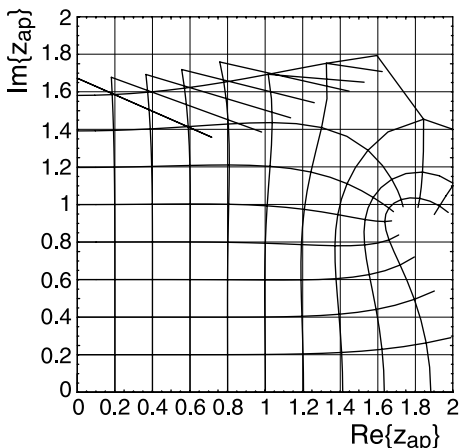
$$z \cdot \tan z = z^2 / z \cot z , \quad (5)$$

and then expand:

$$z \cdot \cot z = 1 - z^2/3 - z^4/45 - \dots . \quad (6)$$

This gives:

$$z^2 \approx \frac{3}{2} \frac{15 + 5jU - \sqrt{225 + 150jU - 45U^2}}{jU} . \quad (7)$$



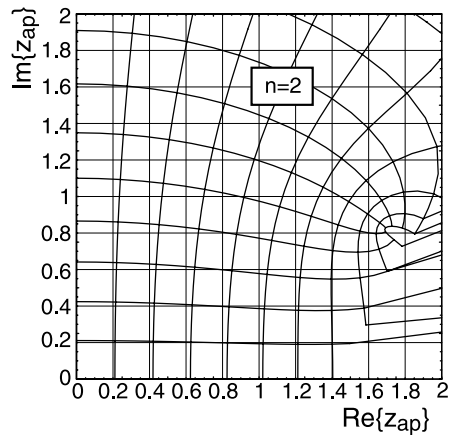
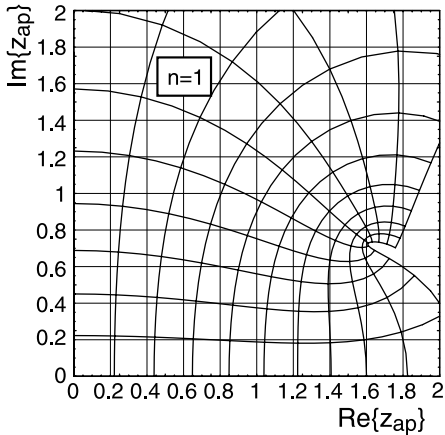
#### Fourth approximation:

This approximation is of some systematic interest because it does not use the characteristic equation. It starts from the general admittance equation:

$$Z_0 G = \frac{1}{k_0} (-\text{grad} \arg(p) + j \text{grad} \ln |p|) \quad (8)$$

and uses the expansion for the sound pressure profile  $q(y) = \cos(\epsilon y)$ :

$$\ln q(y) = \ln \cos(\epsilon y) = \sum_{n=1}^{\infty} \ln \left( 1 - \frac{4(\epsilon y)^2}{\pi^2(2n-1)^2} \right). \quad (9)$$



Simple transformations give:

$$U = -8jz^2 \sum_{n=1}^{\infty} \frac{1}{\pi^2(2n-1)^2 - 4z^2}. \quad (10)$$

The solution with an upper summation limit  $n = 1$  yields:

$$z^2 \approx \frac{\pi^2}{4} \frac{jU}{2 + jU}, \quad (11)$$

and summation up to  $n = 2$  yields:

$$z^2 \approx \frac{\pi^2}{4} \frac{10 + 5jU - \sqrt{100 + 64jU - 16U^2}}{4 + jU}. \quad (12)$$

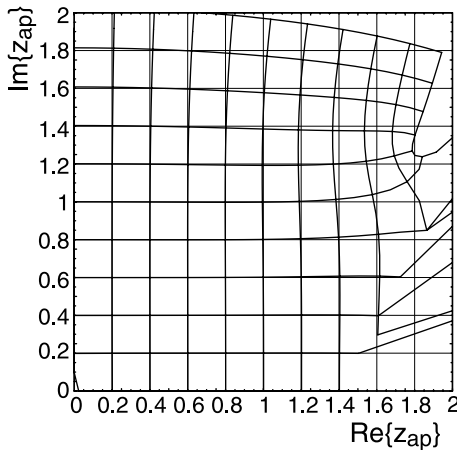
An approximation

$$z^2 \approx \frac{27.40 + 12.34jU - \sqrt{750.56 + 322.47jU - 97.409U^2}}{6.452 + jU} \quad (13)$$

is obtained if one neglects  $4z^2$  in the denominator of the expression for  $U$  for  $n \geq 3$  and applies the numerical series:

$$\sum_{n=1}^{\infty} \frac{1}{(2n-1)^2} = \frac{\pi^2}{8}, \quad (14)$$

which has the value  $1/8 - 10/(9\pi^2)$  if it begins with  $n = 3$ .



#### *Fifth approximation:*

A new class of precision is attained if one applies in the characteristic equations for symmetrical and anti-symmetrical modes

$$z \cdot \tan z = jU; \quad z / \tan z = -jU \quad (15)$$

the continued fraction expansions:

$$z \cdot \tan z = \frac{z^2}{1 - \frac{z^2}{3 - \frac{z^2}{5 - \frac{z^2}{7 - \dots}}}}; \quad z \cdot \cot z = 1 - \frac{z^2}{3 - \frac{z^2}{5 - \frac{z^2}{7 - \dots}}}. \quad (16)$$

They begin to converge with the partial fraction for which

$$2n - 1 > \frac{|z|^2}{2n + 1}; \quad (2n)^2 - 1 > |z|^2. \quad (17)$$

If one truncates the continued fraction with increasing depth, then one gets polynomial equations of higher and higher degrees. The polynomials and explicit solutions (where they exist) are, for *symmetrical modes*:

$$\begin{aligned} z^2 &= jU, \\ z^2 &= \frac{jU}{1 + jU/3}, \end{aligned} \quad (18)$$

$$\begin{aligned} z^4 - (15 + 6jU)z^2 + 15jU &= 0, \\ z^2 &= \frac{1}{2} \left( 15 + 6jU \pm \sqrt{225 + 120jU - 36U^2} \right), \end{aligned} \quad (19)$$

$$(10 + jU)z^4 - (105 + 45jU)z^2 + 105jU = 0, \quad (20)$$

$$z^2 = \frac{105 + 45jU \pm \sqrt{11025 + 5250jU - 1605U^2}}{20 + 2jU}, \quad *) \quad (21)$$

$$\begin{aligned} z^6 - (105 + 15jU)z^4 + (945 + 420jU)z^2 - 945jU &= 0, \\ (21 + jU)z^6 - (1260 + 210jU)z^4 + (10395 + 4725jU)z^2 - 10395jU &= 0, \end{aligned} \quad (22)$$

$$\begin{aligned} z^8 - (378 + 28jU)z^6 + (17325 + 3150jU)z^4 - (135135 + 62370jU)z^2 \\ + 135135jU &= 0, \end{aligned} \quad (23)$$

$$\begin{aligned} (36 + jU)z^8 - (6930 + 630jU)z^6 + (270270 + 51975jU)z^4 \\ - (2027025 + 945945jU)z^2 + 2027025jU &= 0. \end{aligned} \quad (24)$$

The precision test of the approximation (21) is shown in the graph on the next side. In the grey area the sign of the root was chosen so as to make the real part of the root positive and in the other range negative. The limit line passes through the first branch point (where the lines are curved).

Evidently this approximation can be used also for parts of the second "Morse chart", i.e. for the second mode.

Higher-degree polynomials of the continued fraction expansion give more than just one solution for  $z^2$ . They belong (with different precision) to the lower-order modes. To find the solution for the least attenuated mode, exclude all approximations  $z$  which are not in the first quadrant and take from the remaining approximations that which makes  $\text{Re}\{\Gamma h\}$  a minimum.

Frommhold has modified the coefficients of the continued fraction approximations to move the range of application more towards the range of technical values of  $U$ ; he proposes the following:

If  $0 \leq \text{Re}\{Z_0 G\} \leq 3$ ;  $-1.5 \leq \text{Im}\{Z_0 G\} \leq 1.5$ :

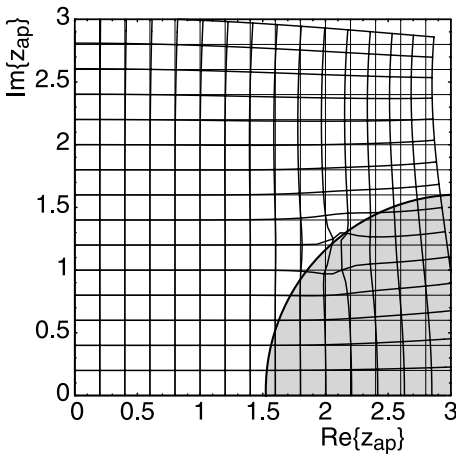
$$z^2 \approx \frac{(2.74 - 0.52 \cdot j)jU}{2.88 - 0.55 \cdot j + jU}. \quad (25)$$

If  $2 \leq \text{Re}\{Z_0 G\} \leq 5$ ;  $3 \leq \text{Im}\{Z_0 G\} \leq 6$ , then:

$$\begin{aligned} z^2 &\approx \frac{(78.94 - 5.43 \cdot j) + (34.47 - 2.2 \cdot j)jU \pm \sqrt{\dots}}{(16.1 - 1.11 \cdot j) + 2jU}, \\ \sqrt{\dots} &= \sqrt{(6203 - 857 \cdot j) + (2887.3 - 372 \cdot j)jU - (867.4 - 130 \cdot j)U^2}. \end{aligned} \quad (26)$$

The sign of the root is determined with the criterion  $\text{Re}\{\Gamma h\} = \text{minimum}$ .

\*) See Preface to the 2<sup>nd</sup> edition.



## J.7 Sets of Mode Solutions in Rectangular, Locally Lined Ducts

---

► See also: Mechel, Vol. III, Ch. 26 (1998)

The charts of the transformation  $z \rightarrow U$  which is induced by the characteristic equation show branch points. The evaluation of sets of mode solutions begins with the determination of these branch points  $z_b$ , and the associated values  $U_b$  follow from the characteristic equations

$$\begin{aligned} z \cdot \tan z &= jU ; && \text{symmetrical modes,} \\ z / \tan z &= -jU ; && \text{anti-symmetrical modes.} \end{aligned} \quad (1)$$

The branch points are solutions of

$$\tan z + \frac{z}{\cos^2 z} = 0 ; \quad \text{symmetrical} ; \quad \cot z - \frac{z}{\sin^2 z} = 0 ; \quad \text{anti-symmetrical.} \quad (2)$$

Approximations of the functions  $z''_b = f(z'_b)$ ;  $U''_b = g(U'_b)$ ;  $z'_b(m)$ ;  $U'_b(m)$  (with  $z_b = z'_b + j \cdot z''_b$ ;  $U_b = U'_b + j \cdot U''_b$  and  $m = 0, 1, 2, \dots$  the mode order) are:

$$\begin{aligned} z''_b &= 0.702568 \cdot (z'_b)^{1/3} + 0.216438 \cdot (z'_b)^{1/2} - 0.036625 \cdot z'_b \\ &\quad + 0.000143119 \cdot z'^2_b ; \quad \text{symm.} \end{aligned} \quad (3)$$

$$\begin{aligned} z''_b &= 0.0232164 + 0.829796 \cdot (z'_b)^{1/2} - 0.0827732 \cdot z'_b \\ &\quad + 0.000351925 \cdot z'^2_b ; \quad \text{anti-symm.} \end{aligned}$$

$$\begin{aligned} U''_b &= 2.02599 \cdot (U'_b)^{1/3} - 0.655631 \cdot (U'_b)^{1/2} + 0.00631631 \cdot U'_b \\ &\quad + 0.00000250827 \cdot U'^2_b ; \quad \text{symm.} \\ U''_b &= 1.0 + 0.553673 \cdot (U'_b)^{1/2} - 0.0412894 \cdot U'_b \\ &\quad + 0.000120216 \cdot U'^2_b ; \quad \text{anti-symm.} \end{aligned} \quad (4)$$

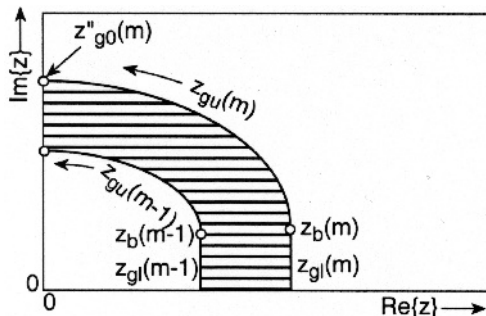
$$\begin{aligned} z'_b(m) &= -1.4403\sqrt{m} + 3.76029 \cdot m - 0.0284415 \cdot m^2 \\ &\quad + 0.000620241 \cdot m^3; \text{ symm.} \end{aligned} \quad (5)$$

$$\begin{aligned} z'_b(m) &= 3.39478 \cdot m - 0.023865 \cdot m^2 \\ &\quad + 0.000669072 \cdot m^3; \text{ anti-symm.} \end{aligned}$$

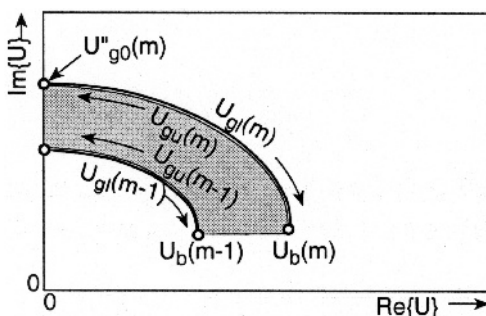
$$\begin{aligned} U'_b(m) &= -1.50237\sqrt{m} + 3.76029 \cdot m - 0.0284415 \cdot m^2 \\ &\quad + 0.000620241 \cdot m^3; \text{ symm.} \end{aligned} \quad (6)$$

$$\begin{aligned} U'_b(m) &= 3.39042 \cdot m - 0.023312 \cdot m^2 \\ &\quad + 0.000651624 \cdot m^3; \text{ anti-symm.} \end{aligned}$$

The characteristic equations transform the U plane (with  $\operatorname{Re}\{U\} \geq 0$ ) into a strip in the first quadrant of the z plane. A one-to-one correspondence of a z-strip and the U plane, with limit curves which can be evaluated (!), is shown in the graph below. The z-strip is limited by lower limit curves  $z_{gl}(m)$  ( $g = \text{Grenze}$  in German), which are vertical lines from the branch point  $z_b(m)$  to the  $\operatorname{Re}\{z\}$  axis, and by upper limit curves  $z_{gu}(m)$ , which are quarter ellipses between  $z_b(m)$  and  $z''_{g0}(m)$  on the  $\operatorname{Im}\{z_b\}$  axis. The associated limit curves in the U plane are shown in the second graph. In the shaded range of the U plane, the surface wave mode is evaluated.



A strip in the z plane into which the U plane (with  $\operatorname{Re}\{U\} \geq 0$ ) is transformed. It is limited by *vertical lower curves* through the branch points and by upper elliptic arcs



Transformation of the limits of the z-strip into the U plane. If U is in the *shaded range*, the surface wave mode is evaluated

**Table 1** Branch points  $z_b$  and associated  $U_b$  for symmetrical and anti-symmetrical modes in flat ducts with locally reacting lining

<b>m</b>	<b>Symmetrical</b>		<b>Anti-symmetrical</b>	
	<b><math>z_b</math></b>	<b><math>U_b</math></b>	<b><math>z_b</math></b>	<b><math>U_b</math></b>
0	0+j 0.	0+j 0.	0+j 0.	0+j 1.
1	2.1062 + j 1.12536	2.05998 + j 1.65061	3.74884 + j 1.38434	3.71944 + j 1.89528
2	5.35627 + j 1.55157	5.33471 + j 2.05785	6.94998 + j 1.6761	6.93297 + j 2.18022
3	8.53668 + j 1.77554	8.52264 + j 2.27847	10.1193 + j 1.85838	10.1073 + j 2.36058
4	11.6992 + j 1.9294	11.6888 + j 2.43112	13.2773 + j 1.99157	13.2681 + j 2.49295
5	14.8541 + j 2.04685	14.8458 + j 2.54799	16.4299 + j 2.09663	16.4224 + j 2.59758
6	18.0049 + j 2.14189	17.9981 + j 2.64271	19.5794 + j 2.1834	19.5731 + j 2.6841
7	21.1534 + j 2.22172	21.1476 + j 2.72234	22.7270 + j 2.25732	22.7216 + j 2.75786
8	24.3003 + j 2.29055	24.2952 + j 2.79103	25.8734 + j 2.32171	25.8686 + j 2.82214
9	27.4462 + j 2.35105	27.4417 + j 2.85144	29.0188 + j 2.37876	29.0146 + j 2.87911
10	30.5913 + j 2.40501	30.5872 + j 2.90533	32.1636 + j 2.42996	32.1598 + j 2.93025
11	33.7358 + j 2.45372	33.7321 + j 2.95399	35.3079 + j 2.4764	35.3044 + j 2.97665
12	36.8799 + j 2.4981	36.8765 + j 2.99833	38.4518 + j 2.5189	38.4486 + j 3.01911
13	40.0236 + j 2.53887	40.0205 + j 3.03906	41.5954 + j 2.55807	41.5924 + j 3.05825
14	43.1671 + j 2.57656	43.1642 + j 3.07673	44.7387 + j 2.59439	44.7359 + j 3.09455
15	46.3103 + j 2.61161	46.3076 + j 3.11176	47.8819 + j 2.62825	47.8793 + j 3.1284
16	49.4534 + j 2.64436	49.4509 + j 3.1445	51.0248 + j 2.65997	51.0224 + j 3.1601
17	52.5963 + j 2.6751	52.5939 + j 3.17522	54.1677 + j 2.68979	54.1654 + j 3.18991
18	55.7390 + j 2.70407	55.7368 + j 3.20417	57.3104 + j 2.71794	57.3082 + j 3.21804
19	58.8817 + j 2.73144	58.8796 + j 3.23154	60.4530 + j 2.74459	60.4509 + j 3.24468
20	62.0242 + j 2.7574	62.0222 + j 3.25748	63.5955 + j 2.76988	63.5935 + j 3.26997

The equation for the limit curve in the U plane in the form  $U'_g(m) = f(U''_g(m))$  for both  $U_{gu}$  and  $U_{gl}$  is:

$$U'_g(m) = U'_b(m) \sqrt{1 - \left( \frac{\frac{U''_g(m) - U''_b(m)}{z'_b(m) \cdot \sin(2z'_b(m))}}{1 + \cos(2z'_b(m)) + U''_b(m)} \right)^2}. \quad (7)$$

The equation for the elliptic limit curve in the  $z$  plane in the form  $z'_{gu}(m) = f(z''_{gu}(m))$  is:

$$z'_{gu}(m) = z'_b(m) \sqrt{1 - \left( \frac{z''_{gu}(m) - z''_b(m)}{z''_{g0}(m) - z''_b(m)} \right)^2}; \quad z''_b(m) \leq z''_{gu}(m) \leq z''_{g0}(m), \quad (8)$$

and in the form  $z''_{gu}(m) = f(z'_{gu}(m))$ :

$$z''_{gu}(m) = z''_b(m) + \left( z''_{g0}(m) - z''_b(m) \right) \sqrt{1 - \left( \frac{z'_{gu}(m)}{z'_b(m)} \right)^2}; \quad 0 \leq z'_{gu}(m) < z'_b(m). \quad (9)$$

Required values of  $z''_{g0}(m)$ ;  $U''_{g0}(m)$  are contained in the table below.

It should be noticed that the branch points, range limit curves and endpoints of the elliptic arcs coincide with the origin for  $m = 0$ .

The modes are counted as  $m = 1, 2, 3, \dots$  in the procedure for the evaluation of a mode solution  $z = \epsilon h$  for given values of  $U$  and  $m$  (usually counting is  $m = 0, 1, 2, \dots$ ). The procedure works with the following steps:

*Step 1: special case  $U = 0$ ?*

$$\text{Take } z = \epsilon h = \begin{cases} (m-1)\pi; & \text{symmetrical} \\ (m-1/2)\pi; & \text{anti-symmetrical} \end{cases}. \quad (10)$$

*Step 2:  $U$  in the surface wave range?*

That is,  $U$  is in the range limited by (a) the curve  $U''_b = g(U'_b)$  which connects the branch point images, (b) the imaginary axis and (c) the curves  $U'_g(n) = f(U''_g(n))$  for  $n = m-1$  and  $n = m$ .

In that case use the fast converging (because  $z \approx U$ ) iteration  $i = 0, 1, 2, \dots$

$$z_{i+1} = jU / \tan(z_i); \quad \text{symm.}; \quad z_{i+1} = -jU / \cot(z_i); \quad \text{anti-symm.} \quad (11)$$

with  $z_0 = U$ .

*Step 3: Else:* Expand the characteristic equation in a continued fraction, using the periodicity of  $\tan(z)$ ,  $\cot(z)$ :

$$\begin{aligned} z \cdot \tan(z - m\pi) &= \frac{z(z - m\pi)}{1 -} \frac{(z - m\pi)^2}{3 -} \frac{(z - m\pi)^2}{5 -} \dots = jU; & \text{symm.} \\ z \cdot \cot(z - m\pi) &= \frac{z}{z - m\pi} \left( 1 - \frac{(z - m\pi)^2}{3 -} \frac{(z - m\pi)^2}{5 -} \dots \right) = -jU; & \text{anti-symm.} \end{aligned} \quad (12)$$

and derive a polynomial equation in  $z^2$  by truncation. Take the solution for which  $z''_b(m) \leq z'' < z''_b(m+1)$ . Produce two start solutions for Muller's procedure by truncating the continued fraction at different depths, and take as the third starter the mean value between them. Then solve the characteristic equation (in its original form) with these

**Table 2** Values of endpoints of elliptic arcs on imaginary axis

<b>m</b>	<b>Symmetrical</b> $z''_{g0}(m) \text{ & } U''_{g0}(m)$	<b>Anti-symmetrical</b> $z''_{g0}(m) \text{ & } U''_{g0}(m)$
0	0.00000	0.00000
1	3.55637	5.39512
2	7.13605	8.83041
3	10.4985	12.1485
4	13.788	15.4182
5	17.0412	18.6597
6	20.276	21.8853
7	23.4928	25.0985
8	26.7013	28.2986
9	29.8984	31.4972
10	33.0907	34.6867
11	36.2800	37.8715
12	39.4623	41.0533
13	42.6456	44.2313
14	45.8196	47.4114
15	48.9979	50.5792
16	52.1657	53.7582
17	55.3359	56.9203
18	58.5124	60.0893
19	61.6746	63.2566
20	64.8482	66.4240

starters and *Muller's procedure* (for many applications the solution of the polynomial equation, if the degree of the polynomial is not too low, is already sufficiently precise).

Because the curves  $U''_{gu}(m) = f(U'_{gu}(m))$  ;  $z''_{gu}(m) = f(z'_{gu}(m))$

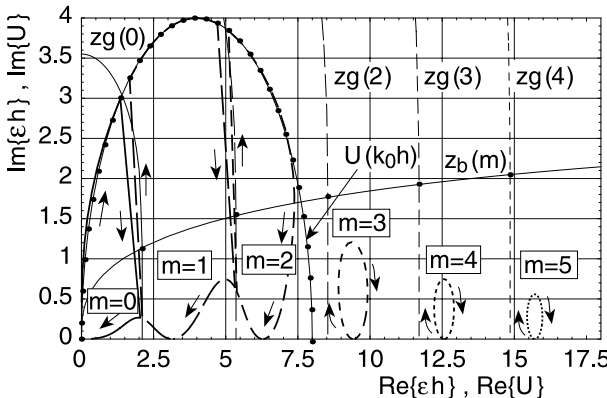
are not exact transforms of each other, it may happen that no solution of the polynomial equation has

$$z''_b(m) \leq z'' < z''_b(m + 1).$$

Then the desired solution is in or near the range of the surface wave mode. Take in this (rare) instance the solution from the iteration above.

The (important) advantage of the procedure is that no mode in a mode set is missed or returned twice; the disadvantage is that the surface wave mode (if any exists) is subdivided and the "pieces" are attributed to different modes, so mode solution curves

in the  $z$  plane do not look “nice”; but this feature does not disturb modal analysis computations. In the numerical example shown below, the surface wave solution (the arc which approximately agrees with the curve  $U(k_0h)$ ) is subdivided; a mode solution jumps whenever this solution crosses a limit of a  $z$ -strip.



The graph shows (in the  $U$  plane) the curve  $U(k_0h)$  (full line with dots); the curve  $z_b(m)$  connecting the branch points (thin full line); the limit curves  $z_g(m)$  of the  $z$ -strips (thin dashed curves); and the mode solutions for the modes  $m = 0, 1, \dots, 5$ . The direction of increasing frequency is indicated by arrows

A procedure for a set of mode solutions and a list of  $k_0h$  values, which avoids the subdivision of the surface wave mode, which returns continuous mode solutions (for a variation of  $k_0h$ ) and which is relatively robust against “mode jumping”, proceeds as follows. It is assumed that the list  $\{k_0h\}$  begins with low values (if necessary, prepend such values; you may drop them later), and the difference  $\Delta k_0h$  is not too large ( $\Delta k_0h \leq 0.1$ ; maximum  $\leq 0.2$ ).

The procedure is first described for symmetrical modes.

Begin to work through the list ( $i = 1, 2, \dots$ ) of  $k_0h$  with starting values  $z_{s1} = m\pi$ ;  $z_{s2} = m\pi + 0.01 \cdot j$ ;  $z_{s3} = m\pi + 0.01 + 0.01 \cdot j$  for *Muller's procedure* and find  $z_{i=1}$ . Write the characteristic equation as:

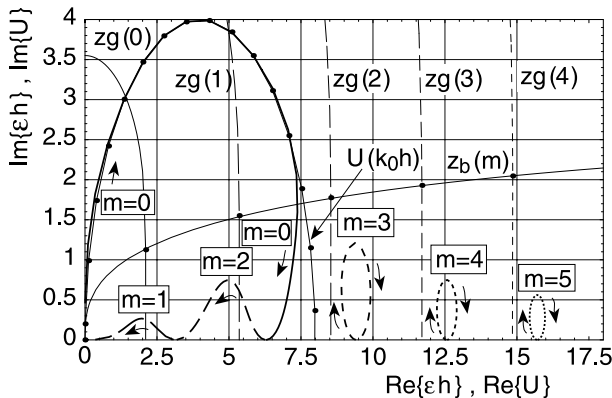
$$z^2 \approx m\pi \cdot z + j \cdot k_0h \cdot Z_0G \cdot \left[ 1 - \frac{(z - m\pi)^2}{3} - \frac{(z - m\pi)^2}{5} - \dots - \frac{(z - m\pi)^2}{(n_{hi} - 2)^2} - \frac{(z - m\pi)^2}{n_{hi}^2} \right] \quad (13)$$

$$\xrightarrow[z \rightarrow m\pi]{} (m\pi)^2 + j \cdot k_0h \cdot Z_0G \xrightarrow[k_0h \rightarrow 0 \text{ and/or } G \rightarrow 0]{} (m\pi)^2,$$

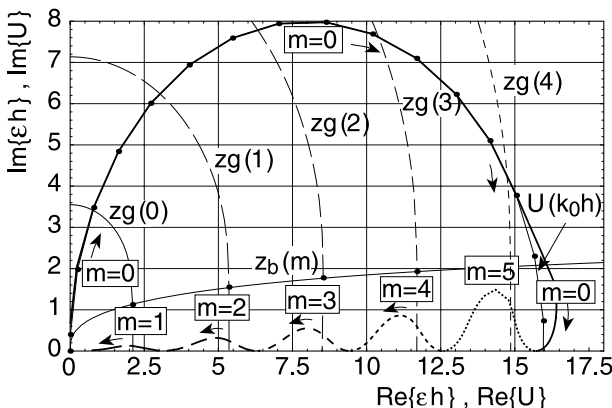
and use on the right-hand side  $z \rightarrow z_{i-1}$  to find a starting approximation  $z_{s3}$  for  $z_i$ . The other starters for *Muller's procedure* are  $z_{s2} = z_{i-2}$ ;  $z_{s1} = z_{i-3}$  (in the second step  $i = 2$ , take the previous solution as  $z_{s2}$  and the mean value of  $z_{s2}, z_{s3}$  as  $z_{s1}$ ). The order

of the starters is important; do not use the Newton-Raphson method; otherwise mode jumping will happen.

The next graph shows again the mode solutions from above, but now with this method; in the second graph the range over which the surface wave mode spans has been enlarged; the mode index  $m = 0$  is attributed to the surface wave mode.



Mode solutions as above, but with a method returning steady curves for the modes



Mode solutions as above, but with an extended span of the surface wave mode ( $m = 0$ )

In the case of anti-symmetrical modes, proceed as above, but replace  $m \rightarrow (m + 1/2)$  (because of  $\cot(z) = -\tan(z - (m + 1/2)\pi)$ ).

## J.8 Flat Duct with a Bulk Reacting Lining

► See also: Mechel, Vol. III, Ch. 27 (1998)

A flat duct with axial co-ordinate  $x$  and lateral co-ordinate  $y$  has a hard wall at  $y = 0$  and is lined with a bulk reacting absorber at  $y = h$ . The lining is a layer of thickness  $d$  of

a porous material with characteristic values  $\Gamma_a$ ,  $Z_a$  (or, in normalised form,  $\Gamma_{an} = \Gamma_a/k_0$ ,  $Z_{an} = Z_a/Z_0$ ), possibly covered with a poro-elastic foil having a partition impedance  $Z_s$  (“ $s$ ” from *series impedance*). Fundamental relations are shown in Table 1.

**Table 1** Relations in the free rectangular duct and in the absorber layer

Relation	Free duct	Absorber layer
Wave equation	$(\Delta + k_0^2) p(x, y) = 0$	$(\Delta - \Gamma_a^2) p_a(x, y) = 0$
Field formulation Profile $\begin{cases} \text{symm.} \\ \text{anti-symm.} \end{cases}$ in $y$	$p(x, y, z) = P_0 q(y) \cdot s(z) \cdot e^{-\Gamma x}$ $q(y) = \begin{cases} \cos(\varepsilon_y y) \\ \sin(\varepsilon_y y) \end{cases}$	$p_a(x, y, z) = P_a q_a(y) \cdot s(z) \cdot e^{-\Gamma x}$ $q_a(y) = \cos(\varepsilon_{ay}(\pm y - h - d))$
Profile $\begin{cases} \text{symm.} \\ \text{anti-symm.} \end{cases}$ in $z$		$s(z) = \begin{cases} \cos(\varepsilon_z z) \\ \sin(\varepsilon_z z) \end{cases}$
Secular equation	$\varepsilon_y^2 = \Gamma + k_0^2 - \varepsilon_z^2$	$\varepsilon_{ay}^2 = \Gamma^2 - \Gamma_a^2 - \varepsilon_z^2$
Velocity in $y$ direction	$v_y = \frac{j}{k_0 Z_0} \frac{\partial p}{\partial y}$	$v_{ay} = \frac{-1}{\Gamma_a Z_a} \frac{\partial p_a}{\partial y}$
Lateral admittance $y = h$ symmetrical	$G_y = -j \frac{\varepsilon_y h}{k_0 h Z_0} \tan(\varepsilon_y h)$	$G_{ay} = -\frac{\varepsilon_{ay} d}{\Gamma_a d Z_a} \tan(\varepsilon_{ay} d)$
Lateral admittance $y = h$ anti-symmetrical	$G_y = j \frac{\varepsilon h}{k_0 h Z_0} \cot(\varepsilon h)$	$G_{ay} = -\frac{\varepsilon_{ay} d}{\Gamma_a d Z_a} \tan(\varepsilon_{ay} d)$

The boundary condition is the agreement of the lateral admittances on both sides of  $y = h$ :

$$G_y \stackrel{!}{=} 1 / (Z_s + 1/G_{ay}) . \quad (1)$$

This gives the following characteristic equations:

$$\text{for symmetrical modes: } \varepsilon_y h \cdot \tan(\varepsilon_y h) = j k_0 h \left/ \left( \frac{Z_s}{Z_0} - \frac{\Gamma_a}{\varepsilon_{ay}} \frac{Z_a}{Z_0} \cot(\varepsilon_{ay} d) \right) \right. = j U; \quad (2)$$

$$\text{for anti-symmetrical modes: } \varepsilon_y h \cdot \cot(\varepsilon_y h) = -j k_0 h \left/ \left( \frac{Z_s}{Z_0} - \frac{\Gamma_a}{\varepsilon_{ay}} \frac{Z_a}{Z_0} \cot(\varepsilon_{ay} d) \right) \right. = -j U; \quad (3)$$

$$\text{secular equation: } (\varepsilon_{ay} h)^2 = (\varepsilon_y h)^2 - (\Gamma_a h)^2 - (k_0 h)^2. \quad (4)$$

Function  $U$  now contains the solution  $\epsilon_y h$  (in contrast to locally reacting linings), and the form of the characteristic equation and the method of its solution thus depend on the structure of the lining. Without a cover of the absorber layer (i.e.  $Z_s = 0$ ), function  $U$  is:

$$U = -\frac{h k_0 Z_0}{d \Gamma_a Z_a} \epsilon_a d \cdot \tan(\epsilon_a d) . \quad (5)$$

If the absorber layer is made locally reacting (e.g. either by a high flow resistivity or by internal partition walls normal to the surface), the characteristic equation for symmetrical modes becomes:

$$\epsilon h \cdot \tan(\epsilon h) = j k_0 h \frac{\tanh(\Gamma_a d)}{Z_a / Z_0} . \quad (6)$$

If, on the other hand, the term  $Z_s / Z_0$  is large compared with the second term in the parentheses of the characteristic equation then  $U \rightarrow \frac{k_0 h}{Z_s / Z_0}$ , i.e. the lining behaves like a locally reacting lining.

The characteristic equation is even in  $\epsilon h$  (as for locally reacting absorbers), but now  $\text{Re}\{U\} < 0$  is possible (in contrast to locally reacting absorbers); therefore solutions  $\epsilon h$  are no longer necessarily in the first quadrant. "Morse charts" for the solutions cannot be drawn.

Modes in a duct with a bulk reacting lining (terminated with a hard wall towards the outer space) are orthogonal to each other if the lateral field profile within the outer walls is written as  $q(y) = q^{(1)}(y) + q^{(2)}(y)$ , where (i) = (1) stands for the free duct and (i) = (2) for the absorber layer. The orthogonality relation is:

$$\frac{1}{j k_0 Z_0} \iint_{A_1} q_m^{(1)} \cdot q_n^{(1)} dA_1 + \frac{1}{\Gamma_a Z_a} \iint_{A_2} q_m^{(2)} \cdot q_n^{(2)} dA_2 = \delta_{m,n} \cdot N_m , \quad (7)$$

where  $\delta_{m,n}$  is the Kronecker symbol and  $N_m$  the mode norm:

$$N_m = \frac{1}{j k_0 Z_0} \iint_{A_1} (q_m^{(1)})^2 dA_1 + \frac{1}{\Gamma_a Z_a} \iint_{A_2} (q_m^{(2)})^2 dA_2 . \quad (8)$$

For multi-layer absorbers an additional term  $i > 2$  will appear on the left-hand side of (7) for each layer.

## J.9 Flat Duct with an Anisotropic, Bulk Reacting Lining

---

► See also: Mechel, Vol. III, Ch. 27 (1998)

The object is the same as in the previous Sect. J.8, but the porous material layer is now assumed to be anisotropic, i.e. with characteristic values  $\Gamma_{ax}, Z_{ax}$  and  $\Gamma_{ay}, Z_{ay}$  in the x, y co-ordinate directions. The relations in the free duct and in the absorber layer are presented in Table 1.

**Table 1** Relations in the free duct and in the anisotropic absorber layer

Relation	Free duct	Absorber layer
Wave equation	$(\Delta + k_0^2) p(x, y) = 0$	$(\partial^2/(\Gamma_{ax}\partial x)^2 + \partial^2/(\Gamma_{ay}\partial y)^2 - 1) p_a(x, y) = 0$
Field formulation	$p(x, y) = P_0 q(y) \cdot e^{-\Gamma x}$	$p_a(x, y) = P_a q_a(y) \cdot e^{-\Gamma x}$
Profile $\left\{ \begin{array}{l} \text{symm.} \\ \text{anti-symm.} \end{array} \right.$	$q(y) = \begin{cases} \cos(\varepsilon_y y) \\ \sin(\varepsilon_y y) \end{cases}$	$q_a(y) = \cos(\varepsilon_{ay}(\pm y - h - d))$
Secular equation	$\varepsilon_y^2 = \Gamma^2 + k_0^2$	$\varepsilon_{ay}^2/\Gamma_{ay}^2 = \Gamma^2/\Gamma_{ax}^2 - 1$
Velocity in y direction	$v_y = \frac{j}{k_0 Z_0} \frac{\partial p}{\partial y}$	$v_{ay} = \frac{-1}{\Gamma_{ay} Z_{ay}} \frac{\partial p_a}{\partial y}$
Lateral admittance symmetrical	$G_y = -j \frac{\varepsilon_y h}{k_0 h Z_0} \tan(\varepsilon_y h)$	$G_{ay} = -\frac{\varepsilon_{ay} d}{\Gamma_{ay} d Z_{ay}} \tan(\varepsilon_{ay} d)$
Lateral admittance anti-symmetrical	$G_y = j \frac{\varepsilon h}{k_0 h Z_0} \cot(\varepsilon h)$	$G_{ay} = -\frac{\varepsilon_{ay} d}{\Gamma_{ay} d Z_{ay}} \tan(\varepsilon_{ay} d)$

The characteristic equations for duct modes are now as follows:

$$\text{symmetrical mode: } \varepsilon_y h \cdot \tan(\varepsilon_y h) = j k_0 h \left/ \left( \frac{Z_s}{Z_0} - \frac{\Gamma_{ay}}{\varepsilon_{ay}} \frac{Z_{ay}}{Z_0} \cot(\varepsilon_{ay} d) \right) \right. = j U ; \quad (1)$$

$$\text{anti-symmetrical mode: } \varepsilon_y h \cdot \cot(\varepsilon_y h) = -j k_0 h \left/ \left( \frac{Z_s}{Z_0} - \frac{\Gamma_{ay}}{\varepsilon_{ay}} \frac{Z_{ay}}{Z_0} \cot(\varepsilon_{ay} d) \right) \right. = -j U ; \quad (2)$$

$$\text{secular equation: } \varepsilon_{ay}^2 = \Gamma^2 \cdot \left( \Gamma_{ay}^2 / \Gamma_{ax}^2 \right) - \Gamma_{ay}^2 = \left( \varepsilon_y^2 - k_0^2 \right) \cdot \left( \Gamma_{ay}^2 / \Gamma_{ax}^2 \right) - \Gamma_{ay}^2 ; \quad (3)$$

$$\text{axial propagation constant: } \Theta h = \sqrt{(\varepsilon_y h)^2 - (k_0 h)^2} . \quad (4)$$

No principally new features are introduced by the anisotropy, only the amount of computation is somewhat increased.

## J.10 Mode Solutions in a Flat Duct with Bulk Reacting Lining

---

► See also: Mechel, Vol. III, Ch. 27 (1998)

Because no transformation between  $z = \epsilon h$  and a meaningful known variable, like  $U$  with locally reacting linings, can be defined drawing Morse charts is no way to solutions for the solutions for characteristic equation.

*Continued fraction expansion, symmetrical mode* (flat duct,  $\epsilon_z = 0$ ; applicable for the least attenuated mode only):

Transform the characteristic equation into:

$$\epsilon_y h \cdot \tan(\epsilon_y h) = j\epsilon_{ay} d \cdot \tan(\epsilon_{ay} d) / \left( \frac{Z_s}{k_0 h \cdot Z_0} \cdot \epsilon_{ay} d \cdot \tan(\epsilon_{ay} d) - \frac{d}{h} \frac{\Gamma_a}{k_0} \frac{Z_a}{Z_0} \right) \quad (1)$$

$$\text{with: } \epsilon_{ay} d = \sqrt{(d/h)^2 ((\epsilon_y h)^2 - (k_0 h)^2) - (\Gamma_a d)^2}, \quad (2)$$

and apply the continued fraction expansion to  $z \cdot \tan z$  (with  $z = \epsilon_y h$  and  $a = (1 + \Gamma_{an}^2)(k_0 h)^2$ ;  $Z_{sn} = Z_s/Z_0$ ).

Even with the rather low precision of expansion up to the second fraction and the special case  $Z_s = 0$  (i. e. no cover foil on the porous layer), the polynomial equation becomes somewhat lengthy:

$$\begin{aligned} & -(z^2)^6 (d/h)^4 (k_0 h)^2 + (z^2)^5 (d/h)^4 (k_0 h)^2 (6 + 4a - \Gamma_{an}^2 Z_{an}^2) \\ & - (z^2)^4 (d/h)^2 (k_0 h)^2 \left( -6\Gamma_{an}^2 Z_{an}^2 + (d/h)^2 (9 + 6a^2 - 2a(-12 + \Gamma_{an}^2 Z_{an}^2)) \right) \\ & + (z^2)^3 (k_0 h)^2 \left( -9\Gamma_{an}^2 Z_{an}^2 - 6(d/h)^2 a \cdot \Gamma_{an}^2 Z_{an}^2 + (d/h)^4 a \cdot (36 + 4a^2 \right. \\ & \left. - a \cdot (-36 + \Gamma_{an}^2 Z_{an}^2)) \right) - (z^2)^2 (d/h)^4 a \cdot (k_0 h)^2 (54 + 24a + a^2) \\ & + (z^2) \cdot 6(d/h)^4 a^3 (k_0 h)^2 (6 + a) - 9(d/h)^4 a^4 (k_0 h)^2 = 0. \end{aligned} \quad (3)$$

With a cover foil (i. e.  $Z_s \neq 0$ ) having the same depth of expansion, the equation becomes, for  $z = \epsilon h$ ,

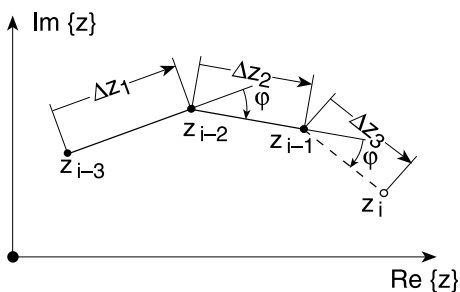
$$\begin{aligned} & z^{14} \cdot 9(d/h)^4 Z_{sn}^2 + z^{13} \cdot 6j(d/h)^4 k_0 h Z_{sn} \\ & - z^{12} \cdot (d/h)^4 ((k_0 h)^2 + 36a Z_{sn}^2) - z^{11} \cdot 6j(d/h)^4 k_0 h (3 + 4a) Z_{sn} \\ & + z^{10} \cdot (d/h)^4 (k_0 h)^2 \left( 6 - \Gamma_{an}^2 Z_{an}^2 + 2a(2 + 27a Z_{sn}^2 / (k_0 h)^2) \right) \\ & + z^9 \cdot 36j(d/h)^4 a k_0 h Z_{sn} (2 + a) \\ & - z^8 \cdot (d/h)^2 (k_0 h)^2 (-6\Gamma_{an}^2 Z_{an}^2 + (d/h)^2 (9 - 2a(-12 + \Gamma_{an}^2 Z_{an}^2))) \\ & + 6a^2 (1 + 6a Z_{sn}^2 / (k_0 h)^2) - z^7 \cdot 12j(d/h)^4 a^2 k_0 h Z_{sn} (9 + 2a) \\ & + z^6 \cdot (k_0 h)^2 \left( -9\Gamma_{an}^2 Z_{an}^2 - 6(d/h)^2 a \Gamma_{an}^2 Z_{an}^2 + (d/h)^4 a (36 - a(-36 + \Gamma_{an}^2 Z_{an}^2)) \right. \\ & \left. + a^2 (4 + 9a Z_{sn}^2 / (k_0 h)^2) \right) \\ & + z^5 \cdot 6j(d/h)^4 a^3 k_0 h Z_{sn} (12 + a) - z^4 \cdot (d/h)^4 a^2 (k_0 h)^2 (54 + 24a + a^2) \\ & - z^3 \cdot 18j(d/h)^4 a^4 k_0 h Z_{sn} + z^2 \cdot 6(d/h)^4 a^3 (k_0 h)^2 (6 + a) - 9(d/h)^4 a^4 (k_0 h)^2 = 0. \end{aligned} \quad (4)$$

The problem is finding the right solution among the roots. Root  $z$  in the first quadrant and with the smallest magnitude is often the right choice.

*Iteration through a list of  $\{k_0 h\}$ :*

At very low  $k_0 h$  the admittance of all linings becomes small. Then the mode solution with the corresponding absorber, in which all layers are assumed to be locally reacting, are suitable starters for Muller's procedure. For later entries of the  $k_0 h$  list, take previous solutions as starters. It may be necessary to make the steps  $\Delta k_0 h$  very small.

It is helpful (and permits larger  $\Delta k_0 h$  values) to use as the third starter for the solution  $z_i$  an extrapolated value. Let  $z_{i-1}$ ,  $z_{i-2}$ ,  $z_{i-3}$  be the previous solutions for the previous  $k_0 h$  values.



The extrapolated  $z_i$  (which is the third start value together with  $z_{i-1}$  and  $z_{i-2}$ ) is evaluated from (with  $\angle z$  the argument of the complex  $z$ ):

$$\begin{aligned} z_i &= |\Delta z_3| \cdot e^{j\angle \Delta z_3}; \quad |\Delta z_3| = c \cdot |\Delta z_2| = c \cdot |z_{i-2} - z_{i-1}|; \\ \angle \Delta z_3 &= \angle \Delta z_2 + \varphi = 2 \cdot \angle \Delta z_2 - \angle \Delta z_1; \\ -\varphi &= \angle \Delta z_1 - \angle \Delta z_2; \\ \Delta z_2 &= z_{i-1} - z_{i-2}; \quad \Delta z_1 = z_{i-2} - z_{i-3}. \end{aligned} \tag{5}$$

*Start the numerical solution with mode values for the locally reacting absorber:*

Sometimes it is proposed to take the mode solution for the absorber, with all layers made locally reacting (and some values nearby as the two other starters) as start values for Muller's method, not only for the lowest entries of a  $k_0 h$  list, as above, but for all  $k_0 h$  values. This method fails, except in very harmless cases (because the numerical procedure may pass on its way from the starters to the true value through apparent resonances of the lining, which do not exist).

*Iteration through the modal angle:*

Define modal angles from the secular equation (below for three dimensions) in the following form:

$$\begin{aligned} 1 &= (\epsilon_y/k_0)^2 + ((\epsilon_z/k_0)^2 - (\Gamma/k_0)^2) \\ &= \cos^2 \varphi + \sin^2 \varphi \cdot (\sin^2 \psi + \cos^2 \psi). \end{aligned} \tag{6}$$

If one associates the terms as  $\cos \varphi = \varepsilon_y/k_0$ ;  $\sin \varphi = \sqrt{1 - (\varepsilon_y/k_0)^2}$ , (7)

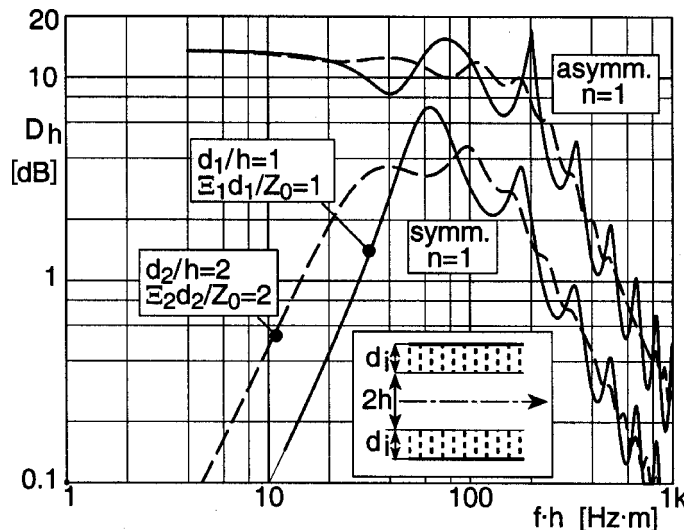
then  $\varphi$  is the angle of incidence on the absorber. The surface admittance of a bulk reacting lining can be written as a function of  $\cos \varphi, \sin \varphi$  (which may be complex). The admittance of the locally reacting absorber is obtained for normal incidence. Start the evaluation by finding the mode solution for the locally reacting absorber with the method described in Sect. J.7. Evaluate with it the mode angle  $\varphi$  as above. Insert this into the admittance formula of  $Z_0 G_{ay}$  of the lining, and solve for the next approximation with the method for locally reacting absorbers (i. e.  $\varphi$  is kept constant during the performance of Muller's procedure). Repeat until the solution becomes stationary.

The advantage of this *method of  $\varphi$ -iteration* is its robustness against mode jumping. It can also be applied for multilayer absorbers, where other methods mostly run into problems. After about eight iterations the result is mostly stationary in its first four to five decimals.

## J.11 Flat Duct with Unsymmetrical, Locally Reacting Lining

► See also: Mechel, Vol. III, Ch. 28 (1998)

The idea behind silencers with unsymmetrical lining is explained with the diagram below. It combines modal attenuations  $D_h$  for the first symmetrical and anti-symmetrical modes in two ducts with symmetrical linings; both ducts are  $2h$  wide, and the lining is a simple, locally reacting layer of glass fibres.



The parameters in the ducts shown,  $i = 1, 2$ , are:

$$d_1/h = 1; \quad \Xi_1 d_1/Z_0 = 1; \quad d_2/h = 2; \quad \Xi_2 d_2/Z_0 = 2,$$

where  $d_i$  = layer thickness and  $\Xi_i$  = flow resistivity.

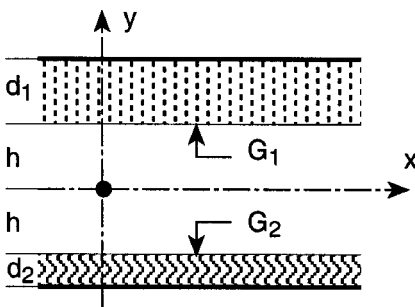
The “idea” expects that in a duct with an unsymmetrical lining the anti-symmetrical mode is used, together with the symmetrical mode, to make up the sound field, and due to its higher attenuation it will increase the attenuation of the least attenuated mode in such ducts.

The field formulation in a flat duct with an unsymmetrical lining is:

$$p(x, y) = (A \cdot \cos(\varepsilon y) + B \cdot \sin(\varepsilon y)) \cdot e^{-\Gamma x}$$

$$Z_0 v_y(x, y) = \frac{j\varepsilon}{k_0} (-A \cdot \sin(\varepsilon y) + B \cdot \cos(\varepsilon y)) \quad (1)$$

$$\Gamma^2 = \varepsilon^2 - k_0^2.$$



The boundary conditions are

$$\left. \frac{Z_0 v_y}{p} \right|_{y=+h} = \frac{j\varepsilon}{k_0} \frac{-A \cdot \sin(\varepsilon h) + B \cdot \cos(\varepsilon h)}{A \cdot \cos(\varepsilon y) + B \cdot \sin(\varepsilon y)} \stackrel{!}{=} Z_0 G_1, \quad (2)$$

$$\left. \frac{Z_0 v_y}{p} \right|_{y=-h} = \frac{j\varepsilon}{k_0} \frac{A \cdot \sin(\varepsilon h) + B \cdot \cos(\varepsilon h)}{A \cdot \cos(\varepsilon h) - B \cdot \sin(\varepsilon h)} \stackrel{!}{=} -Z_0 G_2. \quad (3)$$

First, they give the amplitude ratio:

$$\frac{B}{A} = -\cot(\varepsilon h) \frac{\varepsilon h \cdot \tan(\varepsilon h) - jk_0 h \cdot Z_0 G_2}{\varepsilon h \cdot \cot(\varepsilon h) + jk_0 h \cdot Z_0 G_1}. *) \quad (4)$$

Second, they lead to a characteristic equation for  $\varepsilon h$ , with  $U_i = k_0 h \cdot Z_0 G_i$ :

$$(\varepsilon h \cdot \cot(\varepsilon h) + jU_2)(\varepsilon h \cdot \tan(\varepsilon h) - jU_1) + (\varepsilon h \cdot \cot(\varepsilon h) + jU_1)(\varepsilon h \cdot \tan(\varepsilon h) - jU_2) = 0. \quad (5)$$

$$\text{Setting: } U_s = \frac{1}{2}(U_1 + U_2); \quad U_a = \frac{1}{2}(U_1 - U_2) \quad (6)$$

(where the sides  $i = 1, 2$  are selected so that  $\operatorname{Re}\{U_a\} \geq 0$ ) the equation transforms into:

$$[\varepsilon h \cdot \tan(\varepsilon h) - jU_s] \cdot [\varepsilon h \cdot \cot(\varepsilon h) + jU_s] = U_a^2. \quad (7)$$

\*) See Preface to the 2<sup>nd</sup> edition.

If  $U_a = 0$ , it represents the product of the characteristic equations for symmetrical and anti-symmetrical modes in a symmetrically lined duct. By continued fraction expansions with increasing depth one gets the polynomial equations for  $z^2 = (\epsilon h)^2$ :

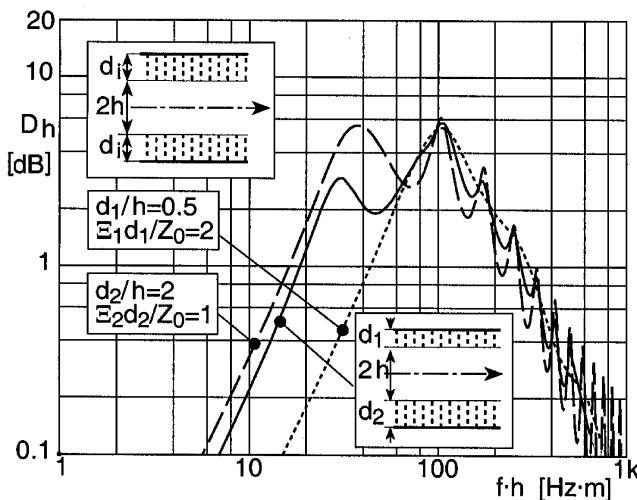
$$5jU_s - 3(U_s^2 - U_a^2) - [-3 - 4jU_s + (U_s^2 - U_a^2)] \cdot z^2 = 0, \quad (8)$$

$$\begin{aligned} & -45jU_s + 45(U_s^2 - U_a^2) + [45 + 78jU_s - 18(U_s^2 - U_a^2)] \cdot z^2 \\ & + [-18 - 9jU_s + (U_s^2 - U_a^2)] \cdot z^4 = 0, \end{aligned} \quad (9)$$

$$\begin{aligned} & -99225jU_s + 99225(U_s^2 - U_a^2) + [99225 + 185850jU_s - 53550(U_s^2 - U_a^2)] \cdot z^2 \\ & + [-53550 - 41895jU_s + 5775(U_s^2 - U_a^2)] \cdot z^4 \\ & + [5775 + 2250jU_s - 150(U_s^2 - U_a^2)] \cdot z^6 \\ & + [-150 - 25jU_s + (U_s^2 - U_a^2)] \cdot z^8 = 0. \end{aligned} \quad (10)$$

The modes in the unsymmetrical duct with solutions of the above characteristic equation are orthogonal to each other over the duct height.

The numerical example compares the attenuation  $D_h = 8.6858 \cdot \text{Re}\{\Gamma_h\}$  [dB] of the least attenuated modes in an unsymmetrically lined duct (full line) with those in the two ducts having each of the linings as a symmetrical lining (dashed lines). The attenuation in the unsymmetrical duct generally lies between the attenuations in the symmetrical ducts, but nearer to the higher attenuation.



Attenuation  $D_h$  of the least attenuated mode in duct with unsymmetrical, locally reacting lining (full line), compared with  $D_h$  in ducts with symmetrical linings (dashed lines)

## J.12 Flat Duct with an Unsymmetrical, Bulk Reacting Lining

► See also: Mechel, Vol. III, Ch. 28 (1998)

The object is as in the previous [Sect. J.11](#), but the lining consists of bulk reacting layers of a porous material (mineral fibre in the numerical examples) having the normalised characteristic values  $\Gamma_{an,i}$ ,  $Z_{an,i}$  on the duct sides  $i = 1, 2$ , possibly covered with a foil having the partition impedance  $Z_{si}$ .

The secular and characteristic equations for the lateral wave number  $z = \epsilon h$  are:

$$\Gamma h = \sqrt{z^2 - (k_0 h)^2};$$

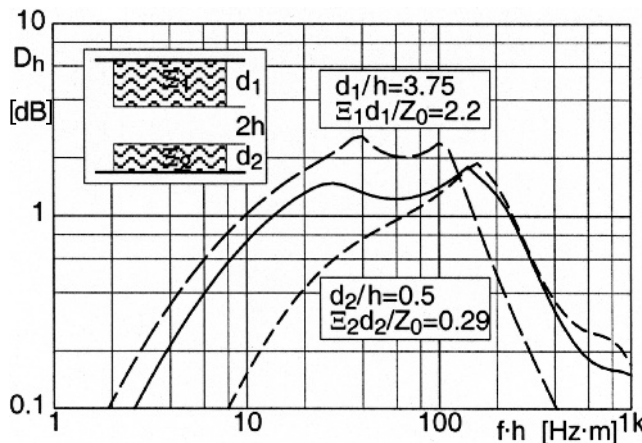
$$[z \cdot \tan z - jU_s] \cdot [z \cdot \cot z + jU_s] = U_a^2; \quad (1)$$

$$U_s = \frac{1}{2} (U_1 + U_2); \quad U_a = \frac{1}{2} (U_1 - U_2)$$

with:

$$U_i = k_0 h \frac{y_i \cdot \tan y_i}{Z_{si}/Z_0 \cdot y_i \cdot \tan y_i - \frac{d_i}{h} k_0 h \cdot \Gamma_{an,i} Z_{an,i}} \xrightarrow{Z_{si} \rightarrow 0} \frac{-y_i \cdot \tan y_i}{\frac{d_i}{h} \cdot \Gamma_{an,i} Z_{an,i}}; \quad (2)$$

$$y_i^2 = (d_i/h)^2 \left( z^2 - (k_0 h)^2 (1 + \Gamma_{an,i}^2) \right); \quad i = 1, 2.$$



Attenuation  $D_h$  of the least attenuated mode in a flat duct with unsymmetrical, bulk reacting lining (*full line*), and in ducts with symmetrical lining (*dashed lines*)

### J.13 Round Duct with a Locally Reacting Lining

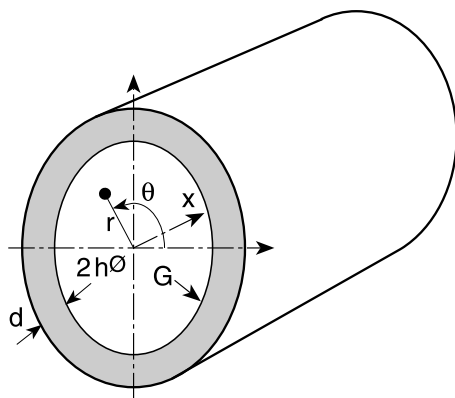
► See also: Mechel, Vol. III, Ch. 29 (1998)

The lining is defined by a surface admittance  $G$ . The form of a mode is:

$$p(r, \theta, x) = P \cdot q(r, \theta) \cdot e^{-\Gamma x}. \quad (1)$$

The lateral profile  $q(r, \theta)$  must satisfy the Bessel differential equation:

$$\left[ \frac{\partial^2}{\partial r^2} + \frac{1}{r} \frac{\partial}{\partial r} + \frac{1}{r^2} \frac{\partial^2}{\partial \theta^2} + \Gamma^2 + k_0^2 \right] q(r, \theta) = 0. \quad (2)$$



Solutions have the general form:

$$q(r, \theta) = \cos(m\theta) [J_m(\varepsilon_m r) + b \cdot Y_m(\varepsilon_m r)] ; \quad m = 0, 1, 2, \dots \quad (3)$$

with Bessel functions  $J_m(z)$  and Neumann functions  $Y_m(z)$ . If the origin  $r = 0$  belongs to the field area, the Neumann function must be excluded because it is singular there. Thus the mode profiles in round ducts are:

$$q(r, \theta) = \cos(m\theta) \cdot J_m(\varepsilon_m r) ; \quad m = 0, 1, 2, \dots . \quad (4)$$

The Bessel differential equation requires (secular equation):  $\varepsilon_m^2 = \Gamma^2 + k_0^2$  (5)

with  $\Gamma \rightarrow \Gamma_m$ .

The radial particle velocity is:

$$v_r = \frac{j}{k_0 Z_0} \frac{\partial p}{\partial r} = \frac{j \varepsilon_m}{k_0 Z_0} P \cos(m\theta) \cdot J'_m(\varepsilon_m r) \cdot e^{-\Gamma x} . \quad (6)$$

With it the boundary condition gives the characteristic equation for  $\varepsilon_m h$ :

$$\left( \varepsilon_m h \right) \frac{J'_m(\varepsilon_m h)}{J_m(\varepsilon_m h)} = -j k_0 h \cdot Z_0 G =: -j \cdot U \quad (7)$$

or, with  $J'_m(z) = J_{m-1}(z) - \frac{m}{z}J_m(z)$ : (8)

$$(\epsilon_m h) \frac{J_{m-1}(\epsilon_m h)}{J_m(\epsilon_m h)} = m - jU . \quad (9)$$

The function  $F_m(z) := z \frac{J_{m-1}(z)}{J_m(z)}$  can be expanded into a continued fraction: (10)

$$F_m(z) = 2m - \frac{z^2}{2(m+1)-} \frac{z^2}{2(m+2)-} \frac{z^2}{2(m+3)-} \dots . \quad (11)$$

Therewith the characteristic equation can be written as (with the abbreviations  $z = \epsilon_m h$ )

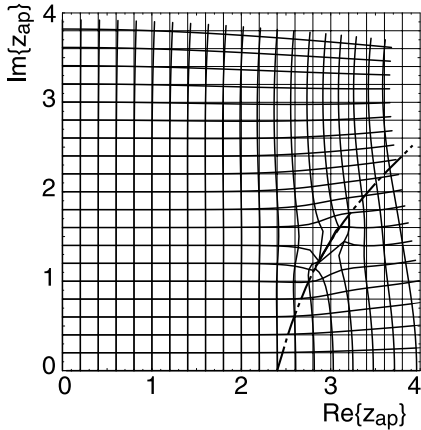
$$\frac{z^2}{2(m+1)-} \frac{z^2}{2(m+2)-} \frac{z^2}{2(m+3)-} \dots = jU + m . \quad (12)$$

It becomes for the fundamental azimuthal mode  $m = 0$ :

$$\frac{z^2}{2-} \frac{z^2}{4-} \frac{z^2}{6-} \frac{z^2}{8-} \dots = jU . \quad (13)$$

The solution with the indicated length of the fraction is:

$$(\epsilon_0 h)^2 \approx \frac{96 + 36jU \pm \sqrt{9216 + 2304jU - 912U^2}}{12 + jU} . \quad (14)$$



Its precision test is contained in the diagram. The root is evaluated with a negative real part in the range above the dash-dotted limit curve and with a positive real part below that curve.

The coefficients  $a_i$  for polynomial approximations

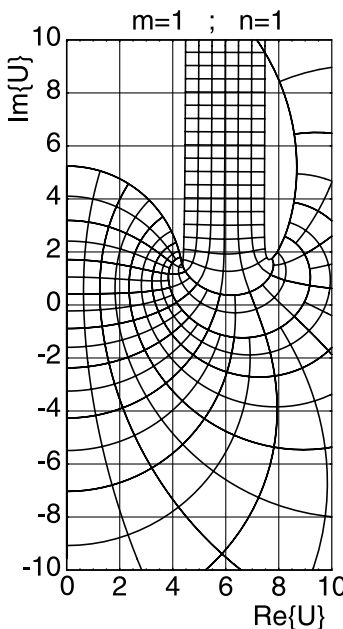
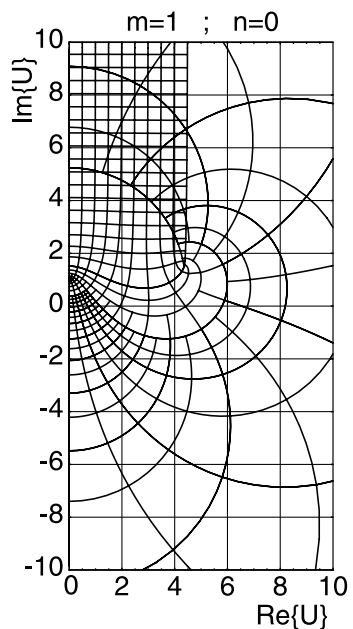
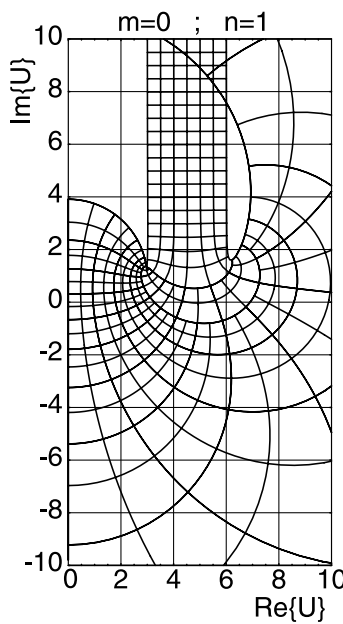
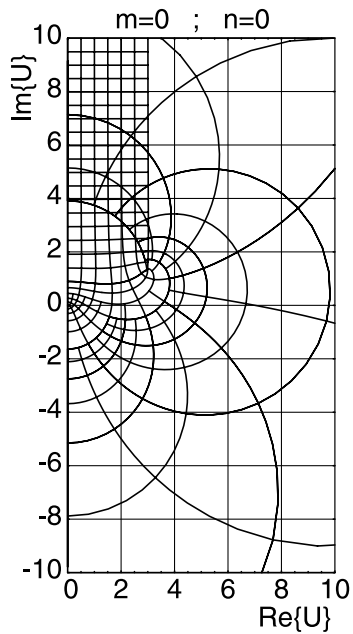
$$a_0 + a_1 \cdot z^2 + a_2 \cdot z^4 + \dots + a_i \cdot z^{2i} = 0 \quad (15)$$

of the characteristic equation with increasing depth of the expansion are given in Table 1.

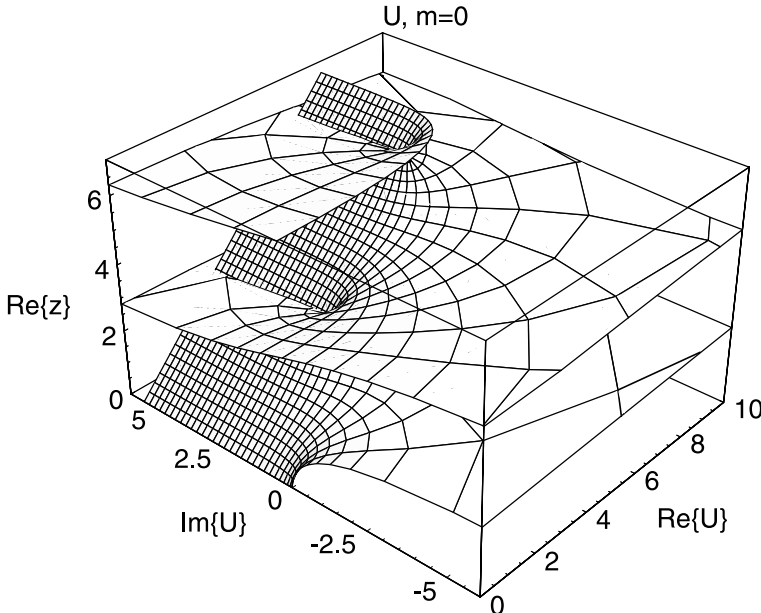
Mode charts can be plotted as lines of  $\text{Re}\{z\} = \text{const}$  and  $\text{Im}\{z\} = \text{const}$  in the complex  $U$  plane for azimuthal mode orders  $m = 0, 1, 2, \dots$  and radial mode orders  $n = 0, 1, 2, \dots$

**Table 1** Coefficients of the polynomial approximations to the characteristic equation for azimuthal modes of orders  $m = 0, 1, 2, 3, 4$

<b>m</b>	<b>a<sub>0</sub></b>	<b>a<sub>1</sub></b>	<b>a<sub>2</sub></b>	<b>a<sub>3</sub></b>	<b>a<sub>4</sub></b>	<b>a<sub>5</sub></b>
<b>0</b>	$8jU$	$-(4 + jU)$	—	—	—	—
	$-384jU$	$24(8 + 3jU)$	$-(12 + jU)$	—	—	—
	$46080jU$	$1920j(12j - 5U)$	$96(20 + 3jU)$	$-(24 + jU)$	—	—
	$-10321920jU$	$322560(16 + 7jU)$	$17280j(28j - 5U)$	$800(12 + jU)$	$-(40 + jU)$	—
<b>1</b>	$24(1 + jU)$	$-7 + jU$	$-$	$-$	$600(56 + 3jU)$	$-(60 + jU)$
	$1920j(j - U)$	$48(13 + 3jU)$	$-(17 + jU)$	—	—	—
	$322560(1 + jU)$	$5760j(19j - 5U)$	$480(9 + jU)$	$-(31 + jU)$	—	—
	$92897280j(j - U)$	$1290240(25 + 7jU)$	$40320j(37j - 5U)$	$1200(15 + jU)$	$-(49 + jU)$	—
	$40874803200(1 + jU)$	$464486400j(3j - 9U)$	$15482880(47 + 7jU)$	$188160j(59 - 5U)4$	$840(67 + 3jU)$	$-(71 + jU)$
<b>2</b>	$48(2 + jU)$	$-(10 + jU)$	—	—	—	—
	$5760j(2j - U)$	$240(6 + jU)$	$-(22 + jU)$	—	—	—
	$1290240(2 + jU)$	$13440j(26j - 5U)$	$240(34 + 3jU)$	$-(38 + jU)$	—	—
	$464486400j(2j - U)$	$3870720(34 + 7jU)$	$80640j(46j - 5U)$	$1680(18 + jU)$	$-(58 + jU)$	—
	$245248819200(2 + jU)$	$5109350400j(14j - 3U)$	$38707200(58 + 7jU)$	$1693440j(14j - U)$	$3360(26 + jU)$	$-(82 + jU)$
<b>3</b>	$80(3 + jU)$	$-(13 + jU)$	—	—	—	—
	$13440j(3j - U)$	$120(23 + 3jU)$	$-(27 + jU)$	—	—	—
	$3870720(3 + jU)$	$26880j(33j - 5U)$	$336(41 + 3jU)$	$-(45 + jU)$	—	—
	$1703116800j(3j - U)$	$9676800(43 + 7jU)$	$725760j(11j - U)$	$2240(21 + jU)$	$-(67 + jU)$	—
	$1062744883200(3 + jU)$	$5109350400j(53j - 9U)$	$85155840(69 + 7jU)$	$564480j(8j - 5U)$	$1440(89 + 3jU)$	$-(93 + jU)$
<b>4</b>	$120(4 + jU)$	$-(16 + jU)$	—	—	—	—
	$26880j(4j - U)$	$168(28 + 3jU)$	$-(32 + jU)$	—	—	—
	$9676800(4 + jU)$	$241920j(8j - U)$	$1344(16 + jU)$	$-(52 + jU)$	—	—
	$5109350400j(4j - U)$	$21288960(52 + 7jU)$	$241920j(64j - 5U)$	$2880(24 + jU)$	$-(76 + jU)$	—
	$3719607091200(4 + jU)$	$13284311040j(64j - 9U)$	$170311680(80 + 7jU)$	$887040j(92j - 5U)$	$1800(100 + 3jU)$	$-(104 + jU)$



Three-dimensional mode charts are created if one plots the mesh points at a height  $\text{Re}\{z\}$  above the U plane for any azimuthal order m.



3D mode chart for the azimuthal mode  $m = 0$  and some radial modes

The evaluation of sets of mode solutions  $z = \epsilon h$  is similar to the task in [Sect. J.7](#). It needs the branch points  $z_b$  and their transforms  $U_b$ . The  $z_b$  are solutions of the equation

$$\frac{J_{m-1}(z)}{J_m(z)} \left( 2m - z \frac{J_{m-1}(z)}{J_m(z)} \right) - z = 0 ; \quad z \neq 0 . \quad (16)$$

The following tables contain branch points  $z_b(m, n)$  and associated  $U_b(m, n)$  for azimuthal orders  $m = 0, 1, \dots, 10$  and radial orders  $n = 0, 1, \dots, 20$ . The entries of the tables are the real and imaginary parts.

Further, the coefficients are given (again with their real and imaginary parts) in tables for the representation of  $z_b(m, n), U_b(m, n)$  as functions of n for given m:

$$\begin{aligned} z_b(m, n) &= a_m + b_m \cdot n^{1/2} + c_m \cdot n + d_m \cdot n^2 + e_m \cdot n^3 , \\ U_b(m, n) &= A_m + B_m \cdot n^{1/2} + C_m \cdot n + D_m \cdot n^2 + E_m \cdot n^3 , \end{aligned} \quad (17)$$

and coefficients for the functions  $z''_b(m, n) = f(z'_b(m, n))$ ;  $U''_b(m, n) = f(U'_b(m, n))$  as:

$$\begin{aligned} z''_b &= \bar{a}_m + \bar{b}_m \cdot z'^{1/2}_b + \bar{c}_m \cdot z'_b + \bar{d}_m \cdot z'^{3/2}_b + \bar{e}_m \cdot z'^2_b + \bar{f}_m \cdot z'^3_b , \\ U''_b &= \bar{A}_m + \bar{B}_m \cdot U'^{1/2}_b + \bar{C}_m \cdot U'_b + \bar{D}_m \cdot U'^{3/2}_b + \bar{E}_m \cdot U'^2_b + \bar{F}_m \cdot U'^3_b . \end{aligned} \quad (18)$$

**Table 2a** Branch points  $z_b(m, n)$  for azimuthal orders  $m$  and radial orders  $n$  in round ducts with a locally reacting lining

$m$	$z_b(m, 0)$	$z_b(m, 1)$	$z_b(m, 2)$	$z_b(m, 3)$	$z_b(m, 4)$	$z_b(m, 5)$	$z_b(m, 6)$	$z_b(m, 7)$	$z_b(m, 8)$	$z_b(m, 9)$	$z_b(m, 10)$
0	0.	2.9803824	6.17515307	9.3419610	12.4985071	15.650104	18.7589117	21.945980	25.0918858	28.2369731	31.381461
	0.	1.2796025	1.61871738	1.8188728	1.96145954	2.0723098	2.16301098	2.2397725	2.30631281	2.36503612	2.4175870
1	0.	4.4662985	7.69410395	10.874574	14.0388913	17.195565	20.3479682	23.497724	26.6457175	29.7924754	32.938331
	0.	1.4674704	1.72697154	1.8949433	2.02006280	2.1199462	2.20312418	2.2744062	2.33677883	2.39222622	2.4421349
2	0.	5.81168507	9.11848718	12.334640	15.5203741	18.691419	21.8541613	25.011725	28.1658298	31.3175030	34.467400
	0.	1.6000118	1.81551915	1.9613351	2.07308877	2.1640392	2.24083200	2.3073267	2.36597916	2.41845412	2.4659342
3	0.	7.1009646	10.4837004	13.743724	16.9575046	20.148156	23.3224221	26.494193	29.6572168	32.8161611	35.972101
	0.	1.7069432	1.89206035	2.0209608	2.12187295	2.2052780	2.27651937	2.3387612	2.39405346	2.44380805	2.4890417
4	0.	8.3439388	11.8075223	15.114516	18.3597199	21.573052	24.7675211	27.949815	31.1237603	34.2917166	37.455223
	0.	1.7983610	1.96027390	2.0754868	2.16727350	2.2441437	2.31047269	2.3688878	2.42111618	2.46836325	2.5115077
5	0.	9.5583600	13.1003688	16.455227	19.7335515	22.971391	26.1848108	29.382231	32.5685480	35.7468196	38.919064
	0.	1.8791146	2.02226408	2.1259798	2.20988517	2.2809907	2.34291347	2.3978501	2.44726287	2.49218466	2.53333769
6	0.	10.751546	14.3689547	17.771528	21.0837394	24.347158	27.5806698	30.794337	33.9940832	37.1836547	40.365546
	0.	1.9519719	2.0937182	2.1731742	2.25014251	2.3160901	2.37401800	2.4257663	2.47257456	2.51532886	2.5546694
7	0.	11.928184	15.6179031	19.067527	22.4138509	25.703439	28.9577821	32.188476	35.4024288	38.6040478	41.796294
	0.	2.0186875	2.13251552	2.2176033	2.28837560	2.3496560	2.40592982	2.4527351	2.49712076	2.53784550	2.5754810
8	0.	13.091486	16.8505539	20.246310	23.7266496	27.042689	30.3183214	33.566582	36.7933083	40.0095430	43.212698
	0.	2.0804554	2.18235758	2.2296692	2.32484276	2.3818611	2.43226785	2.4788405	2.52096170	2.55977848	2.5957841
9	0.	14.243760	18.0694113	21.610265	25.0243271	28.366891	31.6640769	34.930267	38.1741788	41.4014603	44.615958
	0.	2.1381313	2.2939479	2.2996848	2.35975104	2.4128473	2.46063214	2.5041544	2.54415004	2.58116683	2.6156280
10	0.	15.386730	19.2764083	22.861283	26.308655	29.677677	32.9965422	36.280895	39.5402853	42.7809382	46.007117
	0.	2.1923528	2.27401119	2.3378991	2.39326958	2.4427332	2.48760786	2.5287392	2.56673216	2.60204547	2.6350391

**Table 2b** Branch points  $z_b(m, n)$  for azimuthal orders  $m$  and radial orders  $n$  in round ducts with a locally reacting lining (continued)

$m$	$z_b(m, 11)$	$z_b(m, 12)$	$z_b(m, 13)$	$z_b(m, 14)$	$z_b(m, 15)$	$z_b(m, 16)$	$z_b(m, 17)$	$z_b(m, 18)$	$z_b(m, 19)$	$z_b(m, 20)$
0	34.525496 2.4651401	37.6691784 2.50856370	40.8125833 2.5485179	43.9557618 2.58551614	47.098757 2.619657	50.2415986 2.65219513	53.384312 2.6824733	56.5269161 2.71102288	59.6694268 2.73803069	62.811857 2.7636547
1	36.083507 2.4875121	39.2281563 2.52911295	42.372390 2.5675181	45.5162895 2.60318383	48.659915 2.6364750	51.8033147 2.66768817	54.946524 2.6970676	58.0895726 2.72481678	61.2324837 2.75110719	64.375226 2.7760845
2	37.615957 2.5092906	40.7634791 2.5491844	43.910183 2.5861281	47.0562300 2.62052925	50.201740 2.6527155	53.3468057 2.68295513	56.491500 2.7114703	59.6358794 2.73844721	62.7799907 2.76404342	65.923871 2.7883934
3	39.125763 2.5505124	42.2776539 2.56880112	45.428140 2.6043630	48.5774940 2.63756183	51.725920 2.66836927	54.8735766 2.69799875	58.020588 2.7256823	61.1670524 2.75191372	64.3130496 2.77683800	67.458644 2.8005793
4	40.615330 2.5512115	43.7727783 2.58796682	46.928107 2.6222383	50.0817171 2.65429176	53.233915 2.6844132	56.3849379 2.71282291	59.534972 2.7397055	62.6841652 2.76521697	65.8326389 2.78949068	68.980491 2.8126413
5	42.086671 2.5714189	45.2506280 2.60676298	48.411660 2.6397692	51.5703113 2.67072952	54.726996 2.6998839	57.8820393 2.72743228	61.035696 2.7535428	64.1881718 2.7783554	67.339329 2.80200202	70.490216 2.8245792
6	43.541487 2.5911633	46.7127217 2.62515010	49.880164 2.6569703	53.0445061 2.68688559	56.206278 2.7151124	59.3658956 2.74183199	62.523689 2.7671977	65.6799238 2.79134056	68.8348159 2.81437322	71.988543 2.8363935
7	44.981236 2.6104708	48.1603706 2.6431637	51.334805 2.6738558	54.5053795 2.70277034	57.672744 2.7301061	60.8374082 2.75602147	63.999779 2.7806740	67.1601857 2.80416564	70.3188954 2.82660595	73.476130 2.8480852
8	46.407174 2.6593655	49.5947157 2.66083276	52.776622 2.6904391	55.9538830 2.71839384	59.127268 2.7448727	62.2973818 2.77002428	65.464711 2.7939758	68.6296464 2.81683668	71.7925113 2.83870220	74.953571 2.8596555
9	47.80395 2.6478694	51.0167569 2.67816304	54.206533 2.7067329	57.3908614 2.73376582	60.570629 2.7594194	63.7465385 2.78382802	66.919153 2.8071071	70.088997 2.82935880	73.252454 2.85066423	76.421412 2.8711060
10	49.221856 2.6660028	52.4273767 2.69517382	55.6253533 2.7227494	58.8170688 2.74889562	62.003528 2.7737536	65.1855288 2.79744428	68.363712 2.8200725	71.5386020 2.84172925	74.7106281 2.86249447	77.880149 2.8824385

**Table 3a** Branch points  $U_b(m, n)$  for modes with azimuthal order  $m$  and radial order  $n$  in a round duct with a locally reacting lining

$m$	$U_b(m, 0)$	$U_b(m, 1)$	$U_b(m, 2)$	$U_b(m, 3)$	$U_b(m, 4)$	$U_b(m, 5)$	$U_b(m, 6)$	$U_b(m, 7)$	$U_b(m, 8)$	$U_b(m, 9)$	$U_b(m, 10)$
0	0.	2.9803824	6.17515307	9.3419610	12.4985071	15.650104	18.7589117	21.945980	25.0918858	28.2369731	31.381461
	0.	1.2796025	1.61871738	1.8188728	1.96145954	2.0723098	2.16301098	2.2397725	2.30631281	2.36503612	2.4175870
1	0.	4.3645604	7.63203406	10.829870	14.0039585	17.166901	20.3236666	23.476634	26.6270897	29.7757956	32.923331
	1.	1.5016772	1.74101667	1.9027655	2.02510184	2.1234860	2.20575852	2.2764495	2.33841359	2.39356630	2.4432550
2	0.	5.4907943	8.90541529	12.175571	15.3932865	18.585549	21.7634172	24.932316	28.0952333	31.2539566	34.409622
	2.	1.6950243	1.85895745	1.9869593	2.09020428	2.1763663	2.25017531	2.3146755	2.37192429	2.42337139	2.4700748
3	0.	6.4813156	10.0605876	13.419744	16.6943117	19.926292	23.1335608	26.325136	29.5060904	32.6795116	35.847388
	3.	1.8701363	1.97163375	2.0697508	2.15532518	2.2298322	2.29539999	2.3537805	2.40631550	2.45402684	2.4977011
4	0.	7.3835846	11.1309878	14.586504	17.9251176	21.203156	24.4452811	27.664212	30.8672365	34.0588524	37.241995
	4.	2.0326668	2.07941812	2.1506167	2.21981999	2.2832936	2.34092956	2.3933440	2.44123699	2.48523973	2.5258873
5	0.	8.2221186	12.1365161	15.691562	19.0982555	22.426342	25.7070081	28.956619	32.1846863	35.3971529	38.597938
	5.	2.1845043	2.18286741	2.2294453	2.28339614	2.3364279	2.38645997	2.4330944	2.47645099	2.51680343	2.55444540
6	0.	9.0116093	13.0901833	16.745849	20.2228660	23.603546	26.9252866	30.207976	33.4633108	36.6986717	39.918969
	6.	2.3288533	2.28250429	2.3062807	2.34592951	2.3890567	2.43180353	2.4728523	2.51179287	2.54856962	2.5832888
7	0.	9.7617169	14.0010662	17.757338	21.3058567	24.740752	28.1053201	31.422838	34.7071219	37.9669654	41.208261
	7.	2.4667050	2.3877745	2.3812247	2.40738075	2.4410835	2.47884338	2.5124977	2.54714695	2.58043032	2.61222525
8	0.	10.479213	14.8758052	18.732066	22.3526020	25.842719	29.2513290	32.604957	35.9194713	39.2050406	42.468223
	8.	2.5990743	2.47206344	2.4543972	2.46775429	2.4924595	2.52150723	2.5519495	2.58243119	2.61230611	2.6412999
9	0.	11.169070	15.7194383	19.674737	23.3673841	26.913312	30.3667933	33.757471	37.1031938	40.4154669	43.702992
	9.	2.7267290	2.56267754	2.5259193	2.52207712	2.5431644	2.56575149	2.5911533	2.61758702	2.64413811	2.670341
10	0.	11.835078	16.5358998	20.589105	24.3536822	27.955719	31.45462389	34.883035	38.2607134	41.6004613	44.911000
	10.	2.8302677	2.65088497	2.5959057	2.58538746	2.5931956	2.6095514	2.6300728	2.65257265	2.6703511	2.6993511

**Table 3b** Branch points  $U_b(m, n)$  for modes with azimuthal order  $m$  and radial order  $n$  in a round duct with a locally reacting lining (continued)

$m$	$U_b(m, 11)$	$U_b(m, 12)$	$U_b(m, 13)$	$U_b(m, 14)$	$U_b(m, 15)$	$U_b(m, 16)$	$U_b(m, 17)$	$U_b(m, 18)$	$U_b(m, 19)$	$U_b(m, 20)$
0	34.525496	37.6691784	40.812583	43.9557618	47.098757	50.2415986	53.384312	56.5269161	59.6694268	62.811857
	2.4651401	2.50856370	2.5485179	2.585551614	2.6195657	2.65219513	2.6824733	2.71102288	2.73803069	2.7636547
1	36.069713	39.2154611	42.360632	45.5053390	48.649669	51.7936874	54.937445	58.0809635	61.2243340	64.367523
	2.4884634	2.52993170	2.5682308	2.60381027	2.63730303	2.66818403	2.6975133	2.72521973	2.75147339	2.7764189
2	37.562987	40.7145778	43.864770	47.0138402	50.161996	53.3093968	56.456167	59.6024038	62.7481871	65.893580
	2.5128291	2.55224590	2.5888055	2.62289203	2.6548173	2.68483785	2.7131673	2.73998826	2.76544436	2.7896752
3	39.011063	42.1714748	45.329301	48.4850439	51.639082	54.7917072	57.943149	61.0935882	64.2431718	67.392019
	2.5379526	2.57526884	2.6100418	2.64259107	2.6731805	2.70203008	2.7293250	2.75522285	2.77985839	2.8033480
4	40.418666	43.5902778	46.75789	49.9221743	53.083807	56.2432072	59.400731	62.5566605	65.7112253	68.864612
	2.5336249	2.59882201	2.6317861	2.66277443	2.6920041	2.71965912	2.7458970	2.77085312	2.79464478	2.8173741
5	41.789737	44.9744709	48.153544	51.3280090	54.498673	57.6661623	60.830973	63.9935030	67.1540736	70.312949
	2.5896899	2.62276930	2.6539191	2.68333713	2.711952	2.73764260	2.7628097	2.78681032	2.80974448	2.8317003
6	43.127608	46.32270288	49.519028	52.7049613	55.885870	59.0625683	62.235703	65.4057936	68.5732632	71.738459
	2.6160297	2.64700563	2.6763473	2.70419550	2.7306788	2.75591320	2.7800025	2.80305968	2.82510783	2.8462813
7	44.435123	47.6505153	50.856634	54.0551440	57.247328	60.4341950	63.616548	66.7950554	69.9701856	73.142435
	2.6425538	2.67144898	2.6989962	2.72528223	2.7503941	2.77441551	2.7974250	2.81949525	2.84069288	2.8610789
8	45.714733	48.9471592	52.168396	55.3804194	58.584759	61.7826203	64.974968	68.1625812	71.3460989	74.526049
	2.6691925	2.69603480	2.7218066	2.74654278	2.7702909	2.79310361	2.8150351	2.83613827	2.85646395	2.8760600
9	46.868572	50.2189128	53.456107	56.6824395	59.899688	63.1092582	66.312276	69.5096543	72.7021446	75.890368
	2.6568912	2.72071188	2.7447305	2.76793265	2.7903279	2.81193925	2.8327973	2.85293593	2.87239063	2.8911966
10	48.198507	51.4674976	54.721357	57.9626776	61.193485	64.4153818	67.629659	70.8373648	74.0393625	77.236369
	2.7226073	2.74543936	2.7677292	2.78941536	2.8104709	2.83089039	2.8506816	2.86986025	2.88844680	2.9064642

**Table 4** Coefficients for  $z_b(m, n) = f(n)$  for  $n \geq 1$ 

<b>m</b>	<b>a<sub>m</sub></b>	<b>b<sub>m</sub></b>	<b>c<sub>m</sub></b>	<b>d<sub>m</sub></b>	<b>e<sub>m</sub></b>
0	-0.368305765 0.146519108	0.27627919216 1.39955627045	3.071531336840 -0.26955854932	0.0019178022618 0.0064183572442	-0.0000317773239 -0.0001024222785
1	0.9879138803 0.6540921622	0.45297970214 0.96167589506	3.024301642897 -0.15014414119	0.0032892893190 0.0028975202864	-0.0000552435395 -0.0000419843633
2	2.0521650936 0.9577515405	0.83345985094 0.73558052419	2.929014637243 -0.09439767730	0.0058440123552 0.0014452291919	-0.0000970698817 -0.0000186834770
3	3.0330022534 1.1785983848	1.22534943787 0.58911235561	2.839114176362 -0.06130501868	0.0080091011338 0.0006764141953	-0.0001305099148 -7.14670392 · 10 <sup>-6</sup>
4	3.9850498138 1.354592956	1.59208568134 0.48335506807	2.762104033654 -0.03920700769	0.0096590276873 0.0002173543069	-0.0001543296062 -7.29673305 · 10 <sup>-7</sup>
5	4.9274383020 1.50057561805	1.92754209316 0.40182259623	2.697648032647 -0.02333700567	0.0108708424789 -0.000077651008	-0.0001704204923 3.0844587418 · 10 <sup>-6</sup>
6	5.8677962944 1.6275460840	2.23322708646 0.33611110602	2.643937503965 -0.01134703166	0.0117393813727 -0.000277093023	-0.0001807192236 5.445314093 · 10 <sup>-6</sup>
7	6.8093247657 1.7391127229	2.51247480112 0.28141377516	2.599110725057 -0.00193820478	0.0123445094137 -0.000417131079	-0.0001867537156 6.942356734 · 10 <sup>-6</sup>
8	7.7533394623 1.84065628730	2.76875711191 0.23475325470	2.561568904705 0.005668071753	0.0127481558357 -0.000518443632	-0.0001896588790 7.90268874 · 10 <sup>-6</sup>
9	8.7003048861 1.9327222066	3.00519948413 0.19417363167	2.530009158087 0.011967067444	0.0129972690267 -0.000593571691	-0.0001902652854 8.518568157 · 10 <sup>-6</sup>
10	9.6502912998 2.0175497001	3.22448082833 0.15833007251	2.503386726405 0.017288702225	0.0131273172995 -0.000650474842	-0.0001891806589 8.90808346238 · 10 <sup>-6</sup>

**Table 5** Coefficients for  $U_b(m, n) = f(n)$  for  $n \geq 1$ 

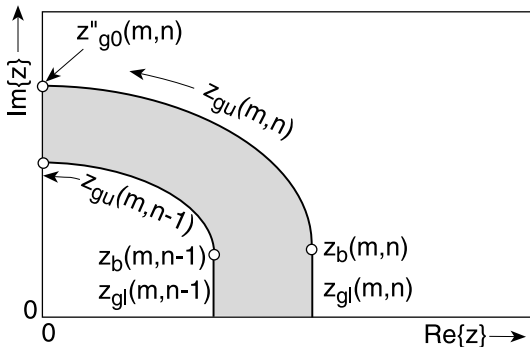
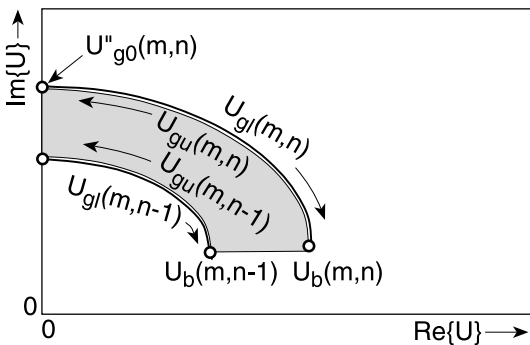
<b>m</b>	<b>A<sub>m</sub></b>	<b>B<sub>m</sub></b>	<b>C<sub>m</sub></b>	<b>D<sub>m</sub></b>	<b>E<sub>m</sub></b>
0	-0.366205759	0.27627918188	3.071531341247	0.0011917802035	-0.00003117773180
	0.1469519014	1.39952628507	-0.26965855525	0.0064183575291	-0.0001024222849
1	0.7282201609	0.66715771889	2.967519068383	0.0049072430267	-0.0000825306369
	0.7715863448	0.84566874624	-0.115294668602	0.00117887755870	-0.0000222567162
2	1.2844860115	1.42244565712	2.779892426397	0.0098790246486	-0.0001633416420
	1.2556576981	0.43704401766	-0.00823731455	-0.001223792151	0.00002813268974
3	1.6588783877	2.21884022363	2.597005607418	0.0142874040691	-0.0002314514703
	1.6855162704	0.11061198552	0.014449811796	-0.0013448411178	0.00006448705901
4	1.9527849797	2.98917578557	2.432549760658	0.0179043227384	-0.0002845999367
	2.0573696067	-0.1665669779	0.142748671627	-0.005231565146	0.00009321965254
5	2.2049928625	3.71899899875	2.28842692153	0.0208394175184	-0.0003256545970
	2.3955102277	-0.4107674316	0.201761528312	-0.006743458033	0.00011740354356
6	2.4339866599	4.40793395345	2.157483380377	0.0232363066293	-0.0003576065424
	2.7085693213	-0.6314780024	0.254380707608	-0.008076867207	0.00013867336588
7	2.6455580966	5.05948744153	2.041808793319	0.0252172122947	-0.0003828178735
	3.0021502783	-0.8346524594	0.302371835308	-0.009286287303	0.00015796641044
8	2.8475035353	5.67793946463	1.937478158243	0.0268771251663	-0.0004030388285
	3.2800950094	-1.0242412011	0.348875537688	-0.010405619456	0.00017585217640
9	3.0416180708	6.26736142134	1.842563478661	0.0282880484561	-0.0004195460889
	3.5451532755	-1.2029842154	0.388662803041	-0.011456954116	0.00019269335736
10	3.2296254730	6.83134055850	1.755509313657	0.0295043406055	-0.0004332708985
	3.7993627839	-1.3728521687	0.428274604376	-0.012455254269	0.00020873028611

**Table 6** Coefficients for  $z_b''(m, n) = f(z'(m, n))$ ;  $U_b''(m, n) = f(U'(m, n))$  of the curve connecting the branch points

$m$	$to$	$\bar{a}_m \& \bar{A}_m$	$\bar{b}_m \& \bar{B}_m$	$\bar{c}_m \& \bar{C}_m$	$\bar{d}_m \& \bar{D}_m$	$\bar{e}_m \& \bar{E}_m$	$\bar{f}_m \& \bar{F}_m$
0	$z''$	0.	1.03255472049	-0.2098911280205	0.02650507820	-0.001547034821	$2.717121859 \cdot 10^{-6}$
	$U''$	0.	1.03255471568	-0.209891125705	0.02650507684	-0.001547034677	$2.717121329 \cdot 10^{-6}$
1	$z''$	0.	1.03768613394	-0.212546972815	0.02699886920	-0.001581192667	$2.7777630939 \cdot 10^{-6}$
	$U''$	1.	0.01695130841	0.1842150467024	-0.0437173781	0.003595268032	$-8.96778277 \cdot 10^{-6}$
2	$z''$	0.	1.04988152225	-0.218290124515	0.02796403550	-0.001641020525	$2.857957129 \cdot 10^{-6}$
	$U''$	2.	-0.7586897835	0.4206222861074	-0.0775339878	0.005545102340	$-0.0000120934311$
3	$z''$	0.	1.07021984409	-0.228003625757	0.02963847580	-0.001749250152	$3.031500895 \cdot 10^{-6}$
	$U''$	3.	-1.4149143941	0.5869873503596	-0.0967221457	0.0064302118295	$-0.0000125320673$
4	$z''$	0.	1.09724052002	-0.240732875512	0.03180605385	-0.001887999641	$3.252218427 \cdot 10^{-6}$
	$U''$	4.	-1.9974527414	0.7142045954165	-0.1084914003	0.0067714996070	$-0.0000119578544$
5	$z''$	0.	1.12979055127	-0.255733684141	0.03430556310	-0.002044526252	$3.490226516 \cdot 10^{-6}$
	$U''$	5.	-2.5297526272	0.8170922590251	-0.1160930652	0.0068500426717	$-0.0000110096253$
6	$z''$	0.	1.16700545337	-0.272501726616	0.03703335580	-0.002211096670	$3.729591742 \cdot 10^{-6}$
	$U''$	6.	-3.02571125991	0.9038948758619	-0.1212266312	0.0067942928935	$-9.96235424 \cdot 10^{-6}$
7	$z''$	0.	1.20830030824	-0.290694642818	0.039992283817	-0.002383059269	$3.962241644 \cdot 10^{-6}$
	$U''$	7.	-3.4943027473	0.9796199915083	-0.1248598502	0.0066724572248	$-8.93938211 \cdot 10^{-6}$
8	$z''$	0.	1.25324561024	-0.310074608988	0.04293030500	-0.002557583186	$4.184329860 \cdot 10^{-6}$
	$U''$	8.	-3.9416611884	1.0474900263916	-0.1275745816	0.006523770294	$-7.99458282 \cdot 10^{-6}$
9	$z''$	0.	1.30152387453	-0.330472119525	0.04602637876	-0.00232925622	$4.394274371 \cdot 10^{-6}$
	$U''$	9.	-4.3721534847	1.1096650362265	-0.1297334263	0.006354705151	$-7.14831915 \cdot 10^{-6}$
10	$z''$	0.	1.35289583687	-0.351763534989	0.04919089721	-0.002098009942	$4.591708949 \cdot 10^{-6}$
	$U''$	10.	-4.7889834598	1.1676373868072	-0.1315676758	0.0062138410826	$-6.40447321 \cdot 10^{-6}$

Above the curve  $U''_b(m, n) = f(U'_b(m, n))$  connecting the branch points in the  $U$  plane for the surface wave mode it is evident that  $z \approx U$ . This permits an iterative approximation to a solution with the following iteration scheme:

$$\begin{aligned} z \approx z_1 &= \frac{(m - jU)U}{F_m(U)} \\ \approx z_2 &= (m - jU) \frac{J_m(z_1)}{J_{m-1}(z_1)} = \frac{(m - jU)z_1}{F_m(z_1)} \\ \approx z_3 &= (m - jU) \frac{J_m(z_2)}{J_{m-1}(z_2)} = \frac{(m - jU)z_2}{F_m(z_2)}. \end{aligned} \quad (19)$$

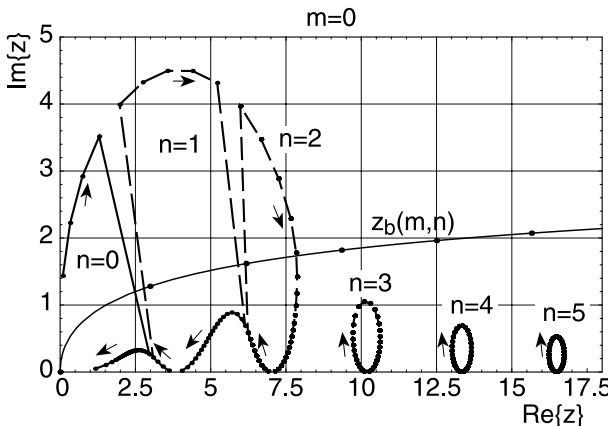


The radial modes  $n$  to a given azimuthal mode order  $m$  subdivide the  $z$  plane into "mode strips". The limits pass through the branch points  $z_b(m, n)$ . The lower-limit branches  $z_{gl}(m, n)$  are vertical lines down to the real axis  $Re\{z\}$ ; the upper branches of the limits  $z_{gu}(m, n)$  are quarter ellipses. The transforms of these limit branches are nearly coincident quarter elliptic arcs with the following forms (prime and double prime indicate real and imaginary parts):

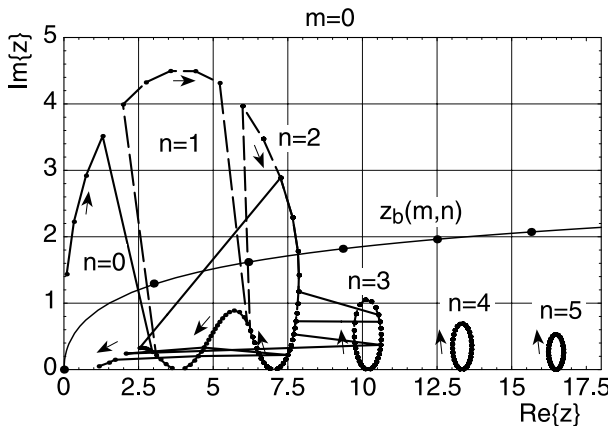
$$U''_g(m, n) = U''_b(m, n) + \left( U''_{g0}(m, n) - U''_b(m, n) \right) \sqrt{1 - U_g'^2(m, n)/U_b'^2(m, n)}, \quad (20)$$

where  $U''_{g0}(m, n)$  are the endpoints of the arcs on the imaginary axis  $Im\{U\}$ ; they have the same values as  $z''_{g0}(m, n)$ :

$$U''_{g0}(m, n) = z''_{g0}(m, n) = \text{Im} \left\{ j \cdot F_m(\text{Re}\{z_b(m, n)\}) - m \right\}. \quad (21)$$



The next graph shows a negative example of what may happen if either imprecise start values and/or an unfavourable method of numerical solution is used; the returned solutions are “hopping” between modes (mode hopping). This would have bad (if not catastrophic) consequences in a modal field analysis attempted with such results (some solutions are missing, others are returned several times).



An example of “mode hopping”

In the following procedure for evaluation of a value  $z(m, n) = \varepsilon_{m,n}h$  of a desired mode set for a given value  $U$ , the radial mode counting is  $n = 0, 1, 2, \dots$  and the azimuthal mode counting is  $m = 0, 1, 2, \dots$ . A solution of radial mode order  $n$  is sought.

*Step 1: special case U = 0?*

Take the  $(n + 1)$ -th (non-zero) root of  $J'_m(z) = 0$ . (22)

*Step 2: U in the surface wave range?*

That is, U is in the range limited by

- the curve  $U''_b = g(U'_b)$  which connects the branch point images  $U_b$ ,
- the imaginary axis,
- the curves  $U'_g(m, n) = f(U''_g(m, n))$  for  $n$  and  $n + 1$ .

Then evaluate z with the above iteration.

*Step 3: Else:*

The solution belongs to the lower part of the z strip, where continued fraction expansions converge quickly. Take as starters  $z_{si}$ ;  $i = 1, 2, 3$  for Muller's procedure

$$\begin{aligned} z_{s1}^2 &= \frac{4(1+m)(2+m)(m+jU)}{4+3m+jU}, \\ z_{s3}^2 &= \frac{2}{12+5m+jU} \left[ (2+m)(3+m)(8+5m+3jU) \right. \\ &\quad \pm ((2+m)(3+m) \cdot (384+608m+294m^2+57m^3+5m^4) \\ &\quad \left. + 6j(2+m)(8+3m+m^2)U - (38+25m+5m^2)U^2)^{1/2} \right], \end{aligned} \quad (23)$$

$$z_{s2} = (z_{s1} + z_{s3})/2.$$

Select the sign of the root in  $z_{s3}$  so that it lies in the lower part of the z strip (i.e.  $z'_b(m, n) < z'_{s3} \leq z'_b(m, n + 1)$  and  $0 \leq z''_{s3} \leq f(z'_b(m, n))$ , with which the curve connecting the branch points  $z_b(m, n)$  is indicated.

## J.14 Admittance of Annular Absorbers Approximated with Flat Absorbers

---

► See also: Mechel, Vol. III, Ch. 29 (1998)

The evaluation of the surface admittance G of annular absorbers may be tedious. This is illustrated with a simple porous layer of thickness d having characteristic values  $\Gamma_a$ ,  $Z_a$ . Let its interior surface be at the radius  $r = h$ .

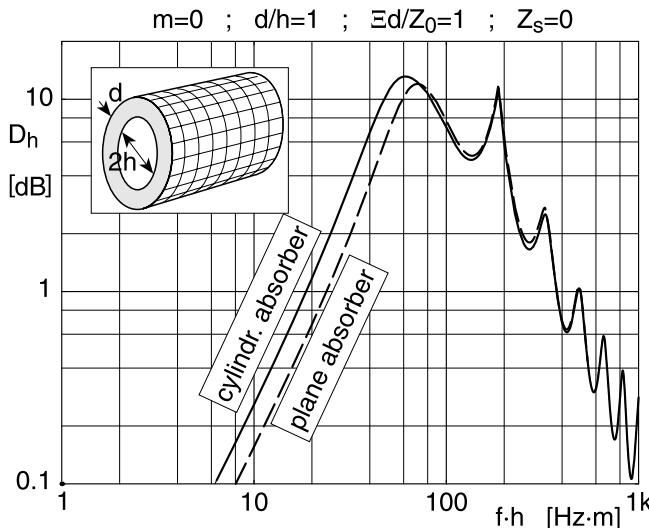
If the layer is made locally reacting by cellular partitions (i.e. locally reacting in all directions), its surface admittance is:

$$Z_0 G = \frac{jk_0 J_1(-j\Gamma_a h) \cdot Y_1(-j\Gamma_a(h+d)) - Y_1(-j\Gamma_a h) \cdot J_1(-j\Gamma_a(h+d))}{Z_{an} J_0(-j\Gamma_a h) \cdot Y_1(-j\Gamma_a(h+d)) - Y_0(-j\Gamma_a h) \cdot J_1(-j\Gamma_a(h+d))}. \quad (1)$$

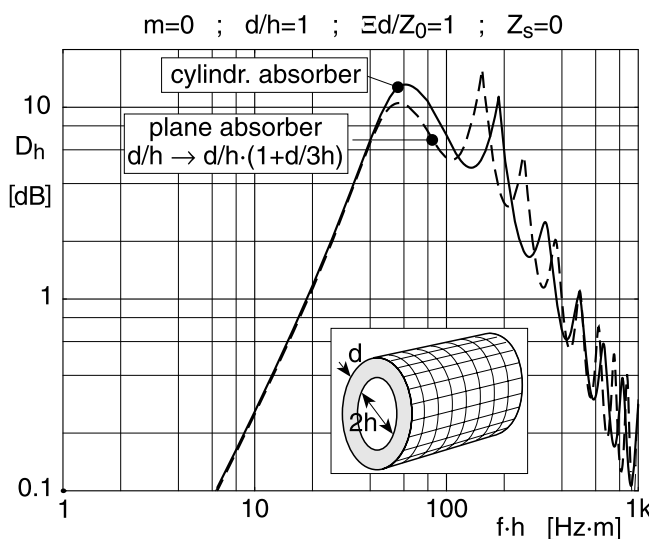
If the layer has ring-shaped partitions, its surface admittance for the mth azimuthal mode is:

$$Z_0 G = \frac{jk_0 J'_m(-j\Gamma_a h) \cdot Y'_m(-j\Gamma_a(h+d)) - Y'_m(-j\Gamma_a h) \cdot J'_m(-j\Gamma_a(h+d))}{Z_{an} J_m(-j\Gamma_a h) \cdot Y'_m(-j\Gamma_a(h+d)) - Y_m(-j\Gamma_a h) \cdot J'_m(-j\Gamma_a(h+d))}. \quad (2)$$

The next graph shows sound attenuation curves  $D_h$  (for the least attenuated mode) in a round duct with a simple glass fibre layer with cellular partitions, first evaluated with the admittance of ring-shaped absorbers, then with the admittance of the same, but plane, absorber.



Attenuation  $D_h$  in a round duct with a locally reacting porous layer, evaluated either as a cylindrical layer or as a plane layer



As above, but the thickness of the plane absorber increased in the evaluation

The rule which can be taken from this example (checked with other examples, too) is as follows:

- For frequencies up to the first maximum in the  $D_h$  curve use the admittance of a plane absorber after increasing the thickness of all air or porous layers in the absorber by  

$$d/h \rightarrow d/h \cdot \left(1 + \frac{1}{3}d/h\right)$$
- For higher frequencies use the plane absorber with the original thicknesses.

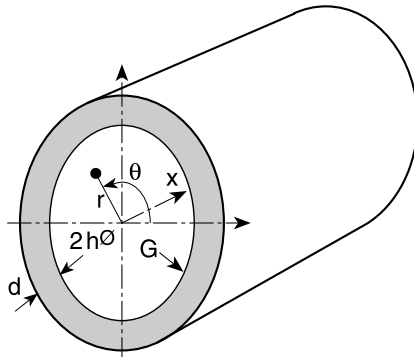
## J.15 Round Duct with a Bulk Reacting Lining

---

► See also: Mechel, Vol. III, Ch. 29 (1998)

A round duct,  $2h$  wide, is lined with a layer of thickness  $d$  of porous material having characteristic values  $\Gamma_a, Z_a$ , or, in normalised form,  $\Gamma_{an} = \Gamma_a/k_0, Z_{an} = Z_a/Z_0$ . The layer is possibly covered with a foil having a partition impedance  $Z_s$ .

The analysis proceeds somewhat in parallel with the analysis in [Sect. J.13](#), but the surface admittance  $G$  of the lining now becomes field dependent.



The field formulation in the free duct for the  $m$ -th azimuthal mode is:

$$\begin{aligned} p(r, \theta, x) &= P \cdot \cos(m\theta) \cdot J_m(\epsilon_m r) \cdot e^{-\Gamma_m x} ; \quad m = 0, 1, 2, \dots , \\ v_r &= \frac{j}{k_0 Z_0} \frac{\partial p}{\partial r} = \frac{j\epsilon_m}{k_0 Z_0} P \cos(m\theta) \cdot J'_m(\epsilon_m r) \cdot e^{-\Gamma_m x} , \\ \epsilon_m^2 &= \Gamma_m^2 + k_0^2 . \end{aligned} \quad (1)$$

The characteristic equation for  $\epsilon_m h$  is:

$$(\epsilon_m h) \frac{J'_m(\epsilon_m h)}{J_m(\epsilon_m h)} = -jk_0 h \cdot Z_0 G \quad (2)$$

or

$$(\epsilon_m h) \frac{J_{m-1}(\epsilon_m h)}{J_m(\epsilon_m h)} = m - jU ; \quad U =: k_0 h \cdot Z_0 G . \quad (3)$$

So far the analysis is as in [Sect. J.13](#). To obtain the surface admittance  $G$ , the field in the absorber layer is formulated as:

$$\begin{aligned} p_a(r, \theta, x) &= [BJ_m(\epsilon_{am}r) + CY_m(\epsilon_{am}r)] \cdot \cos(m\theta) \cdot e^{-\Gamma_m x}, \\ v_{ar}(r, \theta, x) &= \frac{-\epsilon_{am}}{\Gamma_a Z_a} [BJ'_m(\epsilon_{am}r) + CY'_m(\epsilon_{am}r)] \cdot \cos(m\theta) \cdot e^{-\Gamma_m x} \end{aligned} \quad (4)$$

$$\text{with } \epsilon_{am}^2 = \Gamma^2 - \Gamma_a^2 = \epsilon_m^2 - k_0^2 (1 + \Gamma_{an}^2). \quad (5)$$

The boundary condition at the hard outer duct wall gives:

$$C = -B \frac{J'_m(\epsilon_{am}(h+d))}{Y'_m(\epsilon_{am}(h+d))}. \quad (6)$$

The surface admittance of the lining (without  $Z_s$ ) becomes:

$$Z_0 G = \frac{-\epsilon_{am}}{\Gamma_a Z_{an}} \frac{J'_m(\epsilon_{am}h) \cdot Y'_m(\epsilon_{am}(h+d)) - Y'_m(\epsilon_{am}h) \cdot J'_m(\epsilon_{am}(h+d))}{J_m(\epsilon_{am}h) \cdot Y'_m(\epsilon_{am}(h+d)) - Y_m(\epsilon_{am}h) \cdot J'_m(\epsilon_{am}(h+d))}, \quad (7)$$

$$\text{and with } Z_s \quad Z_0 G \rightarrow 1 / (Z_s/Z_0 + 1/Z_0 G). \quad (8)$$

With the derivatives of the Bessel and Neumann functions substituted, function  $U$  becomes for  $Z_s = 0$  and  $y = \epsilon_{am}h$  (for abbreviation):

$$\begin{aligned} U &= \frac{1}{\Gamma_{an} Z_{an}} \\ &\cdot \frac{[mJ_m(y) - yJ_{m-1}(y)] \cdot [mY_m(y(1+d/h)) - y(1+d/h)Y_{m-1}(y(1+d/h))] - \dots}{m \cdot [J_m(y) \cdot Y_m(y(1+d/h)) - Y_m(y) \cdot J_m(y(1+d/h))] + \dots} \\ &\cdot \frac{\dots - [mY_m(y) - yY_{m-1}(y)] \cdot [mJ_m(y(1+d/h)) - y(1+d/h)J_{m-1}(y(1+d/h))] }{\dots + y(1+d/h) \cdot [Y_m(y) \cdot J_{m-1}(y(1+d/h)) - J_m(y) \cdot Y_{m-1}(y(1+d/h))]}, \end{aligned} \quad (9)$$

and for  $Z_s = 0$  and  $m = 0$ :

$$U = k_0 h Z_0 G = \frac{y}{\Gamma_{an} Z_{an}} \frac{J_1(y) \cdot Y_1(y(1+d/h)) - Y_1(y) \cdot J_1(y(1+d/h))}{J_0(y) \cdot Y_1(y(1+d/h)) - Y_0(y) \cdot J_1(y(1+d/h))}. \quad (10)$$

Function  $U$  of the characteristic equation contains in a complicated manner the desired solution  $z = \epsilon_m h$  of that equation.

It is assumed for the following solution methods that modes will be determined for a list of  $k_0 h$  values which begins at low values (if a mode for a single  $k_0 h$  value is needed, a list might have to be prepended).

#### *First method: iteration of layer resistance:*

This method makes use of the fact that a mode-safe method for locally reacting linings exists and that at low frequency and/or high flow resistance values  $R = \Xi \cdot d/Z_0$  ( $\Xi$  = layer flow resistivity) the bulk reacting absorber becomes nearly locally reacting. So start the iteration  $i = 1, 2, \dots$  through the list  $k_0 h$  for  $i = 1, 2, 3$  and begin for each  $i$  the evaluation of the mode for a locally reacting absorber with a high value  $R_k$  (approx.  $R_k > 8$ ); evaluate three solutions for  $R_{k=1}$ ,  $R_{k=2}$ ,  $R_{k=3}$  with the tendency of  $R_k \rightarrow R$  for

increasing  $k$ . Take these values as start values in *Muller's procedure* for the solution of the characteristic equation with the bulk reacting absorber, but with  $R_{k=3}$ . Then iterate with this task through  $R_k$ , taking the previous solutions  $z_k$  as the new starters. For values  $i > 2$  take the previous solutions  $z_{i-2}, z_{i-1}$  as two starters for the new  $z_i$ , and take the approximation from the iteration through  $R_k$  as the third starter (it helps to avoid mode hopping, which happens when only previous  $z_i$  are used, even with small steps  $\Delta k_0 h$ ).

*Second method: start with approximations for low frequencies:*

The iteration through  $R_k$  in the above method may be time consuming.

If the absorber is *locally reacting*, then  $U$  is independent of  $z$ . The characteristic equation reads as follows:

$$\begin{aligned} z \cdot J'_m(z) + jU \cdot J_m(z) &= 0 ; \quad m > 0 , \\ z \cdot J_1(z) - jU \cdot J_0(z) &= 0 ; \quad m = 0 . \end{aligned} \quad (11)$$

The method makes use of the fact that for  $k_0 h \rightarrow 0$  the function for every absorber decreases at least with the square of  $k_0 h$ . Thus starter solutions at low frequency (for the radial modes  $n$ ) are the solutions  $z_{m,n}$  of  $J'_m(z) = 0$  for  $m > 0$  and of  $J_1(z) = 0$  for  $m = 0$ . If  $n \geq 1$ , this value and nearby values with small shifts  $-\Delta z'$  and  $+j \cdot \Delta z''$  are used as starters for *Muller's procedure*. If  $n = 0$  (i.e. the fundamental radial mode), then these approximations are not precise enough; in that case approximations from the continued fraction expansion of Eq. 11 should be applied. From the solution  $i = 4$  on (of the list of  $k_0 h$ ) use previous solutions together with an extrapolated estimate of the new solution (See Sect. J.10).

If the absorber is *bulk reacting*, the statement  $U \xrightarrow[k_0 h \rightarrow 0]{} O((k_0 h)^i); i > 2$  still holds at low frequencies. For  $n > 0$  the same starters can be used as above, but for  $n = 0$  they must be more precise. Either use in this case the "iteration through  $R$ " from above or derive continued fraction approximations for the characteristic equation.

For the *least attenuated mode* one determines solutions for  $n = 0$  and  $n = 1$  and takes the solution with minimum  $\text{Re}\{\Gamma_n h\}$ .

## J.16 Annular Ducts

---

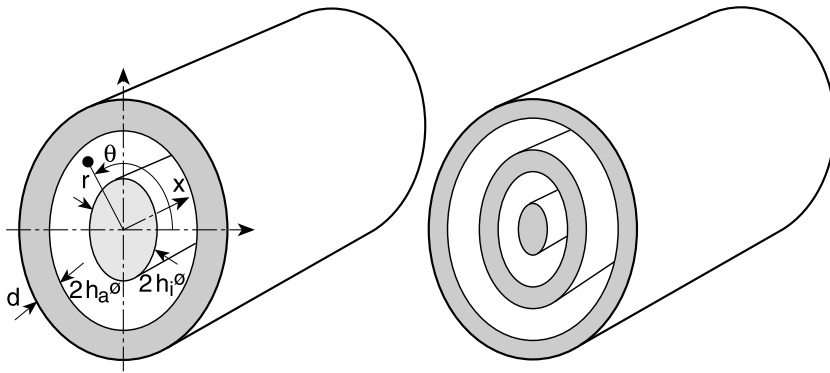
► See also: Mechel, Vol. III, Ch. 30 (1998)

Such ducts are in principle different from round ducts because now the Neumann functions appear.

We distinguish with indices  $i$ , a radii  $h_i, h_a$  and absorber functions  $U_i = k_0 h_i \cdot Z_0 G_i$  and  $U_a = k_0 h_a \cdot Z_0 G_a$  on the interior or outer side, respectively, of the free duct, which spans over  $h_i \leq r \leq h_a$ .

The field formulation for the  $m$ -th azimuthal mode is:

$$\begin{aligned} p(r, \theta, x) &= [A \cdot J_m(\epsilon r) + B \cdot Y_m(\epsilon r)] \cdot \cos(m\theta) \cdot e^{-\Gamma x} , \\ v_r(r, \theta, x) &= \frac{j\epsilon}{k_0 Z_0} [A \cdot J'_m(\epsilon r) + B \cdot Y'_m(\epsilon r)] \cdot \cos(m\theta) \cdot e^{-\Gamma x} \end{aligned} \quad (1)$$



(we neglect for the moment the indexing of  $\epsilon, \Gamma$  with  $m$ ). The boundary conditions give the following system of equations:

$$\begin{aligned} A \cdot [j\epsilon \cdot J'_m(\epsilon h_a) - k_0 Z_0 G_a \cdot J_m(\epsilon h_a)] + B \cdot [j\epsilon \cdot Y'_m(\epsilon h_a) - k_0 Z_0 G_a \cdot Y_m(\epsilon h_a)] &= 0, \\ A \cdot [j\epsilon \cdot J'_m(\epsilon h_i) + k_0 Z_0 G_i \cdot J_m(\epsilon h_i)] + B \cdot [j\epsilon \cdot Y'_m(\epsilon h_i) + k_0 Z_0 G_i \cdot Y_m(\epsilon h_i)] &= 0. \end{aligned} \quad (2)$$

A solution must nullify the determinant:

$$\begin{aligned} &[j\epsilon \cdot J'_m(\epsilon h_a) - k_0 Z_0 G_a \cdot J_m(\epsilon h_a)] \cdot [j\epsilon \cdot Y'_m(\epsilon h_i) + k_0 Z_0 G_i \cdot Y_m(\epsilon h_i)] \\ &- [j\epsilon \cdot J'_m(\epsilon h_i) + k_0 Z_0 G_i \cdot J_m(\epsilon h_i)] \cdot [j\epsilon \cdot Y'_m(\epsilon h_a) - k_0 Z_0 G_a \cdot Y_m(\epsilon h_a)] = 0. \end{aligned} \quad (3)$$

With the recurrence relations for derivatives of Bessel and Neumann functions, and using the abbreviations  $z = \epsilon h_a$ ;  $\alpha = h_i/h_a$ , a different form of the equation is:

$$\begin{aligned} &[z \cdot J_{m-1}(z) + (jU_a - m) \cdot J_m(z)] \cdot [\alpha z \cdot Y_{m-1}(\alpha z) - (jU_i + m) \cdot Y_m(\alpha z)] \\ &- [\alpha z \cdot J_{m-1}(\alpha z) - (jU_i + m) \cdot J_m(\alpha z)] \cdot [z \cdot Y_{m-1}(z) + (jU_a - m) \cdot Y_m(z)] = 0. \end{aligned} \quad (4)$$

In the special case  $m = 0$  with  $J'_0(z) = -J_1(z)$ ;  $Y'_0(z) = -Y_1(z)$  it becomes:

$$\begin{aligned} &[z \cdot J_1(z) - jU_a \cdot J_0(z)] \cdot [\alpha z \cdot Y_1(\alpha z) + jU_i \cdot Y_0(\alpha z)] \\ &- [\alpha z \cdot J_1(\alpha z) + jU_i \cdot J_0(\alpha z)] \cdot [z \cdot Y_1(z) - jU_a \cdot Y_0(z)] = 0, \end{aligned} \quad (5)$$

and after multiplication:

$$\begin{aligned} &\alpha z^2 \cdot [J_1(z) \cdot Y_1(\alpha z) - J_1(\alpha z) \cdot Y_1(z)] - jU_a \alpha z \cdot [J_0(z) \cdot Y_1(\alpha z) - J_1(\alpha z) \cdot Y_0(z)] \\ &+ jU_i z \cdot [J_1(z) \cdot Y_0(\alpha z) - J_0(\alpha z) \cdot Y_1(z)] + U_a U_i \cdot [J_0(z) \cdot Y_0(\alpha z) - J_0(\alpha z) \cdot Y_0(z)] = 0. \end{aligned} \quad (6)$$

An interior porous layer of thickness  $d_i < h_i$  has the following surface admittance ( $\Gamma_i$ ,  $Z_i$  the characteristic values of the material):

$$Z_0 G_i = \frac{-jk_0}{Z_i} \frac{J_1(j\Gamma_i h_i) \cdot Y_1(j\Gamma_i(h_i - d_i)) - Y_1(j\Gamma_i h_i) \cdot J_1(j\Gamma_i(h_i - d_i))}{J_0(j\Gamma_i h_i) \cdot Y_1(j\Gamma_i(h_i - d_i)) - Y_0(j\Gamma_i h_i) \cdot J_1(j\Gamma_i(h_i - d_i))}, \quad (7)$$

and if  $d_i = h_i$ , i.e. a central absorber (locally reacting):

$$Z_0 G_i = \frac{-jk_0}{Z_i} \frac{J_1(j\Gamma_i h_i)}{J_0(j\Gamma_i h_i)}. \quad (8)$$

An outer porous layer has the admittance:

$$Z_0 G_a = \frac{jk_0}{Z_a} \frac{J_1(j\Gamma_a h_a) \cdot Y_1(j\Gamma_a(h_a + d_a)) - Y_0(j\Gamma_a h_a) \cdot J_1(j\Gamma_a(h_a + d_a))}{J_0(j\Gamma_a h_a) \cdot Y_1(j\Gamma_a(h_a + d_a)) - Y_0(j\Gamma_a h_a) \cdot J_1(j\Gamma_a(h_a + d_a))}. \quad (9)$$

For the numerical solution, an iterative scheme over a list of  $k_0 h$  which begins at low values is recommended.

*For  $m = 0$  and locally reacting absorbers:*

For low  $k_0 h$  the last three terms in the last form of the characteristic equation disappear with the highest order in  $k_0 h$ ; therefore an approximate solution is found from:

$$[J_1(z) \cdot Y_1(\alpha z) - J_1(\alpha z) \cdot Y_1(z)] = 0. \quad (10)$$

Such solutions are tabulated in the literature. A regression for  $z_{m=0, n=1}$  over  $0 \leq \alpha \leq 0.8$  is:

$$\begin{aligned} z_{0,1} \approx & 3.8050757 + 2.65957569 \cdot \alpha - 21.764629204 \alpha^2 \\ & + 135.27002785 \cdot \alpha^3 - 249.58953616 \cdot \alpha^4 + 172.92523266 \cdot \alpha^5 \end{aligned} \quad (11)$$

(use small shift  $-\Delta z'$  and  $+j \cdot \Delta z''$  for the two other starters of *Muller's procedure*). A starter at low  $k_0 h$  for the case  $n = 0$  (i.e. lowest radial mode) is taken from the following power series expansion of the characteristic equation:

$$\begin{aligned} & \frac{2}{\pi} [j(U_a + U_i) + U_a U_i \ln \alpha] \\ & - \frac{z^2}{2\pi} \{(1 - \alpha^2) [2 + j(U_a - U_i) + U_a U_i] + \ln \alpha \cdot [(U_a - 2j) U_i + \alpha^2 (U_i + 2j) U_a]\} \\ & + \frac{z^4}{64\pi} \{(1 - \alpha^2) [8 + 2jU_a - 10jU_i + 3U_a U_i + \alpha^2 (8 + 10jU_a - 2jU_i + 3U_a U_i)] \\ & + 2 \ln \alpha \cdot [(U_a - 4j) U_i + 4\alpha^2 (U_a - 2j) (U_i + 2j) + \alpha^4 U_a (U_i + 4j)]\} = 0. \end{aligned} \quad (12)$$

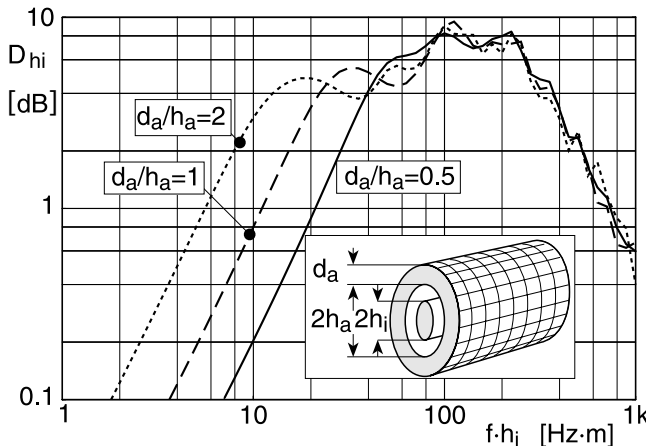
Take in the solution for  $z^2$  the root with a negative real part. Further, take the solution of this equation with the fourth power term  $z^4$  neglected as a second starter, and the mean value of both as the third starter.

*If the absorber is bulk reacting and  $m = 0$ :*

Find initial starters (at the lower end of the  $k_0 h$  list) with the assumption that the absorber is approximately locally reacting. Take these solutions as starters with the equation for the bulk reacting absorber, and for later  $k_0 h$  values take previous solutions and an extrapolated new solution (see Sect. J.10).

*If the absorber is bulk reacting and  $m > 0$ :*

For  $n > 0$  take the solution of the term without  $U_a, U_i$  in the expanded characteristic equation as starter. For  $n = 0$  solve the power series expansion of the characteristic equation, now with expansion of  $U_a, U_i$ , for a starter.



Attenuation curves  $D_{hi}$  for ring-shaped silencers with locally reacting glass fibre layers for different thickness ratios of the outer layer. Input parameters:  $h_i/h_a = 0.5$ ;  $d_i/h_i = 1$ ;  $\Xi_a d_a / Z_0 = \Xi_i d_i / Z_0 = 1.5$ ;  $Z_{sa} = Z_{si} = 0$

## J.17 Duct with a Cross-Layered Lining

► See also: Mechel, Vol. III, Ch. 32 (1998)

Often silencers need low values of the (normalised) flow resistance  $R = \Xi \cdot d/Z_0$  of porous layers to obtain high attenuation values  $D_h$ , but the layer thickness  $d$  must not be small, otherwise the lower-limit frequency of attenuation would be high. The necessarily low flow resistance values  $\Xi$  lead to low bulk densities or to coarse fibres; both measures reduce the mechanical stability of the absorber. A remedy can be to place layers side by side, one of the layers just being a “placeholder” made out of (e.g.) scrambled wire mats.

If characteristic values  $\Gamma_\alpha$ ,  $Z_\alpha$ ,  $\alpha = a, b$ , are normalised with  $k_0$ ,  $Z_0$ , respectively, this is indicated with an additional index  $n$ .

In case (a), in which both layers are separated from each other, if both layer thicknesses  $a$ ,  $b$  are small compared to the wavelength, the effective lining admittance is the weighted average

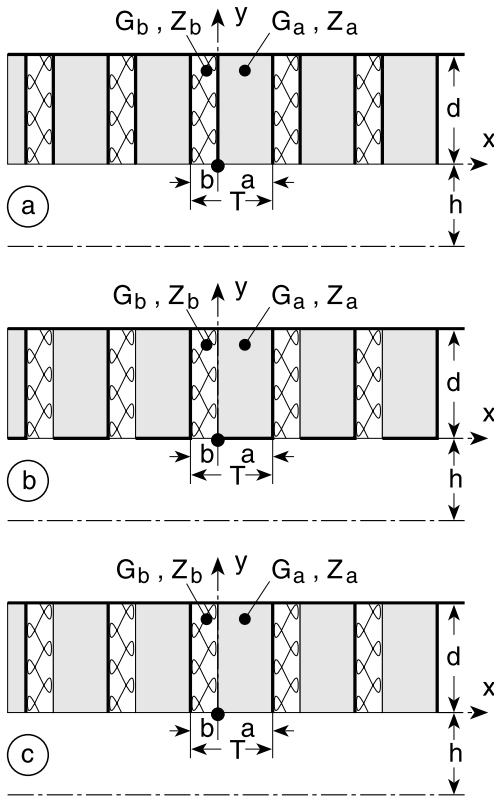
$$Z_0 G_Y = \frac{a/T}{Z_{an}} \tanh(\Gamma_a d) + \frac{b/T}{Z_{bn}} \tanh(\Gamma_b d) . \quad (1)$$

In case (b) a couple of layers form a lined cross-directed duct, and one of the layer heads is covered towards the main duct.

In case (c) layer couples form cross-directed, lined ducts, and both layer heads are open towards the main duct.

In cases (b) and (c) first the propagation constant  $\Gamma_s$  in the side ducts is determined. For arrangement (b) the average wall admittance seen from the main duct is approximately:

$$Z_0 G_Y = \frac{b/T \Gamma_s}{Z_{bn} \Gamma_b} \tanh(\Gamma_s d) . \quad (2)$$



For arrangement (c) the average admittance of the cross-layered lining of the main duct is:

$$Z_0 G_y = \left[ \frac{a/T}{\Gamma_a Z_{an}} + \frac{b/T}{\Gamma_b Z_{bn}} \right] \cdot \Gamma_s \tanh(\Gamma_s d). \quad (3)$$

Average admittance values  $G_y$  are sufficient only for small  $T/\lambda_0$ . Otherwise the main duct should be treated as a duct with an axially periodic lining. Formulas will be given below, first with the assumption of only the fundamental mode in the side duct, second with higher modes in the side duct. Sometimes the layer indices will be collected as  $\alpha = a, b$ .

*Only the fundamental mode in the side duct:*

The wave and impulse equations in the layers are:

$$(\Delta - \Gamma_\alpha^2) p_\alpha(x, y) = 0; \quad v_{\alpha,x}(x, y) = \frac{-1}{\Gamma_\alpha Z_\alpha} \frac{\partial p_\alpha}{\partial x}. \quad (4)$$

Field formulations in the layers are as follows ( $\alpha$  may assume the values of a, b):

$$\begin{aligned} p_\alpha(x, y) &= P_\alpha \cdot \frac{\cosh(\Gamma_s(y - d))}{\cosh(\Gamma_s d)} \cdot \cos(\epsilon_\alpha(x \mp \alpha)) ; \quad \alpha = \begin{cases} a ; & x \in a \\ b ; & x \in b \end{cases} , \\ v_{x\alpha}(x, y) &= \frac{1}{Z_\alpha} P_\alpha \cdot \frac{\cosh(\Gamma_s(y - d))}{\cosh(\Gamma_s d)} \cdot \frac{\epsilon_\alpha}{\Gamma_\alpha} \sin(\epsilon_\alpha(x \mp \alpha)) , \\ v_{y\alpha}(x, y) &= \frac{-1}{Z_\alpha} P_\alpha \cdot \frac{\Gamma_s}{\Gamma_\alpha} \frac{\sinh(\Gamma_s(y - d))}{\cosh(\Gamma_s d)} \cdot \cos(\epsilon_\alpha(x \mp \alpha)) , \end{aligned} \quad (5)$$

and from the wave equation  $\epsilon_\alpha^2 = \Gamma_s^2 - \Gamma_\alpha^2$ . (6)

If the main duct carries higher modes in the z direction, this changes to:

$$\epsilon_\alpha^2 = \Gamma_s^2 - \Gamma_\alpha^2 - \epsilon_z^2 . \quad (7)$$

(This will be ignored below.)

The characteristic equation of the side duct is:

$$\frac{-\epsilon_a}{\Gamma_a Z_a} \tan(\epsilon_a a) = \frac{\epsilon_b}{\Gamma_b Z_b} \tan(\epsilon_b b) \quad (8)$$

or, with the abbreviations:

$$z_b = \epsilon_b b ; \quad A = \frac{b}{a} \frac{\Gamma_b Z_b}{\Gamma_a Z_a} ; \quad B = (\Gamma_b b)^2 - (\Gamma_a b)^2 , \quad (9)$$

it is:

$$z_b \cdot \tan(z_b) + A \cdot \left( \frac{a}{b} \sqrt{z_b^2 + B} \right) \cdot \tan \left( \frac{a}{b} \sqrt{z_b^2 + B} \right) = 0 . \quad (10)$$

An approximate equation  $C_0 + C_1 \cdot z_b^2 - C_2 \cdot z_b^4 + C_3 \cdot z_b^6 - C_4 \cdot z_b^8 = 0$  (11)

is obtained by continued fraction expansion with the following coefficients:

$$\begin{aligned} C_0 &= 525(a/b)^2 A \cdot B (21 - 2(a/b)^2 B) , \\ C_1 &= 15 \left\{ 5(a/b)^2 A [147 - 7(9 + 4(a/b)^2) B + 6(a/b)^2 B^2] \right. \\ &\quad \left. + 7(105 - 45(a/b)^2 B + (a/b)^4 B^2) \right\} , \\ C_2 &= 5 \left\{ 210 + 3(a/b)^2 [315 + 7A(45 - B) - 30B] \right. \\ &\quad \left. - 2(a/b)^4 [(21 - B)B - A(105 - 90B + B^2)] \right\} , \\ C_3 &= 5(a/b)^2 \{90 + A[21 + (a/b)^2(90 - 4B)] + (a/b)^2(21 - 4B)\} , \\ C_4 &= 10(1 + A)(a/b)^4 . \end{aligned} \quad (12)$$

One obtains with its solution:

$$\Gamma_s d = \frac{d}{b} \sqrt{z_b^2 + (k_0 b)^2 \Gamma_{bn}^2} \quad (13)$$

or, in the case of a higher mode in the z direction:

$$\Gamma_s d = \frac{d}{b} \sqrt{z_b^2 + (k_0 b)^2 \Gamma_{bn}^2 + (\epsilon_z b)^2}. \quad (14)$$

Select from the polynomial solutions the solution with minimum  $\operatorname{Re}\{\Gamma_s d\} > 0$ .

The normalised surface admittances of the layer heads are:

$$Z_0 G_{\alpha y} = \frac{\Gamma_s d}{k_0 d \Gamma_{\alpha n} Z_{\alpha n}} \tanh(\Gamma_s d). \quad (15)$$

The field formulation in the main duct with spatial harmonics is:

$$\begin{aligned} p(x, y) &= \sum_{n=-\infty}^{+\infty} P_n \cdot \frac{\cos(\epsilon_n(y + h))}{\cos(\epsilon_n h)} \cdot e^{-j\beta_n x}, \\ Z_0 v_v(x, y) &= -j \sum_n P_n \cdot \frac{\epsilon_n}{k_0} \frac{\sin(\epsilon_n(y + h))}{\cos(\epsilon_n h)} \cdot e^{-j\beta_n x} \end{aligned} \quad (16)$$

with axial wave numbers

$$\beta_n = \beta_0 + n \frac{2\pi}{T}; \quad \operatorname{Im}\{\beta_0\} \leq 0; \quad \epsilon_n^2 = k_0^2 - \beta_n^2. \quad (17)$$

The wall admittance at  $y = 0$  is periodic with period  $T = a + b$  and has the axial profile:

$$Z_0 G(x) = \begin{cases} Z_0 G_{by}; & -b \leq x < 0 \\ Z_0 G_{ay}; & 0 < x \leq a \end{cases}. \quad (18)$$

When written as a Fourier series it is:

$$Z_0 G(x) = \sum_v g_v \cdot e^{+j2v\pi \cdot x/T}; \quad g_v = \frac{1}{T} \int_T Z_0 G(x) \cdot e^{-j2v\pi \cdot x/T} dx \quad (19)$$

with coefficients

$$\begin{aligned} g_v &= \frac{1}{a+b} \left[ a \cdot Z_0 G_{ay} \frac{\sin(v\pi a/T)}{v\pi a/T} \cdot e^{-jv\pi a/T} + b \cdot Z_0 G_{by} \frac{\sin(v\pi b/T)}{v\pi b/T} \cdot e^{+jv\pi b/T} \right], \\ g_0 &= \frac{1}{a+b} [a \cdot Z_0 G_{ay} + b \cdot Z_0 G_{by}] = Z_0 G_y \end{aligned} \quad (20)$$

(notice in general  $g_{-v} \neq g_{+v}$ ).

One splits the main duct field into a periodic factor and a propagation factor:

$$p(x, y) = P(x, y) \cdot e^{-j\beta_0 x}; \quad v_y(x, y) = V_y(x, y) \cdot e^{-j\beta_0 x}. \quad (21)$$

The boundary conditions at  $y = 0$  give the following linear, homogeneous system of equations:

$$\sum_n P_n \cdot \left[ \delta_{m,n} \cdot j \frac{\epsilon_n}{k_0} \tan(\epsilon_n h) + g_{n-m} \right] = 0; \quad m, n = 0, \pm 1, \pm 2, \dots. \quad (22)$$

The determinant set to zero represents the characteristic equation for  $\beta_0$ . A simplified boundary condition requires the matching of the periodic factor  $V_y(x, 0)$  with the particle velocity  $V_{abs}(x, 0)$  in the surface of the lining:

$$-jP_n \frac{\epsilon_n}{k_0} \tan(\epsilon_n h) = \frac{1}{T} \int_T Z_0 V_{abs}(x, 0) \cdot e^{+j2\pi nx/T} dx . \quad (23)$$

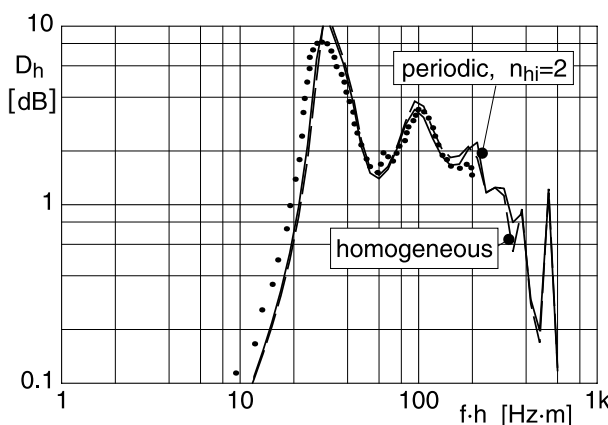
This leads to:

$$\sum_n \left\{ \delta_{m,n} - jk_0 h \frac{g_{n-m}}{\epsilon_n h \cdot \tan(\epsilon_n h)} \right\} \cdot \frac{1}{T} \int_T Z_0 V_{abs}(x, 0) \cdot e^{+j2\pi nx/T} dx = 0 . \quad (24)$$

If only one mode exists in the side duct, and this is supposed to have a plane velocity profile, so that  $V_{abs} = G \cdot P$  for an exciting pressure  $P$ , then this equation becomes:

$$\begin{aligned} \sum_n \left\{ \delta_{m,n} - jk_0 h \frac{g_{n-m}}{\epsilon_n h \cdot \tan(\epsilon_n h)} \right\} \cdot g_{-n} &= 0 ; \quad m \neq 0 , \\ g_0 - jk_0 h \sum_n \frac{g_n \cdot g_{-n}}{\epsilon_n h \cdot \tan(\epsilon_n h)} &= 0 ; \quad m = 0 . \end{aligned} \quad (25)$$

The equation for  $m = 0$  is the characteristic equation for  $\beta_0 h$ , which is contained in the  $\epsilon_n h$  (the leading term plus the term with  $n = 0$  in the sum form the characteristic equation for a duct with a homogeneous lining). One can take the mode wave numbers  $\epsilon_n h$  in a duct with the average admittance from  $Z_0 G_{ay}$ ,  $Z_0 G_{by}$  as starting approximations in the numerical solution with Muller's procedure for  $(\beta_0 h)^2 = (k_0 h)^2 - (\epsilon_0 h)^2$ .



Mineral fibre boards,  $a = 4$  [cm] thick,  $\Xi = 30$  [kPas/m<sup>2</sup>], with mutual distance  $b = 6$  [cm], form a cross-layered lining of  $d = 20$  [cm] thickness (air in the layers  $\alpha = a$ ) of a  $h = 10$  [cm] wide duct. Points: measured; Full line: periodic duct with spatial harmonics; Dashed: homogeneous duct with average admittance of the layers treated as side ducts

The assumption of a plane mode profile, made above, can be dropped. One obtains with the true mode profile:

$$Z_0 V_{\text{abs}}(x, 0) = \begin{cases} Z_0 v_{ay}(x, 0) = \frac{\Gamma_s \tanh(\Gamma_s d)}{\Gamma_a Z_{an}} P_a \cos(\epsilon_a a) \frac{\cos(\epsilon_a(x - a))}{\cos(\epsilon_a a)} ; & x \in a \\ Z_0 v_{by}(x, 0) = \frac{\Gamma_s \tanh(\Gamma_s d)}{\Gamma_b Z_{bn}} P_b \cos(\epsilon_b b) \frac{\cos(\epsilon_b(x + b))}{\cos(\epsilon_b b)} ; & x \in b \end{cases}, \quad (26)$$

and (notice the definition of the abbreviation  $\gamma_n$ )

$$\begin{aligned} \frac{1}{T} \int_T^T Z_0 V_{\text{abs}}(x, 0) \cdot e^{+j2\pi n \alpha x / T} dx &:= P \cdot \gamma_n \\ &= P \cdot \left\{ \frac{1}{\Gamma_a d Z_{an}} \frac{a/T}{(\epsilon_a a)^2 - (2\pi n \alpha / T)^2} \left[ j2\pi n \frac{a}{T} \left( \frac{e^{j2\pi n \alpha a / T}}{\cos(\epsilon_a a)} - 1 \right) + \epsilon_a a \cdot \tan(\epsilon_a a) \right] \right. \\ &\quad \left. + \frac{1}{\Gamma_b d Z_{bn}} \frac{b/T}{(\epsilon_b b)^2 - (2\pi n \alpha / T)^2} \left[ j2\pi n \frac{b}{T} \left( 1 - \frac{e^{-j2\pi n \alpha b / T}}{\cos(\epsilon_b b)} \right) + \epsilon_b b \cdot \tan(\epsilon_b b) \right] \right\}. \end{aligned} \quad (27)$$

Therewith the equation to be solved is:

$$\gamma_0 - jk_0 h \sum_n \frac{g_n \cdot \gamma_n}{\epsilon_n h \cdot \tan(\epsilon_n h)} = 0. \quad (28)$$

The changes in the result due to the mode profile (26) as compared with a plane profile often are not worth the larger amount of computations.

*Higher modes in the side duct* (mode index  $\sigma$  in the side ducts):

The field formulation in the side ducts  $\alpha = a, b$  is:

$$\begin{aligned} p_\alpha(x, y) &= \sum_\sigma P_{\alpha\sigma} \cdot \frac{\cosh(\Gamma_{s\sigma}(y - d))}{\cosh(\Gamma_{s\sigma}d)} \cdot \frac{\cos(\epsilon_{\alpha\sigma}(x \mp \alpha))}{\cos(\epsilon_{\alpha\sigma}\alpha)} ; \quad \alpha = \begin{cases} a ; & x \in a \\ b ; & x \in b, \end{cases} \\ v_{x\alpha}(x, y) &= \frac{1}{Z_\alpha} \sum_\sigma P_{\alpha\sigma} \cdot \frac{\cosh(\Gamma_{s\sigma}(y - d))}{\cosh(\Gamma_{s\sigma}d)} \cdot \frac{\epsilon_{\alpha\sigma} \sin(\epsilon_{\beta\sigma}(x \mp \alpha))}{\Gamma_\alpha \cos(\epsilon_{\alpha\sigma}\alpha)}, \\ v_{y\alpha}(x, y) &= \frac{-1}{Z_\alpha} \sum_\sigma P_{\alpha\sigma} \cdot \frac{\Gamma_{s\sigma}}{\Gamma_\alpha} \frac{\sinh(\Gamma_{s\sigma}(y - d))}{\cosh(\Gamma_{s\sigma}d)} \cdot \frac{\cos(\epsilon_{\alpha\sigma}(x \mp \alpha))}{\cos(\epsilon_{\alpha\sigma}\alpha)} \end{aligned} \quad (29)$$

with  $\epsilon_{\alpha\sigma}^2 = \Gamma_{s\sigma}^2 - \Gamma_\alpha^2$  and the characteristic equation:

$$\frac{-\epsilon_{a\sigma}}{\Gamma_a Z_a} \tan(\epsilon_{a\sigma} a) = \frac{\epsilon_{b\sigma}}{\Gamma_b Z_b} \tan(\epsilon_{b\sigma} b). \quad (30)$$

With the transversal mode profiles:  $q_{\alpha\sigma}(x) = \frac{\cos(\epsilon_{\alpha\sigma}(x \mp \alpha))}{\cos(\epsilon_{\alpha\sigma}\alpha)}$ ,

the orthogonality relation in the side ducts

$$\frac{1}{\Gamma_a Z_{an}} \int_0^a q_{a\sigma}(x) \cdot q_{a\tau}(x) dx + \frac{1}{\Gamma_b Z_{bn}} \int_{-b}^0 q_{b\sigma}(x) \cdot q_{b\tau}(x) dx = \delta_{\sigma,\tau} \cdot TN_\sigma \quad (32)$$

gives the mode norms  $N_\sigma$ :

$$T \cdot N_\sigma = \frac{a/2}{\Gamma_{an} Z_{an} \cos^2(\epsilon_{a\sigma} a)} \left[ 1 + \frac{\sin(2\epsilon_{a\sigma} a)}{2\epsilon_{a\sigma} a} \right] + \frac{b/2}{\Gamma_{bn} Z_{bn} \cos^2(\epsilon_{b\sigma} b)} \left[ 1 + \frac{\sin(2\epsilon_{b\sigma} b)}{2\epsilon_{b\sigma} b} \right]. \quad (33)$$

The field formulation in the main duct remains as above.

Matching the sound fields in the plane  $y = 0$  leads to the homogeneous linear system of equations for the amplitudes  $P_n$  of the space harmonics:

$$\sum_n P_n \left[ \delta_{m,n} \cdot \epsilon_m h \cdot \tan(\epsilon_m h) - j \frac{h}{d} \sum_\sigma \Gamma_{s\sigma} d \tanh(\Gamma_{s\sigma} d) \cdot \frac{R_{n,\sigma} R_{-m,\sigma}}{N_\sigma} \right] = 0 \quad (34)$$

with the coupling coefficients  $R_{n,\sigma}$  between side duct modes and main duct spatial harmonics:

$$\begin{aligned} T \cdot R_{n,\sigma} := & \frac{1}{\Gamma_{an} Z_{an}} \int_0^a e^{-j\beta_n x} \cdot \frac{\cos(\epsilon_{a\sigma}(x-a))}{\cos(\epsilon_{a\sigma} a)} dx \\ & + \frac{1}{\Gamma_{bn} Z_{bn}} \int_{-b}^0 e^{-j\beta_n x} \cdot \frac{\cos(\epsilon_{b\sigma}(x+b))}{\cos(\epsilon_{b\sigma} b)} dx \\ = & \frac{j/2}{\Gamma_{an} Z_{an} \cos(\epsilon_{a\sigma} a)} \cdot \left[ \frac{-1}{\beta_n} + \frac{2}{\beta_n} \frac{2\epsilon_{a\sigma}^2 - \beta_n^2}{4\epsilon_{a\sigma}^2 - \beta_n^2} e^{-j\beta_n a} \right. \\ & \left. + \frac{1}{4\epsilon_{a\sigma}^2 - \beta_n^2} (\beta_n \cos(2\epsilon_{a\sigma} a) - 2j\epsilon_{a\sigma} \sin(2\epsilon_{a\sigma} a)) \right] \\ & + \frac{j/2}{\Gamma_{bn} Z_{bn} \cos(\epsilon_{b\sigma} b)} \cdot \left[ \frac{1}{\beta_n} - \frac{2}{\beta_n} \frac{2\epsilon_{b\sigma}^2 - \beta_n^2}{4\epsilon_{b\sigma}^2 - \beta_n^2} e^{+j\beta_n b} \right. \\ & \left. - \frac{1}{4\epsilon_{b\sigma}^2 - \beta_n^2} (\beta_n \cos(2\epsilon_{b\sigma} b) + 2j\epsilon_{b\sigma} \sin(2\epsilon_{b\sigma} b)) \right]. \end{aligned} \quad (35)$$

The determinant of the above system of equations set to zero is the characteristic equation of the system. It can be simplified if only the periodic factor of the main duct field is matched to the field in the side ducts:

$$\sum_n P_n \left[ \delta_{m,n} \cdot \epsilon_m h \cdot \tan(\epsilon_m h) - j \frac{h}{d} \sum_\sigma \Gamma_{s\sigma} d \tanh(\Gamma_{s\sigma} d) \cdot \frac{S_{n,\sigma} S_{-m,\sigma}}{N_\sigma} \right] = 0, \quad (36)$$

where the  $S_{n,\sigma}$  are obtained from the  $R_{n,\sigma}$  by the substitution  $\beta_n \rightarrow 2n\pi/T$ , especially for  $n = 0$ :

$$\begin{aligned} T \cdot S_{0,\sigma} &= \frac{a/2}{\Gamma_{an} Z_{an} \cos(\epsilon_{a\sigma} a)} \left[ 1 + \frac{\sin(2\epsilon_{a\sigma} a)}{2\epsilon_{a\sigma} a} \right] + \frac{b/2}{\Gamma_{bn} Z_{bn} \cos(\epsilon_{b\sigma} b)} \left[ 1 + \frac{\sin(2\epsilon_{b\sigma} b)}{2\epsilon_{b\sigma} b} \right] \\ &\xrightarrow{|\epsilon_{a\sigma} a|, |\epsilon_{b\sigma} b| \ll 1} \frac{a/T}{\Gamma_{an} Z_{an}} + \frac{b/T}{\Gamma_{bn} Z_{bn}}. \end{aligned} \quad (37)$$

The determinant equation of the second system can be approximated by:

$$\varepsilon_0 h \cdot \tan(\varepsilon_0 h) - j \frac{h}{d} (\Gamma_{s0} d) \cdot \tanh(\Gamma_{s0} d) \left( \frac{a/T}{\Gamma_{an} Z_{an}} + \frac{b/T}{\Gamma_{bn} Z_{bn}} \right) = 0, \quad (38)$$

which is just the characteristic equation with the average head admittance.

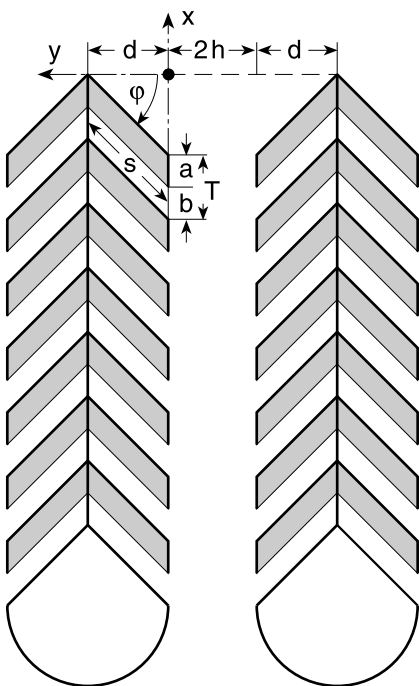
A special form of ducts with cross-layered linings is the “pine-tree silencer”. These silencers are used in air flows with heavy dust load. Their axis is vertical. The intention is that dust deposits on the branches of the trees will slide down due to the vibrations of the structure.

The pine-tree baffles mostly belong to type (b) of the initial graph of this section.

Because of the inclination of the branches, the layer thicknesses change to  $a \rightarrow a \cdot \cos\varphi$ ,  $b \rightarrow b \cdot \cos\varphi$  and the admittances  $G_{ay} \rightarrow G_{ay} \cdot \cos\varphi$ .

Sometimes the air-filled channels (layers with  $b$  in the sketch) are terminated near the “trunk” with an absorber layer having a reflection factor  $r$  for the incident fundamental side duct mode. The surface admittance at  $y = 0$  then becomes approximately:

$$Z_0 G_{by} = \frac{\Gamma_s}{\Gamma_b Z_{bn}} \frac{1 - r \cdot e^{-2\Gamma_s s}}{1 + r \cdot e^{-2\Gamma_s s}} \cos \varphi. \quad (39)$$



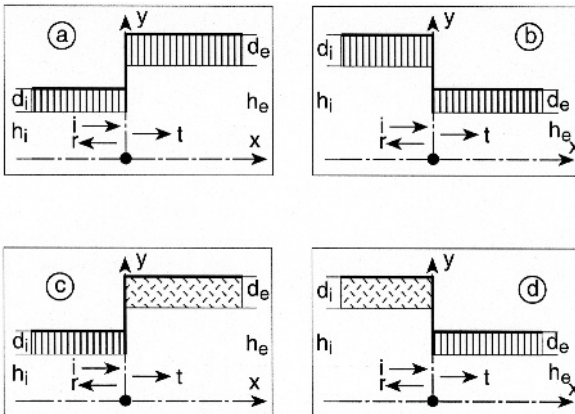
Frommhold derived a correction formula to be applied to the reflection factor  $r$  for normal incidence to obtain approximately the reflection factor  $r_{eff}$  for the incident mode (claimed to be applicable for  $f > 70$  [Hz]):

$$r_{eff} = r \cdot \left( \sqrt{\cos \varphi} + \frac{1 - \sqrt{\cos \varphi}}{1 - (f [\text{Hz}] / 70)^3} \right). \quad (40)$$

## J.18 Single Step of Duct Height and/or Duct Lining

► See also: Mechel, Vol. III, Ch. 33 (1998)

The steps are isolated, i. e. the ducts on both sides are infinitely long, in principle; in practice it will be sufficient if the next step is far enough to neglect reflections from there at the original step.



One must distinguish:

- expanding (a, c) or contracting (b, d) ducts (as seen in the direction of sound);
- locally (a, b) or bulk reacting linings;
- the same (a, b) or different (c, d) types (local or bulk) on both sides of the step;
- if the lining in the narrow duct is bulk reacting, whether its head is open or covered with a hard sheet.

There are more combinations than the few examples shown above. Vertical hatching will be used in the sketches below to indicate a locally reacting lining; crossed hatching indicates bulk reacting absorbers.

An index  $\beta = i, e$  will indicate the duct (and its parameters) on the side of the incident sound and on the exit side. The incident sound  $p_i$  may be a sum of modes of the entrance duct or, as a special case, one mode of order  $\mu$ . Both the reflected wave  $p_r$  and the transmitted wave  $p_t$  are formulated as sums of modes in their ducts.

*Fundamental relations in a duct with a locally reacting lining:*

Field formulations:

$$p_i(x, y) = \sum_m P_{im} \cdot \cos(\epsilon_{im}y) \cdot e^{-\gamma_{im}x}, \quad (1)$$

$$v_{ix}(x, y) = \frac{1}{jk_0 Z_0} \sum_m P_{im} \cdot \gamma_{im} \cos(\epsilon_{im}y) \cdot e^{-\gamma_{im}x}.$$

In the special case of a single incident mode,  $P_{im} \rightarrow \delta_{m,\mu} \cdot P_{ip}$ . (2)

$$p_r(x, y) = \sum_m P_{rm} \cdot \cos(\epsilon_{im}y) \cdot e^{+\gamma_{im}x}, \quad (3)$$

$$v_{rx}(x, y) = \frac{-1}{jk_0 Z_0} \sum_m P_{rm} \cdot \gamma_{im} \cos(\epsilon_{im}y) \cdot e^{+\gamma_{im}x},$$

$$\begin{aligned} p_t(x, y) &= \sum_n P_{tn} \cdot \cos(\epsilon_{en} y) \cdot e^{-\gamma_{en} x}, \\ v_{tx}(x, y) &= \frac{1}{jk_0 Z_0} \sum_n P_{tn} \cdot \gamma_{en} \cos(\epsilon_{en} y) \cdot e^{-\gamma_{en} x}. \end{aligned} \quad (4)$$

The secular equation is:  $\epsilon_{\beta k}^2 = k_0^2 + \gamma_{\beta k}^2$ ;  $\beta = i, e$ ;  $k = \mu, m, n$ . (5)

If there is a higher mode in the z direction, then it becomes:  $\epsilon_{\beta k}^2 = k_0^2 + \gamma_{\beta k}^2 - \epsilon_z^2$ ;  $\beta = i, e$ ;  $k = \mu, m, n$ . (6)

The characteristic equation for the modes is:

$$(\epsilon_{\beta k} h_\beta) \cdot \tan(\epsilon_{\beta k} h_\beta) = jk_0 h_\beta \cdot Z_0 G_\beta, \quad (7)$$

and if  $G_\beta = 0$ , then  $\epsilon_{\beta k} = (k - 1)\pi$ ;  $k = 0, 1, 2, \dots$ . (8)

The mode norms  $N_{\beta k}$  are:

$$\begin{aligned} \frac{1}{h_\beta} \int_0^{h_\beta} \cos(\epsilon_{\beta k} y) \cdot \cos(\epsilon_{\beta k'} y) dy &= \delta_{k,k'} \cdot N_{\beta k}, \\ N_{\beta k} &:= \frac{1}{h_\beta} \int_0^{h_\beta} \cos^2(\epsilon_{\beta k} y) dy = \frac{1}{2} \left[ 1 + \frac{\sin(2\epsilon_{\beta k} h_\beta)}{2\epsilon_{\beta k} h_\beta} \right]. \end{aligned} \quad (9)$$

The mode coupling coefficients of the modes of both ducts are:

$$\begin{aligned} R_{m,n}(h, \beta, \beta') &:= \frac{1}{h} \int_0^h \cos(\epsilon_{\beta m} y) \cdot \cos(\epsilon_{\beta' n} y) dy \\ &= \frac{1}{2} \left[ \frac{\sin((\epsilon_{\beta m} - \epsilon_{\beta' n})h)}{(\epsilon_{\beta m} - \epsilon_{\beta' n})h} + \frac{\sin((\epsilon_{\beta m} + \epsilon_{\beta' n})h)}{(\epsilon_{\beta m} + \epsilon_{\beta' n})h} \right]. \end{aligned} \quad (10)$$

Evidently  $R_{m,n}(h, \beta, \beta') = R_{n,m}(h, \beta', \beta)$ . Other coupling coefficients over the range  $\Delta h$  of the height difference are:

$$\begin{aligned} S_{m,n}(h, \beta, \beta') &:= \frac{1}{h_\beta} \int_h^{h_\beta} \cos(\epsilon_{\beta m} y) \cdot \cos(\epsilon_{\beta' n} y) dy \\ &= R_{m,n}(h_\beta, \beta, \beta') - \frac{h}{h_\beta} R_{m,n}(h, \beta, \beta') \xrightarrow[h \rightarrow h_\beta]{} 0. \end{aligned} \quad (11)$$

In ducts with a locally reacting lining:

$$S_{m,n}(h, \beta, \beta') := \delta_{m,n} \cdot N_{\beta m} - \frac{h}{h_\beta} R_{m,n}(h, \beta, \beta'). \quad (12)$$

*Fundamental relations in a duct with a bulk reacting lining:*

In order to write the mode field in a single line, a “switch function” is introduced by:

$$s_y(a, b) := \begin{cases} 1 & a \leq y < b \\ 0 & \text{else} \end{cases} . \quad (13)$$

The field formulations are:

$$\begin{aligned} p_i(x, y) &= \sum_m P_{im} \cdot e^{-\gamma_{im}x} \\ &\cdot \left[ s_y(0, h_i) \frac{\cos(\epsilon_{im}y)}{\cos(\epsilon_{im}h_i)} + s_y(h_i, h_i + d_i) \frac{\cos(\kappa_{im}(y - h_i - d_i))}{\cos(\kappa_{im}d_i)} \right], \\ v_{ix}(x, y) &= \frac{1}{jk_0 Z_0} \sum_m P_{im} \cdot \gamma_{im} e^{-\gamma_{im}x} \\ &\cdot \left[ s_y(0, h_i) \frac{\cos(\epsilon_{im}y)}{\cos(\epsilon_{im}h_i)} - j \frac{s_y(h_i, h_i + d_i)}{\Gamma_{in} Z_{in}} \frac{\cos(\kappa_{im}(y - h_i - d_i))}{\cos(\kappa_{im}d_i)} \right], \\ p_r(x, y) &= \sum_m P_{rm} \cdot e^{+\gamma_{im}x} \\ &\cdot \left[ s_y(0, h_i) \frac{\cos(\epsilon_{im}y)}{\cos(\epsilon_{im}h_i)} + s_y(h_i, h_i + d_i) \frac{\cos(\kappa_{im}(y - h_i - d_i))}{\cos(\kappa_{im}d_i)} \right], \\ v_{rx}(x, y) &= \frac{-1}{jk_0 Z_0} \sum_m P_{rm} \cdot \gamma_{im} e^{+\gamma_{im}x} \\ &\cdot \left[ s_y(0, h_i) \frac{\cos(\epsilon_{im}y)}{\cos(\epsilon_{im}h_i)} - j \frac{s_y(h_i, h_i + d_i)}{\Gamma_{in} Z_{in}} \frac{\cos(\kappa_{im}(y - h_i - d_i))}{\cos(\kappa_{im}d_i)} \right], \\ p_t(x, y) &= \sum_n P_{tn} \cdot e^{-\gamma_{en}x} \\ &\cdot \left[ s_y(0, h_e) \frac{\cos(\epsilon_{en}y)}{\cos(\epsilon_{en}h_e)} + s_y(h_e, h_e + d_e) \frac{\cos(\kappa_{en}(y - h_e - d_e))}{\cos(\kappa_{en}d_e)} \right], \\ v_{tx}(x, y) &= \frac{1}{jk_0 Z_0} \sum_n P_{tn} \cdot \gamma_{en} e^{-\gamma_{en}x} \\ &\cdot \left[ s_y(0, h_e) \frac{\cos(\epsilon_{en}y)}{\cos(\epsilon_{en}h_e)} - j \frac{s_y(h_e, h_e + d_e)}{\Gamma_{en} Z_{en}} \frac{\cos(\kappa_{en}(y - h_e - d_e))}{\cos(\kappa_{en}d_e)} \right]. \end{aligned} \quad (14)$$

The secular equation is:

$$\epsilon_{\beta k}^2 = k_0^2 + \gamma_{\beta k}^2 ; \quad \kappa_{\beta k}^2 = \gamma_{\beta k}^2 - \Gamma_{\beta}^2 = \epsilon_{\beta k}^2 - k_0^2 - \Gamma_{\beta}^2 . \quad (15)$$

The characteristic equation in the case of a simple porous layer is:

$$\epsilon_{\beta k} h_{\beta} \cdot \tan(\epsilon_{\beta k} h_{\beta}) = -jk_0 h_{\beta} \cdot \frac{\kappa_{\beta k}}{\Gamma_{\beta} Z_{\beta n}} \cdot \tan(\kappa_{\beta k} d_{\beta}) . \quad (16)$$

The relation of mode orthogonality is:

$$\frac{1}{h_\beta} \left[ \int_0^{h_\beta} \frac{\cos(\epsilon_{\beta m} y)}{\cos(\epsilon_{\beta m} h_\beta)} \frac{\cos(\epsilon_{\beta n} y)}{\cos(\epsilon_{\beta n} h_\beta)} dy - \frac{j}{\Gamma_{\beta n} Z_{\beta n}} \int_{h_\beta}^{h_\beta + d_\beta} \frac{\cos(\kappa_{\beta m}(y - h_\beta - d_\beta))}{\cos(\kappa_{\beta m} d_\beta)} \frac{\cos(\kappa_{\beta n}(y - h_\beta - d_\beta))}{\cos(\kappa_{\beta n} d_\beta)} dy \right] = \delta_{m,n} \cdot M_{\beta m}. \quad (17)$$

The mode norms are:

$$M_{\beta k} = \frac{1}{2 \cos^2(\epsilon_{\beta k} h_\beta)} \left[ 1 + \frac{\sin(2\epsilon_{\beta k} h_\beta)}{2\epsilon_{\beta k} h_\beta} \right] - \frac{1}{2} \frac{d_\beta}{h_\beta} \frac{j}{\Gamma_{\beta k} Z_{\beta k}} \frac{1}{\cos^2(\kappa_{\beta k} d_\beta)} \left[ 1 + \frac{\sin(2\kappa_{\beta k} d_\beta)}{2\kappa_{\beta k} d_\beta} \right]. \quad (18)$$

The mode coupling coefficients are:

$$\begin{aligned} Q'_{m,n}(h, \beta, \beta') &:= \frac{1}{h} \int_0^h \frac{\cos(\epsilon_{\beta m} y)}{\cos(\epsilon_{\beta m} h_\beta)} \frac{\cos(\epsilon_{\beta' n} y)}{\cos(\epsilon_{\beta' n} h_{\beta'})} dy \\ &= \frac{R_{m,n}(h, \beta, \beta')}{\cos(\epsilon_{\beta m} h_\beta) \cdot \cos(\epsilon_{\beta' n} h_{\beta'})}, \\ Q''_{m,n}(h_\beta, \beta, \beta') &:= \frac{1}{h_\beta} \int_{h_\beta}^{h_\beta + d_\beta} \frac{\cos(\kappa_{\beta m}(y - h_\beta - d_\beta))}{\cos(\kappa_{\beta m} d_\beta)} \frac{\cos(\epsilon_{\beta' n} y)}{\cos(\epsilon_{\beta' n} h_{\beta'})} dy \\ &= \frac{1}{\cos(\epsilon_{\beta' n} h_{\beta'}) \cos(\kappa_{\beta m} d_\beta)} \\ &\quad \cdot \left[ \frac{\epsilon_{\beta' n} h_{\beta'}}{(\epsilon_{\beta' n}^2 - \kappa_{\beta m}^2) h_\beta h_{\beta'}} \sin(\epsilon_{\beta' n}(h_\beta + d_\beta)) \right. \\ &\quad \left. - \frac{\sin(\epsilon_{\beta' n} h_\beta - \kappa_{\beta m} d_\beta)}{2(\epsilon_{\beta' n} + \kappa_{\beta m}) h_\beta} - \frac{\sin(\epsilon_{\beta' n} h_\beta + \kappa_{\beta m} d_\beta)}{2(\epsilon_{\beta' n} - \kappa_{\beta m}) h_\beta} \right] \end{aligned} \quad (19)$$

with the following combination:

$$Q_{m,n}(h, \beta, \beta') := Q'_{m,n}(h, \beta, \beta') - \frac{j}{\Gamma_{\beta n} Z_{\beta n}} Q''_{m,n}(h_\beta, \beta, \beta'). \quad (20)$$

Other coupling coefficients needed include the following:

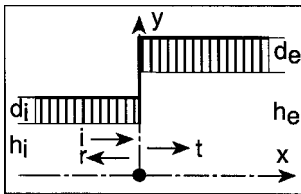
$$\begin{aligned} T'_{m,n}(h, \beta, \beta') &= \frac{1}{h_\beta} \int_h^{h_\beta} \frac{\cos(\epsilon_{\beta m} y)}{\cos(\epsilon_{\beta m} h_\beta)} \frac{\cos(\epsilon_{\beta' n} y)}{\cos(\epsilon_{\beta' n} h_{\beta'})} dy \\ &= \frac{S_{m,n}(h, \beta, \beta')}{\cos(\epsilon_{\beta m} h_\beta) \cos(\epsilon_{\beta' n} h_{\beta'})}, \end{aligned} \quad (21)$$

$$\begin{aligned}
 T''_{m,n}(h_\beta, \beta, \beta') &= \frac{1}{h_\beta} \int_{h_\beta}^{h_\beta + d_\beta} \frac{\cos(\kappa_{\beta m}(y - h_\beta - d_\beta))}{\cos(\kappa_{\beta m}d_\beta)} \frac{\cos(\kappa_{\beta n}(y - h_\beta - d_\beta))}{\cos(\kappa_{\beta n}d_\beta)} dy \\
 &= \frac{d_\beta/h_\beta}{2 \cos(\kappa_{\beta m}d_\beta) \cos(\kappa_{\beta n}d_\beta)} \\
 &\cdot \left[ \frac{\sin((\kappa_{\beta m} - \kappa_{\beta n})d_\beta)}{(\kappa_{\beta m} - \kappa_{\beta n})d_\beta} + \frac{\sin((\kappa_{\beta m} + \kappa_{\beta n})d_\beta)}{(\kappa_{\beta m} + \kappa_{\beta n})d_\beta} \right]
 \end{aligned} \tag{22}$$

with the combination:

$$T_{m,n}(h, \beta, \beta') = T'_{m,n}(h, \beta, \beta') - \frac{j}{\Gamma_{\beta n} Z_{\beta n}} T''_{m,n}(h_\beta, \beta, \beta') . \tag{23}$$

*Expanding local → local:*



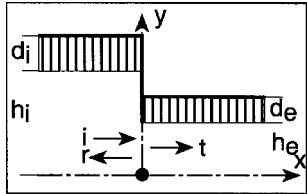
$$P_{rm} = -\delta_{\mu,m} \cdot P_{i\mu} + \frac{1}{N_{im}} \sum_n P_{tn} \cdot R_{m,n}(h_i, i, e) , \tag{24}$$

$$\begin{aligned}
 &\sum_n P_{tn} \left[ \delta_{n,k} \cdot \gamma_{ek} h_e N_{ek} + \sum_m \gamma_{im} h_i \frac{R_{m,k}(h_i, i, e) \cdot R_{m,n}(h_i, i, e)}{N_{im}} \right] \\
 &= 2 \sum_m P_{im} \gamma_{im} h_i R_{m,k}(i, e) .
 \end{aligned} \tag{25}$$

Alternatively (with reduced precision, however):

$$\begin{aligned}
 P_{tn} &= \frac{1}{\gamma_{en} h_e N_{en}} \sum_m (P_{im} - P_{rm}) \cdot \gamma_{im} h_i R_{m,n}(h_i, i, e), \\
 \sum_m P_{rm} \left[ \delta_{m,k} N_{ik} + \gamma_{im} h_i \sum_n \frac{R_{k,n}(h_i, i, e) \cdot R_{m,n}(h_i, i, e)}{\gamma_{en} h_e N_{en}} \right] \\
 &= \sum_m P_{im} \left[ -\delta_{m,k} N_{ik} + \gamma_{im} h_i \sum_n \frac{R_{k,n}(h_i, i, e) \cdot R_{m,n}(h_i, i, e)}{\gamma_{en} h_e N_{en}} \right] .
 \end{aligned} \tag{26}$$

*Contracting, local → local:*



$$P_{rm} = P_{im} - \frac{1}{\gamma_{im} h_i N_{im}} \sum_n P_{tn} \gamma_{en} h_e R_{n,m}(h_e, e, i) , \quad (27)$$

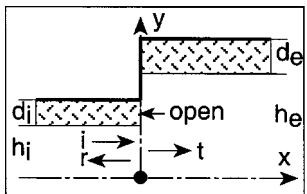
$$\begin{aligned} & \sum_n P_{tn} \left[ \delta_{k,n} N_{ek} + \gamma_{en} h_e \sum_m \frac{R_{k,m}(h_e, e, i) \cdot R_{n,m}(h_e, e, i)}{\gamma_{im} h_i N_{im}} \right] \\ & = 2 \sum_m P_{im} R_{k,m}(h_e, e, i) . \end{aligned} \quad (28)$$

Alternatively:

$$P_{tn} = \frac{1}{N_{en}} \sum_m (P_{im} + P_{rm}) R_{n,m}(h_e, e, i) , \quad (29)$$

$$\begin{aligned} & \sum_m P_{rm} \left[ \delta_{m,k} \gamma_{im} h_i N_{im} + \sum_n \gamma_{en} h_e \frac{R_{n,k}(h_e, e, i) \cdot R_{n,m}(h_e, e, i)}{N_{en}} \right] \\ & = \sum_m P_{im} \left[ \delta_{m,k} \gamma_{im} h_i N_{im} - \sum_n \gamma_{en} h_e \frac{R_{n,k}(h_e, e, i) \cdot R_{n,m}(h_e, e, i)}{N_{en}} \right] . \end{aligned} \quad (30)$$

*Expanding, lateral → lateral, open head:*



$$P_{rm} = -P_{im} + \frac{1}{M_{im}} \sum_n P_{tn} \cdot Q_{m,n}(h_i, i, e) , \quad (31)$$

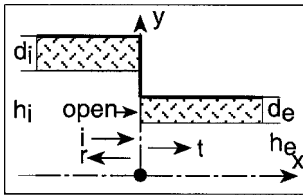
$$\begin{aligned} & \sum_n P_{tn} \left[ \delta_{n,k} \gamma_{ek} h_e M_{ek} + \sum_m \gamma_{im} h_i \frac{Q_{m,k}(h_i, i, e) \cdot Q_{m,n}(h_i, i, e)}{M_{im}} \right] \\ & = \sum_m P_{im} \gamma_{im} h_i Q_{m,k}(h_i, i, e) (1 + \delta_{m,k}) . \end{aligned} \quad (32)$$

Alternatively:

$$P_{tn} = \frac{1}{\gamma_{en} h_e M_{en}} \sum_m (P_{im} - P_{rm}) \cdot \gamma_{im} h_i Q_{m,n}(h_i, i, e), \quad (33)$$

$$\begin{aligned} & \sum_m P_{rm} \left[ \delta_{m,k} M_{ik} - \gamma_{im} h_i \sum_n \frac{Q_{k,n}(h_i, i, e) \cdot Q_{m,n}(h_i, i, e)}{\gamma_{en} h_e M_{en}} \right] \\ &= \sum_m P_{im} \left[ -\delta_{m,k} M_{ik} + \gamma_{im} h_i \sum_n \frac{Q_{k,n}(h_i, i, e) \cdot Q_{m,n}(h_i, i, e)}{\gamma_{en} h_e M_{en}} \right]. \end{aligned} \quad (34)$$

*Contracting, lateral → lateral, open head:*



$$P_{rm} = P_{im} - \frac{1}{\gamma_{im} h_i M_{im}} \sum_n P_{tn} \gamma_{en} h_e Q_{n,m}(h_e, e, i), \quad (35)$$

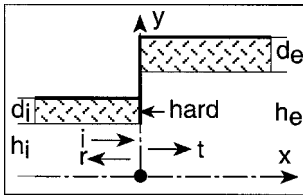
$$\begin{aligned} & \sum_n P_{tn} \left[ \delta_{n,k} M_{ek} + \gamma_{en} h_e \sum_m \frac{Q_{k,m}(h_e, e, i) \cdot Q_{n,m}(h_e, e, i)}{\gamma_{im} h_i M_{im}} \right] \\ &= \sum_m P_{im} Q_{k,m}(h_e, e, i) (1 + \delta_{m,k}). \end{aligned} \quad (36)$$

Alternatively:

$$P_{tn} = \frac{1}{M_{en}} \sum_m (P_{im} + P_{rm}) Q_{n,m}(h_e, e, i), \quad (37)$$

$$\begin{aligned} & \sum_m P_{rm} \left[ \delta_{m,k} \gamma_{ik} h_i M_{ik} + \sum_n \gamma_{en} h_e \frac{Q_{n,k}(h_e, e, i) \cdot Q_{n,m}(h_e, e, i)}{M_{en}} \right] \\ &= \sum_m P_{im} \left[ \delta_{m,k} \gamma_{ik} h_i M_{ik} - \sum_n \gamma_{en} h_e \frac{Q_{n,k}(h_e, e, i) \cdot Q_{n,m}(h_e, e, i)}{M_{en}} \right]. \end{aligned} \quad (38)$$

Expanding, lateral  $\rightarrow$  lateral, covered head:



A combined system of equations for  $\{P_{rn}, P_{tn}\}$  is:

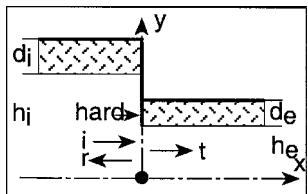
$$\sum_n P_{tn} Q'_{k,n}(h_i, i, e) - \sum_m P_{rm} \left[ \delta_{m,k} M_{ik} + \frac{j}{\Gamma_{in} Z_{in}} T''_{k,m}(h_i, i, i) \right] \quad (39)$$

$$= \sum_m P_{im} \left[ \delta_{m,k} M_{ik} - \frac{j}{\Gamma_{in} Z_{in}} T''_{k,m}(h_i, i, i) \right],$$

$$\sum_m P_{rm} \left[ \delta_{k,m} \gamma_{ik} h_i M_{ik} - \frac{h_i}{h_e} \gamma_{im} h_i \sum_n \frac{Q'_{k,n}(h_i, i, e) \cdot Q'_{m,n}(h_i, i, e)}{M_{en}} \right] \quad (40)$$

$$= \sum_m P_{im} \left[ \delta_{k,m} \gamma_{ik} h_i M_{ik} - \frac{h_i}{h_e} \gamma_{im} h_i \sum_n \frac{Q'_{k,n}(h_i, i, e) \cdot Q'_{m,n}(h_i, i, e)}{M_{en}} \right].$$

Contracting, lateral  $\rightarrow$  lateral, covered head:



A combined system of equations for  $\{P_{rn}, P_{tn}\}$  is:

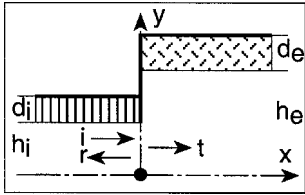
$$\sum_n P_{tn} \left[ \delta_{n,k} M_{ek} + \frac{j}{\Gamma_{en} Z_{en}} T''_{k,n}(h_e, e, e) \right] \quad (41)$$

$$- \sum_m P_{rm} Q'_{k,m}(h_e, e, i) = \sum_m P_{im} Q'_{k,m}(h_e, e, i),$$

$$\sum_m P_{rm} \left[ \delta_{m,k} \gamma_{ik} h_i M_{ik} - \gamma_{im} h_i \frac{h_e}{h_i} \sum_n \frac{Q'_{n,k}(h_e, e, i) \cdot Q'_{n,m}(h_e, e, i)}{M_{en}} \right] \quad (42)$$

$$= \sum_m P_{im} \left[ \delta_{m,k} \gamma_{ik} h_i M_{ik} - \gamma_{im} h_i \frac{h_e}{h_i} \sum_n \frac{Q'_{n,k}(h_e, e, i) \cdot Q'_{n,m}(h_e, e, i)}{M_{en}} \right].$$

Expanding, local  $\rightarrow$  lateral:



$$P_{tn} = \frac{1}{\gamma_{en} h_e M_{en} \cos(\epsilon_{en} h_e)} \sum_m (P_{im} - P_{rm}) \gamma_{im} h_i R_{m,n}(h_i, i, e), \quad (43)$$

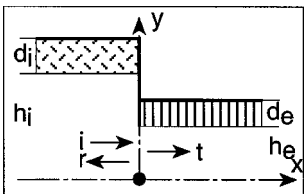
$$\begin{aligned} & \sum_m P_{rm} \left[ \delta_{m,k} N_{ik} + \gamma_{im} h_i \sum_n \frac{R_{k,n}(h_i, i, e) \cdot R_{m,n}(h_i, i, e)}{\gamma_{en} h_e M_{en} \cos^2(\epsilon_{en} h_e)} \right] \\ &= \sum_m P_{im} \left[ -\delta_{m,k} N_{im} + \gamma_{im} h_i \sum_n \frac{R_{k,n}(h_i, i, e) \cdot R_{m,n}(h_i, i, e)}{\gamma_{en} h_e M_{en} \cos^2(\epsilon_{en} h_e)} \right]. \end{aligned} \quad (44)$$

Alternatively:

$$P_{rm} = -P_{im} + \frac{1}{N_{im}} \sum_n P_{tn} \frac{R_{m,n}(h_i, i, e)}{\cos(\epsilon_{en} h_e)}, \quad (45)$$

$$\begin{aligned} & \sum_n P_{tn} \left[ \delta_{n,k} \gamma_{ek} h_e M_{ek} + \frac{1}{\cos(\epsilon_{ek} h_e) \cos(\epsilon_{en} h_e)} \right. \\ & \quad \left. \cdot \sum_m \gamma_{im} h_i \frac{R_{m,k}(h_i, i, e) \cdot R_{m,n}(h_i, i, e)}{N_{im}} \right] \\ &= \sum_m P_{im} \frac{\gamma_{im} h_i R_{m,k}(h_i, i, e)}{\cos(\epsilon_{ek} h_e)} (1 + \delta_{m,k}). \end{aligned} \quad (46)$$

Contracting, lateral  $\rightarrow$  local:



$$P_{rm} = P_{im} - \frac{1}{\gamma_{im} h_i M_{im} \cos(\epsilon_{im} h_i)} \sum_n P_{tn} \gamma_{en} h_e R_{n,m}(h_e, e, i), \quad (47)$$

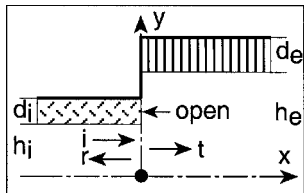
$$\begin{aligned} \sum_n P_{tn} & \left[ \delta_{n,k} N_{ek} + \gamma_{en} h_e \sum_m \frac{R_{k,m}(h_e, e, i) \cdot R_{n,m}(h_e, e, i)}{\gamma_{im} h_i M_{im} \cos^2(\epsilon_{im} h_i)} \right] \\ & = 2 \sum_m P_{im} \frac{R_{k,m}(h_e, e, i)}{\cos(\epsilon_{im} h_i)}. \end{aligned} \quad (48)$$

Alternatively:

$$P_{tn} = \frac{1}{N_{en}} \left[ \sum_m (P_{im} + P_{rm}) \frac{R_{n,m}(h_e, e, i)}{\cos(\epsilon_{im} h_i)} \right], \quad (49)$$

$$\begin{aligned} \sum_m P_{rm} & \left[ \delta_{k,m} \gamma_{ik} h_i M_{ik} + \frac{1}{\cos(\epsilon_{ik} h_i) \cos(\epsilon_{im} h_i)} \right. \\ & \cdot \left. \sum_n \gamma_{en} h_e \frac{R_{n,k}(h_e, e, i) \cdot R_{n,m}(h_e, e, i)}{N_{en}} \right] \\ & = \sum_m P_{im} \left[ \delta_{k,m} \gamma_{ik} h_i M_{ik} - \frac{1}{\cos(\epsilon_{ik} h_i) \cos(\epsilon_{im} h_i)} \right. \\ & \cdot \left. \sum_n \gamma_{en} h_e \frac{R_{n,k}(h_e, e, i) \cdot R_{n,m}(h_e, e, i)}{N_{en}} \right]. \end{aligned} \quad (50)$$

Expanding, lateral  $\rightarrow$  local, open head:



$$P_{tn} = \frac{\cos(\epsilon_{en} h_e)}{\gamma_{en} h_e N_{en}} \sum_m (P_{im} - P_{rm}) \gamma_{im} h_i Q_{m,n}(h_i, i, e), \quad (51)$$

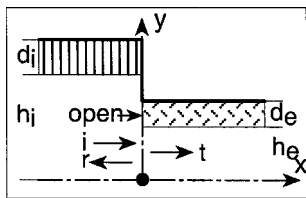
$$\begin{aligned} \sum_m P_{rm} & \left[ \delta_{m,k} M_{ik} + \gamma_{im} h_i \sum_n \cos^2(\epsilon_{en} h_e) \frac{Q_{k,n}(h_i, i, e) \cdot Q_{m,n}(h_i, i, e)}{\gamma_{en} h_e N_{en}} \right] \\ & = \sum_m P_{im} \left[ -\delta_{m,k} M_{im} + \gamma_{im} h_i \sum_n \cos^2(\epsilon_{en} h_e) \frac{Q_{k,n}(h_i, i, e) \cdot Q_{m,n}(h_i, i, e)}{\gamma_{en} h_e N_{en}} \right]. \end{aligned} \quad (52)$$

Alternatively:

$$P_{rm} = -P_{im} + \frac{1}{M_{im}} \sum_n P_{tn} Q_{m,n}(h_i, i, e) \cos(\epsilon_{en} h_e), \quad (53)$$

$$\begin{aligned}
 & \sum_n P_{tn} \left[ \delta_{n,k} \gamma_{ek} h_e N_{ek} + \cos(\epsilon_{ek} h_e) \cos(\epsilon_{en} h_e) \right. \\
 & \quad \cdot \sum_m \gamma_{im} h_i \frac{Q_{m,k}(h_i, i, e) \cdot Q_{m,n}(h_i, i, e)}{M_{im}} \Big] \\
 & = \sum_m P_{im} \gamma_{im} h_i \cos(\epsilon_{ek} h_e) Q_{m,k}(h_i, i, e) (1 + \delta_{m,k}) .
 \end{aligned} \tag{54}$$

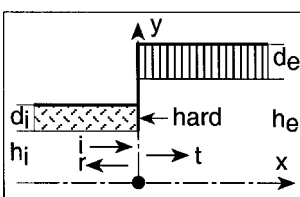
*Contracting, local  $\rightarrow$  lateral, open head:*



$$\begin{aligned}
 P_{rm} = P_{im} - \frac{1}{\gamma_{im} h_i N_{im}} \sum_n P_{tn} \gamma_{en} h_e \\
 \cdot \left[ \frac{R_{n,m}(h_e, e, i)}{\cos(\epsilon_{en} h_e)} + Q''_{n,m}(h_e, e, i) \cos(\epsilon_{im} h_i) \right] ,
 \end{aligned} \tag{55}$$

$$\begin{aligned}
 & \sum_n P_{tn} \left[ \delta_{n,k} M_{ek} + \gamma_{en} h_e \sum_m \frac{1}{\gamma_{im} h_i N_{im}} \right. \\
 & \cdot \left( \frac{R_{k,m}(h_e, e, i)}{\cos(\epsilon_{ek} h_e)} - \frac{j}{\Gamma_{en} Z_{en}} Q''_{k,m}(h_e, e, i) \cos(\epsilon_{im} h_i) \right) \\
 & \cdot \left. \left( \frac{R_{n,m}(h_e, e, i)}{\cos(\epsilon_{en} h_e)} + Q''_{n,m}(h_e, e, i) \cos(\epsilon_{im} h_i) \right) \right] \\
 & = \sum_m P_{im} \left[ \frac{R_{k,m}(h_e, e, i)}{\cos(\epsilon_{ek} h_e)} - \frac{j}{\Gamma_{en} Z_{en}} Q''_{k,m}(h_e, e, i) \cos(\epsilon_{im} h_i) \right] (1 + \delta_{m,k}) .
 \end{aligned} \tag{56}$$

*Expanding, lateral  $\rightarrow$  local, covered head:*

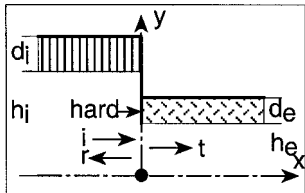


Two combined systems of equations for the  $P_{rn}$ ,  $P_{tn}$ :

$$\begin{aligned} & \sum_m P_{rm} \left[ \delta_{m,k} \gamma_{ik} h_i N_{ik} - \gamma_{im} h_i \frac{h_i}{h_e} \sum_n \cos^2(\epsilon_{en} h_e) \frac{Q'_{k,n}(h_i, i, e) \cdot Q'_{m,n}(h_i, i, e)}{N_{ek}} \right] \\ &= \sum_m P_{im} \left[ \delta_{m,k} \gamma_{ik} h_i N_{ik} - \gamma_{im} h_i \frac{h_i}{h_e} \sum_n \cos^2(\epsilon_{en} h_e) \frac{Q'_{k,n}(h_i, i, e) \cdot Q'_{m,n}(h_i, i, e)}{N_{ek}} \right], \end{aligned} \quad (57)$$

$$\begin{aligned} & \sum_n P_{tn} Q'_{k,n}(h_i, i, e) \cos(\epsilon_{en} h_e) - \sum_m P_{rm} \left[ \delta_{m,k} M_{ik} + \frac{j}{\Gamma_{in} Z_{in}} T''_{k,m}(h_i, i, i) \right] \\ &= \sum_m P_{im} \left[ \delta_{m,k} M_{ik} + \frac{j}{\Gamma_{in} Z_{in}} T''_{k,m}(h_i, i, i) \right]. \end{aligned} \quad (58)$$

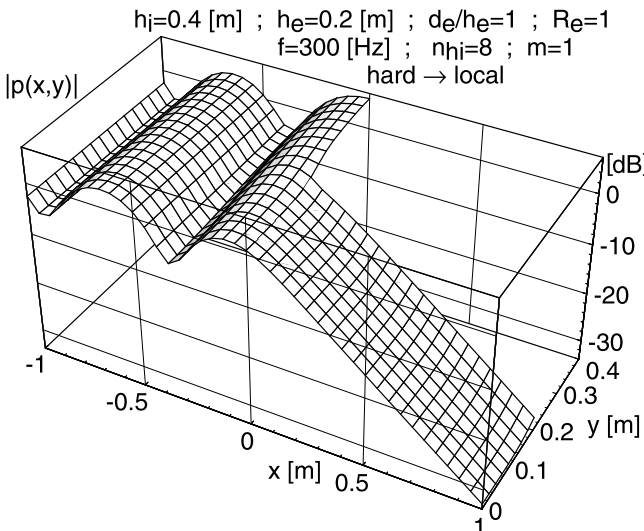
*Contracting, local  $\rightarrow$  lateral, covered head:*



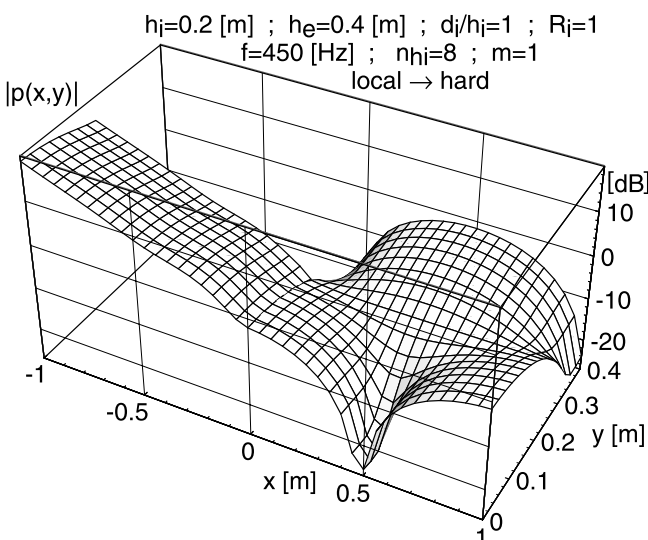
Two combined systems of equations for the  $P_{rn}$ ,  $P_{tn}$ :

$$\begin{aligned} & \sum_m P_{rm} \left[ \delta_{m,k} \gamma_{ik} h_i N_{ik} - \cos(\epsilon_{ik} h_i) \cos(\epsilon_{im} h_i) \right. \\ & \quad \left. \cdot \sum_n \gamma_{en} h_e \frac{Q'_{n,k}(h_e, e, i) \cdot Q'_{n,m}(h_e, e, i)}{M_{en}} \right] \\ &= \sum_m P_{im} \left[ \delta_{m,k} \gamma_{ik} h_i N_{ik} - \cos(\epsilon_{ik} h_i) \cos(\epsilon_{im} h_i) \right. \\ & \quad \left. \cdot \sum_n \gamma_{en} h_e \frac{Q'_{n,k}(h_e, e, i) \cdot Q'_{n,m}(h_e, e, i)}{M_{en}} \right], \end{aligned} \quad (59)$$

$$\begin{aligned} & \sum_m P_{rm} Q'_{k,m}(h_e, e, i) \cos(\epsilon_{im} h_e) - \sum_n P_{tn} \left[ \delta_{n,k} M_{ek} + \frac{j}{\Gamma_{en} Z_{en}} T''_{k,n}(h_e, e, e) \right] \\ &= - \sum_m P_{im} Q'_{k,m}(h_e, e, i) \cos(\epsilon_{im} h_e). \end{aligned} \quad (60)$$



Sound pressure magnitude at a contracting duct step from hard to locally absorbing duct for the lowest duct mode incident

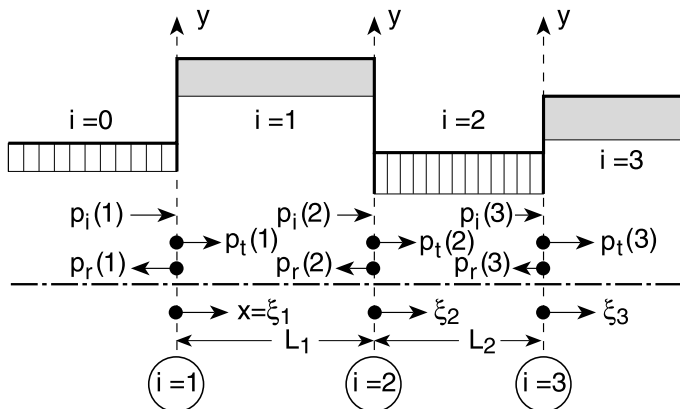


Sound pressure magnitude at an expanding duct step from a locally absorbing duct to a hard duct with the least attenuated mode as incident wave. The first higher mode in the hard duct is a cut-on mode

## J.19 Sections and Cascades of Silencers, no Feedback

► See also: Mechel, Vol. III, Ch. 34 (1998)

Lined duct sections  $i = 1, 2, 3, \dots$  have finite lengths  $L_i$  (except the entrance duct  $i = 0$  and the last duct). The ducts may have bulk or locally reacting linings or be hard. The (half) duct heights are  $h_i$ .



The condition is that there *is no feedback*, i.e. at a duct step  $i$  the reflected waves from the steps  $i - 1$  and/or  $i + 1$  can be neglected.

$$\text{Axial section co-ordinates are } \xi_i \text{ with: } x = \xi_i + \begin{cases} 0; & i = 1 \\ \sum_{k=1}^{i-1} L_k; & i > 1 \end{cases} \quad (1)$$

The incident wave is a sum of modes of the duct  $i = 0$  with a list of amplitudes  $\{P_{im}(1)\}$  or a single mode with amplitude  $P_{iu}(1)$  (note that the index  $i$  in field components and amplitudes counts the duct steps).

The field formulations of the incident wave  $p_i(i)$ , reflected wave  $p_r(i)$ , and transmitted wave  $p_t(i)$  at the  $i$ th duct step are:

$$\begin{aligned} p_i(i) &= p_i(i, \xi_i, y) = \sum_m p_{im}(i, \xi_i, y) = \sum_m P_{im}(i) \cdot q_m(i-1, y) \cdot e^{-\gamma_m(i-1) \cdot \xi_i}, \\ p_i(1) &= p_i(1, \xi_1, y) = \sum_m p_{im}(1, \xi_1, y) = \sum_m P_{im}(1) \cdot q_m(0, y) \cdot e^{-\gamma_m(0) \cdot \xi_1}, \\ p_r(i) &= p_r(i, \xi_i, y) = \sum_m p_{rm}(i, \xi_i, y) = \sum_m P_{rm}(i) \cdot q_m(i-1, y) \cdot e^{+\gamma_m(i-1) \cdot \xi_i}, \\ p_t(i) &= p_t(i, \xi_i, y) = \sum_n p_{tn}(i, \xi_i, y) = \sum_n P_{tn}(i) \cdot q_n(i, y) \cdot e^{-\gamma_n(i) \cdot \xi_i}. \end{aligned} \quad (2)$$

The  $p_{\beta k}(i, \xi_i, y)$ ,  $\beta = i, r, t$ , are the mode components;  $q_m(i, y)$  are their lateral profiles; and  $P_{\beta k}(i)$  are their amplitudes. The secular equations between lateral mode wave number  $\varepsilon_k(i)$  and axial propagation constant  $\gamma_k(i)$  are:

$$\gamma_k^2(i) = \epsilon_k^2(i) - k_0^2 \quad \text{if the field is constant in the } z \text{ direction ,} \quad (3)$$

$$\gamma_k^2(i) = \epsilon_k^2(i) - k_0^2 - \epsilon_z^2(i) \quad \text{if there is a mode in the } z \text{ direction .} \quad (4)$$

The lateral wave numbers are solutions of the characteristic equation in duct section i. The lateral mode pressure profiles are:

$$q_n(i, y) = \begin{cases} \cos(\epsilon_n(i)y) & ; \text{ locally reacting} \\ s_y(0, h_i) \frac{\cos(\epsilon_n(i)y)}{\cos(\epsilon_n(i)h_i)} \\ + s_y(h_i, h_i + d_i) \frac{\cos(\kappa_n(i)(y - h_i - d_i))}{\cos(\kappa_n(i)d_i)} & ; \text{ bulk reacting} \end{cases} \quad (5)$$

the lateral profiles of the axial particle velocity are:

$$q_{vn}(i, y) = \begin{cases} \cos(\epsilon_n(i)y) & ; \text{ locally reacting} \\ s_y(0, h_i) \frac{\cos(\epsilon_n(i)y)}{\cos(\epsilon_n(i)h_i)} \\ - \frac{j s_y(h_i, h_i + d_i) \cos(\kappa_n(i)(y - h_i - d_i))}{\Gamma_{in} Z_{in}} & ; \text{ bulk reacting} \end{cases} \quad (6)$$

with the “switch function”  $s_y(a, b) := \begin{cases} 1 & ; a \leq y < b \\ 0 & ; \text{else} \end{cases}$ ; the (half) duct height  $h_i$  and the layer thickness  $d_i$  for a bulk reacting absorber consisting of a simple porous layer with normalised characteristic values  $\Gamma_{in}, Z_{in}$ .

The identity  $p_{im}(i+1, \xi_{i+1}, y) = p_{tm}(i, \xi_i, y); i = 1, 2, \dots, I-1$

leads to  $P_{im}(i+1) = P_{tm}(i) \cdot e^{-\gamma_m(i) \cdot L_i}; i = 1, 2, \dots, I-1$ , (7)

where the  $P_{im}(1)$  are given.

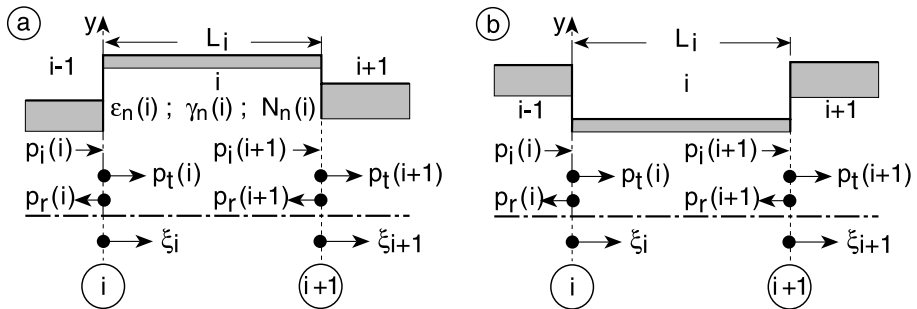
The field evaluation is an iterative procedure which uses the equations of the previous  
 ➤ Sect. J.18. Begin with the given  $P_{im}(1)$  and evaluate with those equations the transmitted mode amplitudes  $P_{tm}(1)$  at the first duct step. With the last relation from above, they give the incident mode amplitudes  $P_{im}(i+1)$  at the next step. Repeat the evaluation until the last step.

## J.20 A Section with Feedback Between Sections Without Feedback

---

► See also: Mechel, Vol. III, Ch. 34 (1998)

A duct section is said to have feedback if the reflected waves from its exit influence the boundary conditions at its entrance. Neglecting feedback (because the section is long and/or its attenuation is high) simplifies the field evaluation in cascades to a straightforward computation. Feedback in all sections, on the other hand, leads to chains of systems of equations. The amount of computational work is still reasonably low if only one section is assumed to have feedback between sections without feedback.



These sketches show two examples of a duct section  $i$  with feedback between duct sections  $i - 1$  and  $i + 1$  without feedback.  $\epsilon_n(i)$ ,  $\gamma_n(i)$ ,  $N_n(i)$  are, respectively, the lateral mode wave numbers, axial mode propagation constants, and mode norms in section  $i$ . The (half) duct height are  $h_i$ ;  $\xi_i$  are the axial co-ordinates of the sections (► Sect. J.18).

Sound pressure and axial particle velocity conditions at the entrance  $\xi_i = 0$  of the  $i$ -th section are:

$$\begin{aligned} & \sum_m (P_{im}(i) + P_{rm}(i)) \cdot \cos(\epsilon_n(i-1)y) \\ &= \sum_n (P_{tn}(i) + P_{rn}(i+1) \cdot e^{-\gamma_n(i) \cdot L_i}) \cdot \cos(\epsilon_n(i)y), \end{aligned} \quad (1)$$

$$\begin{aligned} & \sum_m (P_{im}(i) - P_{rm}(i)) \gamma_n(i-1) \cdot \cos(\epsilon_n(i-1)y) \\ &= \sum_n (P_{tn}(i) - P_{rn}(i+1) \cdot e^{-\gamma_n(i) \cdot L_i}) \gamma_n(i) \cdot \cos(\epsilon_n(i)y). \end{aligned} \quad (2)$$

Sound pressure and axial particle velocity conditions at the exit  $\xi_i = L_i$  of the  $i$ -th section are:

$$\begin{aligned} & \sum_n (P_{tn}(i) \cdot e^{-\gamma_n(i) \cdot L_i} + P_{rn}(i+1)) \cdot \cos(\epsilon_n(i)y) \\ &= \sum_n P_{tn}(i+1) \cdot \cos(\epsilon_n(i+1)y), \end{aligned} \quad (3)$$

$$\begin{aligned} & \sum_n (P_{tn}(i) \cdot e^{-\gamma_n(i) \cdot L_i} - P_{rn}(i+1)) \gamma_n(i) \cdot \cos(\epsilon_n(i)y) \\ &= \sum_n P_{tn}(i+1) \gamma_n(i+1) \cdot \cos(\epsilon_n(i+1)y). \end{aligned} \quad (4)$$

The special case of a wide section  $i$  with a locally reacting lining between narrow sections  $i - 1$  and  $i + 1$  with locally reacting linings (see sketch (a) above) is as follows.

There exist two coupled linear systems of equations for the double vector of amplitudes  $\{P_{tn}(i), P_{rn}(i+1)\}$  (the mode coupling coefficients  $R_{m,n}(h, \beta, \beta')$  are defined in  $\Rightarrow$  Sect. J.18):

$$\begin{aligned} & \sum_n P_{tn}(i) \left[ \delta_{k,n} \gamma_k(i) h_i N_k(i) + \sum_m \gamma_m(i-1) h_{i-1} \frac{R_{m,k}(h_{i-1}, i-1, i) \cdot R_{m,n}(h_{i-1}, i-1, i)}{N_m(i-1)} \right] \\ & - \sum_n P_{rn}(i+1) e^{-\gamma_n(i) \cdot L_i} \\ & \cdot \left[ \delta_{k,n} \gamma_k(i) h_i N_k(i) - \sum_m \gamma_m(i-1) h_{i-1} \frac{R_{m,k}(h_{i-1}, i-1, i) \cdot R_{m,n}(h_{i-1}, i-1, i)}{N_m(i-1)} \right] \\ & = 2 \sum_m P_{im}(i) \gamma_m(i-1) h_{i-1} R_{m,k}(h_{i-1}, i-1, i) \end{aligned} \quad (5)$$

and

$$\begin{aligned} & \sum_n P_{tn}(i) e^{-\gamma_n(i) \cdot L_i} \\ & \cdot \left[ \delta_{k,n} \gamma_k(i) h_i N_k(i) - \sum_m \gamma_m(i+1) h_{i+1} \frac{R_{m,k}(h_{i+1}, i+1, i) \cdot R_{m,n}(h_{i+1}, i+1, i)}{N_m(i+1)} \right] \\ & - \sum_n P_{rn}(i+1) \\ & \cdot \left[ \delta_{k,n} \gamma_k(i) h_i N_k(i) + \sum_m \gamma_m(i+1) h_{i+1} \frac{R_{m,k}(h_{i+1}, i+1, i) \cdot R_{m,n}(h_{i+1}, i+1, i)}{N_m(i+1)} \right] = 0. \end{aligned} \quad (6)$$

Using the solutions evaluate:

$$P_{tm}(i+1) = \frac{1}{N_m(i+1)} \sum_n (P_{tn}(i) \cdot e^{-\gamma_n(i) \cdot L_i} + P_{rn}(i+1)) \cdot R_{m,n}(h_{i+1}, i+1, i), \quad (7)$$

$$P_{rm}(i) = -P_{im}(i) + \frac{1}{N_m(i-1)} \sum_n (P_{tn}(i) + P_{rn}(i+1) e^{-\gamma_n(i) \cdot L_i}) \cdot R_{m,n}(h_{i-1}, i-1, i). \quad (8)$$

The special case of a narrow section  $i$  between wider sections  $i-1$  and  $i+1$ , all with locally reacting lining (see sketch (b) above), is as follows:

There exist two coupled linear systems of equations for the double vector of amplitudes  $\{P_{tn}(i), P_{rn}(i+1)\}$ :

$$\begin{aligned} & \sum_n P_{tn}(i) \left[ \delta_{k,n} N_k(i) + \gamma_n(i) h_i \sum_m \frac{R_{k,m}(h_i, i, i-1) \cdot R_{n,m}(h_i, i, i-1)}{\gamma_m(i-1) h_{i-1} N_m(i-1)} \right] \\ & + \sum_n P_{rn}(i+1) e^{-\gamma_n(i) L_i} \left[ \delta_{k,n} N_k(i) - \gamma_n(i) h_i \sum_m \frac{R_{k,m}(h_i, i, i-1) \cdot R_{n,m}(h_i, i, i-1)}{\gamma_m(i-1) h_{i-1} N_m(i-1)} \right] \\ & = 2 \sum_m P_{im}(i) R_{k,m}(h_i, i, i-1) \end{aligned} \quad (9)$$

and

$$\sum_n P_{tn}(i) e^{-\gamma_n(i) \cdot L_i} \left[ \delta_{k,n} N_k(i) - \gamma_n(i) h_i \sum_m \frac{R_{k,m}(h_i, i, i+1) \cdot R_{n,m}(h_i, i, i+1)}{\gamma_m(i+1) h_{i+1} N_m(i+1)} \right] + \sum_n P_{rn}(i+1) \left[ \delta_{k,n} N_k(i) + \gamma_n(i) h_i \sum_m \frac{R_{k,m}(h_i, i, i+1) \cdot R_{n,m}(h_i, i, i+1)}{\gamma_m(i+1) h_{i+1} N_m(i+1)} \right] = 0. \quad (10)$$

Using the solutions evaluate:

$$\begin{aligned} P_{tm}(i+1) &= \frac{1}{\gamma_m(i+1) h_{i+1} N_m(i+1)} \\ &\cdot \sum_n (P_{tn}(i) e^{-\gamma_n(i) \cdot L_i} - P_{rn}(i+1)) \gamma_n(i) h_i R_{n,m}(h_i, i, i+1), \\ P_{rm}(i) &= P_{im}(i) - \frac{1}{\gamma_m(i-1) h_{i-1} N_m(i-1)} \\ &\cdot \sum_n (P_{tn}(i) - P_{rn}(i+1) e^{-\gamma_n(i) \cdot L_i}) \gamma_n(i) h_i R_{n,m}(h_i, i, i-1). \end{aligned} \quad (11)$$

Other step configurations, as in Sect. J.18, can be treated as follows. The equations at the exit of section  $i$  do not change with feedback. The equations at the entrance are modified by:

$$\begin{aligned} P_{tn}(i) &\rightarrow (P_{tn}(i) + P_{rn}(i+1) e^{-\gamma_n(i) \cdot L_i}) ; && \text{pressure,} \\ P_{tn}(i) \gamma_n(i) &\rightarrow (P_{tn}(i) - P_{rn}(i+1) e^{-\gamma_n(i) \cdot L_i}) \gamma_n(i); && \text{axial velocity.} \end{aligned} \quad (12)$$

The systems of equations from the boundary conditions at the entrance will have the form:

$$\begin{aligned} \sum_n P_{tn}(i) [\delta_{k,n} \cdot A_k + B_{k,n}] &\mp \sum_n P_{rn}(i+1) e^{-\gamma_n(i) \cdot L_i} [\delta_{k,n} \cdot A_k - B_{k,n}] \\ &= \sum_m P_{im}(i) \cdot C_{k,m}; \quad \left\{ \begin{array}{l} \text{expanding} \\ \text{contracting} \end{array} \right.. \end{aligned} \quad (13)$$

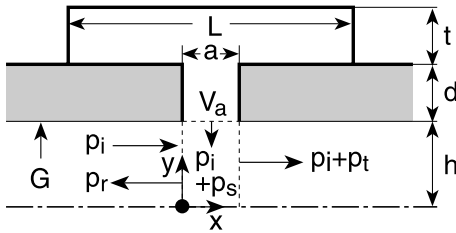
The  $A_k$ ,  $B_{k,n}$ ,  $C_{k,m}$  can be taken from the corresponding systems for sections without feedback.

## J.21 Concentrated Absorber in an Otherwise Homogeneous Lining

---

► See also: Mechel, Vol. III, Ch. 35 (1998)

Sometimes the attenuation produced by a homogeneous lining (say, locally reacting with an admittance  $G$ ) shall be improved around some (preferably low) frequency. The idea is to place some isolated resonators into the lining; the resonator orifice is the “concentrated absorber”.



The task is treated with the method of a fictitious volume source in the orifice, having the particle velocity  $V_a$ . The sound field  $p = p_r + p_s + p_t$  which the source produces in the duct satisfies the inhomogeneous wave equation:

$$(\Delta + k_0^2) p(x, y) = -jk_0 Z_0 \cdot V_a(x_0) dx_0 \cdot \delta(x - x_0) \cdot \delta(y - y_0) \quad (1)$$

with  $y_0 = h$ ;  $0 \leq x_0 \leq a$ . The Dirac delta function  $\delta(y - y_0)$  is synthesised with modes of the homogeneously lined duct having the lateral profiles  $q_n(y)$  and axial propagation constants  $\gamma_n$ , and the mode norms  $N_{hn}$ :

$$\delta(y - y_0) = \sum_n c_n \cdot q_n(y); \quad c_n = \frac{q_n(y_0)}{y_0 \cdot N_{hn}}; \quad N_{hn} = \frac{1}{h} \int_0^h q_n^2(y) dy. \quad (2)$$

The sound pressure contribution  $dp(x, y)$  of the elementary source  $V_a(x_0) \cdot dx_0$  is:

$$dp(x, y) = \frac{jk_0 Z_0 V_a(x_0) dx_0}{2h} \sum_n \frac{q_n(h) \cdot q_n(y)}{\gamma_n N_{hn}} e^{-\gamma_n |x-x_0|}. \quad (3)$$

The source contributions  $p_r, p_s, p_t$  ahead of, in front of, and after the orifice are:

$$\begin{aligned} p_r(x, y) &= \frac{jk_0 a}{2} \sum_n \frac{q_n(h)}{\gamma_n h N_{hn}} \cdot q_n(y) e^{+\gamma_n x} \cdot I_{rn}(0); \quad x < 0, \\ p_s(x, y) &= \frac{jk_0 a}{2} \sum_n \frac{q_n(h)}{\gamma_n h N_{hn}} \cdot q_n(y) [e^{-\gamma_n x} \cdot I_{tn}(x) + e^{+\gamma_n x} \cdot I_{rn}(x)]; \quad 0 < x < a, \\ p_t(x, y) &= \frac{jk_0 a}{2} \sum_n \frac{q_n(h)}{\gamma_n h N_{hn}} \cdot q_n(y) e^{-\gamma_n x} \cdot I_{tn}(a); \quad x > a \end{aligned} \quad (4)$$

with the integrals

$$I_{rn}(x) := \frac{1}{a} \int_x^a Z_0 V_a(x_0) \cdot e^{-\gamma_n x_0} dx_0; \quad I_{tn}(x) := \frac{1}{a} \int_0^x Z_0 V_a(x_0) \cdot e^{+\gamma_n x_0} dx_0. \quad (5)$$

If the source occupies a resonator neck  $0 \leq x \leq a$  with hard walls, its velocity profile can be synthesised as follows:

$$V_a(x_0) = \sum_m A_m \cos(k_{xm} x_0), \quad (6)$$

which leads to:

$$It_n(x) = \sum_m A_m It_{n,m}(x); \quad Ir_n(x) = \sum_m A_m Ir_{n,m}(x) \quad (7)$$

with

$$\begin{aligned} It_{n,m}(x) &:= \frac{1}{a} \int_0^x \cos(k_{xm}x_0) \cdot e^{+\gamma_n x_0} dx_0 \\ &= \gamma_n a \frac{-1 + e^{+\gamma_n x}}{(\gamma_n a)^2 + (m\pi)^2} (\cos(m\pi x/a) + (m\pi/\gamma_n a) \sin(m\pi x/a)) \\ &\xrightarrow{x=a} \gamma_n a \frac{-1 + (-1)^m e^{+\gamma_n a}}{(\gamma_n a)^2 + (m\pi)^2} \\ &\xrightarrow{m=0} \frac{-1 + e^{+\gamma_n x}}{\gamma_n a} \xrightarrow{x=a} \frac{-1 + e^{+\gamma_n a}}{\gamma_n a}; \end{aligned} \quad (8)$$

$$\begin{aligned} Ir_{n,m}(x) &:= \frac{1}{a} \int_x^a \cos(k_{xm}x_0) \cdot e^{-\gamma_n x_0} dx_0 \\ &= \gamma_n a \frac{(-1)^{m+1} e^{-\gamma_n a} + e^{-\gamma_n x}}{(\gamma_n a)^2 + (m\pi)^2} (\cos(m\pi x/a) - (m\pi/\gamma_n a) \sin(m\pi x/a)) \\ &\xrightarrow{x=0} \gamma_n a \frac{1 - (-1)^m e^{-\gamma_n a}}{(\gamma_n a)^2 + (m\pi)^2} \\ &\xrightarrow{m=0} \frac{e^{-\gamma_n x} - e^{+\gamma_n a}}{\gamma_n a} \xrightarrow{x=0} \frac{1 - e^{-\gamma_n a}}{\gamma_n a}. \end{aligned} \quad (9)$$

*Special case:* • The  $\mu$ -th mode of the homogeneous duct is the incident wave  $p_i$ ;  
• only a plane wave is in the resonator neck.

$$p_i(x, y) = P_{i\mu} \cdot \cos(\epsilon_\mu y) \cdot e^{-\gamma_\mu x}; \quad -\infty < x < +\infty. \quad (10)$$

The field formulations with  $q_n(y) = \cos(\epsilon_n y)$  are as follows:

$$\begin{aligned} p_r(x, y) &= \sum_n P_{rn} \cdot \cos(\epsilon_n y) \cdot e^{+\gamma_n x}; \quad -\infty < x < 0, \\ p_t(x, y) &= \sum_n P_{tn} \cdot \cos(\epsilon_n y) \cdot e^{-\gamma_n x}; \quad a < x < \infty, \\ p_s(x, y) &= \sum_n P_{sn} \cdot \cos(\epsilon_n y) \cdot [a_n(x) + b_n e^{+\gamma_n x} + c_n e^{-\gamma_n x}]; \quad 0 < x < a. \end{aligned} \quad (11)$$

The lateral mode wave numbers  $\varepsilon_n h$  are solutions of the characteristic equation:

$$\varepsilon_n h \cdot \tan(\varepsilon_n h) = j \cdot k_0 h Z_0 G =: j \cdot U ; \quad n = 1, 2, \dots , \quad (12)$$

and have the following axial wave numbers and mode norms:

$$\begin{aligned} \gamma_n h &= \sqrt{(\varepsilon_n h)^2 - (k_0 h)^2} \xrightarrow[G=0]{} \sqrt{((n-1)\pi)^2 - (k_0 h)^2}, \\ N_{hn} &= \frac{1}{2} \left( 1 + \frac{\sin(2\varepsilon_n h)}{2\varepsilon_n h} \right) \xrightarrow[G=0]{} \frac{1}{\delta_{n-1}} ; \quad \delta_i = \begin{cases} 1; i = 0 \\ 2; i > 0 \end{cases} . \end{aligned} \quad (13)$$

The particle velocity profile  $V_a(x_0)$  of the fictitious source is:

$$-V_a(x_0) = v_{ay}(x_0) - G \cdot p_i(x_0, h) . \quad (14)$$

If, on the other hand, the orifice input admittance  $G_a$  is known, then:

$$\begin{aligned} -V_a(x_0) &\approx G_a \cdot \langle p_i(x_0, h) + p_s(x_0, h) \rangle_a - G \cdot \langle p_i(x_0, h) \rangle_a ; \quad 0 < x_0 < a \\ &= \langle p_i(x_0, h) \rangle_a \cdot (G_a - G) - \langle p_s(x_0, h) \rangle_a \cdot G_a \end{aligned} \quad (15)$$

(with  $\langle \dots \rangle_a$  the average over the orifice) and  $V_a(x_0) \rightarrow \langle V_a(x_0) \rangle \rightarrow A_0$ .

This gives:

$$\begin{aligned} p_r(x, y) &= \frac{j k_0 h}{2} Z_0 A_0 \sum_n \frac{1 - e^{-\gamma_n a}}{(\gamma_n h)^2 N_{hn}} q_n(h) \cdot q_n(y) e^{+\gamma_n x} ; \quad x < 0 , \\ p_s(x, y) &= \frac{j k_0 h}{2} Z_0 A_0 \sum_n \frac{1}{(\gamma_n h)^2 N_{hn}} q_n(h) \\ &\quad \cdot q_n(y) [2 - e^{-\gamma_n x} + e^{+\gamma_n (x-a)}] ; \quad 0 < x < a , \\ p_t(x, y) &= \frac{j k_0 h}{2} Z_0 A_0 \sum_n \frac{-1 + e^{+\gamma_n a}}{(\gamma_n h)^2 N_{hn}} q_n(h) \cdot q_n(y) e^{-\gamma_n x} ; \quad x > a \end{aligned} \quad (16)$$

with the following required average values:

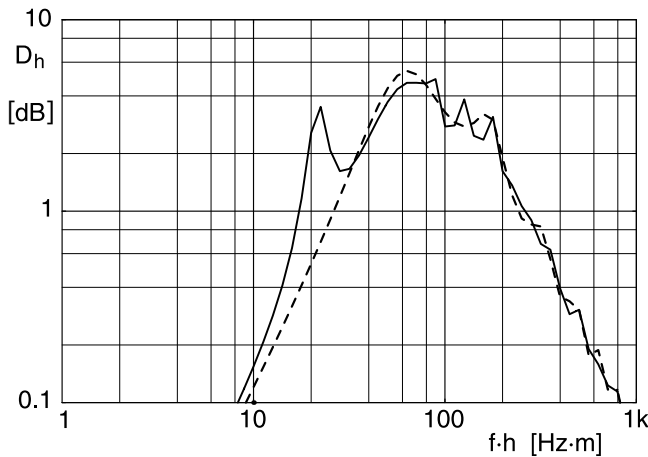
$$\begin{aligned} \langle p_i(x, h) \rangle_a &= P_{ip} q_p(h) \frac{1 - e^{-\gamma_p a}}{\gamma_p a} , \\ \langle p_s(x, h) \rangle_a &= j Z_0 A_0 k_0 h \sum_n \frac{q_n^2(h)}{(\gamma_n h)^2 N_{hn}} \left( 1 - \frac{1 - e^{-\gamma_n a}}{\gamma_n a} \right) . \end{aligned} \quad (17)$$

The final equation for  $A_0$  is:

$$\begin{aligned} Z_0 A_0 &= \left[ P_{ip} q_p(h) \frac{1 - e^{-\gamma_p a}}{\gamma_p a} (Z_0 G_a - Z_0 G) \right] \\ &\quad \cdot \left[ 1 + j Z_0 G_a k_0 h \sum_n \frac{q_n^2(h)}{(\gamma_n h)^2 N_{hn}} \left( 1 - \frac{1 - e^{-\gamma_n a}}{\gamma_n a} \right) \right]^{-1} . \end{aligned} \quad (18)$$

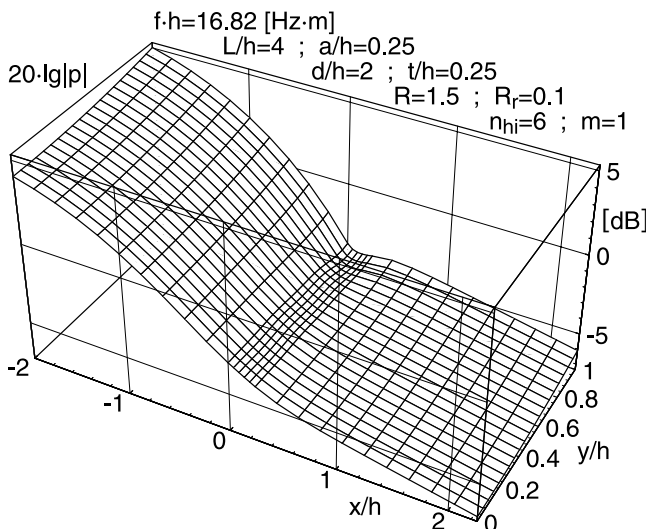
The numerical example shows the attenuation  $D_h = -\Delta L/h$  as the sound pressure level decreases per travel distance  $h$  in a duct with a (locally reacting) porous layer of thickness  $d$  and a normalised flow resistance  $R = \Xi \cdot d/Z_0$  having T-shaped Helmholtz

resonators (see initial sketch) at distances  $L$  with an orifice width  $a$  and a normalised flow resistance  $R_r$  in the orifice (e.g. by a wire mesh). The lowest duct mode  $\mu = 1$  is incident.



Attenuation  $D_h$  in a duct with homogeneous lining (dashed line) and additional T-shaped Helmholtz resonators (solid line).

Input parameters:  $L/h = 4$ ;  $a/h = 0.25$ ;  $d/h = 1$ ;  $t/h = 0.25$ ;  $R = 1.5$ ;  $R_r = 0.1$ ;  $n_{hi} = 6$ ;  $\mu = 1$



Sound pressure magnitude in a lined duct with single T-shaped Helmholtz resonators, at the resonance frequency.

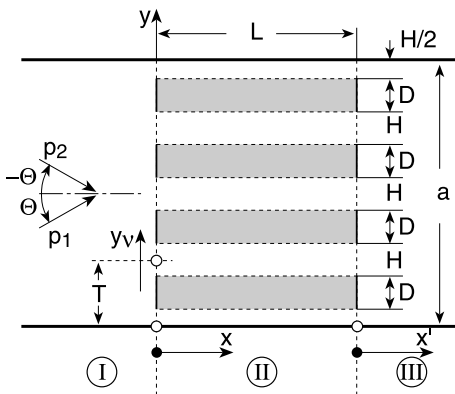
Input parameters:  $f \cdot h = 16.82$  [Hz · m];  $L/h = 4$ ;  $a/h = 0.25$ ;  $d/h = 2$ ;  $t/h = 0.25$ ;  $R = 1.5$ ;  $R_r = 0.1$ ;  $n_{hi} = 6$ ;  $\mu = 1$

## J.22 Wide Splitter-Type Silencer with Locally Reacting Splitters

► See also: Mechel, Vol. III, Ch. 36 (1998)

Splitters (or “baffles”) with thickness  $D = 2d$  and length  $L$  are at mutual distances  $H = 2h$ . They form a periodic structure with period length  $T = D + H$ . The heads of the splitters are hard.

This section treats an arrangement with many splitters, i. e. with a large lateral extent  $a$ . A single plane wave  $p_1$  is assumed as the incident wave. The next section will treat splitters in a hard duct; then an additional mirror-reflected wave  $p_2$  will be incident, and the angle  $\Theta$  of incidence is determined so that  $p_1 + p_2$  make a mode of the hard duct.



Incident plane wave:

$$p_1(x, y) = P_1 \cdot e^{-jk_x x} \cdot e^{-jk_y y}; \quad v_{1x}(x, y) = \frac{k_x}{k_0 Z_0} \cdot p_1(x, y), \quad (1)$$

$$k_x = k_0 \cos \Theta; \quad k_y = k_0 \sin \Theta.$$

Backscattered wave  $p_s$  as the sum of spatial harmonics is:

$$p_s(x, y) = \sum_{n=-\infty}^{+\infty} A_n \cdot e^{jk_n x} \cdot e^{-j\beta_n y}, \quad (2)$$

$$\beta_n = \beta_0 + \frac{2\pi n}{T}; \quad n = 0, \pm 1, \pm 2, \dots; \quad \beta_0 = k_y = k_0 \sin \Theta,$$

$$\kappa_0 = k_x = k_0 \cos \Theta; \quad \kappa_n = \sqrt{k_0^2 - \beta_n^2} = k_0 \sqrt{1 - (\sin \Theta + n\lambda_0/T)^2}.$$

The field in Zone I  $p_I = p_1 + p_s$  is:

$$p_I(x, y) = P_1 e^{-jk_x x} e^{-jk_y y} + \sum_{n=-\infty}^{+\infty} A_n \cdot e^{jk_n x} \cdot e^{-j\beta_n y}, \quad (3)$$

$$v_{Ix}(x, y) = \frac{j}{k_0 Z_0} \frac{\partial p_{I1}}{\partial x} = \frac{k_x}{k_0 Z_0} P_1 e^{-jk_x x} e^{-jk_y y} - \frac{1}{Z_0} \sum_{n=-\infty}^{+\infty} \frac{\kappa_n}{k_0} A_n \cdot e^{jk_n x} \cdot e^{-j\beta_n y}.$$

The field in Zone III is:

$$\begin{aligned} p_{III}(x', y) &= \sum_{n=-\infty}^{+\infty} D_n e^{-jk_n x'} e^{-j\beta_n y} = e^{-j\beta_0 y} \sum_{n=-\infty}^{+\infty} D_n e^{-jk_n x'} e^{-jn2\pi y/T}, \\ v_{IIIx}(x', y) &= \frac{1}{Z_0} e^{-j\beta_0 y} \sum_{n=-\infty}^{+\infty} D_n \frac{k_n}{k_0} e^{-jk_n x'} e^{-jn2\pi y/T}. \end{aligned} \quad (4)$$

The field in the  $v$ -th splitter duct in Zone II as the sum of silencer modes is:

$$p_{II}(x, y_v) = e^{-j\beta_0 v T} \sum_{m=0}^{\infty} [B_m e^{-\gamma_m x} + C_m e^{+\gamma_m x}] \cdot q_m(y_v) \quad (5)$$

with the following lateral mode profiles:

$$q_m(y_v) = \begin{cases} \cos(\epsilon_m y_v); & m = 0, 2, 4, \dots \\ \sin(\epsilon_m y_v); & m = 1, 3, 5, \dots \end{cases}; \quad \gamma_m = \sqrt{\epsilon_m^2 - k_0^2}; \quad \operatorname{Re}\{\gamma_m\} \geq 0. \quad (6)$$

The lateral mode wave numbers  $\epsilon_m h$  are solutions of the following equations (the splitter surfaces are locally reacting with admittance  $G$ ):

$$jk_0 h \cdot Z_0 G = \begin{cases} \epsilon_m h \cdot \tan(\epsilon_m h); & m = 0, 2, 4, \dots \\ -\epsilon_m h \cdot \cot(\epsilon_m h); & m = 1, 3, 5, \dots \end{cases}. \quad (7)$$

The mode norms are:

$$\begin{aligned} \frac{1}{2h} \int_{-h}^{+h} q_m(\epsilon_m y_v) \cdot q_{m'}(\epsilon_{m'} y_v) dy_v &= \begin{cases} 0 & ; \quad m \neq m' \\ N_m & ; \quad m = m' \end{cases}, \\ N_m &= \begin{cases} \frac{1}{2} \left( 1 + \frac{\sin(2\epsilon_m h)}{2\epsilon_m h} \right) & ; \quad m = 0, 2, 4, \dots \\ \frac{1}{2} \left( 1 - \frac{\sin(2\epsilon_m h)}{2\epsilon_m h} \right) & ; \quad m = 1, 3, 5, \dots \end{cases}. \end{aligned} \quad (8)$$

Auxiliary amplitudes are defined by:

$$X_m := B_m - C_m; \quad Y_m := B_m e^{-\gamma_m L} - C_m e^{+\gamma_m L}. \quad (9)$$

The field matching at the zone limits gives for them two coupled, linear, homogeneous systems of equations:

$$\begin{aligned} \sum_{m'=0}^{\infty} X_{m'} \left[ -j \frac{\gamma_{m'}}{k_0} \frac{h}{T} \sum_n \frac{k_0}{\kappa_n} S_{m,n} S_{m',n} + 2\delta_{m',m} (-1)^m N_m \frac{1 + e^{-2\gamma_m L}}{1 - e^{-2\gamma_m L}} \right] \\ = 2P_1 S_{m,0} + 4(-1)^m N_m \frac{e^{-\gamma_m L}}{1 - e^{-2\gamma_m L}} \cdot Y_m, \end{aligned} \quad (10)$$

$$\begin{aligned} \sum_{m'=0}^{\infty} Y_{m'} \left[ -j \frac{\gamma_{m'}}{k_0} \frac{h}{T} \sum_n \frac{k_0}{\kappa_n} S_{m,n} S_{m',n} + 2\delta_{m',m} (-1)^m N_m \frac{1 + e^{-2\gamma_m L}}{1 - e^{-2\gamma_m L}} \right] \\ = 4(-1)^m N_m \frac{e^{-\gamma_m L}}{1 - e^{-2\gamma_m L}} \cdot X_m, \end{aligned} \quad (11)$$

$$\begin{array}{c}
 \begin{array}{|c|c|c|c|} \hline
 & m'=0 & \dots & m'=0 \\ \hline
 m=0 & A_{mm'} & & F_m \\ \hline
 \vdots & & 0 & \\ \hline
 m=0 & & 0 & \\ \hline
 \vdots & & & \\ \hline
 & 0 & & A_{mm'} \\ \hline
 \end{array} & \bullet & \begin{array}{|c|} \hline X_m \\ \hline Y_m \\ \hline \end{array} & = & \begin{array}{|c|} \hline b_m \\ \hline 0 \\ \hline \end{array} \\
 \end{array}$$

i.e. a system of equations of the form shown above with the coefficients:

$$\begin{aligned}
 F_m &= -4(-1)^m N_m \frac{e^{-\gamma_m L}}{1 - e^{-2\gamma_m L}}, \\
 b_m &= 2P_1 S_{m,0},
 \end{aligned} \tag{12}$$

$$A_{m,m'} = -j \frac{\gamma_{m'}}{k_0} \frac{h}{T} \sum_n \frac{k_0}{\kappa_n} S_{m,n} S_{m',n} + 2\delta_{m',m} (-1)^m N_m \frac{1 + e^{-2\gamma_m L}}{1 - e^{-2\gamma_m L}}, \tag{13}$$

where  $S_{m,n}$  are the coupling coefficients between the spatial harmonics and the silencer modes:

$$\begin{aligned}
 S_{m,n} &:= \frac{1}{h} \int_{-h}^{+h} e^{j\beta_n y} q_m(y) dy \\
 &= \begin{cases} 2 \frac{(\epsilon_m h) \sin(\epsilon_m h) \cos(\beta_n h) - (\beta_n h) \cos(\epsilon_m h) \sin(\beta_n h)}{(\epsilon_m^2 - \beta_n^2) h^2}; & m = 0, 2, 4, \dots \\ 2j \frac{(\beta_n h) \sin(\epsilon_m h) \cos(\beta_n h) - (\epsilon_m h) \cos(\epsilon_m h) \sin(\beta_n h)}{(\epsilon_m^2 - \beta_n^2) h^2}; & m = 1, 3, 5, \dots \end{cases} \\
 &\xrightarrow[\beta_n \rightarrow -\beta_n]{} (-1)^m S_{m,n} \\
 &\xrightarrow[\beta_n \rightarrow \epsilon_m]{} \begin{cases} 2N_m; & m = 0, 2, 4, \dots \\ 2jN_m; & m = 1, 3, 5, \dots \end{cases}
 \end{aligned} \tag{14}$$

Using the solutions for  $X_m, Y_m$  follow the amplitudes in the field formulations:

$$A_n = \frac{k_0}{\kappa_n} [\delta_{0,n} P_1 \cos \Theta + j \frac{h}{T} \sum_{m=0}^{\infty} X_m \frac{Y_m}{k_0} S_{m,n}]; \quad D_n = -j \frac{k_0}{\kappa_n} \frac{h}{T} \sum_{m=0}^{\infty} Y_m \frac{Y_m}{k_0} S_{m,n}; \tag{15}$$

$$B_m = \frac{X_m - Y_m e^{-\gamma_m L}}{1 - e^{-2\gamma_m L}}; \quad C_m = \frac{X_m e^{-\gamma_m L} - Y_m}{1 - e^{-2\gamma_m L}} e^{-\gamma_m L}.$$

The sound transmission coefficient  $\tau = \Pi_i / \Pi_t$ , with incident effective sound power  $\Pi_i$  (on one baffle unit) is:

$$\Pi_i = T \frac{|P_1|^2}{2Z_0} \cos \Theta, \tag{16}$$

and the transmitted effective sound power is:

$$\Pi_t = \frac{1}{2} \operatorname{Re} \int_0^T p_{III}(0, y) \cdot v_{III}^*(0, y) dy = \frac{T}{2Z_0} \sum_{n_s} |D_{n_s}|^2 \sqrt{1 - (\sin \Theta + n_s \frac{\lambda_0}{T})^2}, \quad (17)$$

where the summation index  $n_s$  extends over the range of “radiating spatial harmonics”:

$$-(1 + \sin \Theta) \cdot T/\lambda_0 < n_s < (1 - \sin \Theta) \cdot T/\lambda_0 \quad (18)$$

(harmonics with orders outside this range only contribute to near fields).

The spatial harmonics in Zone III are plane waves with effective intensity:

$$I_{n_s} = \frac{1}{2Z_0} |D_{n_s}|^2 \sqrt{1 - \left(\sin \Theta + n_s \frac{\lambda_0}{T}\right)^2}, \quad (19)$$

and angle of radiation (relative to the x axis):

$$\vartheta_{n_s} = \arctan \frac{\beta_{n_s}}{\kappa_{n_s}} = \arctan \frac{\sin \Theta + n_s \frac{\lambda_0}{T}}{\sqrt{1 - \left(\sin \Theta + n_s \frac{\lambda_0}{T}\right)^2}}. \quad (20)$$

Using this equation the radiation directivity of the transmitted sound can be evaluated.

## J.23 Splitter-Type Silencer with Locally Reacting Splitters in a Hard Duct

---

► See also: Mechel, Vol. III, Ch. 36 (1998)

See the sketch in Sect. J.22. There are K splitter elements in the main duct; the splitter ducts are counted with  $v = 0, 1, 2, \dots, K$ . Let the incident wave be the  $\mu$ -th mode of the hard duct ahead of the splitters. It is made up of two plane waves  $p_1, p_2$  incident at angles  $\pm \Theta_\mu$  (relative to the x axis):

$$p_1(x, y) = P_1 \cdot e^{-jk_{xp}x} \cdot e^{-jk_{yp}y}; \quad p_2(x, y) = P_1 \cdot e^{-jk_{xp}x} \cdot e^{+jk_{yp}y},$$

$$k_{yp} = \frac{\mu\pi}{a} = k_0 \sin \Theta_\mu; \quad k_{xp} = k_0 \cos \Theta_\mu = \sqrt{k_0^2 - \left(\frac{\mu\pi}{a}\right)^2}; \quad \mu = 0, 1, 2, \dots, \quad (1)$$

$$\sin \Theta_\mu = \frac{k_{yp}}{k_0} = \frac{\mu\lambda_0}{2a}.$$

The field formulations are:

$$\begin{aligned} p_{l\mu}(x, y) &= 2P_1 e^{-jk_0x \cos \Theta_\mu} \cdot \cos(k_0y \sin \Theta_\mu) + 2 \sum_{n=-\infty}^{+\infty} A_n e^{jk_n x} \cdot \cos(\beta_n y), \\ v_{l\mu x}(x, y) &= \frac{2}{Z_0} \left[ P_1 \cos \Theta_\mu \cdot e^{-jk_0x \cos \Theta_\mu} \cdot \cos(k_0y \sin \Theta_\mu) \right. \\ &\quad \left. - \sum_{n=-\infty}^{+\infty} A_n \frac{\kappa_n}{k_0} e^{jk_n x} \cdot \cos(\beta_n y) \right], \end{aligned} \quad (2)$$

$$p_{III\mu}(x', y) = 2 \sum_{n=-\infty}^{+\infty} D_n e^{-jk_n x'} \cdot \cos(\beta_n y), \quad (3)$$

$$p_{III\mu}(x, y_v) = 2 \cos(v\beta_0 T) \sum_{m=0}^{\infty} [B_m e^{-Y_m x} + C_m e^{+Y_m x}] \cdot q_m(y_v). \quad (4)$$

With these formulations the amplitudes  $A_n, D_n, B_m, C_m$  are evaluated as in the previous  
► Sect. J.22.

The range of the index  $n_s$  for radiating spatial harmonics can now be formulated as follows:

$$-\left(\frac{T}{\lambda_0} + \frac{\mu}{2K}\right) < n_s < \frac{T}{\lambda_0} - \frac{\mu}{2K} \quad \text{or:} \quad -\left(\frac{2a}{\lambda_0} + \mu\right) < 2n_s K < \frac{2a}{\lambda_0} - \mu. \quad (5)$$

The incident effective sound power is:

$$\Pi_{i\mu} = \frac{2a}{\delta_\mu Z_0} \cos \Theta_\mu |P_1|^2; \quad \delta_\mu = \begin{cases} 1; & \mu = 0 \\ 2; & \mu > 0 \end{cases}. \quad (6)$$

The transmitted effective sound power is:

$$\Pi_{t\mu} = \frac{2a}{\delta_\mu Z_0} \sum_{n_s} |D_{n_s}|^2 \sqrt{1 - \left(\frac{\lambda_0}{2a}\right)^2 (\mu + 2n_s K)^2}. \quad (7)$$

The effective sound power reflected at the front side of the splitters is:

$$\Pi_{r\mu} = \frac{2a}{\delta_\mu Z_0} \left[ |A_0|^2 \cos \Theta_\mu + \sum_{n_s \neq 0} |A_{n_s}|^2 \sqrt{1 - \left(\frac{\lambda_0}{2a}\right)^2 (\mu + 2n_s K)^2} \right]. \quad (8)$$

*Special cases:*

The transmission loss of the entrance plane of the splitters can be studied using  $L \rightarrow \infty$ . Then  $C_m \rightarrow 0, D_m \rightarrow 0; X_m \rightarrow B_m, Y_m \rightarrow 0$ . In the system of equations of ► Sect. J.22 go  $F_m \rightarrow 0$ , and

$$A_{m,m'} = -j \frac{Y_{m'}}{k_0} \frac{h}{T} \sum_n \frac{k_0}{\kappa_n} S_{m,n} S_{m',n}; \quad b_m = 2P_1 S_{m,0}. \quad (9)$$

*Special case of incident plane wave  $\mu = 0$ : Consequences:*

$$\begin{aligned} \mu &= 0; & \Theta &= \Theta_\mu = 0; \\ \beta_0 &= 0; & \beta_n &= \frac{2\pi n}{T}; \\ \kappa_0 &= k_0; & \kappa_n &= k_0 \sqrt{1 - \left(\frac{2\pi n}{k_0 T}\right)^2}; \\ \beta_{-n} &= -\beta_n; & \kappa_{-n} &= \kappa_n; \end{aligned} \quad (10)$$

$$S_{m,n} = \begin{cases} 2 \frac{(jk_0 h Z_0 G) \cos(2n\pi h/T) - (2n\pi h/T) \sin(2n\pi h/T)}{(\epsilon_m h)^2 - (2n\pi h/T)^2} \cos(\epsilon_m h); \\ m = 0, 2, 4, \dots \\ 2 \frac{j(2n\pi h/T) \cos(2n\pi h/T) - (k_0 h Z_0 G) \sin(2n\pi h/T)}{(\epsilon_m h)^2 - (2n\pi h/T)^2} \sin(\epsilon_m h); \\ m = 1, 3, 5, \dots \end{cases}; \quad (11)$$

$$S_{m,0} = \begin{cases} 2jk_0 h Z_0 G \cdot \frac{\cos(\epsilon_m h)}{\epsilon_m h}; & m = 0, 2, 4, \dots \\ 0; & m = 1, 3, 5, \dots \end{cases}; \quad (12)$$

$$S_{m,-n} = (-1)^m \cdot S_{m,n}.$$

The sums  $\sum_{n=-\infty}^{\infty} \frac{k_0}{\kappa_n} S_{m,n} S_{m',n}$  disappear in the coefficients  $A_{m,m'}$ ; therefore anti-symmetrical waves play no role. The system of equations for the auxiliary amplitudes  $X_m, Y_m$  has the coefficients

$$\begin{aligned} A_{m,m'} &= -j \frac{y_{m'}}{k_0} \frac{h}{T} \sum_{n \geq 0} \delta_n \frac{k_0}{\kappa_n} S_{m,n} S_{m',n} + 2\delta_{m',m} (-1)^m N_m \frac{1 + e^{-2y_m L}}{1 - e^{-2y_m L}}, \\ F_m &= 4(-1)^m N_m \frac{e^{-y_m L}}{1 - e^{-2y_m L}}, \\ b_m &= 2P_1 S_{m,0}. \end{aligned} \quad (13)$$

Using its solution the other amplitudes are evaluated from:

$$\begin{aligned} A_{-n} &= A_n = \delta_{0,n} P_1 + \frac{j}{\kappa_n T} \sum_m X_m \cdot y_m h \cdot S_{m,n}; \\ D_{-n} &= D_n = \frac{-j}{\kappa_n T} \sum_m Y_m \cdot y_m h \cdot S_{m,n}; \\ B_m &= \frac{X_m - Y_m e^{-y_m L}}{1 - e^{-2y_m L}}; \quad C_m = \frac{X_m e^{-y_m L} - Y_m}{1 - e^{-2y_m L}} e^{-y_m L}. \end{aligned} \quad (14)$$

The sound fields in the zones then follow from:

$$\begin{aligned} p_I(x, y) &= 2P_1 e^{-jk_0 x} + 2 \sum_{n=0}^{\infty} \delta_n \cdot A_n e^{jk_0 x \sqrt{1-(n\lambda_0/T)^2}} \cdot \cos\left(\frac{2\pi n}{T} y\right), \\ p_{III}(x', y) &= 2 \sum_{n=0}^{\infty} \delta_n \cdot D_n e^{-jk_0 x' \sqrt{1-(n\lambda_0/T)^2}} \cdot \cos\left(\frac{2\pi n}{T} y\right), \\ p_{II}(x, y_v) &= 2 \sum_m [B_m e^{-y_m x} + C_m e^{+y_m x}] \cdot \cos(\epsilon_m y_v). \end{aligned} \quad (15)$$

(The number K of the splitters in the main duct has disappeared, as expected.) The range of radiating spatial harmonics is:

$$-\frac{T}{\lambda_0} < n_s < \frac{T}{\lambda_0}. \quad (16)$$

The expressions for the effective sound powers simplify to:

$$\begin{aligned}\Pi_i &= 2a|P_1^2|/Z_0, \\ \Pi_r &= \frac{2a}{Z_0} \sum_{n_s} \delta_{n_s} \cdot |A_{n_s}|^2 \cdot \sqrt{1 - (n_s \lambda_0/T)^2}, \\ \Pi_t &= \frac{2a}{Z_0} \sum_{n_s} \delta_{n_s} \cdot |D_{n_s}|^2 \cdot \sqrt{1 - (n_s \lambda_0/L)^2}.\end{aligned}\quad (17)$$

*Approximations:*

$$\begin{array}{c} m'=0 \\ \vdots \\ m=0 \end{array} \xrightarrow{\quad} \boxed{A_{mm'}} \bullet \boxed{X_m} = \boxed{b_m}$$

Neglect the reflections at the splitter duct exit, i.e. set everywhere  $C_m = 0$ . The consequence is

$$X_m = B_m; \quad Y_m = B_m \cdot e^{-\gamma_m L} = X_m \cdot e^{-\gamma_m L}. \quad (18)$$

This simplifies the system of equations with the following coefficients:

$$A_{m,m'} = -j \frac{\gamma_{m'}}{k_0} \frac{h}{T} \sum_n \frac{k_0}{\kappa_n} S_{m,n} S_{m',n} + 2\delta_{m,m'}(-1)^m N_m, \quad (19)$$

$$b_m = 2P_1 S_{m,0}.$$

The amplitudes  $A_n$  are evaluated as before, and the  $D_n$  follow from:

$$D_n = -j \frac{k_0}{\kappa_n} \frac{h}{T} \sum_{m=0}^{\infty} X_m e^{-\gamma_m L} \frac{\gamma_m}{k_0} S_{m,n}. \quad (20)$$

Assume only a single mode in the splitter duct (usually the least attenuated mode): The  $X_m, Y_m$  follow from the two equations:

$$\begin{aligned}A_{m,m} \cdot X_m + F_m \cdot Y_m &= b_m, \\ F_m \cdot X_m + A_{m,m} \cdot Y_m &= 0\end{aligned}\quad (21)$$

with the coefficients:

$$\begin{aligned}A_{m,m} &= -j \frac{\gamma_m}{k_0} \frac{h}{T} \sum_n \frac{k_0}{\kappa_n} S_{m,n}^2 + 2(-1)^m N_m \coth(\gamma_m L), \\ F_m &= 2(-1)^{m+1} N_m \frac{1}{\sinh(\gamma_m L)},\end{aligned}\quad (22)$$

$$b_m = 2P_1 S_{m,0},$$

or, as explicit solutions:

$$X_m = \frac{A_{m,m} b_m}{A_{m,m}^2 - F_m^2}; \quad Y_m = -\frac{F_m b_m}{A_{m,m}^2 - F_m^2}, \quad (23)$$

and the amplitudes in the main duct from:

$$A_n = \delta_{0,n} P_1 + j \frac{h}{T} \frac{\gamma_m}{\kappa_n} S_{m,n} \cdot X_m ; \quad D_n = -j \frac{h}{T} \frac{\gamma_m}{\kappa_n} S_{m,n} \cdot Y_m . \quad (24)$$

Assume only a single mode in the splitter duct and neglect its reflection at the splitter duct exit: Then, using the coefficients from above:

$$X_m = B_m = \frac{b_m}{A_{mm} + F_m e^{-\gamma_m L}} ; \quad (25)$$

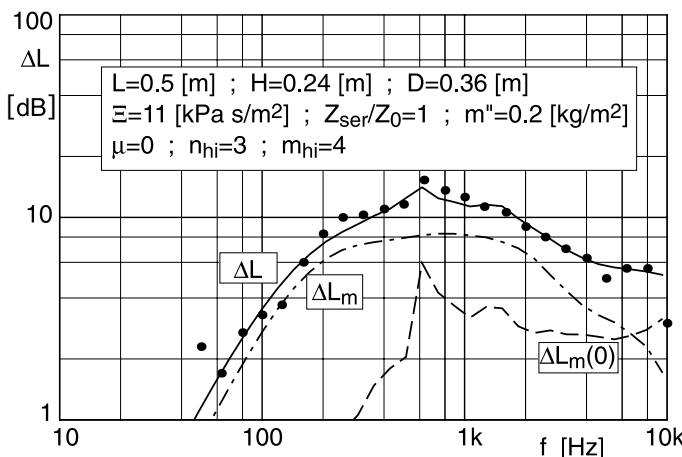
$$A_n = \delta_{0,n} P_1 + j \frac{h}{T} \frac{\gamma_m}{\kappa_n} S_{m,n} \cdot X_m ; \quad D_n = -j \frac{h}{T} \frac{\gamma_m}{\kappa_n} S_{m,n} \cdot X_m \cdot e^{-\gamma_m L} . \quad (26)$$

Assume an incident plane wave ( $\mu = 0$ ), and neglect reflections at the splitter duct exit. The simplified system of equations for the  $X_m$  from above has the coefficients:

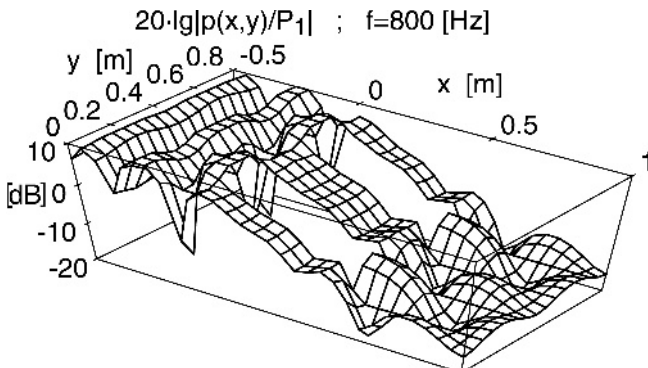
$$A_{m,m'} = 2\delta_{m,m'}(-1)^m N_m - j \frac{\gamma_{m'}}{k_0} \frac{h}{T} \sum_{n=0}^{\infty} \delta_n \frac{k_0}{\kappa_n} S_{m,n} S_{m',n} ; \quad b_m = 2P_1 S_{m,0} , \quad (27)$$

and the amplitudes in the main duct are:

$$\begin{aligned} A_{-n} = A_n &= \delta_{0,n} P_1 + \frac{j}{\kappa_n T} \sum_m X_m \cdot \gamma_m h \cdot S_{m,n} , \\ D_{-n} = D_n &= -j \frac{k_0}{\kappa_n} \frac{h}{T} \sum_m X_m e^{-\gamma_m L} \frac{\gamma_m}{k_0} S_{m,n} . \end{aligned} \quad (28)$$



Transmission loss of a splitter silencer; *points*: measured; *solid*: theory; *dash-dotted*: propagation loss of the least attenuated mode; *dashed*: loss by reflection at the splitter duct entrance



Sound pressure level in front of, within, and behind a splitter silencer with two splitters in a main duct

The splitters in the numerical example shown consist of layers of mineral fibres with a flow resistivity of  $\Xi = 11 \text{ [kPa} \cdot \text{s/m}^2\text{]}$ , covered with a porous foil of surface mass density  $m'' = 0.2 \text{ [kg/m}^2\text{]}$  and a flow resistance  $Z_{\text{ser}} = 1 \cdot Z_0$ . The points are measured transmission loss values for plane wave incidence; the full curve is evaluated as explained above; the dash-dotted curve represents the propagation loss of the least attenuated mode of the splitter duct; the dashed curve shows the loss by reflection at the entrance of the splitter ducts.

## J.24 Splitter Type Silencer with Simple Porous Layers as Bulk Reacting Splitters

---

► See also: Mechel, Vol. III, Ch. 37 (1998)

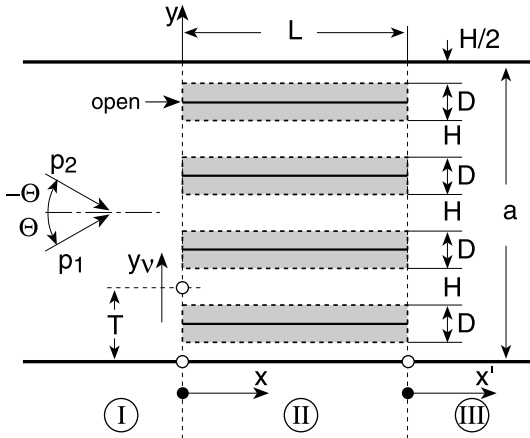
Splitters consist of simple porous layers with characteristic values of the material  $\Gamma_a$ ,  $Z_a$ , or, in normalised form,  $\Gamma_{an} = \Gamma_a/k_0$ ,  $Z_{an} = Z_a/Z_0$ . The heads of splitters are open. Splitters are not sound transmissive from one splitter duct to the neighbouring splitter duct, either due to a sufficiently high flow resistance of the splitter or due to a central partition (the condition is not necessary for plane wave incidence parallel to the x axis).  $H = 2h$ ;  $D = 2d$ .

The incident wave is a mode of the hard main duct; it is composed of two plane waves  $p_1 + p_2$  with mirror-reflected incidence under the modal angle  $\Theta \rightarrow \Theta_\mu$ :

$$p_1(x, y) = P_1 \cdot e^{-jk_x x} \cdot e^{-jk_y y}; \quad p_2(x, y) = P_1 \cdot e^{-jk_x x} \cdot e^{+jk_y y};$$

$$k_y \rightarrow k_{y\mu} = k_0 \sin \Theta_\mu; \quad k_x \rightarrow k_{x\mu} = k_0 \cos \Theta_\mu = \sqrt{k_0^2 - (\frac{\mu\pi}{a})^2}; \quad (1)$$

$$\sin \Theta_\mu = \frac{k_{y\mu}}{k_0} = \frac{\mu\lambda_0}{2a}.$$



The backscattered wave  $p_s$  in Zone I and the transmitted wave  $p_t$  in Zone III are sums of spatial harmonics; thus the fields in these zones are formulated as follows:

$$p_{I\mu}(x, y) = 2P_1 e^{-jk_0 x \cos \Theta_\mu} \cdot \cos(k_0 y \sin \Theta_\mu) + 2 \sum_{n=-\infty}^{+\infty} A_n e^{jk_n x} \cdot \cos(\beta_n y), \quad (2)$$

$$p_{III\mu}(x', y) = 2 \sum_{n=-\infty}^{+\infty} D_n e^{-jk_n x'} \cdot \cos(\beta_n y) \quad (3)$$

with

$$\beta_n = \beta_0 + \frac{2\pi n}{T}; \quad n = 0, \pm 1, \pm 2, \dots; \quad \beta_0 = k_y = k_0 \sin \Theta_\mu; \quad (4)$$

$$\kappa_0 = k_x = k_0 \cos \Theta_\mu; \quad \kappa_n = \sqrt{k_0^2 - \beta_n^2} = k_0 \sqrt{1 - (\sin \Theta_\mu + n\lambda_0/T)^2}. \quad (5)$$

The field in the  $v$ -th splitter duct is a sum of splitter duct modes:

$$p_{II\mu}(x, y_v) = 2 \cos(v\beta_0 T) \sum_{m=0}^{\infty} [B_m e^{-\gamma_m x} + C_m e^{+\gamma_m x}] \cdot q_m(y_v) \quad (6)$$

with lateral mode profiles:

$$q_m(y) = \begin{cases} s_{|y|}(0, h) \cdot \frac{\cos(\epsilon_m y)}{\cos(\epsilon_m h)} + s_{|y|}(h, h+d) \\ \cdot \frac{\cos(\alpha_m(y-h-d))}{\cos(\alpha_m d)}; \quad m = 0, 2, 4 \dots \\ s_{|y|}(0, h) \cdot \frac{\sin(\epsilon_m y)}{\sin(\epsilon_m h)} + s_{|y|}(h, h+d) \\ \cdot \frac{y}{|y|} \cdot \frac{\cos(\alpha_m(y-h-d))}{\cos(\alpha_m d)}; \quad m = 1, 3, 5 \dots \end{cases} \quad (7)$$

which use the “switch function”  $s_y(a, b) = \begin{cases} 1 & ; a \leq y < b \\ 0 & ; \text{else} \end{cases}$ . (8)

The wave equations in the splitter duct and in the absorber material imply:

$$\epsilon_m^2 = k_0^2 + y_m^2 ; \quad \alpha_m^2 = y_m^2 - \Gamma_a^2 = \epsilon_m^2 - k_0^2 - \Gamma_a^2 , \quad (9)$$

and the lateral mode wave numbers are solutions of:

$$\begin{aligned} \epsilon_m h \cdot \tan(\epsilon_m h) &= -j \frac{h}{d} \frac{\alpha_m d}{\Gamma_{an} Z_{an}} \tan(\alpha_m d) ; \quad m = 0, 2, 4, \dots , \\ \epsilon_m h \cdot \cot(\epsilon_m h) &= +j \frac{h}{d} \frac{\alpha_m d}{\Gamma_{an} Z_{an}} \tan(\alpha_m d) ; \quad m = 1, 3, 5, \dots . \end{aligned} \quad (10)$$

The modes of all orders are orthogonal to each other over  $(-T/2, +T/2)$  with the mode norms  $M_m$ :

$$\frac{1}{h} \left[ \int_0^h q_m(y) \cdot q_{m'}(y) dy - \frac{j}{\Gamma_{an} Z_{an}} \int_h^{h+d} q_m(y) \cdot q_{m'}(y) dy \right] = \delta_{m,m'} \cdot M_m, \quad (11)$$

$$M_m = \begin{cases} \frac{1}{2} \frac{1}{\cos^2(\epsilon_m h)} \left[ 1 + \frac{\sin(2\epsilon_m h)}{2\epsilon_m h} \right] - \frac{j}{2} \frac{d/h}{\Gamma_{an} Z_{an}} \frac{1}{\cos^2(\alpha_m d)} \left[ 1 + \frac{\sin(2\alpha_m d)}{2\alpha_m d} \right] ; \\ m = 0, 2, 4 \dots \\ \frac{1}{2} \frac{1}{\sin^2(\epsilon_m h)} \left[ 1 - \frac{\sin(2\epsilon_m h)}{2\epsilon_m h} \right] - \frac{j}{2} \frac{d/h}{\Gamma_{an} Z_{an}} \frac{1}{\cos^2(\alpha_m d)} \left[ 1 + \frac{\sin(2\alpha_m d)}{2\alpha_m d} \right] ; \\ m = 1, 3, 5 \dots . \end{cases}$$

Coupling coefficients between modes in the hard main duct and in the splitter duct, respectively, will be needed:

$$S_{m,n} = \begin{cases} \frac{1}{d+h} \int_0^h \cos(\beta_n y) \cdot q_m(|y| \leq h) dy = \frac{1}{d+h} \int_0^h \cos(\beta_n y) \frac{\cos(\epsilon_m y)}{\cos(\epsilon_m h)} dy ; \\ m = 0, 2, \dots \\ \frac{j}{d+h} \int_0^h \sin(\beta_n y) \cdot q_m(|y| \leq h) dy = \frac{j}{d+h} \int_0^h \sin(\beta_n y) \frac{\sin(\epsilon_m y)}{\sin(\epsilon_m h)} dy ; \\ m = 1, 3, \dots \end{cases} \quad (12)$$

$$R_{m,n} = \begin{cases} \frac{1}{d+h} \int_h^{h+d} \cos(\beta_n y) \cdot q_m(|y| \geq h) dy \\ = \frac{1}{d+h} \int_h^{h+d} \cos(\beta_n y) \frac{\cos(\alpha_m(y-h-d))}{\cos(\alpha_m d)} dy; \quad m = 0, 2, \dots \\ \frac{j}{d+h} \int_h^{h+d} \sin(\beta_n y) \cdot q_m(|y| \geq h) dy \\ = \frac{j}{d+h} \int_h^{h+d} \sin(\beta_n y) \frac{\cos(\alpha_m(y-h-d))}{\cos(\alpha_m d)} dy; \quad m = 1, 3, \dots . \end{cases} \quad (13)$$

Their values are:

$$S_{m,n} = \begin{cases} \frac{1}{2(1+d/h) \cos(\epsilon_m h)} \left( \frac{\sin((\beta_n - \epsilon_m)h)}{(\beta_n - \epsilon_m)h} + \frac{\sin((\beta_n + \epsilon_m)h)}{(\beta_n + \epsilon_m)h} \right); \quad m = 0, 2, \dots \\ \frac{j}{2(1+d/h) \sin(\epsilon_m h)} \left( \frac{\sin((\beta_n - \epsilon_m)h)}{(\beta_n - \epsilon_m)h} - \frac{\sin((\beta_n + \epsilon_m)h)}{(\beta_n + \epsilon_m)h} \right); \quad m = 1, 3, \dots \end{cases} \quad (14)$$

$$R_{m,n} = \begin{cases} \frac{1}{2(1+d/h) \cos(\alpha_m d)} \\ \cdot \left( \frac{2\beta_n h}{(\beta_n^2 - \alpha_m^2)h^2} \sin(\beta_n h(1+d/h)) - \frac{\sin(\beta_n h + \alpha_m d)}{(\beta_n + \alpha_m)h} \right. \\ \left. - \frac{\sin(\beta_n h - \alpha_m d)}{(\beta_n - \alpha_m)h} \right); \quad m = 0, 2, \dots \\ \frac{j}{2(1+d/h) \cos(\alpha_m d)} \\ \cdot \left( \frac{-2\beta_n h}{(\beta_n^2 - \alpha_m^2)h^2} \cos(\beta_n h(1+d/h)) \right. \\ \left. + \frac{\cos(\beta_n h + \alpha_m d)}{(\beta_n - \alpha_m)h} + \frac{\cos(\beta_n h - \alpha_m d)}{(\beta_n + \alpha_m)h} \right); \quad m = 1, 3, \dots \end{cases} \quad (15)$$

Introduce the auxiliary amplitudes:

$$X_m = B_m - C_m; \quad Y_m = B_m e^{-Y_m L} - C_m e^{+Y_m L}. \quad (16)$$

The boundary conditions of field matching at  $x = 0$  and  $x = L$  give for them the following coupled systems of linear equations:

$$\sum_{m'} X_{m'} \left[ -j \frac{Y_{m'}}{k_0} \sum_n \frac{k_0}{\kappa_n} \left( S_{m,n} - \frac{j}{\Gamma_{an} Z_{an}} R_{m,n} \right) \left( S_{m',n} + \frac{j}{\Gamma_{an} Z_{an}} R_{m',n} \right) \right. \\ \left. + \delta_{m',m} (-1)^m \frac{H}{T} M_m \frac{1 + e^{-2Y_m L}}{1 - e^{-2Y_m L}} \right] - 2(-1)^m \frac{H}{T} M_m \frac{e^{-Y_m L}}{1 - e^{-2Y_m L}} \cdot Y_m \\ = 2 P_1 \left( S_{m,0} - \frac{j}{\Gamma_{an} Z_{an}} R_{m,0} \right); \quad \begin{cases} m, m' = 0, 1, 2, \dots, \\ n = 0, \pm 1, \pm 2 \dots, \end{cases} \quad (17)$$

$$\sum_{m'} Y_{m'} \left[ -j \frac{\gamma_{m'}}{k_0} \sum_n \frac{k_0}{\kappa_n} \left( S_{m,n} - \frac{j}{\Gamma_{an} Z_{an}} R_{m,n} \right) \left( S_{m',n} + \frac{j}{\Gamma_{an} Z_{an}} R_{m',n} \right) \right. \\ \left. + \delta_{m',m} (-1)^m \frac{H}{T} M_m \frac{1 + e^{-2\gamma_m L}}{1 - e^{-2\gamma_m L}} \right] - 2(-1)^m \frac{H}{T} M_m \frac{e^{-\gamma_m L}}{1 - e^{-2\gamma_m L}} \cdot X_m = 0 . \quad (18)$$

Using their solutions the amplitudes are evaluated as follows:

$$A_n = \delta_{n,0} P_1 + j \frac{k_0}{\kappa_n} \sum_m X_m \frac{\gamma_m}{k_0} \left( S_{m,n} + \frac{j}{\Gamma_{an} Z_{an}} R_{m,n} \right); \\ D_n = -j \frac{k_0}{\kappa_n} \sum_m Y_m \frac{\gamma_m}{k_0} \left( S_{m,n} + \frac{j}{\Gamma_{an} Z_{an}} R_{m,n} \right); \\ B_m = \frac{X_m - Y_m e^{-\gamma_m L}}{1 - e^{-2\gamma_m L}}; \quad C_m = \frac{X_m e^{-\gamma_m L} - Y_m}{1 - e^{-2\gamma_m L}} e^{-\gamma_m L} . \quad (19)$$

The effective incident and transmitted sound powers are evaluated as in [Sect. J.23](#), and the transmission coefficient follows from there.

## J.25 Splitter-Type Silencer with Splitters of Porous Layers Covered with a Foil

---

► See also: Mechel, Vol. III, Ch. 37 (1998)

The arrangement and sound incidence are as in the previous [Sect. J.24](#), but the splitters are covered with a (poro-elastic) foil having a partition impedance  $Z_s$ .

The field formulations in Zones I and III remain as in [Sect. J.24](#). The field in a splitter duct and in the porous layer is formulated as:

$$p_{IIp}(x, y_v) = 2 \cos(\nu \beta_0 T) \sum_{m=0}^{\infty} [B_m e^{-\gamma_m x} + C_m e^{+\gamma_m(x-L)}] \cdot q_m(y_v) \quad (1)$$

with the following mode profiles:

$$q_m(y) = \\ = \begin{cases} s_{|y|}(0, h) \cdot \cos(\epsilon_m y) + s_{|y|}(h, h+d) \cdot b_m \cos(\alpha_m(y-h-d)); & m = 0, 2, 4 \dots \\ s_{|y|}(0, h) \cdot \sin(\epsilon_m y) + s_{|y|}(h, h+d) \cdot \frac{y}{|y|} \cdot b_m \cos(\alpha_m(y-h-d)); & m = 1, 3, 5 \dots \end{cases} \quad (2)$$

( $s_y(a,b)$  is the switch function as in [Sect. J.24](#)). The wave equations in the splitter duct and in the porous layer imply:

$$(\alpha_m h)^2 = (\epsilon_m h)^2 - (k_0 h)^2 (1 + \Gamma_{an}^2), \quad (3)$$

and either the  $\epsilon_m h$  or the  $\alpha_m h$  are solutions of:

$$\left| \begin{array}{cc} \epsilon_m h \cdot \sin(\epsilon_m h) & \frac{j \alpha_m h \cdot \sin(\alpha_m d)}{\Gamma_{an} Z_{an}} \\ \left( k_0 h \cdot \cos(\epsilon_m h) + \frac{j Z_s}{Z_0} \epsilon_m h \cdot \sin(\epsilon_m h) \right) & -k_0 h \cdot \cos(\alpha_m d) \end{array} \right| = 0; \\ m = 0, 2, 4, \dots, \quad (4)$$

$$\left| \begin{array}{cc} \varepsilon_m h \cdot \cos(\varepsilon_m h) & -j\alpha_m h \cdot \sin(\alpha_m d) \\ \left( k_0 h \cdot \sin(\varepsilon_m h) - \frac{jZ_s}{Z_0} \varepsilon_m h \cdot \cos(\varepsilon_m h) \right) & -k_0 h \cdot \cos(\alpha_m d) \end{array} \right| = 0 ; m = 1, 3, \dots \quad (5)$$

The amplitudes  $B_m, C_m$  are solutions of the following coupled systems of linear equations:

$$\sum_m B_m \left[ (T_{m,n} + Q_{m,n}) - j \frac{\gamma_m}{\kappa_n} \left( T_{m,n} + \frac{j}{\Gamma_{an} Z_{an}} Q_{m,n} \right) \right] + C_m e^{-\gamma_m L} \left[ (T_{m,n} + Q_{m,n}) + j \frac{\gamma_m}{\kappa_n} \left( T_{m,n} + \frac{j}{\Gamma_{an} Z_{an}} Q_{m,n} \right) \right] = 2\delta_{0,n} \cdot P_1 , \quad (6)$$

$$\sum_m B_m e^{-\gamma_m L} \left[ (T_{m,n} + Q_{m,n}) + j \frac{\gamma_m}{\kappa_n} \left( T_{m,n} + \frac{j}{\Gamma_{an} Z_{an}} Q_{m,n} \right) \right] + C_m \left[ (T_{m,n} + Q_{m,n}) - j \frac{\gamma_m}{\kappa_n} \left( T_{m,n} + \frac{j}{\Gamma_{an} Z_{an}} Q_{m,n} \right) \right] = 0 \quad (7)$$

with mode coupling coefficients:

$$T_{m,n} = \begin{cases} S_{m,n} \cos(\varepsilon_m h) ; & m = 0, 2, 4 \dots \\ S_{m,n} \sin(\varepsilon_m h) ; & m = 1, 3, 5 \dots \end{cases} , \quad (8)$$

$$Q_{m,n} = R_{m,n} b_m \cos(\alpha_m d) ; \quad m = 0, 1, 2 \dots , \quad (9)$$

where

$$b_m = \begin{cases} j\Gamma_{an} Z_{an} \frac{\varepsilon_m \sin(\varepsilon_m h)}{\alpha_m \sin(\alpha_m d)} ; & m = 0, 2, 4, \dots \\ -j\Gamma_{an} Z_{an} \frac{\varepsilon_m \cos(\varepsilon_m h)}{\alpha_m \sin(\alpha_m d)} ; & m = 1, 3, 5, \dots \end{cases} . \quad (10)$$

Using the solutions  $B_m, C_m$  the other amplitudes follow as:

$$A_n = -\delta_{0,n} \cdot P_1 + \sum_m (B_m + C_m e^{-\gamma_m L}) (T_{m,n} + Q_{m,n}) ,$$

$$D_n = \sum_m (B_m e^{-\gamma_m L} + C_m) (T_{m,n} + Q_{m,n}) . \quad (11)$$

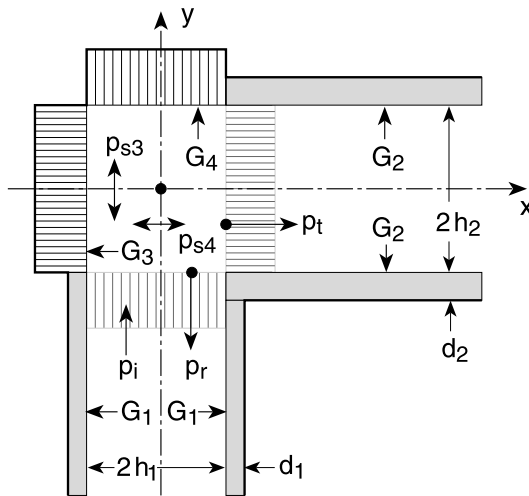
## J.26 Lined Duct Corners and Junctions

---

► See also: Mechel, Vol. III, Ch. 38 (1998)

See also  Sect. J.41 about TV splitters.

Two lined ducts  $i = 1, 2$  form a corner. The corner walls  $i = 3, 4$  opposite the ducts are lined, too. All linings are supposed to be locally reacting (for ease of formulation, mainly) with surface admittances  $G_i$ .



Let the incident wave  $p_i$  be the  $\mu$ -th mode of the duct  $i = 1$ . Each of the corner linings with  $G_3, G_4$ , when mirror-reflected at the  $y$  axis and  $x$  axis, respectively, will form a fictitious lined duct  $i = 3, 4$ .

The reflected wave  $p_r$  in the duct  $i = 1$  is formulated as a mode sum of that duct, and the transmitted wave  $p_t$  in the duct  $i = 2$  is formulated as a mode sum of the duct  $i = 2$ . The scattered waves  $p_{s3}, p_{s4}$  in the corner area are written as mode sums of the fictitious ducts  $i = 3, 4$ .

The inlet duct  $i = 1$ , the exit duct  $i = 2$ , and the corner area form Zones I, II, and III, respectively, of the sound field. The sound fields in the zones are:

$$\begin{aligned} p_I(x, y) &= p_i(x, y) + p_r(x, y), \\ p_{II}(x, y) &= p_t(x, y), \\ p_{III}(x, y) &= p_{s3}(x, y) + p_{s4}(x, y) \end{aligned} \quad (1)$$

with the formulations of the component fields:

$$\begin{aligned} p_i(x, y) &= P_i \cdot q1_\mu(x) \cdot e^{-\gamma 1_\mu(y+h_2)}, \\ p_r(x, y) &= \sum_m A_m \cdot q1_m(x) \cdot e^{+\gamma 1_\mu(y+h_2)}, \\ p_t(x, y) &= \sum_n D_n \cdot q2_n(y) \cdot e^{-\gamma 2_n(x-h_1)}, \\ p_{s3}(x, y) &= \sum_\alpha B_\alpha \cdot q3_\alpha(x) \cdot [e^{-\gamma 3_\alpha(y+h_2)} + R_\alpha \cdot e^{+\gamma 3_\alpha(y+h_2)}], \\ p_{s4}(x, y) &= \sum_\beta C_\beta \cdot q4_\beta(y) \cdot [e^{+\gamma 4_\beta(x-h_1)} + R_\beta \cdot e^{-\gamma 4_\beta(x-h_1)}], \end{aligned} \quad (2)$$

where the  $q_{ik}(z)$  are symmetrical and anti-symmetrical mode profiles:

$$q_{ik}(z) = \begin{cases} \cos(\epsilon i_k z); & k = 0, 2, 4, \dots; \text{ symm.} \\ \sin(\epsilon i_k z); & k = 1, 3, 5, \dots; \text{ anti-symm.} \end{cases} \quad (3)$$

with the axial propagation constants  $\gamma i_k$  from the wave equation  $\gamma i_k^2 = \epsilon i_k^2 - k_0^2$  (4) and the lateral wave numbers  $\epsilon i_k h_i$  solutions of the characteristic equation:

$$\epsilon i_k h_i \cdot q i'_k (\epsilon i_k h_i) = -j k_0 h_i \cdot Z_0 G_i \cdot q i_k (\epsilon i_k h_i) . \quad (5)$$

The mode norms are:  $N_{i_k} := \frac{1}{2h_i} \int_{-h_i}^{h_i} q i_k^2(\eta_i) d\eta_i = \frac{1}{2} \left[ 1 + (-1)^k \frac{\sin(2\epsilon i_k h_i)}{2\epsilon i_k h_i} \right] . \quad (6)$

$R_\alpha, R_\beta$  are modal reflection factors of the corner linings  $G_4, G_3$ , respectively, "measured" in the orifice planes of the ducts  $i = 1, 2$ ; they follow from the reflection factors  $r_\alpha, r_\beta$  at the lining surfaces by:

$$\begin{aligned} R_\alpha &= r_\alpha \cdot e^{-4\gamma 3_\alpha h_2} ; \quad r_\alpha = \frac{j\gamma 3_\alpha/k_0 + Z_0 G_4}{j\gamma 3_\alpha/k_0 - Z_0 G_4} = \frac{j\gamma 3_\alpha h_2 + U_4}{j\gamma 3_\alpha h_2 - U_4} , \\ R_\beta &= r_\beta \cdot e^{-4\gamma 4_\beta h_1} ; \quad r_\beta = \frac{j\gamma 4_\beta/k_0 + Z_0 G_3}{j\gamma 4_\beta/k_0 - Z_0 G_3} = \frac{j\gamma 4_\beta h_1 + U_3}{j\gamma 4_\beta h_1 - U_3} . \end{aligned} \quad (7)$$

Matching of the sound fields at the zone limits leads to a coupled system of linear equations for the amplitudes  $B_\alpha, C_\beta$ :

$$\begin{aligned} &\sum_\alpha B_\alpha \cdot S_{\alpha,k} [\gamma 3_\alpha h_2 (1 - R_\alpha) + \gamma 1_k h_2 (1 + R_\alpha)] \\ &+ \sum_\beta C_\beta \cdot (-1)^\beta q 4_\beta(h_2) (\gamma 1_k h_2 - jU_4) (e^{-\gamma 4_\beta h_1} \cdot I a_{\beta,k} + R_\beta e^{+\gamma 4_\beta h_1} \cdot I b_{\beta,k}) \\ &= 2\delta_{\mu,k} \cdot P_i \cdot \gamma 1_\mu h_2 N 1_\mu , \end{aligned} \quad (8)$$

$$\begin{aligned} &\sum_\alpha B_\alpha \cdot q 3_\alpha h_1 (\gamma 2_k h_1 - jU_3) (e^{-\gamma 3_\alpha h_2} \cdot I B_{\alpha,k} + R_\alpha e^{+\gamma 3_\alpha h_2} \cdot I A_{\alpha,k}) \\ &+ \sum_\beta C_\beta \cdot T_{\beta,k} [\gamma 4_\beta h_1 (1 - R_\beta) + \gamma 2_k h_1 (1 + R_\beta)] = 0 . \end{aligned} \quad (9)$$

These contain the following mode coupling coefficients:

$$\begin{aligned} S_{\alpha,k} &:= \frac{1}{2h_1} \int_{-h_1}^{h_1} q 3_\alpha(x) \cdot q 1_k(x) dx = 0 ; \quad \alpha + k = \text{odd} \\ &= \frac{1}{2} \left[ \frac{\sin((\epsilon 3_\alpha - \epsilon 1_k)h_1)}{(\epsilon 3_\alpha - \epsilon 1_k)h_1} + (-1)^{(\alpha+k)/2} \cdot \frac{\sin((\epsilon 3_\alpha + \epsilon 1_k)h_1)}{(\epsilon 3_\alpha + \epsilon 1_k)h_1} \right] ; \quad \alpha + k = \text{even} \end{aligned} \quad (10)$$

$$\begin{aligned} T_{\beta,k} &:= \frac{1}{2h_2} \int_{-h_2}^{h_2} q 4_\beta(y) \cdot q 2_k(y) dy = 0 ; \quad \beta + k = \text{odd} \\ &= \frac{1}{2} \left[ \frac{\sin((\epsilon 4_\beta - \epsilon 2_k)h_2)}{(\epsilon 4_\beta - \epsilon 2_k)h_2} + (-1)^{(\beta+k)/2} \cdot \frac{\sin((\epsilon 4_\beta + \epsilon 2_k)h_2)}{(\epsilon 4_\beta + \epsilon 2_k)h_2} \right] ; \quad \beta + k = \text{even} \end{aligned} \quad (11)$$

with  $S_{\alpha k} \rightarrow \delta_{\alpha k} \cdot N 1_k$  if the lining  $i = 3$  agrees with the lining  $i = 1$ , and  $T_{\beta,k} \rightarrow \delta_{\beta,k} \cdot N 2_k$  if the lining  $i = 4$  agrees with the lining  $i = 2$ .

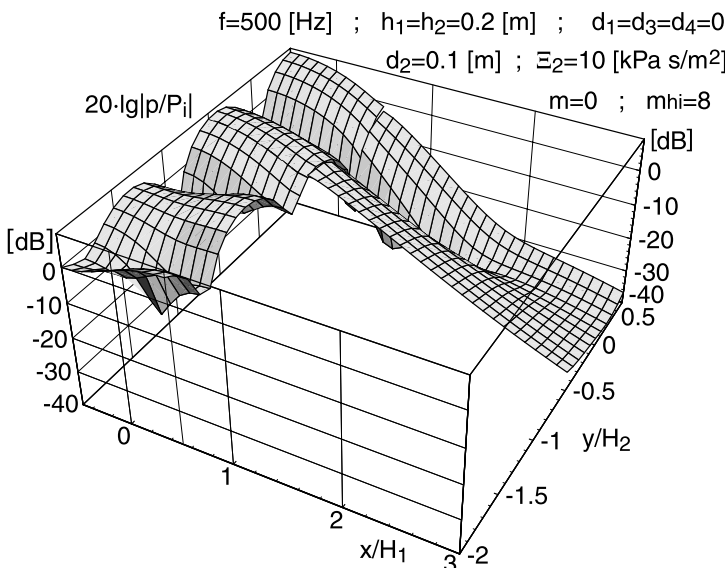
Further needed are the integrals:

$$\begin{aligned} Ia_{\beta,k} &:= \frac{1}{2h_1} \int_{-h_1}^{h_1} e^{+\gamma^4 \beta x} \cdot q1_k(x) dx ; \quad Ib_{\beta,k} := \frac{1}{2h_1} \int_{-h_1}^{h_1} e^{-\gamma^4 \beta x} \cdot q1_k(x) dx ; \\ IA_{\alpha,k} &:= \frac{1}{2h_2} \int_{-h_2}^{h_2} e^{+\gamma^3 \alpha y} \cdot q2_k(y) dy ; \quad IB_{\alpha,k} := \frac{1}{2h_2} \int_{-h_2}^{h_2} e^{-\gamma^3 \alpha y} \cdot q2_k(y) dy , \end{aligned} \quad (12)$$

which are easily evaluated with the mode profile functions  $q1_k(z)$ . With the solutions  $B_\alpha$ ,  $C_\beta$  the other amplitudes follow as:

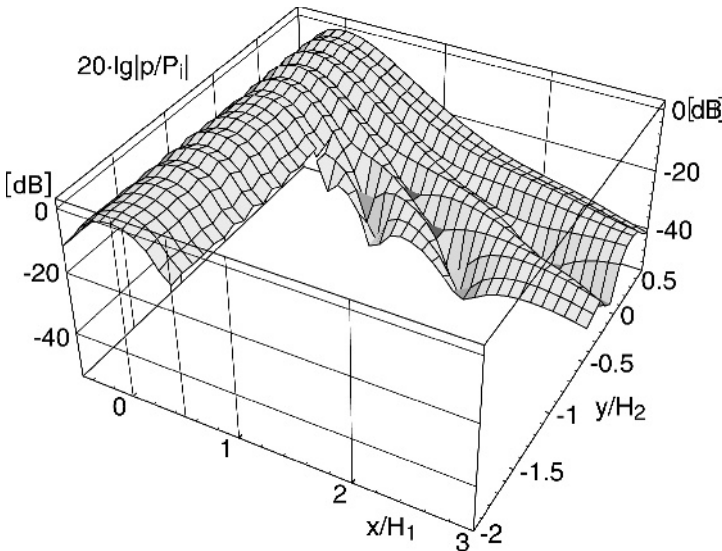
$$A_k = \frac{1}{N1_k} \left[ -\delta_{\mu,k} \cdot P_i \cdot N1_\mu + \sum_{\alpha} B_\alpha (1+R_\alpha) \cdot S_{\alpha,k} + \sum_{\beta} C_\beta \cdot q4_\beta(-h_2) (e^{-\gamma^4 \beta h_1} \cdot Ia_{\beta,k} + R_\beta e^{+\gamma^4 \beta h_1} \cdot Ib_{\beta,k}) \right], \quad (13)$$

$$D_k = \frac{1}{N2_k} \sum_{\alpha} B_\alpha q3_\alpha(h_1) (e^{-\gamma^3 \alpha h_2} \cdot IB_{\alpha,k} + R_\alpha e^{+\gamma^3 \alpha h_2} \cdot IA_{\alpha,k}) + \sum_{\beta} C_\beta \cdot (1+R_\beta) \cdot T_{\beta,k} . \quad (14)$$



Sound pressure level in two ducts and their corner. The entrance duct  $i = 1$  and the corner walls are hard; only the exit duct  $i = 2$  is lined. Because the standing wave pattern in the corner agrees well with the first higher mode pattern in the exit duct, this higher mode is predominantly excited, and a high extra corner transmission loss is produced (as compared with the least attenuated mode propagation loss)

The linings in the numerical examples shown are simple glass fibre layers of thickness  $d_i$  with flow resistivity  $\Xi_i$ , made locally absorbing (if a duct or corner wall is hard, then  $d_i = 0$  and no  $\Xi$  value is given).



Sound pressure level in two lined ducts and their corner. Both ducts and the corner walls are equally lined.

Input parameters:  $f = 2000[\text{Hz}]$ ;  $\mu = 0$ ;  $m_{hi} = 8$ ;  $h_1 = h_2 = 0.2[\text{m}]$ ;  $d_1 = d_2 = d_3 = d_4 = 0.1[\text{m}]$ ;  $\Xi_1 = \Xi_2 = \Xi_3 = \Xi_4 = 10[\text{kPas/m}^2]$

T-joints and cross-joints of ducts can be approximately evaluated with the present method if one or both corner wall linings are given a lining admittance  $G_i = 1/Z_0$ . See references for a more precise method.

## J.27 Sound Radiation from a Lined Duct Orifice

---

► See also: Mechel, Vol. III, Ch. 39 (1998); Mechel, Mathieu Functions (1997)

A two-dimensional, flat duct of width  $2h$  with locally reacting lining of surface admittance  $G$  has its orifice in a hard baffle wall. The  $\mu$ -th duct mode  $p_\mu$  is incident on the orifice.

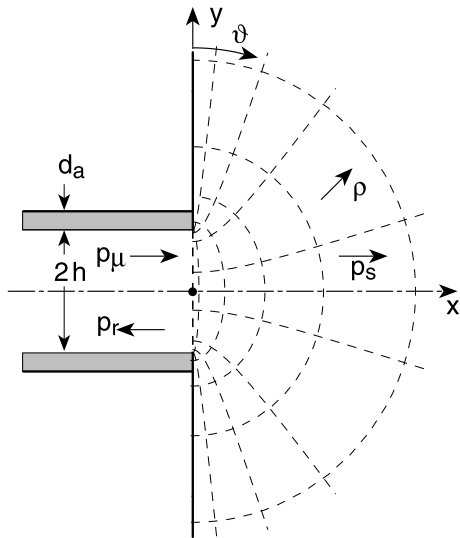
Cartesian co-ordinates  $x, y$  are used inside the duct; outside the duct an elliptic-hyperbolic system of co-ordinates  $\rho, \vartheta$  is applied. The orifice is in the plane  $x = 0$  and  $\rho = 0$ .

The reflected wave  $p_r$  inside the duct is composed of duct modes; the radiated field  $p_s$  is formulated as a sum of azimuthal and radial Mathieu functions  $ce_m(\vartheta), Hc_m^{(2)}(\rho)$ .

Field formulations:

$$p_\mu(x, y) = P_\mu \cdot \cos(\epsilon_\mu y) \cdot e^{-\gamma_\mu x}; \quad v_{\mu x} = -P_\mu \frac{j\gamma_\mu}{k_0 Z_0} \cos(\epsilon_\mu y) \cdot e^{-\gamma_\mu x}; \quad (1)$$

$$\gamma_\mu^2 = \epsilon_\mu^2 - k_0^2;$$



$$\begin{aligned} p_r(x, y) &= \sum_n A_n \cdot \cos(\epsilon_n y) \cdot e^{j\gamma_n x}; \quad v_{nx}(0, y) = \frac{j\gamma_n h}{k_0 h Z_0} A_n \cdot \cos(\epsilon_n y); \\ p_s(\rho, \vartheta) &= \sum_m D_m \cdot Hc_m^{(2)}(\rho) \cdot ce_m(\vartheta); \end{aligned} \quad (2)$$

$$\begin{aligned} v_{mp}(0, \vartheta) &= v_{mx}(0, \vartheta) = \frac{j}{k_0 Z_0 \cdot h \sin \vartheta} \left. \frac{\partial p_{s,m}}{\partial \rho} \right|_{\rho=0} \\ &= \frac{j}{k_0 Z_0 \cdot h \sin \vartheta} D_m \cdot Hc_m'^{(2)}(0) \cdot ce_m(\vartheta). \end{aligned} \quad (3)$$

Both the duct modes and the azimuthal Mathieu functions are orthogonal with norms:

$$\begin{aligned} N_n &:= \frac{1}{h} \int_{-h}^h q_n^2(y) dy = 1 + \frac{\sin(2\epsilon_n h)}{2\epsilon_n h}; \\ \int_0^\pi ce_m^2(\vartheta) d\vartheta &= \frac{\pi}{2}. \end{aligned} \quad (4)$$

Coupling coefficients:

$$R_{m,n} := \int_0^\pi c e_m(\vartheta) \cdot \cos(\epsilon_n h \cdot \cos \vartheta) d\vartheta = \pi \sum_{s \geq 0} A_{2s} \cdot (-1)^s J_{2s}(\epsilon_n h), \quad (5)$$

where  $J_k(z)$  is a Bessel function and  $A_{2s}$  are Fourier coefficients for the representation of  $c e_m(\vartheta)$  ( $\Rightarrow$  Sect. J.15).

The field matching in the orifice gives a system of linear equations for the  $A_n$ :

$$\begin{aligned} \sum_n A_n \cdot \left[ \delta_{n,k} \cdot \gamma_k h N_k - \frac{2}{\pi} \sum_m \frac{Hc_m^{(2)}(0)}{Hc_m^{(2)}(0)} R_{m,k} \cdot R_{m,n} \right] \\ = P_\mu \cdot \left[ \delta_{\mu,k} \cdot \gamma_\mu h N_\mu + \frac{2}{\pi} \sum_m \frac{Hc_m^{(2)}(0)}{Hc_m^{(2)}(0)} R_{m,k} \cdot R_{m,\mu} \right] \end{aligned} \quad (6)$$

(a prime indicates the derivative). Using its solutions the  $D_m$  can be determined from:

$$D_m = \frac{2}{\pi Hc_m^{(2)}(0)} \sum_n (\delta_{\mu,n} P_\mu + A_n) \cdot R_{m,n}. \quad (7)$$

A “radiation loss” can be defined by  $\Delta L = -10 \cdot \lg(\tau_\mu)$  with the transmission coefficient  $\tau_\mu$  being the ratio of the radiated effective power  $\Pi'_s$  to the effective incident power  $\Pi'_\mu$  of the  $\mu$ -th duct mode:

$$\begin{aligned} \Pi_\mu &= \frac{1}{2} \int_{-h}^h p_\mu(0, y) \cdot v_{\mu x}^*(0, y) dy = \frac{1}{2} \frac{j \gamma_\mu^*}{k_0 Z_0} |P_\mu|^2 \int_{-h}^h |\cos(\epsilon_\mu y)|^2 dy \\ &= \frac{1}{2} \frac{j \gamma_\mu^* h}{k_0 Z_0} |P_\mu|^2 \left( \frac{\sin(2\epsilon'_\mu h)}{2\epsilon'_\mu h} + \frac{\sinh(2\epsilon''_\mu h)}{2\epsilon''_\mu h} \right), \end{aligned} \quad (8)$$

$$\begin{aligned} \Pi_s &= \frac{1}{2} \int_{-h}^h p_s(0, y) \cdot v_{sx}^*(0, y) dy \\ &= \frac{h}{2} \int_0^\pi p_s(0, \vartheta) \cdot v_{s\rho}^*(0, \vartheta) \sin \vartheta d\vartheta \\ &= \frac{\pi}{4k_0 Z_0} \sum_m |D_m|^2 Yc_m'(0) \cdot (Jc_m(0) - jYc_m(0)), \end{aligned} \quad (9)$$

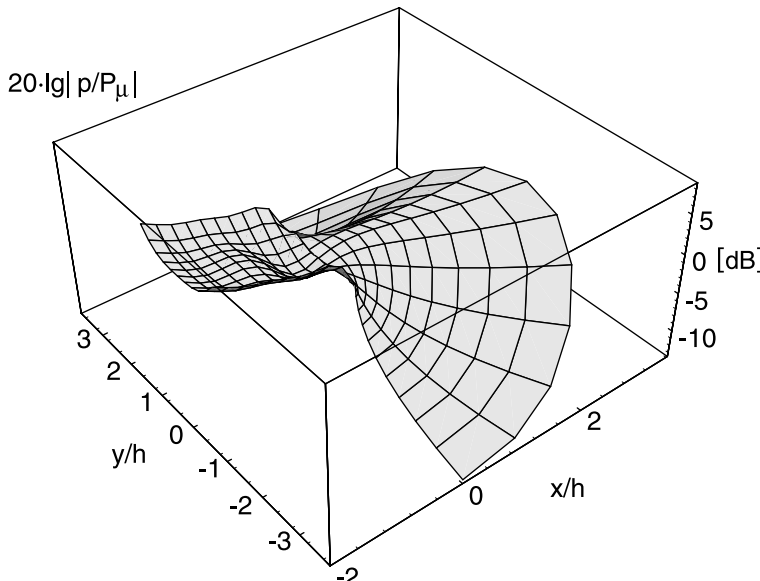
where  $Jc_m(z)$ ,  $Yc_m(z)$  are Mathieu–Bessel and Mathieu–Neumann functions associated with  $c e_m(\vartheta)$ . The transmission coefficient is thus (writing  $\epsilon_n = \epsilon'_n + j\epsilon''_n$ ;  $\gamma_n = \gamma'_n + j\gamma''_n$ ;  $\gamma_n^* = \gamma'_n - j\gamma''_n$ ):

$$\tau_\mu = \frac{\Pi'_s}{\Pi'_\mu} = \frac{\pi}{2\gamma_\mu'' h} \frac{\sum_m \frac{|D_m|^2}{|P_\mu|^2} Yc_m'(0) \cdot Jc_m(0)}{\left( \frac{\sin(2\epsilon'_\mu h)}{2\epsilon'_\mu h} + \frac{\sinh(2\epsilon''_\mu h)}{2\epsilon''_\mu h} \right)}. \quad (10)$$

In the special case of a hard duct:

$$\tau_\mu = \frac{\pi\delta_\mu}{4\sqrt{(k_0 h)^2 - (\mu\pi)^2}} \sum_m \frac{|D_m|^2}{|P_\mu|^2} Yc'_m(0) \cdot Jc_m(0); \quad \delta_\mu = \begin{cases} 1; & \mu = 0 \\ 2; & \mu > 0 \end{cases} \quad (11)$$

(with  $\gamma_\mu h = \sqrt{(\mu\pi)^2 - (k_0 h)^2}$ ).



3D plot of sound pressure level inside and behind a lined duct

#### Approximate determination of radiation loss $\Delta L$ :

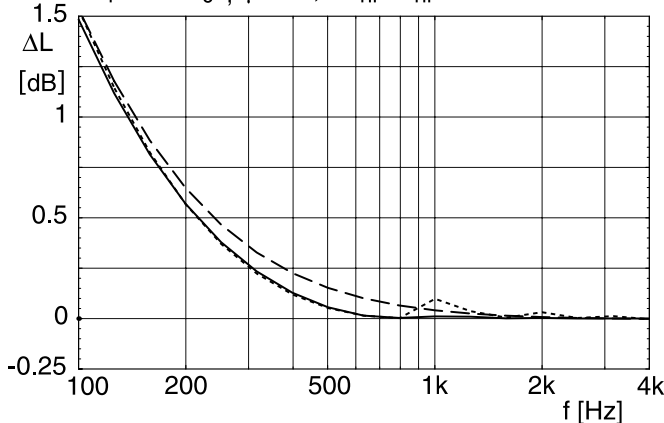
The radiation loss  $\Delta L$  of the orifice (in a baffle wall) of a lined duct can be evaluated approximately by:

$$\Delta L = -10 \cdot \lg(1 - |R|^2); \quad R = \frac{Z_r - Z_\mu}{Z_r + Z_\mu}; \quad (12)$$

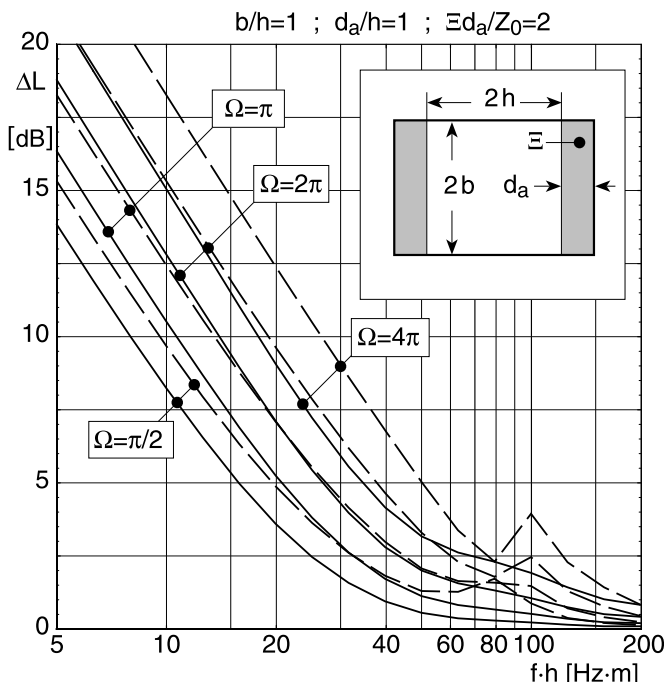
$$Z_\mu = jk_0 Z_0 / \gamma_\mu,$$

where  $Z_\mu$  is the axial wave impedance of the incident  $\mu$ th mode and  $Z_r$  is the radiation impedance either of a piston radiator with an area equal to the orifice area (if  $\mu$  belongs to the lowest or least attenuated mode) or of a cylindrical radiator with radius  $a = 2h/\pi$  (see  $\gg$  Sects. F.4, F.7 for radiation impedances).

$$h=0.2 \text{ [m]} ; d_a=0.1 \text{ [m]} ; \Xi=20 \text{ [kPas/m}^2\text{]} ; \\ Z_f=100 \cdot Z_0 ; \mu=1 ; n_{hi}=r_{hi}=4$$



Radiation loss  $\Delta L$  of duct orifice, lined with a layer of glass fibres, covered with a resistive foil having a flow resistance  $Z_f$ . *solid line*: with a piston radiator; *long dash*: with a cylindrical radiator; *short dash*: with elliptic co-ordinates



Radiation loss  $\Delta L$  of duct orifices of a hard duct (*solid*) and of a lined duct (*dashed*) for different radiation angles  $\Omega$ . Evaluated with the radiation impedance  $Z_r$  of a hemispherical radiator with radius  $a = \sqrt{S/\Omega}$  ( $S$  = orifice area)

The radiation loss depends on the volume angle  $\Omega$  into which the orifice radiates ( $\Omega = 4\pi$ : free space;  $\Omega = 2\pi$ : orifice in a baffle wall;  $\Omega = \pi$ : orifice in the corner of two walls;  $\Omega = \pi/2$ : orifice in the corner of three walls).

## J.28 Conical Duct Transitions; Special Case: Hard Walls

► See also: Mechel, J. Sound Vibr. 216, pp. 649–671 (1998)

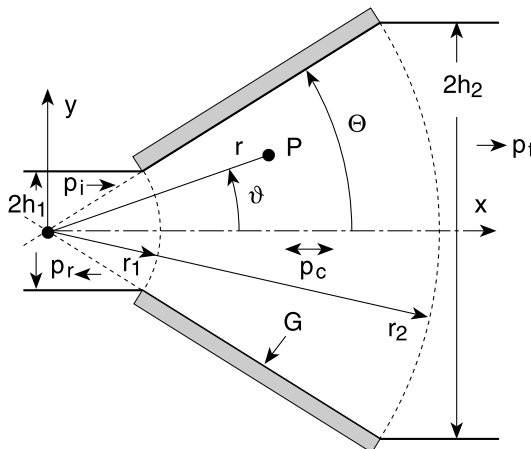
It seems appropriate to describe the sound field in conical (wedge-shaped) duct transitions in cylindrical co-ordinates  $r, \vartheta$  because the flanks would then be on co-ordinate surfaces and to separate modes in them as  $p(r, \vartheta) = T(\vartheta) \cdot R(r)$  with azimuthal profiles:

$$T(\vartheta) = \begin{cases} \cos(\eta\vartheta); & \text{symmetrical} \\ \sin(\eta\vartheta); & \text{anti-symmetrical} \end{cases} \quad (1)$$

for symmetrical or anti-symmetrical distributions relative to the  $x$  axis. Such modes would be orthogonal over  $\vartheta$  and, therefore, would be suitable for modal analysis of the fields. If the lining of the cone is locally reacting with a surface admittance  $G$ , the azimuthal wave numbers  $\eta$  have to be solutions of the equation:

$$jk_0 r \cdot \Theta Z_0 G = \begin{cases} (\eta\Theta) \cdot \tan(\eta\Theta); & \text{symmetrical} \\ -(\eta\Theta) \cdot \cot(\eta\Theta); & \text{anti-symmetrical} \end{cases} \quad (2)$$

In general,  $\eta = \eta(r)$ , and this prevents a separation of the mode into factors depending on only one co-ordinate.



*Special cases with separation are:*

- $G = 0$  (i.e. hard flank):

$$\eta\Theta = \begin{cases} m\pi; & \text{symmetrical} \\ (m + 1/2)\pi; & \text{anti-symmetrical} \end{cases}; \quad m = 0, 1, 2, \dots, \quad (3)$$

- $G = \infty$  (i.e. soft flank):

$$\eta\Theta = \begin{cases} (m + 1/2)\pi; & \text{symmetrical} \\ m\pi; & \text{anti-symmetrical} \end{cases}; \quad m = 0, 1, 2, \dots, \quad (4)$$

- $G = G(r) \sim 1/r: \quad \eta\Theta = \text{const}(r),$
- parallel walls (in distance  $2h$ ) with characteristic equation:

$$jk_0h \cdot Z_0G = \begin{cases} (\eta h) \cdot \tan(\eta h); & \text{symmetrical} \\ -(\eta h) \cdot \cot(\eta h); & \text{anti-symmetrical} \end{cases}. \quad (6)$$

In these cases the radial part of the wave equation becomes the Bessel differential equation:

$$\left[ \frac{d^2}{d(k_0r)^2} + \frac{1}{k_0r} \frac{d}{d(k_0r)} + \left( \kappa^2 - \frac{\eta^2}{(k_0r)^2} \right) \right] R(k_0r) = 0; \quad \kappa^2 = 1 - (k_z/k_0)^2, \quad (7)$$

where  $k_z \neq 0$  if in the  $z$  direction a field variation with  $\cos(k_z z), \sin(k_z z), e^{\pm jk_z z}$  or a linear combination thereof exists. Thus, if  $\kappa = 1$ , the radial factors  $R(k_0r)$  are Bessel, Neumann, and Hankel functions of order  $\eta$ .

This section further deals with the *first special case of hard flanks*; the next sections will present methods for the evaluation of sound fields in lined cones.

Both the entrance duct with height  $2h_1$  and the exit duct with height  $2h_2$  are assumed to be hard also (if they are lined, mainly the lateral mode wave numbers in the ducts  $\epsilon_{i,n}$  have to be solutions of the characteristic equations in these ducts). The terminating ducts are infinite; the  $\mu$ th mode of the entrance duct is the incident wave  $p_i$ ; it is assumed to be a symmetrical mode. The reflected wave  $p_r$  in the entrance duct, the transmitted wave  $p_t$  in the exit duct, and the field  $p_c$  in the cone are formulated as mode sums. The fields are matched with respect to their pressures and radial particle velocities  $v_r = v_x \cdot \cos \vartheta + v_y \cdot \sin \vartheta$  at the arcs  $r_i$ ;  $i = 1, 2$ ; with  $h_i = r_i \cdot \sin \Theta$ . On these arcs is:  $x = r_i \cdot \cos \vartheta; y = r_i \cdot \sin \vartheta$ .

Field formulations:

$$p_i(x, y) = P_i \cdot \cos(\epsilon_{1\mu} y) \cdot e^{-\gamma_{1\mu} x};$$

$$p_r(x, y) = \sum_{n \geq 0} A_n \cdot \cos(\epsilon_{1n} y) \cdot e^{+\gamma_{1n} x}; \quad \epsilon_{1n} h_1 = n \cdot \pi; \quad \gamma_{1n}^2 = \epsilon_{1n}^2 - k_0^2; \quad (8)$$

$$p_t(x, y) = \sum_{n \geq 0} D_n \cdot \cos(\epsilon_{2n} y) \cdot e^{-\gamma_{2n} x};$$

$$p_c(x, y) = \sum_{m \geq 0} \cos(\eta_m \vartheta) \cdot (B_m \cdot J_{\eta_m}(k_0 r) + C_m \cdot Y_{\eta_m}(k_0 r)); \quad \eta_m \Theta = m \cdot \pi;$$

$$Nc_m := \frac{1}{2\Theta} \int_{-\Theta}^{+\Theta} \cos^2(\eta_m \vartheta) d\vartheta = \frac{1}{2} \left( 1 + \frac{\sin(2\eta_m \Theta)}{2\eta_m \Theta} \right) = \frac{1}{\delta_m}; \quad \delta_m = \begin{cases} 1; & m = 0 \\ 2; & m > 0 \end{cases}. \quad (9)$$

Introduce the integrals ( $i = 1, 2$ ):

$$\begin{aligned} I_{n,k}^{(\pm)}(r_i) &:= \frac{1}{2\Theta} \int_{-\Theta}^{+\Theta} \cos(\epsilon_{in} r_i \sin \vartheta) \cdot e^{\pm \gamma_{in} r_i \cos \vartheta} \cdot \cos(\eta_k \vartheta) d\vartheta, \\ J_{n,k}^{(\pm)}(r_i) &:= \frac{1}{2\Theta} \int_{-\Theta}^{+\Theta} \cos(\epsilon_{in} r_i \sin \vartheta) \cdot e^{\pm \gamma_{in} r_i \cos \vartheta} \cdot \cos(\eta_k \vartheta) \cdot \cos \vartheta d\vartheta, \\ K_{n,k}^{(\pm)}(r_i) &:= \frac{1}{2\Theta} \int_{-\Theta}^{+\Theta} \sin(\epsilon_{in} r_i \sin \vartheta) \cdot e^{\pm \gamma_{in} r_i \cos \vartheta} \cdot \cos(\eta_k \vartheta) \cdot \sin \vartheta d\vartheta. \end{aligned} \quad (10)$$

The integrals must be evaluated by numerical integration.

(Because the integrands are even in  $\vartheta$ , they can be evaluated as

$$\frac{1}{2\Theta} \int_{-\Theta}^{+\Theta} \dots d\vartheta = \frac{1}{\Theta} \int_0^{+\Theta} \dots d\vartheta.)$$

Application of the operator  $\frac{1}{2\Theta} \int_{-\Theta}^{+\Theta} \dots \cos(\eta_k \vartheta) d\vartheta$

$$(11)$$

on the boundary condition for the sound pressure  $p_i(r_1, \vartheta) + p_r(r_1, \vartheta) = p_c(r_1, \vartheta)$  on the arc with  $r_1$  gives the following system of equations:

$$P_i \cdot I_{\mu,k}^{(-)}(r_1) + \sum_{n \geq 0} A_n \cdot I_{n,k}^{(+)}(r_1) = N c_k [B_k \cdot J_{\eta_k}(k_0 r_1) + C_k \cdot Y_{\eta_k}(k_0 r_1)]. \quad (12)$$

The same operator applied to the boundary condition for the radial particle velocity at  $r_1$  leads to (the prime indicates the derivative):

$$\begin{aligned} P_i \cdot \left[ \frac{-\gamma_{1\mu}}{k_0} J_{\mu,k}^{(-)}(r_1) - \frac{\epsilon_{1\mu}}{k_0} K_{\mu,k}^{(-)}(r_1) \right] + \sum_{n \geq 0} A_n \cdot \left[ \frac{\gamma_{1n}}{k_0} J_{n,k}^{(+)}(r_1) - \frac{-\epsilon_{1n}}{k_0} K_{n,k}^{(+)}(r_1) \right] \\ := P_i \cdot b_{\mu,k} + \sum_{n \geq 0} A_n \cdot a_{n,k} = N c_k [B_k \cdot J'_{\eta_k}(k_0 r_1) + C_k \cdot Y'_{\eta_k}(k_0 r_1)]. \end{aligned} \quad (13)$$

On the arc with  $r_2$  drop terms with  $P_i$  as factor; substitute  $r_1 \rightarrow r_2$ ;  $A_n \rightarrow D_n$ ;  $\epsilon_{1n} \rightarrow \epsilon_{2n}$ ;  $\gamma_{1n} \rightarrow -\gamma_{2n}$ ; and substitute the integrals correspondingly; this gives:

$$\sum_{n \geq 0} D_n \cdot I_{n,k}^{(-)}(r_2) = N c_k [B_k \cdot J_{\eta_k}(k_0 r_2) + C_k \cdot Y_{\eta_k}(k_0 r_2)], \quad (14)$$

$$\begin{aligned} \sum_{n \geq 0} D_n \cdot \left[ \frac{-\gamma_{2n}}{k_0} J_{n,k}^{(-)}(r_2) - \frac{-\epsilon_{2n}}{k_0} K_{n,k}^{(-)}(r_2) \right] \\ := \sum_{n \geq 0} D_n \cdot d_{n,k} = N c_k [B_k \cdot J'_{\eta_k}(k_0 r_2) + C_k \cdot Y'_{\eta_k}(k_0 r_2)]. \end{aligned} \quad (15)$$

Solve these two equations at  $r_2$  (with fixed but arbitrary integer  $k \geq 0$ ) for  $B_k, C_k$ :

$$\begin{aligned} B_k &= \frac{\pi k_0 r_2}{2Nc_k} \sum_{n \geq 0} D_n \cdot \left( I2_{n,k}^{(-)}(r_2) \cdot Y'_{\eta_k}(k_0 r_2) - d_{n,k} \cdot Y_{\eta_k}(k_0 r_2) \right), \\ C_k &= -\frac{\pi k_0 r_2}{2Nc_k} \sum_{n \geq 0} D_n \cdot \left( I2_{n,k}^{(-)}(r_2) \cdot J'_{\eta_k}(k_0 r_2) - d_{n,k} \cdot J_{\eta_k}(k_0 r_2) \right). \end{aligned} \quad (16)$$

This inserted into the equations at  $r_1$  leads to two coupled systems of linear equations for the sets  $A_n, D_n$  of amplitudes:

$$\begin{aligned} \sum_{n \geq 0} A_n \cdot I1_{n,k}^{(+)}(r_1) + \frac{\pi k_0 r_2}{2} \sum_{n \geq 0} D_n \cdot \left[ d_{n,k} \cdot (J_{\eta_k}(k_0 r_1) \right. \\ \left. \cdot Y_{\eta_k}(k_0 r_2) - J_{\eta_k}(k_0 r_2) \cdot Y'_{\eta_k}(k_0 r_1)) \right] \end{aligned} \quad (17)$$

$$+ I2_{n,k}^{(-)}(r_2) \cdot \left( J'_{\eta_k}(k_0 r_2) \cdot Y_{\eta_k}(k_0 r_1) - J_{\eta_k}(k_0 r_1) \cdot Y'_{\eta_k}(k_0 r_2) \right) \Big] = -P_i \cdot I1_{\mu,k}^{(-)}(r_1),$$

$$\begin{aligned} \sum_{n \geq 0} A_n \cdot a_{n,k} + \frac{\pi k_0 r_2}{2} \sum_{n \geq 0} D_n \cdot \left[ d_{n,k} \cdot \left( J'_{\eta_k}(k_0 r_1) \cdot Y_{\eta_k}(k_0 r_2) - J_{\eta_k}(k_0 r_2) \cdot Y'_{\eta_k}(k_0 r_1) \right) \right. \\ \left. + I2_{n,k}^{(-)}(r_2) \cdot \left( J'_{\eta_k}(k_0 r_2) \cdot Y'_{\eta_k}(k_0 r_1) - J'_{\eta_k}(k_0 r_1) \cdot Y'_{\eta_k}(k_0 r_2) \right) \right] = -P_i \cdot b_{\mu,k}. \end{aligned} \quad (18)$$

The  $B_k, C_k$  can be evaluated with the solutions  $D_n$ . The sound field is determined.

## J.29 Lined Conical Duct Transition, Evaluated with Stepping Duct Sections

---

► See also: Mechel, J. Sound Vibr. 216, pp. 673–696 (1998)

This section makes use of the last special case in Sect. J.28, i. e. it composes a lined (locally reacting) duct cone with stepping duct sections having parallel walls.

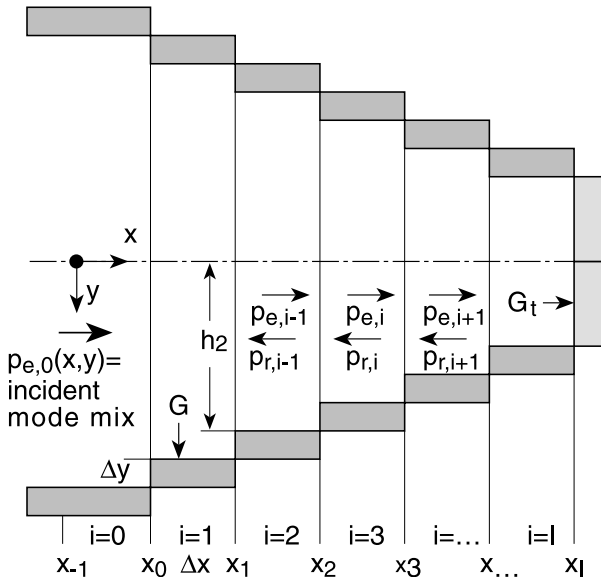
All duct sections may have equal linings (for ease of representation) with surface admittance  $G$ .

The duct section  $i = 0$  is the entrance duct (infinitely long); it sends a mode mix to the stepping sections. The last section  $i = I$  is terminated with an admittance  $G_t$ .

The heads of the steps are assumed to be hard. In each section the forward wave  $p_{e,i}$  and the backward wave  $p_{r,i}$  are written as sums of modes of that section. The fields are matched at the section limits with their sound pressure and axial particle velocity.

Field formulation:

$$\begin{aligned} p_{e,i}(x, y) &= \sum_{m \geq 0} A_{i,m} \cdot q_{i,m}(y) \cdot e^{-\gamma_{i,m}(x-x_{i-1})}, \\ p_{r,i}(x, y) &= \sum_{m \geq 0} B_{i,m} \cdot q_{i,m}(y) \cdot e^{+\gamma_{i,m}(x-x_i)} \end{aligned} \quad (1)$$



with lateral mode profiles:

$$q_{i,m}(y) = \begin{cases} \cos(\epsilon_{i,m}y) ; & \text{symmetrical} \\ \sin(\epsilon_{i,m}y) ; & \text{anti-symmetrical.} \end{cases} \quad (2)$$

The axial propagation constants  $\gamma_{i,m}$  are obtained by:

$$\gamma_{i,m}^2 = \epsilon_{i,m}^2 - k_0^2 ; \quad \operatorname{Re}\{\gamma_{i,m}\} \geq 0 \quad (3)$$

from the lateral wave numbers, and these in turn are solutions of the characteristic equations:

$$\begin{aligned} (\epsilon_{i,m}h_i) \cdot \tan(\epsilon_{i,m}h_i) &= jk_0h_i \cdot G ; & \text{symmetrical ,} \\ (\epsilon_{i,m}h_i) \cdot \cot(\epsilon_{i,m}h_i) &= -jk_0h_i \cdot G ; & \text{anti-symmetrical .} \end{aligned} \quad (4)$$

The mode norms are:

$$\frac{1}{h_i} \int_0^{h_i} q_{i,m}(y) \cdot q_{i,n}(y) dy = \delta_{m,n} \cdot N_{i,m} ; \quad N_{i,m} = \frac{1}{2} \left( 1 \pm \frac{\sin(2\epsilon_{i,m}h_i)}{2\epsilon_{i,m}h_i} \right), \quad (5)$$

and the mode coupling coefficients  $C(i, m; k, n)$  of the mode of order  $m$  in section  $i$  with the mode of order  $n$  in section  $k$  are:

$$\begin{aligned} \frac{1}{h_i} \int_0^{h_i} q_{i,m}(y) \cdot q_{k,n}(y) dy &= C(i, m; k, n) , \\ C(i, m; k, n) &= \frac{1}{2} \left( \frac{\sin((\epsilon_{i,m} - \epsilon_{k,n})h_i)}{(\epsilon_{i,m} - \epsilon_{k,n})h_i} \pm \frac{\sin((\epsilon_{i,m} + \epsilon_{k,n})h_i)}{(\epsilon_{i,m} + \epsilon_{k,n})h_i} \right) \end{aligned} \quad (6)$$

( $\pm$  for symmetrical or anti-symmetrical modes, respectively; cross-coupling coefficients between both types of symmetry are zero).

By the special termination of the wedge with an admittance  $G_t$  one has:

$$\{B_{I,m}\} = \{M_t\} \circ \{A_{I,m}\} = \{r_m \cdot e^{-Y_{I,m} \Delta x}\} \circ \{A_{I,m}\}, \quad (7)$$

where  $\{M_t\}$  is a general coupling matrix ( $\circ$  is the symbol for matrix multiplication), which in the present case is a diagonal matrix with the values  $r_m \cdot e^{-Y_{I,m} \Delta x}$  on the main diagonal,  $r_m$  being the modal reflection factors at the exit of the last section  $i = I$ :

$$r_m = \frac{g_m - G_t}{g_m + G_t} = \frac{jY_{I,m}/k_0 + G_t}{jY_{I,m}/k_0 - G_t}, \quad (8)$$

and  $g_m$  the normalised axial modal admittances of the modes of  $p_{e,I}(x, y)$ :

$$g_m = Z_0 \frac{v_{x,I,m}(x_I)}{p_{e,I,m}(x_I)} = -j \frac{Y_{I,m}}{k_0}. \quad (9)$$

*Converging cone:*

The boundary condition for the sound pressure at the entrance  $x = x_{i-1}$  of the  $i$ -th section ( $i \geq 1$ ) is:

$$p_{e,i-1}(x_{i-1}, y) + p_{r,i-1}(x_{i-1}, y) \stackrel{!}{=} p_{e,i}(x_{i-1}, y) + p_{r,i}(x_{i-1}, y); \quad 0 \leq y \leq h_i, \\ \sum_m (A_{i-1,m} \cdot e^{-Y_{i-1,m} \Delta x} + B_{i-1,m}) \cdot q_{i-1,m}(y) \stackrel{!}{=} \sum_m (A_{i,m} + B_{i,m} \cdot e^{-Y_{i,m} \Delta x}) \cdot q_{i,m}(y). \quad (10)$$

Application of the operation  $\frac{1}{h_i} \int_0^{h_i} \dots \cdot q_{i,m}(y) dy$  on both sides gives the following system of equations:

$$(A_{i,m} + B_{i,m} \cdot e^{-Y_{i,m} \Delta x}) \cdot N_{i,m} = \sum_n (A_{i-1,n} \cdot e^{-Y_{i-1,n} \Delta x} + B_{i-1,n}) \cdot C(i, m; i-1, n). \quad (11)$$

This is an upward iteration scheme.

The boundary condition for the axial particle velocity at  $x = x_{i-1}$  is:

$$v_{xe,i-1}(x_{i-1}, y) + v_{xr,i-1}(x_{i-1}, y) \stackrel{!}{=} \begin{cases} 0 & ; h_i \leq y \leq h_{i-1} \\ v_{xe,i}(x_{i-1}, y) + v_{xr,i}(x_{i-1}, y) & ; 0 \leq y \leq h_i \end{cases}, \\ \sum_m (A_{i-1,m} \cdot e^{-Y_{i-1,m} \Delta x} - B_{i-1,m}) \cdot Y_{i-1,m} \cdot q_{i-1,m}(y) \stackrel{!}{=} \\ \left\{ \begin{array}{ll} 0 & ; h_i \leq y \leq h_{i-1} \\ \sum_m (A_{i,m} - B_{i,m} \cdot e^{-Y_{i,m} \Delta x}) \cdot Y_{i,m} \cdot q_{i,m}(y) & ; 0 \leq y \leq h_i \end{array} \right.. \quad (12)$$

Application of the operators  $\frac{1}{h_i} \int_0^{h_i} \dots \cdot q_{i,m}(y) dy$  left;  $\frac{1}{h_{i-1}} \int_0^{h_{i-1}} \dots \cdot q_{i,m}(y) dy$  right produces the following system of equations:

$$(A_{i,m} - B_{i,m} \cdot e^{-Y_{i,m} \Delta x}) \cdot Y_{i,m} \cdot N_{i,m} = \frac{h_{i-1}}{h_i} \sum_n (A_{i-1,n} \cdot e^{-Y_{i-1,n} \Delta x} - B_{i-1,n}) \\ \cdot Y_{i-1,n} \cdot C(i-1, n; i, m). \quad (13)$$

One gets, by combination of both systems of equations:

$$\begin{aligned} A_{i,m} &= \frac{1}{2N_{i,m}} \sum_n A_{i-1,n} \cdot e^{-\gamma_{i-1,m} \Delta x} \cdot \left( C(i, m; i-1, n) + C(i-1, n; i, m) \frac{\gamma_{i-1,n} h_{i-1}}{\gamma_{i,m} h_i} \right) \\ &\quad + B_{i-1,n} \cdot \left( C(i, m; i-1, n) - C(i-1, n; i, m) \frac{\gamma_{i-1,n} h_{i-1}}{\gamma_{i,m} h_i} \right), \\ B_{i,m} &= \frac{1}{2N_{i,m} \cdot e^{-\gamma_{i,m} \Delta x}} \sum_n A_{i-1,n} \cdot e^{-\gamma_{i-1,n} \Delta x} \\ &\quad \cdot \left( C(i, m; i-1, n) - C(i-1, n; i, m) \frac{\gamma_{i-1,n} h_{i-1}}{\gamma_{i,m} h_i} \right) \\ &\quad + B_{i-1,n} \cdot \left( C(i, m; i-1, n) + C(i-1, n; i, m) \frac{\gamma_{i-1,n} h_{i-1}}{\gamma_{i,m} h_i} \right). \end{aligned} \quad (14)$$

The upward iterations begin at  $i = 1$ , where  $A_{i-1,m} = A_{0,m}$  have given numerical values and  $B_{0,m}$  are unknown symbols. At any step  $i$  of the iteration one will have systems of equations of the form:

$$A_{i,m} = \sum_n a_{i,n} + b_{i,n} \cdot B_{0,n}; \quad B_{i,m} = \sum_n \alpha_{i,n} + \beta_{i,n} \cdot B_{0,n} \quad (15)$$

with numerical  $a_{i,n}, b_{i,n}, \alpha_{i,n}, \beta_{i,n}$ . The iteration ends with  $i = I$ , where on the left-hand sides of the iterative equations stand  $\{A_{I,m}\}$  and  $\{B_{I,m}\}$ , which, with the above relation of reflection, reduce to only the  $\{A_{I,m}\}$  as yet unknown amplitudes. Thus the equations for  $i = I$  are two linear systems of equations in the two sets of amplitudes  $\{A_{I,m}\}, \{B_{0,n}\}$ , and they are inhomogeneous systems of equations because of the numerical terms  $a_{I,n}, \alpha_{I,n}$ . After they are solved for  $\{B_{0,n}\}$ , all amplitudes  $\{A_{i,m}\}, \{B_{i,m}\}$  can be evaluated by insertion. The described iteration with mixed numerical and symbolic expressions can easily be performed with *Mathematica* or other computer programs for both numerical and symbolic mathematics.

#### Diverging cone:

One gets in a similar way the following two downward iterative systems of equations:

$$\begin{aligned} A_{i-1,m} &= \frac{1}{2N_{i-1,m} \cdot e^{-\gamma_{i-1,m} \Delta x}} \cdot \sum_n A_{i,n} \cdot \left( C(i-1, m; i, n) + \frac{\gamma_{i,n} h_i}{\gamma_{i-1,m} h_{i-1}} \cdot C(i, n; i-1, m) \right) \\ &\quad + B_{i,n} \cdot e^{-\gamma_{i,n} \Delta x} \cdot \left( C(i-1, m; i, n) - \frac{\gamma_{i,n} h_i}{\gamma_{i-1,m} h_{i-1}} \cdot C(i, n; i-1, m) \right), \\ B_{i-1,m} &= \frac{1}{2N_{i-1,m}} \cdot \sum_n A_{i,n} \cdot \left( C(i-1, m; i, n) - \frac{\gamma_{i,n} h_i}{\gamma_{i-1,m} h_{i-1}} \cdot C(i, n; i-1, m) \right) \\ &\quad + B_{i,n} \cdot e^{-\gamma_{i,n} \Delta x} \cdot \left( C(i-1, m; i, n) + \frac{\gamma_{i,n} h_i}{\gamma_{i-1,m} h_{i-1}} \cdot C(i, n; i-1, m) \right). \end{aligned} \quad (16)$$

If one begins the iteration with  $i = I$ , the equations have the form:

$$A_{I-1,m} = \sum_n b_{I,n} \cdot A_{I,n}; \quad B_{I-1,m} = \sum_n \beta_{I,n} \cdot A_{I,n} \quad (17)$$

with still unknown amplitudes  $\{A_{I,n}\}$ , and in the general step  $i$ :

$$A_{i-1,m} = \sum_n b_{i,n} \cdot A_{i,n}; \quad B_{i-1,m} = \sum_n \beta_{i,n} \cdot A_{i,n} \quad (18)$$

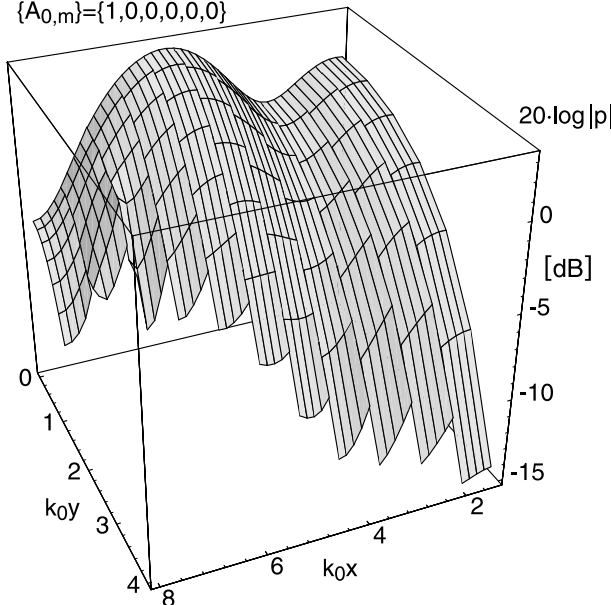
with numerical values of  $b_{i,n}, \beta_{i,n}$ . At the end, with  $i = 1$ , one has the known amplitudes  $\{A_{0,m}\}$  of the incident modes on the left-hand side of the first equation. Thus it can be solved for the  $\{A_{1,n}\}$ , and with these all other amplitudes  $\{A_{i,m}\}, \{B_{i,m}\}$  are computed by insertion.

The numerical examples show 3D plots of the sound pressure level; the spatial coordinates are  $k_0x, k_0y$ .

$$G=2-j; \quad G_t=1; \quad m_{hi}=5; \quad I=10$$

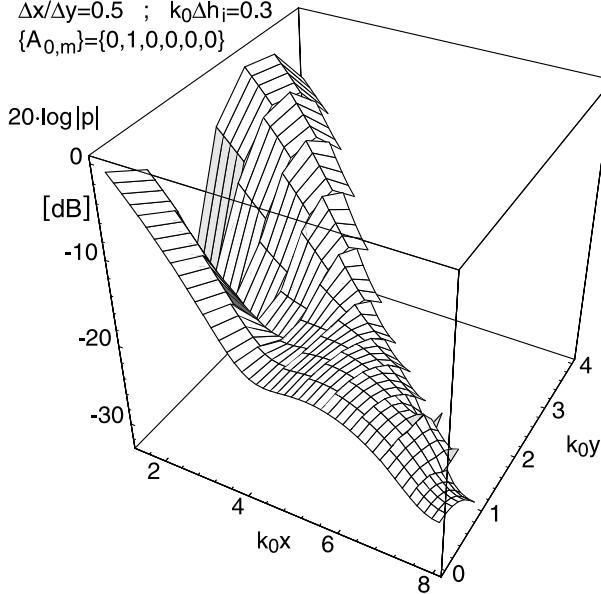
$$\Delta x/\Delta y=0.5; \quad k_0\Delta h_i=0.3$$

$$\{A_{0,m}\}=\{1,0,0,0,0,0\}$$



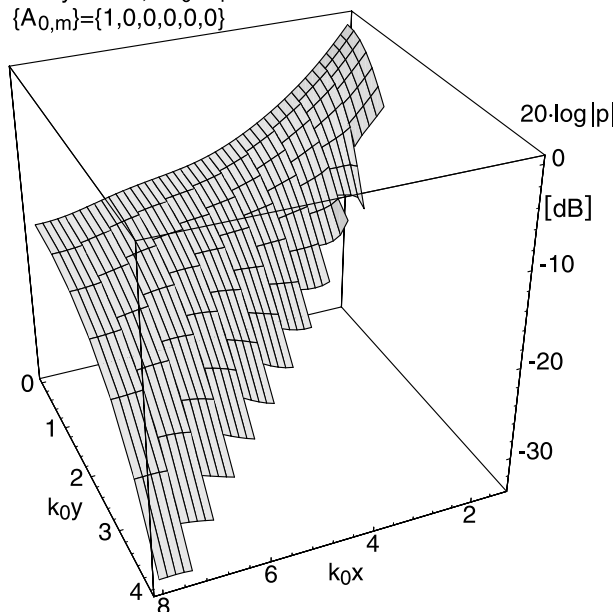
Sound pressure level in a converging cone, with the fundamental duct mode incident

$G=2-j$  ;  $G_t=1$  ;  $m_{hi}=5$  ;  $l=10$   
 $\Delta x/\Delta y=0.5$  ;  $k_0\Delta h_i=0.3$   
 $\{A_{0,m}\}=\{0,1,0,0,0,0\}$



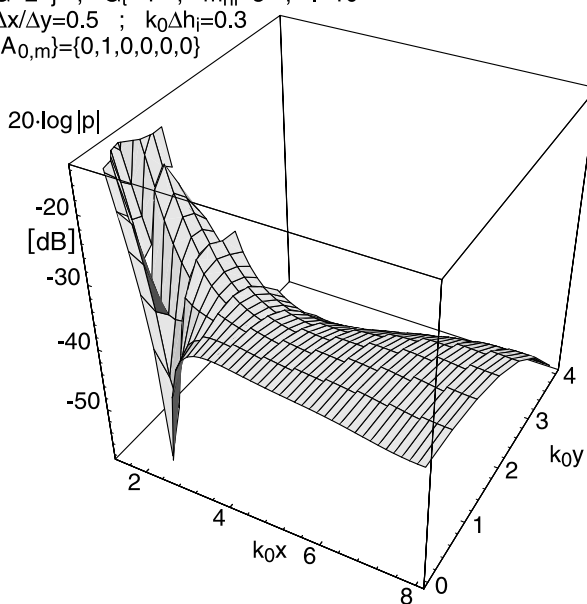
As above, but with the first higher duct mode incident

$G=2-j$  ;  $G_t=1$  ;  $m_{hi}=5$  ;  $l=10$   
 $\Delta x/\Delta y=0.5$  ;  $k_0\Delta h_i=0.3$   
 $\{A_{0,m}\}=\{1,0,0,0,0,0\}$



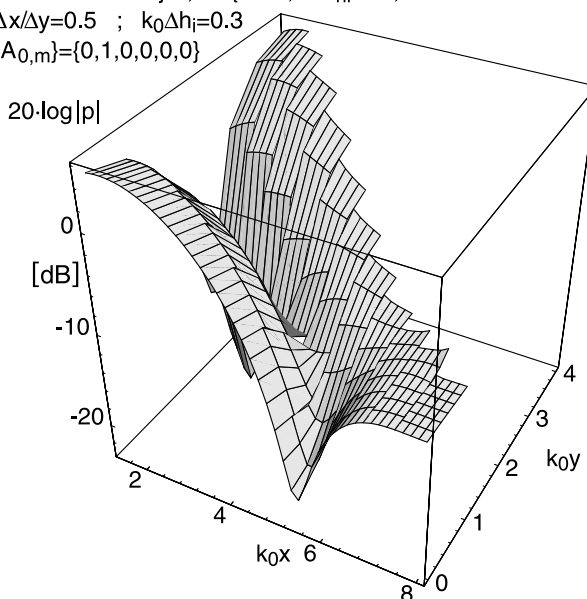
Sound pressure level in a diverging cone, with the fundamental duct mode incident

$$\begin{aligned}
 G &= 2-j ; \quad G_t = 1 ; \quad m_{hi} = 5 ; \quad l = 10 \\
 \Delta x / \Delta y &= 0.5 ; \quad k_0 \Delta h_i = 0.3 \\
 \{A_{0,m}\} &= \{0, 1, 0, 0, 0, 0\}
 \end{aligned}$$



As in the previous graph, but now with the first higher mode incident

$$\begin{aligned}
 G &= 0.01 - 0.01 \cdot j ; \quad G_t = 1 ; \quad m_{hi} = 5 ; \quad l = 10 \\
 \Delta x / \Delta y &= 0.5 ; \quad k_0 \Delta h_i = 0.3 \\
 \{A_{0,m}\} &= \{0, 1, 0, 0, 0, 0\}
 \end{aligned}$$



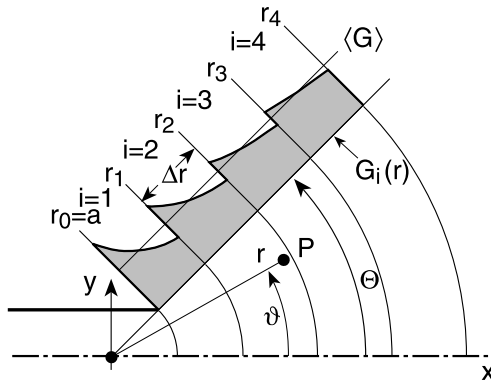
Sound pressure level in a converging, nearly hard cone, with the first higher mode incident. It becomes cut off inside the cone

### J.30 Lined Conical Duct Transition, Evaluated with Stepping Admittance Sections

► See also: Mechel, J. Sound Vibr. 219 (1999)

This section applies the third special case of Sect. J.28:  $\eta\Theta = \text{const}(r)$  if the lining admittance  $G = G(r) \sim 1/r$ . This condition is not satisfied over the entire radial range, but in radial sections  $i = 1, 2, \dots$ , such that  $G_i(r) \sim 1/r$ , and the average admittance in the sections equals a given value  $G$ :

$$\langle G_i \rangle = G. \quad (1)$$



The computational sectional admittances are:

$$G_i(r) = \frac{G}{r} \frac{r_i - r_{i-1}}{\ln(r_i/r_{i-1})}. \quad (2)$$

If the section width  $\Delta r$  is small compared to the wavelength, and if the variation of  $G_i(r)$  is not too strong, the sectored lining will approximately produce a sound field like that for a homogeneous lining with admittance  $G$  (the conditions mentioned exclude a lining reaching to the origin  $r = 0$ ).

The sound fields in the sections can be written as sums of modes, which are orthogonal over  $0 \leq \vartheta \leq \Theta$ :

$$p_i(r, \vartheta, z) = \sum_{\eta} R_{\eta}(kr) \cdot T(\eta\vartheta) \cdot Z(k_z z) \quad (3)$$

with  $k^2 = k_0^2 - k_z^2$  if the variation  $Z(k_z z)$  in the  $z$  direction is like  $\cos(k_z z)$ ,  $\sin(k_z z)$ ,  $e^{\pm jk_z z}$  or a linear combination thereof, with

$$T(\eta\vartheta) = \begin{cases} \cos(\eta\vartheta); & \text{symmetrical modes} \\ \sin(\eta\vartheta); & \text{anti-symmetrical modes} \end{cases}, \quad (4)$$

where the radial functions  $R_{\eta}(kr)$  are Bessel, Neumann, or Hankel functions of order  $\eta$ , and with  $\eta\Theta$  solutions of:

$$\begin{aligned} (\eta\Theta_0) \cdot \tan(\eta\Theta_0) &= jkr \cdot \Theta_0 G; & \text{symmetrical modes} \\ (\eta\Theta_0) \cdot \cot(\eta\Theta_0) &= -jkr \cdot \Theta_0 G; & \text{anti-symmetrical modes} \end{aligned}, \quad (5)$$

or, more definitely (with the mode counter  $n$  in the  $i$ -th section):

$$(\eta_{i,n}\Theta) \cdot \begin{cases} \tan & (\eta_{i,n}\Theta) = \pm j\Theta \frac{k_0\Delta r}{\ln(r_i/r_{i-1})} G \end{cases} \begin{cases} \text{rigid} & \text{flank at } \vartheta = 0 \\ \text{soft} & \end{cases} . \quad (6)$$

The mode norms are

$$N_{i,n} = \frac{1}{\Theta} \int_0^\Theta \frac{\cos^2}{\sin^2} (\eta_{i,n}\vartheta) d\vartheta = \frac{1}{2} \left( 1 \pm \frac{\sin(2\eta_{i,n}\Theta)}{2\eta_{i,n}\Theta} \right) . \quad (7)$$

The sound field in zone  $i$  is formulated as (henceforth only symmetrical modes are assumed; a possible variation in the  $z$  direction with  $Z(k_z z)$  will be dropped):

$$\begin{aligned} p_i(r, \vartheta) &= \sum_{m \geq 0} \left[ A_{i,m} \cdot H_{\eta_{i,m}}^{(1)}(kr) + B_{i,m} \cdot H_{\eta_{i,m}}^{(2)}(kr) \right] \cdot \cos(\eta_{i,m}\vartheta) , \\ Z_0 \cdot v_{r,i} &= \frac{jk}{k_0} \sum_{m \geq 0} \left[ A_{i,m} \cdot H_{\eta_{i,m}}'^{(1)}(kr) + B_{i,m} \cdot H_{\eta_{i,m}}'^{(2)}(kr) \right] \cdot \cos(\eta_{i,m}\vartheta) \end{aligned} \quad (8)$$

(a prime indicates the derivative). The amplitudes  $A_{i,m}$ ,  $B_{i,m}$  are determined by field matching at the section limits.

In a simple example of application of the method assume the following:

1. A given radial particle velocity distribution  $V_0(\vartheta)$  on the arc  $r = a$ .

(Some incident duct mode in the duct in front of  $r = a$  would lead to a method as described in the previous Sect. J.29.)

2. The cone is infinitely long.

(In practice it is sufficient if it is so long that the admittance step at the outer zone limit becomes small, so that reflections at the cone can be neglected, and the cone has an anechoic termination; other terminations are handled as in Sect. J.29, see also below.)

One needs coupling coefficients between modes of adjacent zones given by the integrals ( $T_{i,m}(\vartheta)$  are the azimuthal mode functions):

$$\begin{aligned} X_{m,n}^{(i)} &= \frac{1}{\Theta} \int_0^\Theta T_{i,m}(\vartheta) \cdot T_{i+1,n}(\vartheta) d\vartheta , \\ Y_{m,n}^{(i)} &= \frac{1}{\Theta} \int_0^\Theta T_{i,m}(\vartheta) \cdot T_{i-1,n}(\vartheta) d\vartheta = X_{n,m}^{(i-1)} . \end{aligned} \quad (9)$$

They assume the following values if the flank at  $\vartheta = 0$  is rigid:

$$X_{m,n}^{(i)} = \frac{1}{2} \left[ \frac{\sin((\eta_{i,m} - \eta_{i+1,n})\Theta)}{(\eta_{i,m} - \eta_{i+1,n})\Theta} + \frac{\sin((\eta_{i,m} + \eta_{i+1,n})\Theta)}{(\eta_{i,m} + \eta_{i+1,n})\Theta} \right] , \quad (10)$$

$$Y_{m,n}^{(i)} = \frac{1}{2} \left[ \frac{\sin((\eta_{i,m} - \eta_{i-1,n})\Theta)}{(\eta_{i,m} - \eta_{i-1,n})\Theta} + \frac{\sin((\eta_{i,m} + \eta_{i-1,n})\Theta)}{(\eta_{i,m} + \eta_{i-1,n})\Theta} \right] , \quad (11)$$

and if that flank at  $\vartheta = 0$  is soft:

$$\begin{aligned} X_{m,n}^{(i)} &= \frac{1}{2} \left[ \frac{\sin((\eta_{i,m} - \eta_{i+1,n})\Theta)}{(\eta_{i,m} - \eta_{i+1,n})\Theta} - \frac{\sin((\eta_{i,m} + \eta_{i+1,n})\Theta)}{(\eta_{i,m} + \eta_{i+1,n})\Theta} \right], \\ Y_{m,n}^{(i)} &= \frac{1}{2} \left[ \frac{\sin((\eta_{i,m} - \eta_{i-1,n})\Theta)}{(\eta_{i,m} - \eta_{i-1,n})\Theta} - \frac{\sin((\eta_{i,m} + \eta_{i-1,n})\Theta)}{(\eta_{i,m} + \eta_{i-1,n})\Theta} \right]. \end{aligned} \quad (12)$$

The boundary condition (source condition) at  $r = a$  is:

$$Z_0 \cdot v_{r,1} = \frac{jk}{k_0} \sum_{m \geq 0} \left[ A_{1,m} \cdot H'_{\eta_{1,m}}^{(1)}(ka) + B_{1,m} \cdot H'_{\eta_{1,m}}^{(2)}(ka) \right] \cdot \cos(\eta_{1,m}\vartheta) \stackrel{!}{=} Z_0 V_0(\vartheta) \quad (13)$$

leading to:

$$\frac{jkN_{1,m}}{k_0} \left[ A_{1,m} \cdot H'_{\eta_{1,m}}^{(1)}(ka) + B_{1,m} \cdot H'_{\eta_{1,m}}^{(2)}(ka) \right] = \frac{1}{\Theta} \int_0^\Theta Z_0 V_0(\vartheta) \cdot \cos(\eta_{1,m}\vartheta) d\vartheta \quad (14)$$

with known Fourier coefficients on the right-hand side.

Applying the integral operation  $\frac{1}{\Theta} \int_0^\Theta \dots \cos(\eta_{i+1,m}\vartheta) d\vartheta$  on both sides of the boundary condition for the sound pressure at the zone limit  $r_i$  between two zones  $i$  and  $i + 1$  gives:

$$\begin{aligned} & \left[ A_{i+1,m} \cdot H'_{\eta_{i+1,m}}^{(1)}(kr_i) + B_{i+1,m} \cdot H'_{\eta_{i+1,m}}^{(2)}(kr_i) \right] \cdot N_{i+1,m} \\ &= \sum_{n \geq 0} \left[ A_{i,n} \cdot H'_{\eta_{i,n}}^{(1)}(kr_i) + B_{i,n} \cdot H'_{\eta_{i,n}}^{(2)}(kr_i) \right] \cdot X_{n,m}^{(i)}, \end{aligned} \quad (15)$$

and for the radial particle velocity:

$$\begin{aligned} & \left[ A_{i+1,m} \cdot H'_{\eta_{i+1,m}}^{(1)}(kr_i) + B_{i+1,m} \cdot H'_{\eta_{i+1,m}}^{(2)}(kr_i) \right] \cdot N_{i+1,m} \\ &= \sum_{n \geq 0} \left[ A_{i,n} \cdot H'_{\eta_{i,n}}^{(1)}(kr_i) + B_{i,n} \cdot H'_{\eta_{i,n}}^{(2)}(kr_i) \right] \cdot X_{n,m}^{(i)}. \end{aligned} \quad (16)$$

Elimination of the  $B_{i+1,m}$  and use of the Wronski determinant for Hankel functions returns the upward iterative systems of equations:

$$\begin{aligned} A_{i+1,m} &= j \frac{\pi kr_i}{4N_{i+1,m}} \sum_{n \geq 0} \left[ A_{i,n} \cdot \left( H_{\eta_{i,n}}^{(1)}(kr_i) \cdot H'_{\eta_{i+1,m}}^{(2)}(kr_i) - H'_{\eta_{i,n}}^{(1)}(kr_i) \cdot H_{\eta_{i+1,m}}^{(2)}(kr_i) \right) \right. \\ & \quad \left. + B_{i,n} \cdot \left( H_{\eta_{i,n}}^{(2)}(kr_i) \cdot H'_{\eta_{i+1,m}}^{(2)}(kr_i) - H'_{\eta_{i,n}}^{(2)}(kr_i) \cdot H_{\eta_{i+1,m}}^{(2)}(kr_i) \right) \right] \cdot X_{n,m}^{(i)}, \end{aligned} \quad (17)$$

$$\begin{aligned} B_{i+1,m} &= -j \frac{\pi kr_i}{4N_{i+1,m}} \sum_{n \geq 0} \left[ A_{i,n} \cdot \left( H_{\eta_{i,n}}^{(1)}(kr_i) \cdot H'_{\eta_{i+1,m}}^{(1)}(kr_i) - H_{\eta_{i+1,m}}^{(1)}(kr_i) \cdot H_{\eta_{i,n}}^{(1)}(kr_i) \right) \right. \\ & \quad \left. + B_{i,n} \cdot \left( H_{\eta_{i,n}}^{(2)}(kr_i) \cdot H'_{\eta_{i+1,m}}^{(1)}(kr_i) - H_{\eta_{i+1,m}}^{(1)}(kr_i) \cdot H_{\eta_{i,n}}^{(2)}(kr_i) \right) \right] \cdot X_{n,m}^{(i)}. \end{aligned}$$

If we begin with  $i = 1$ , the  $B_{1,n}$  on the right-hand sides can be expressed by the (numerical) Fourier coefficients of the particle velocity distribution  $Z_0 V_0(\vartheta)$  at  $r_0 = a$  and the symbolic  $A_{1,n}$ . The equations will have the following general form during the iteration:

$$\begin{aligned} A_{i+1,m} &= j \frac{\pi k r_i}{4N_{i+1,m}} \sum_{n \geq 0} (a_{i,n} \cdot A_{1,n} + b_{i,n}) ; \\ B_{i+1,m} &= -j \frac{\pi k r_i}{4N_{i+1,m}} \sum_{n \geq 0} (\alpha_{i,n} \cdot A_{1,n} + \beta_{i,n}) , \end{aligned} \quad (18)$$

where  $a_{i,n}, b_{i,n}, \alpha_{i,n}, \beta_{i,n}$  are numerical quantities. When the iteration has proceeded up to a value  $i = I$ , for which the admittance step at  $r = r_I$  is small enough to neglect the inward reflection, i. e.  $B_{i \geq I, m} = 0$ , the equations will have the form:

$$A_{I+1,m} = j \frac{\pi k r_I}{4N_{I+1,m}} \sum_{n \geq 0} (a_{I,n} \cdot A_{1,n} + b_{I,n}) ; \quad 0 = -j \frac{\pi k r_I}{4N_{I+1,m}} \sum_{n \geq 0} (\alpha_{I,n} \cdot A_{1,n} + \beta_{I,n}) . \quad (19)$$

Then they are a coupled system of equations for the amplitude sets  $A_{1,n}, A_{I+1,n}$ . After the solution of this system, all other amplitudes follow by insertion.

If the cone is not infinitely long but ends with some termination at  $r = r_I$ , this termination will give a prescription of how to express the  $B_{I+1,m}$  by the  $A_{I+1,m}$ , and the procedure remains the same, in principle.

In general, the upper limit  $n_{hi}$  of the required mode orders will not be high, except if  $V_0(\vartheta)$  has many details.

### J.31 Mode Mixtures

---

► See also: Mechel, Vol. III, Ch. 40 (1998)

Modes are elementary solutions of a wave equation and of boundary conditions. For some kinds of boundaries they are orthogonal over the duct cross section and therefore suited for a synthesis of sound fields in the duct. Like the “science fiction” of a diffuse sound field in room acoustics, it may be useful to define in duct acoustics mode mixtures in which the modes obey some rules of mixing but may have random phases.

Consider a rectangular hard duct with the duct axis in the  $z$  direction and the origin of the transversal co-ordinates  $x, y$  in a duct corner. A sound wave propagating in the  $z$  direction may be described by:

$$p(x, y, z) = \sum_{m,n} p_{m,n}(x, y, z) = \sum_{m,n} A_{m,n} \cdot q_{m,n}(x, y) \cdot e^{-jk_{m,n}z} \quad (1)$$

with mode profiles (containing both symmetrical and anti-symmetrical modes with respect to the duct central axis):

$$q_{m,n}(x, y) = \cos(\varepsilon_m x) \cdot \cos(\eta_n y) ; \quad \varepsilon_m a = m \cdot \pi ; \quad \eta_n b = n \cdot \pi ; \quad m, n = 0, 1, 2, \dots \quad (2)$$

and

$$k_0^2 = \varepsilon_m^2 + \eta_n^2 + k_{m,n}^2 ; \quad k_{m,n}^2 = \varepsilon_m^2 + \eta_n^2 = (m\pi/a)^2 + (n\pi/b)^2 \quad (3)$$

with mode norms  $N_{m,n}$  ( $S$  = duct cross-section area):

$$\iint_S q_{m,n} \cdot q_{\mu,\nu} dx dy = \begin{cases} 0; & m, n \neq \mu, \nu; \\ S \cdot N_{m,n}; & m, n = \mu, \nu; \end{cases} \quad (4)$$

$$N_{m,n} = \frac{1}{\delta_m \cdot \delta_n}; \quad \delta_k = \begin{cases} 1; & k = 0 \\ 2; & k > 0 \end{cases}.$$

The modal angles (relative to the duct axis) are:

$$\Phi_{m,n} = \arccos \left( \frac{k_{m,n}}{k_0} \right) = \arcsin \left( \frac{k_{m,n}}{k_0} \right); \cos \Phi_{m,n} = \sqrt{1 - (m\pi/k_0 a)^2 - (n\pi/k_0 b)^2}. \quad (5)$$

Thus modes have the form:

$$p_{m,n}(x, y, z) = A_{m,n} \cdot \cos \left( \frac{m\pi}{a} x \right) \cdot \cos \left( \frac{n\pi}{b} y \right) \cdot e^{-jk_{m,n} z}, \quad (6)$$

$$v_{z_{m,n}}(x, y, z) = \frac{k_{m,n}}{k_0 Z_0} p_{m,n}(x, y, z) = G_{z_{m,n}} \cdot p_{m,n}(x, y, z),$$

where  $G_{z_{m,n}}$  are the modal axial field admittances:

$$G_{z_{m,n}} = \frac{k_{m,n}}{k_0 Z_0} = \frac{1}{Z_0} \sqrt{1 - (\kappa_{m,n}/k_0)^2} \quad (7)$$

$$= \frac{1}{Z_0} \sqrt{1 - (m\pi/k_0 a)^2 - (n\pi/k_0 b)^2} = \frac{\cos \Phi_{m,n}}{Z_0}.$$

The modal axial effective intensity at a point  $x$  is:

$$I_{z_{m,n}}(x) = \frac{1}{2} \operatorname{Re} \{ p_{m,n}(x) \cdot v_{z_{m,n}}^*(x) \} = \frac{1}{2} |p_{m,n}(x)|^2 \cdot \operatorname{Re}\{G_{z_{m,n}}\}. \quad (8)$$

The axial effective intensity of the sound wave (a mode mixture) is:

$$I_z(x) = \frac{1}{2} \operatorname{Re} \left\{ \sum_{m,n} p_{m,n}(x) \cdot v_{z_{m,n}}^*(x) \right\} = \frac{1}{2} \sum_{m,n} |p_{m,n}(x)|^2 \cdot \operatorname{Re}\{G_{z_{m,n}}\}. \quad (9)$$

The effective sound power through a duct cross section is:

$$\Pi = \frac{1}{2} \iint_S \operatorname{Re}\{p \cdot v^*\} dS = \frac{1}{2} S \cdot \operatorname{Re} \left\{ \sum_{m,n} \frac{k_{m,n}}{k_0 Z_0} \cdot |A_{m,n}|^2 \cdot N_{m,n} \right\} \quad (10)$$

$$= \frac{1}{2} S \sum_{m,n} \frac{1}{\delta_m \delta_n} \cdot |A_{m,n}|^2 \cdot \operatorname{Re}\{G_{z_{m,n}}\} = \sum_{m,n} \Pi_{m,n},$$

where  $\Pi_{m,n}$  are the modal effective powers.

A mode can transport effective power only if it is cut on (propagating); the condition for cut-on is (the summations in  $\Pi$  extend up to these limits):

$$(\kappa_{m,n}/k_0)^2 < 1 \quad \text{or:} \quad (m/a)^2 + (n/b)^2 < (k_0/\pi)^2 = 4/\lambda_0^2 = (2f/c_0)^2. \quad (11)$$

Below, the sound power  $\Pi$  sometimes will be referred to as the sound power  $\Pi_0$  of a plane wave with sound pressure  $p_0$  such that  $\Pi_0 = \frac{S p_0^2}{2 Z_0} = 1$ . (12)

The condition  $\Pi/\Pi_0 = 1$  is equivalent to:

$$\sum_{m,n} \frac{1}{\delta_m \delta_n} \left| \frac{A_{m,n}}{p_0} \right|^2 \cdot \operatorname{Re}\{k_{m,n}/k_0\} = \sum_{m,n} \frac{1}{\delta_m \delta_n} \left| \frac{A_{m,n}}{p_0} \right|^2 \cdot \operatorname{Re}\{Z_0 G_{z_{m,n}}\} = 1 . \quad (13)$$

*Mode mixture with equal modal amplitudes  $A_{m,n}$ :*

$$\left| \frac{A_{m,n}}{p_0} \right|^2 \stackrel{!}{=} \left[ \sum_{m,n} \frac{\operatorname{Re}\{Z_0 G_{z_{m,n}}\}}{\delta_m \delta_n} \right]^{-1} = \operatorname{const}(m, n) . \quad (14)$$

*Mode mixture with equal modal sound powers (or intensities):*

$$\sum_{m,n} \frac{\Pi_{m,n}}{\Pi_0} = 1 ; \quad \frac{\Pi_{m,n}}{\Pi_0} = \operatorname{const}(m, n) = \frac{1}{N} , \quad (15)$$

where  $N$  is the total number of cut-on modes. This leads to the mode amplitudes:

$$\left| \frac{A_{m,n}}{p_0} \right|^2 \stackrel{!}{=} \frac{\delta_m \delta_n}{N} \frac{1}{\operatorname{Re}\{Z_0 G_{z_{m,n}}\}} = \frac{1}{N} \frac{\delta_m \delta_n}{\cos \Phi_{m,n}} . \quad (16)$$

If a mode approaches cut-off, then  $\cos \Phi_{m,n} \rightarrow 0$ , i.e. this mode-mixing model would require large mode amplitudes near cut-off, and also for large mode orders, because then  $\Phi_{m,n} \rightarrow \pi/2$ .

*Mode mixture with equal mode energy density  $E_{m,n}$ :*

The mode energy density averaged over the duct cross section follows from the mode power:  $\Pi_{m,n} = c_{gm,n} \cdot S \cdot E_{m,n}$  with the modal group velocity:

$$c_g = \frac{1}{dk/d\omega} = \frac{c_{ph}}{1 - \frac{\omega}{c_{ph}} \frac{\partial c_{ph}}{\partial \omega}} ,$$

$$k_{m,n} = \sqrt{(\omega/c_0)^2 - \kappa_{m,n}^2} ; \quad \frac{dk_{m,n}}{d\omega} = \frac{1}{c_0} \frac{1}{\sqrt{1 - (\kappa_{m,n}/k_0)^2}} , \quad (18)$$

$$c_{gm,n} = c_0 \sqrt{1 - (\kappa_{m,n}/k_0)^2} = c_0 \cdot Z_0 G_{z_{m,n}} .$$

Therefore the averaged modal energy density is:

$$E_{m,n} = \frac{\Pi_{m,n}}{S \cdot c_{gm,n}} = \frac{1}{2} \frac{1}{\delta_m \delta_n} \left| A_{m,n} \right|^2 \frac{\operatorname{Re}\{G_{z_{m,n}}\}}{c_0 Z_0 G_{z_{m,n}}} . \quad (19)$$

The model of equal modal energy density demands (with restriction to propagating modes, for which  $\operatorname{Re}\{G_{zm,n}\} = G_{zm,n}$ ):

$$E_{m,n} = \frac{1}{2} \frac{1}{c_0 Z_0} \frac{\left| A_{m,n} \right|^2}{\delta_m \delta_n} = \operatorname{const}(m, n) , \quad (20)$$

or, with the above power normalisation:

$$\left| \frac{A_{m,n}}{p_0} \right|^2 = \frac{\delta_m \delta_n}{\sum_{m,n} \operatorname{Re}\{Z_0 G_{z_{m,n}}\}} = \frac{\delta_m \delta_n}{\sum_{m,n} \cos \Phi_{m,n}} . \quad (21)$$

This is the most plausible model for the simulation of random sound fields.

## J.32 Mode Excitation Coefficients

---

► See also: Mechel, Vol. III, Ch. 40 (1998)

Sometimes one is interested in exciting predominantly higher modes (because they are easier to attenuate than lower modes); sometimes one would like to avoid the excitation of higher modes (e.g. in experiments with low modes). It is reasonable to introduce a coefficient which describes the excitation probability of a mode under some standard conditions.

Consider a flat lined duct extending over  $-h \leq y \leq +h$  (other duct geometries are treated similarly) with a sound field formulated as a mode sum, with mode norms  $N_n$ :

$$p(x, y) = \sum_n A_n \cdot q_n(y) \cdot e^{-\gamma_n x}; \quad N_n = \frac{1}{2h} \int_{-h}^h q_n^2(y) dy. \quad (1)$$

If the excitation is performed by a given sound pressure profile  $p_i(0, y)$  in the plane  $x = 0$ , then the mode amplitudes are:

$$A_n = \frac{1}{N_n} \cdot \frac{1}{2h} \int_{-h}^h p_i(0, y) \cdot q_n(y) dy. \quad (2)$$

If the excitation is done by a given axial particle velocity  $v_{ix}(0, y)$ , then the mode amplitudes are:

$$A_n = \frac{j}{N_n \cdot \gamma_n / k_0} \cdot \frac{1}{2h} \int_{-h}^h Z_0 v_{ix}(0, y) \cdot q_n(y) dy. \quad (3)$$

One plausible standard excitation is the excitation by a plane wave pressure profile  $p_i(0, y) = 1$  and to introduce mode excitation coefficients  $F_n$  for that excitation:

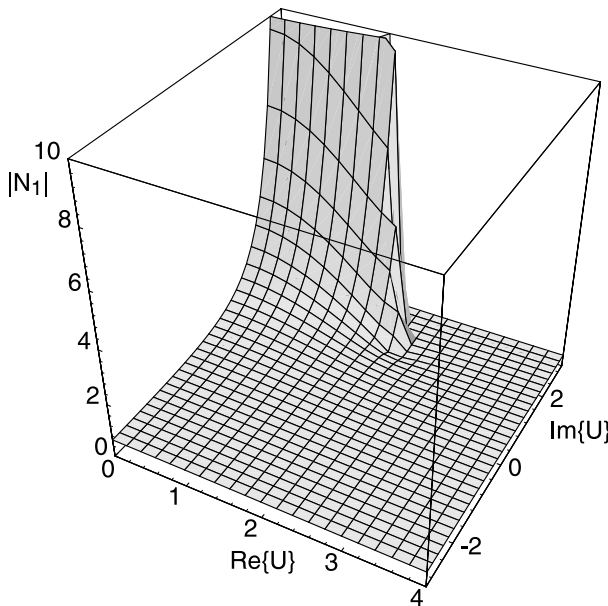
$$F_n = \frac{1}{N_n} \cdot \frac{1}{2h} \int_{-h}^h q_n(y) dy. \quad (4)$$

For modes with symmetrical (relative to  $y = 0$ ) profiles  $q_n(y) = \cos(\epsilon_n y)$ : (5)

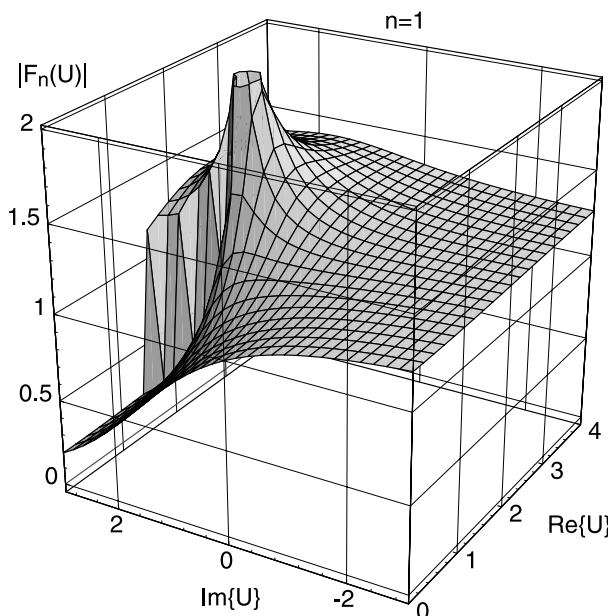
$$F_n = 2 \frac{\sin(\epsilon_n h) / (\epsilon_n h)}{1 + \sin(2\epsilon_n h) / (2\epsilon_n h)} \xrightarrow{\epsilon_n h=0} 1. \quad (6)$$

For anti-symmetrical modes with  $q_n(y) = \sin(\epsilon_n y)$ :

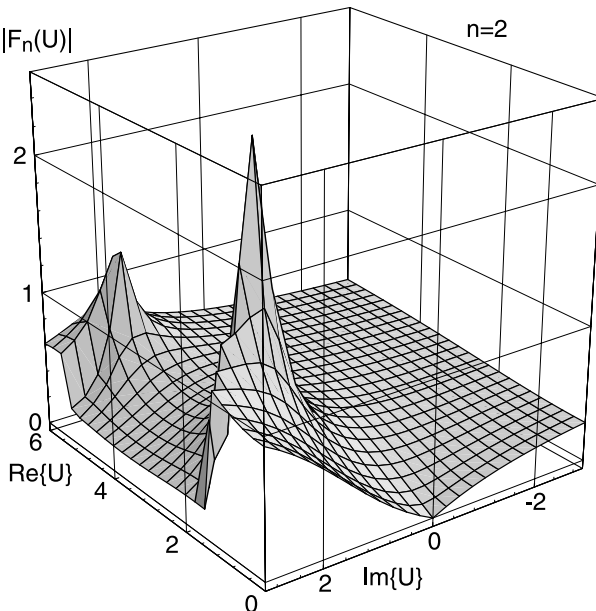
$$F_n = 2 \frac{(1 - \cos(\epsilon_n h)) / (\epsilon_n h)}{1 - \sin(2\epsilon_n h) / (2\epsilon_n h)}. \quad (7)$$



Magnitude of the mode norm in the range of the first mode in a flat, lined (locally reacting) duct over the plane  $U = k_0 h \cdot Z_0 G$



Magnitude of mode excitation coefficient  $F_n(U)$  for  $n = 1$  in a flat lined (locally reacting) duct over the plane  $U = k_0 h \cdot Z_0 G$ . The low values are in the range of the surface wave mode; the peak maximum is at the branch point between the first and second modes.



Magnitude of mode excitation coefficient  $F_n(U)$  for  $n = 2$  in a flat lined (locally reacting) duct over the plane  $U = k_0 h \cdot Z_0 G$ . Low values are in the range of the surface wave mode; the peak maxima are at the branch points between the first and second and the second and third modes

### J.33 Cremer's Admittance

► See also: Cremer (1953); Mechel, Vol. III, Ch. 41 (1998)

(The author wondered whether he should include this section because its topic requires more words than formulas; but the use of Cremer's admittance is a modern design of silencers if powerful computing programs for sound absorbers are available. Duct linings are assumed to be locally reacting.)

Cremer's question:

Under what condition will the least attenuated mode in a lined duct have its maximum attenuation?

Answer (for a flat duct):

When  $U := k_0 h \cdot Z_0 G \stackrel{!}{=} U_{b,1} = 2.05998 + j \cdot 1.65061$ , (1)

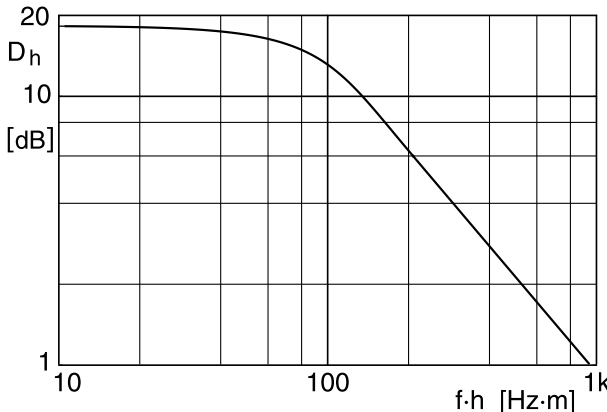
where  $G$  is the lining admittance and  $U_{b,1}$  is the value of  $U$  in the first branch point of symmetrical modes.

In circular ducts  $U := k_0 h \cdot Z_0 G \stackrel{!}{=} U_{b,1} = 2.9803824 + j \cdot 1.2796025$ . (2)

The attenuation  $D_h$  in the duct is the sound pressure level decrease per half duct height  $h$  (or radius) travel distance:  $D_h = 8.6858 \cdot \text{Re}\{\Gamma_h\} \quad (\Gamma_h)^2 = (\epsilon h)^2 - (k_0 h)^2$ , where  $\epsilon =$

$\varepsilon_h$  is the solution of the characteristic equation for the least attenuated mode. If the admittance is in the branch point, then:

$$\varepsilon_h = z_{b,1} = \begin{cases} 2.1062 + j \cdot 1.12536 & \text{flat duct} \\ 2.9803824 + j \cdot 1.2796025 & \text{round duct} \end{cases} \quad (3)$$



Attenuation  $D_h$  of least attenuated mode in a flat duct if the lining admittance  $G$  has Cremer's admittance value at all frequencies

#### Facts:

1.  $U = k_0 h \cdot Z_0 G = U_{b,1}$  is the condition for maximum attenuation of the least attenuated mode.
2.  $G$  has the sign of a spring-like reaction but the frequency dependence of a mass-like reaction.
3.  $\tan \delta = \text{Im}\{U_{b,1}\}/\text{Re}\{U_{b,1}\} = \text{Im}\{G\}/\text{Re}\{G\} = 0.801$  is a value which is typical at frequencies in the lower half-value point of resonances.
4.  $U_{b,1}$  is at a coincidence of  $\varepsilon_0 h$  and  $\varepsilon_1 h$ , i. e. at the cut-on of the first higher mode.
5. Onset of the first higher mode is the criterion for the beginning of "ray formation" in the duct, where the slope  $D_h \sim 1/f^2$  begins.
6. From the second and third facts it follows that a lining with Cremer's admittance typically is a narrow-band lining.
7. From the fourth and fifth facts it follows that a lining with Cremer's admittance is no low-frequency lining (i. e. with small  $h/\lambda_0$  or small  $f \cdot h$ ).
8. The least attenuated mode for Cremer's admittance has a large mode excitation coefficient (see previous Sect. J.32).

### Extension of Cremer's rule:

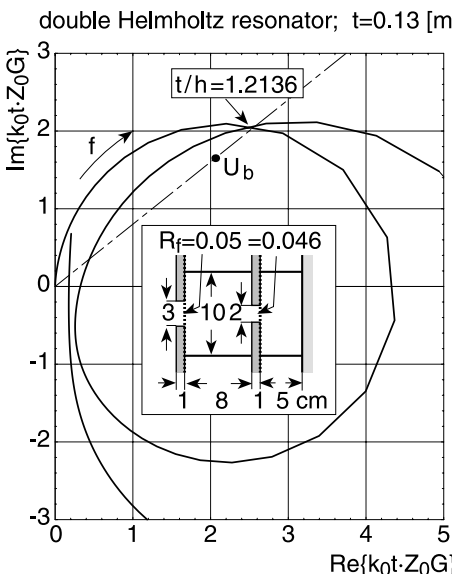
The condition  $U = U_{b,1}$  is unnecessarily restrictive. The following extension is more flexible in its application.

*Every absorber with a characteristic length  $t$  and a function  $U_t = k_0 t \cdot Z_0 G$  which crosses the straight line  $(0, U_{b,1})$  has a Cremer admittance at the crossing point if it is applied in a duct with the (half) height  $h$  for which  $t/h = |U_t|/|U_{b,1}|$ .*

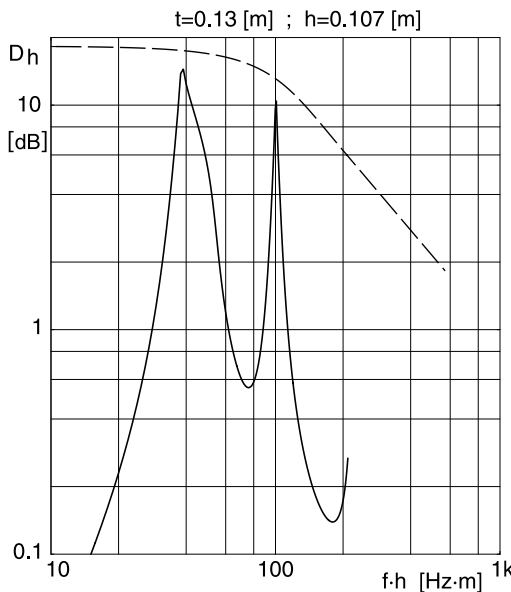
The crossing point  $t/h \cdot U_{b,1}$  on the straight line  $(0, U_{b,1})$  will be called the “*design point*”. Design points with  $t/h > 1$  in general are reached more easily, but the maximum of their attenuation curve  $D_h(f \cdot h)$  is often in the range  $f \cdot h$  of ray formation, so that the attenuation is of little practical use. Therefore design points with  $t/h < 1$  are of greater interest.

In order to extend the frequency range of Cremer's admittance, one must combine resonators which are tuned differently, so that the curve of  $U$  for the combination in the complex  $U$  plane forms narrow double loops around  $U_{b,1}$ . This combination can be made by resonators in series (one behind the other) or in parallel (resonators side by side). Series combinations must be found by trial and error;  Sect. J.33 below will describe an algorithm for finding parallel combinations. The following graphs are examples for series combinations (more examples in [Mechel, Vol. III, Ch. 41 (1998)]). Pairs of graphs will be shown; the first graph contains the curve of  $U_t$  in the complex plane with indications of possible design points, while the second graph shows the  $D_h(f \cdot h)$  curve for the indicated design point, together with the (dashed) curve of maximum possible attenuation. The characteristic length  $t$  in all examples is the sum of the layer thicknesses of the absorber.

The first example is for two Helmholtz resonators (with slit-shaped necks) in series; in each orifice is a resistance foil with normalised flow resistance  $R_f$ .

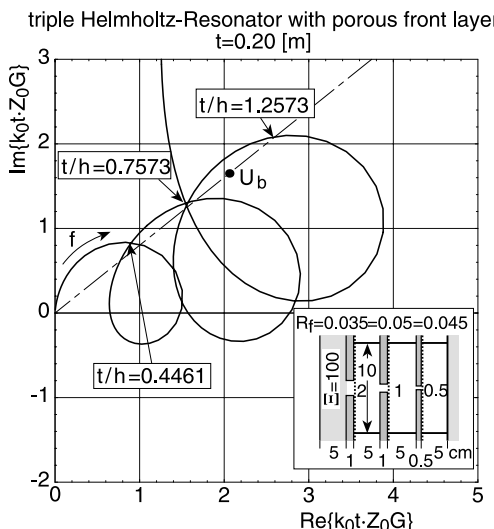


Function  $U_t$  in the complex plane for two Helmholtz resonators in series

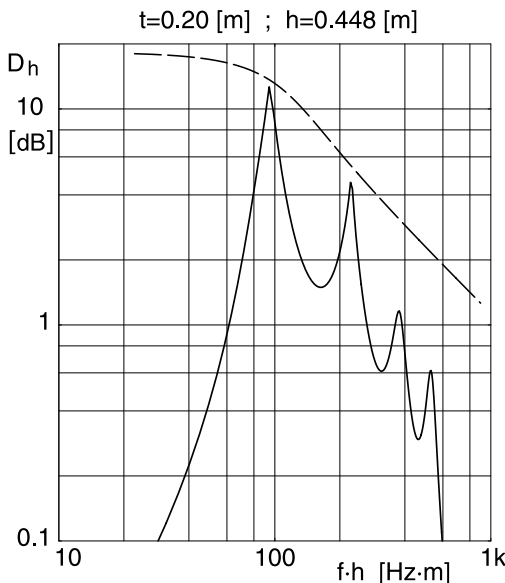


Attenuation  $D_h$  for the above absorber arrangement with a design ratio  $t/h = 1.2136$ . The two maxima belong to the two crossings of the line  $(0, U_b)$  at about the same design point

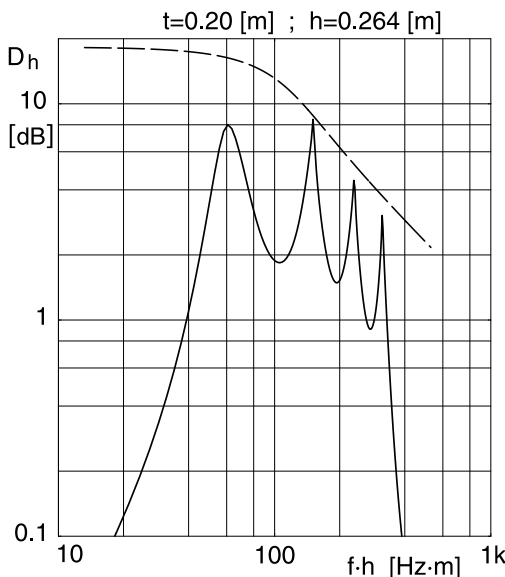
The next example, for a triple Helmholtz resonator with a front side porous layer, shows the influence of the selection of the design point on the attenuation curve.



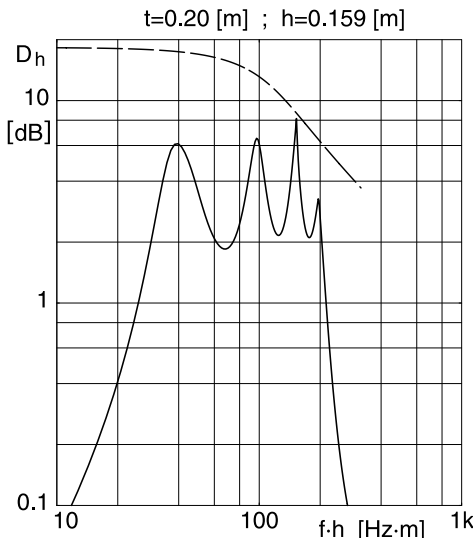
Function  $U_t$  in the complex plane for three Helmholtz resonators in series with a porous front layer. Three design points can be selected



$$t/h = 0.4461$$



$$t/h = 0.7573$$



$$t/h = 1.2573$$

It is possible to construct design points with multiple cross-overs with resonators in series, but the individual crossings are separated by full resonance circles and, therefore, in the  $D_h$  curves by wide frequency steps. This can be avoided with resonators in a parallel arrangement; see next section.

### J.34 Cremer's Admittance with Parallel Resonators

► See also: Mechel, Vol. III, Ch. 41 (1998); Press et al., (1989)

The lining consists of repeated couples of absorbers. If the dimensions of the absorbers (in the direction of the duct axis) are small compared to the wavelength, the weighted (with the absorber surface areas) average of their admittances will determine the attenuation. One of the absorbers will be called the *primary* absorber (with index p), the other the *adjoint* absorber (with index a). Let  $F_p, F_a$  be the surface areas of the absorbers,  $G_p$  and  $G_a$  their surface admittances,  $\beta = F_a/F_p$  the surface ratio, and  $t$  a common characteristic length of both absorbers. Then the extended principle of Cremer's admittance (see ➤ Sect. J.33) demands that:

$$\langle U_t \rangle = \frac{F_p U_{t,p} + F_a U_{t,a}}{F_p + F_a} = \frac{U_{t,p} + \beta U_{t,a}}{1 + \beta} = \frac{t}{h} U_b ; \quad U_{t,\alpha} = k_0 t \cdot Z_0 G_\alpha ; \quad \alpha = p, a . \quad (1)$$

This conditional equation defines the  $U$  function  $\hat{U}_{t,a}$  of a *fictitious adjoint absorber*:

$$\hat{U}_{t,a} = \frac{1}{\beta} [(1 + \beta) \cdot t/h \cdot U_b - U_{t,p}] . \quad (2)$$

It is called "fictitious" because it is not clear whether and how it can be realised. If, for example, the real part of the brackets is negative, then the associate admittance  $\hat{G}_a$  should have a negative real part, which cannot be realised with passive absorber elements. The conditional equation gives the "rule of construction" for  $\hat{U}_{t,a}$  in the  $U$  plane:

$$\beta \cdot \left[ t/h \cdot U_b - \hat{U}_{t,a} \right] \stackrel{!}{=} - \left[ t/h \cdot U_b - U_{t,p} \right]. \quad (3)$$

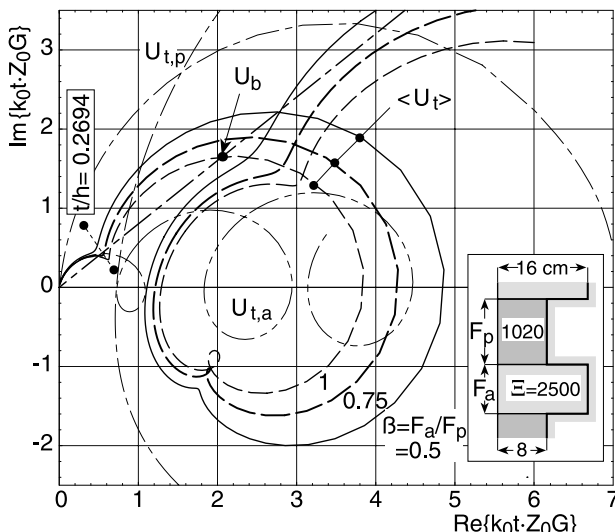
According to this condition, the point  $\hat{U}_{t,a}$  belonging to a value  $U_{t,p}$  is on a straight line through  $U_{t,p}$  and the design point  $t/h \cdot U_b$  on the opposite side (with respect to  $t/h \cdot U_b$ ) at a distance  $\beta$  times the distance between  $U_{t,p}$  and  $t/h \cdot U_b$ . Thus, if  $U_{t,p}$  is above the line  $(0, U_b)$ , the point for  $\hat{U}_{t,a}$  is below that line; if  $U_{t,p}$  is above  $(0, U_b)$  and right-turning (which is normal),  $\hat{U}_{t,a}$  is below  $(0, U_b)$  and right-turning also. All curves for functions  $U$  of passive absorbers begin at sufficiently low frequencies near the origin of the  $U$  plane; thus  $\hat{U}_{t,a}$  begins near the line  $(0, U_b)$  beyond  $U_b$ , which physically is not possible. Therefore no realisation of  $\hat{U}_{t,a}$  is possible at very low frequencies.

First the steps of the procedure for finding a lining with parallel absorbers with an effective Cremer admittance will be described (with a concrete example), then an algorithm for finding a suitable adjoint absorber will be derived. The first example simply consists of two porous absorbers with different flow resistivity values  $\Xi$  and thicknesses  $t_p, t_a$ , arranged side by side. The characteristic length is  $t = t_p$ .

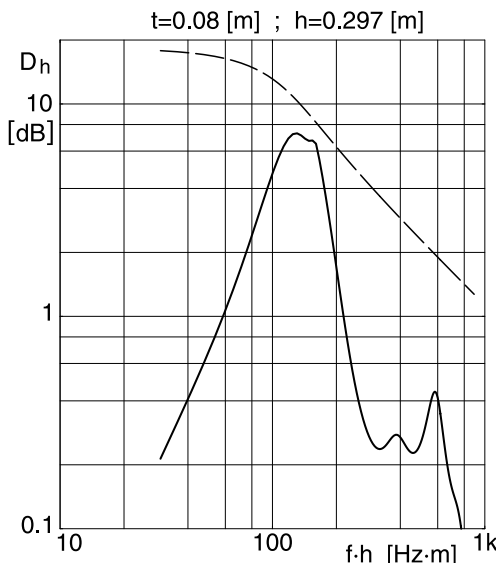
1. Find a suitable primary absorber (i.e. an absorber with the  $U$  function on an arc above the line  $(0, U_b)$ , possibly crossing that line beyond  $U_b$ ).
2. Conceive an adjoint absorber whose function  $U_{t,a}$  approximates  $\hat{U}_{t,a}$  in some frequency interval of interest ( $\hat{U}_{t,a}$  can be drawn with the above rule of construction).

Thus  $U_{t,p}, U_{t,a}$  are known as functions of frequency and  $\langle U_t \rangle$  is their average function. Plot these curves in the  $U$  plane.

The diagram below shows these curves together with the straight line  $(0, U_b)$  and the curve  $\langle U_t \rangle$  for three surface ratios  $\beta = F_a/F_p$ . A design point at  $t/h = 0.2694$  is marked.

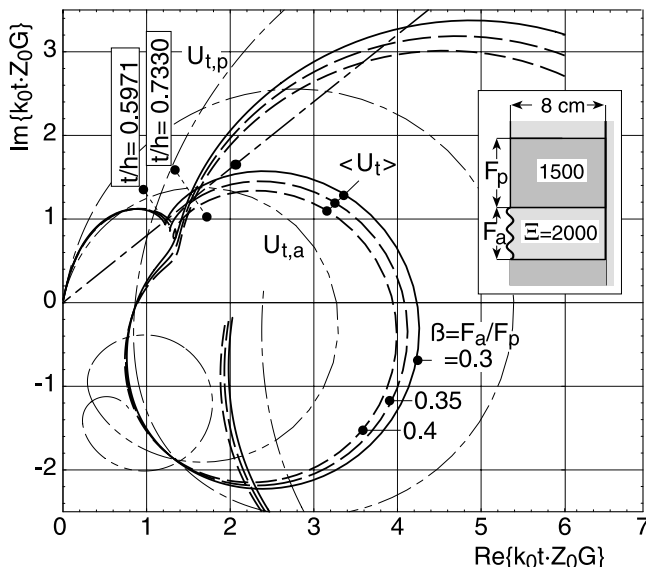


Branch point  $U_b$ , curves  $U_{t,p}, U_{t,a}$  for the component absorbers, and average  $\langle U_t \rangle$  in the  $U$  plane. A design point  $t/h = 0.2694$  is marked at which two resonances have contracted to a dent

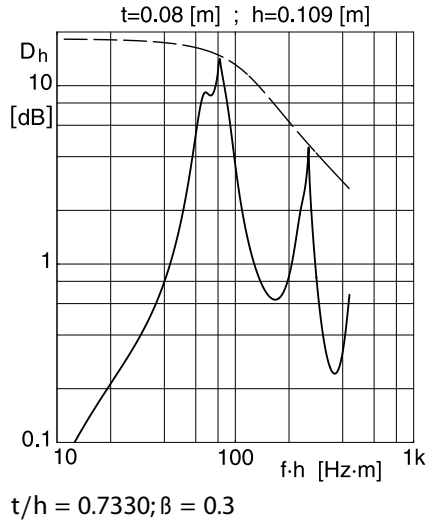
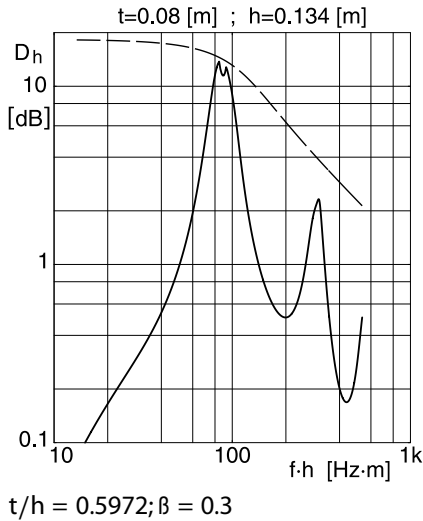


Maximum possible attenuation (dashed) and attenuation curve of the least attenuated mode in a duct with the lining from above at a surface ratio  $\beta = F_a/F_p = 0.2694$

The next example is for a similar arrangement, but now with equal thicknesses  $t = t_p = t_a = 8 \text{ [cm]}$ . The adjoint absorber is covered with a tight, limp foil with surface mass density  $m_f = 0.06 \text{ [kg/m}^2\text{]}$ . Two design points are of interest, one at  $t/h = 0.5971$ , the other at  $t/h = 0.7330$ .



A surface area ratio  $\beta = F_a/F_p = 0.3$  is selected for the attenuation curves at the two design points.

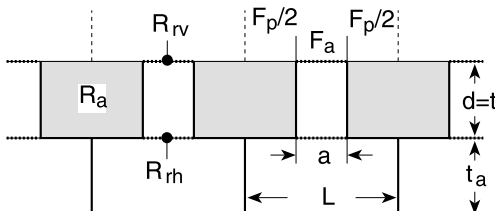


The main problem is the determination of suitable parameters of the adjoint absorber. This task can be performed with a computation algorithm. The initial step is the same as above:

1. Find a suitable primary absorber (i.e. an absorber with the U function on an arc above the straight line  $(0, U_b)$ , possibly crossing that line beyond  $U_b$ ).
2. Establish the structure of an adjoint absorber.

The lining in the example used below consists of a *primary absorber*, which is a porous layer of thickness  $d = t$  and a flow resistance (normalised)  $R_a = \Xi \cdot d/Z_0$ ;  $\Xi = 1000 \text{ [Pa} \cdot \text{s/m}^2]$  is fixed.

an *adjoint absorber*, which is a Helmholtz resonator with (normalised) flow resistances  $R_{rv}$ ,  $R_{rh}$  in the orifices.



Experience shows that if both component absorbers have resonances at frequencies  $f_p$ ,  $f_a$ , respectively, the resonance of the adjoint absorber should be at about  $f_a \approx f_p/2$ . The

resonances of the component absorbers in the example are at about ( $d'$  = resonator neck length):

$$\begin{aligned} f_p &\approx \frac{c_0}{4} \cdot \frac{1}{t}, \\ f_a &\approx \frac{c_0}{2\pi} \sqrt{\frac{F_a}{(F_a + F_p) \cdot d' \cdot t_a}} = \frac{c_0}{2\pi} \sqrt{\frac{\beta}{(1 + \beta) \cdot d' \cdot t_a}} \\ &\xrightarrow{d' \rightarrow t} \frac{c_0}{2\pi t} \sqrt{\frac{\beta}{(1 + \beta) \cdot t_a/t}} = f_p \cdot \frac{2}{\pi} \sqrt{\frac{\beta}{(1 + \beta) \cdot t_a/t}}. \end{aligned} \quad (4)$$

Thus the condition  $f_a \approx f_p/2$  can be satisfied. The U functions of the component absorbers are evaluated from ( $\Gamma_{an}$ ,  $Z_{an}$  are normalised characteristic values of the porous material of the primary absorber; E is the variable needed for their evaluation):

*Primary absorber:*

$$U_{t,p} = k_0 t \cdot G_p = k_0 t \cdot \tanh(k_0 t \cdot \Gamma_{an}) / Z_{an}; \quad E = \frac{\rho_0 f}{\Xi} = \frac{1}{2\pi} \frac{k_0 t}{R_a}; \quad R_a = \frac{\Xi \cdot t}{Z_0}. \quad (5)$$

*Adjoint absorber:*

$$\begin{aligned} U_{t,a} &= k_0 t \cdot G_a = k_0 t / Z_a; \quad Z_a = jk_0 a \frac{\Delta l_0}{a} + R_{rv} + Z_{sv}; \\ Z_{sv} &= \frac{Z_{sh} + j \tan(k_0 t)}{1 + j \cdot Z_{sh} \cdot \tan(k_0 t)}; \end{aligned} \quad (6)$$

$$Z_{sh} = R_{rh} + jk_0 a \frac{\Delta l_i}{a} - j \frac{a/L}{\tan(k_0 t_a)}; \quad \frac{\Delta l_i}{a} = \frac{\Delta l_0(x)}{a} [1 + f(y)] \cdot [1 + g(z)]; \quad (7)$$

$$\begin{aligned} x &= \lg(a/L) = \lg \frac{\beta}{1 + \beta}; \quad y = \lg(d/a) = -\lg(a/t); \\ z &= \lg(t_a/L) = x + y + \lg(t_a/t), \end{aligned} \quad (8)$$

where  $\Delta l_i$  is the interior end correction of the neck; the functions  $\Delta l_0(x)$ ,  $f(y)$ ,  $g(z)$  are taken from  Sect. H.4. The parameters to be optimised are  $\beta = a/L$ ;  $t/h$ ;  $t_a/t$ ;  $a/t$ ;  $R_{rv}$ ;  $R_{rh}$ .

The conditional equation for the Cremer admittance can be written as:

$$U_{t,p} \stackrel{!}{=} (1 + \beta) \cdot t/h \cdot U_b - \beta \cdot \hat{U}_{t,a}. \quad (9)$$

If one replaces on the right-hand side  $\hat{U}_{t,a} \rightarrow U_{t,a}$ , the task is to find a good approximation to the known  $U_{t,p}$  by variation of parameters. It can be formulated as a task to find a minimum by parameter variation. Find a minimum of the squared-error sum:

$$q(a_1, a_2, \dots) = \sum_n w_n \cdot |z_n - f(x_n; a_1, a_2, \dots; b_1, b_2, \dots)|^2 \left/ \sum_n w_n \right. \stackrel{!}{=} \text{Min}, \quad (10)$$

where  $x_n = (k_0 t)_n$  are discrete values of the frequency variable in a range for which the approximation should be found,  $z_n = (U_{t,p})_n = z_n(x_n)$  are the known values to be

approximated,  $f_n(x_n; \dots)$  are the values of the right-hand side of the above conditional equation (after substitution  $\hat{U}_{t,a} \rightarrow U_{t,a}$ ),  $a_k$  are parameters to be varied,  $b_k$  are parameters to remain fixed, and  $w_n(x_n)$  is a weight function which may be centred at some point  $x$  (e.g. with the form of a sine arc  $w(x) = \sin((x - x_{lo})/(x_{hi} - x_{lo}) \cdot \pi)$ ) for easier location of a parameter set in a preliminary run, or it is  $w_n(x_n) = \text{const}$  in later runs. Use a program for minimum seeking which accepts start values for the parameters  $a_k$  and which accepts limits for the parameter ranges (in order to avoid parameter variation to negative or even complex values of the  $a_k$  which should be real positive, see [Press et al., (1989)]).

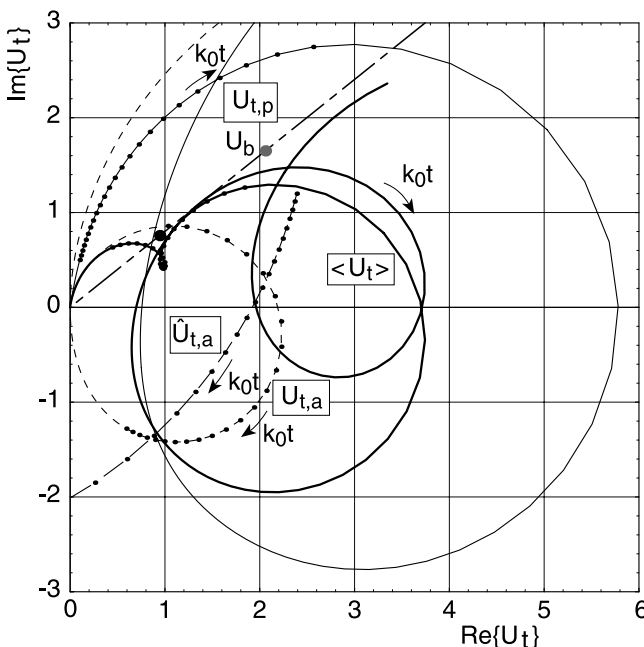
The following diagram shows in the  $U$  plane the curve for  $U_{t,p}$  with sampling points in the  $k_0 t$  interval used, the fictitious adjoint  $\hat{U}_{t,a}$  in its range used (also with sampling points), the final  $U_{t,a}$  after optimisation of the parameters (sampling points in the  $k_0 t$  interval used), and the average  $\langle U_t \rangle$  (thick line). The reference dimension  $t$  was set to  $t = 0.1$  [m]; the ratio  $a/t$  was kept on a fixed value  $a/t = 0.1$ ; the starters for the other parameters  $a_k$  were:

$$\beta = 0.5, ; \quad t/h = 1.0 ; \quad t_a/t = 0.5 ; \quad a/t = 0.1 ; \quad R_{rv} = 0.05 ; \quad R_{rh} = 0.05 .$$

The optimised values were:

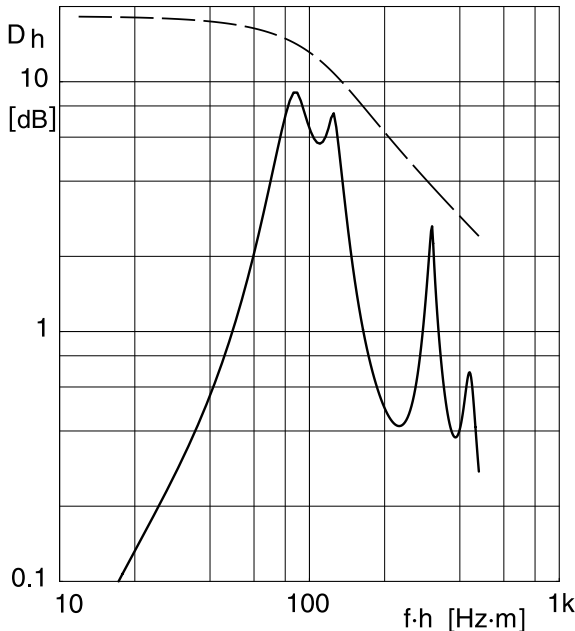
$$\begin{aligned} \beta &= 0.5832; \quad t/h = 0.4585; \quad t_a/t = 0.4267; \quad a/t = 0.1; \\ R_{rv} &= 0.3579; \quad R_{rh} = 0.0 . \end{aligned}$$

The weight function was  $w(x) = 1$ . The (computed) design point is indicated as a point on the straight line  $(0, U_b)$ .



The design point is on the *straight line*  $(0, U_b)$  near the small loop in the curve of  $\langle U_t \rangle$

$$\begin{aligned} t &= 0.10 \text{ [m]} ; \quad h = 0.218 \text{ [m]} ; \\ t/h &= 0.4585 ; \quad \beta = 0.583 \end{aligned}$$



Attenuation curve  $D_h$  for the combination of a porous layer primary absorber with a Helmholtz resonator as adjoint absorber with the optimised values of the free parameters listed above

### J.35 Influence of Flow on Attenuation

► See also: Mechel, Vol. III, Ch. 25.4 (1998); Mechel, Vol. III, Ch. 42 (1998)

Consider a duct with axial co-ordinate  $x$  and transversal co-ordinate  $y$ . A stationary flow with velocity profile  $V(y)$  is in the  $+x$  direction if  $V > 0$  and in the  $-x$  direction if  $V < 0$ . Sound waves are assumed to propagate in the  $+x$  direction. In this section the simplifying assumption  $V(y) = \text{const}$  is made; for more details see the chapter "Flow Acoustics".

The presence of flow will modify the fundamental equations mainly by the replacement of the partial time derivative  $\partial/\partial t$  by the "substantial derivative"  $D/Dt$ :

$$\begin{aligned} \rho_0 \operatorname{div} \mathbf{v} + \frac{\partial \rho}{\partial t} &\stackrel{V \neq 0}{\longrightarrow} \rho_0 \operatorname{div} \mathbf{v} + \frac{D\rho}{Dt} = 0, \\ \rho_0 \frac{\partial \mathbf{v}}{\partial t} + \operatorname{grad} p &\stackrel{V \neq 0}{\longrightarrow} \rho_0 \frac{D\mathbf{v}}{Dt} + \operatorname{grad} p = 0, \\ \left( \Delta - \frac{1}{c_0^2} \frac{\partial^2}{\partial t^2} \right) p &\stackrel{V \neq 0}{\longrightarrow} \left( \Delta - \frac{1}{c_0^2} \frac{D^2}{Dt^2} \right) p = 0. \end{aligned} \quad (1)$$

The substitution for the time derivative can be written for an assumed time factor  $e^{j\omega t}$  and a sound wave of the form  $p(x, y) = P_0 \cdot q(y) \cdot e^{-j\Gamma x}$  as:

$$\begin{aligned} \frac{\partial}{\partial t} = j\omega &= jc_0 k_0 \xrightarrow[V \neq 0]{} \frac{D}{Dt} = \frac{\partial}{\partial t} + V \frac{\partial}{\partial x} = c_0 \left[ jk_0 + M \frac{\partial}{\partial x} \right] \\ &= jc_0 k_0 \left[ 1 + jM \frac{\Gamma}{k_0} \right] \end{aligned} \quad (3)$$

(with  $M = V/c_0$  the Mach number). So this effect of the flow can be taken into account by the substitution:

$$k_0 \xrightarrow[V \neq 0]{} k_0 \left[ 1 - j \frac{M}{k_0} \frac{\partial}{\partial x} \right] = k_0 \left[ 1 + jM \frac{\Gamma}{k_0} \right]. \quad (4)$$

Using the abbreviation w one can write:

$$\begin{aligned} w &= \left[ 1 - j \frac{M}{k_0} \frac{\partial}{\partial x} \right] = \left[ 1 + jM \frac{\Gamma}{k_0} \right], \\ k_0 \xrightarrow[V \neq 0]{} k_0 \cdot w. \end{aligned} \quad (5)$$

The wave equation, for example, becomes  $(\Delta + k_0^2 w^2) p(x, y) = 0$ .

If the lateral sound wave profile  $q(y)$  is (for example)  $q(y) = \cos(\epsilon y)$ , the characteristic equation for the determination of  $\epsilon h$  in a duct of (half) width  $h$  and with a locally reacting lining with surface admittance  $G$  changes to:

$$\epsilon h \cdot \tan(\epsilon h) = jk_0 h Z_0 G \xrightarrow[V \neq 0]{} \epsilon h \cdot \tan(\epsilon h) = jk_0 h Z_0 G \cdot w. \quad (7)$$

This form assumes that the boundary conditions at the lining surface are the continuity of sound pressure and normal particle velocity  $v_y$ . Some authors claim that not the particle velocity should be continuous, but the elongation  $e_y$  with  $v_y = \partial e_y / \partial t$ . This time derivative introduces a new factor  $w$  wherever  $G$  appears:

$$\epsilon h \cdot \tan(\epsilon h) = jk_0 h Z_0 G \xrightarrow[V \neq 0]{} \epsilon h \cdot \tan(\epsilon h) = jk_0 h Z_0 G \cdot w^2. \quad (8)$$

One can combine both theories of the boundary condition to give:

$$\epsilon h \cdot \tan(\epsilon h) = jk_0 h Z_0 G \xrightarrow[V \neq 0]{} \epsilon h \cdot \tan(\epsilon h) = jk_0 h Z_0 G \cdot w^\alpha; \quad \alpha = 1, 2. \quad (9)$$

The secular equation, which follows from the wave equation, changes to:

$$(\Gamma/k_0)^2 + 1 - (\epsilon/k_0)^2 = 0 \xrightarrow[V \neq 0]{} (\Gamma/k_0)^2 (1 - M^2) + 2jM \cdot \Gamma/k_0 + 1 - (\epsilon/k_0)^2 = 0. \quad (10)$$

Because the solution shall be without flow:

$$\frac{\Gamma}{k_0} \xrightarrow[M \rightarrow 0]{} \frac{1}{k_0 h} \sqrt{(\epsilon h)^2 - (k_0 h)^2}, \quad (11)$$

the solution with flow is:

$$\frac{\Gamma}{k_0} = \frac{-j}{1 - M^2} \left[ M + j \frac{1}{k_0 h} \sqrt{(1 - M^2)(\epsilon h)^2 - (k_0 h)^2} \right]. \quad (12)$$

Thus w has the form:

$$w = \frac{1}{1 - M^2} \left[ 1 + j \frac{M}{k_0 h} \sqrt{(\epsilon h)^2 (1 - M^2) - (k_0 h)^2} \right]. \quad (13)$$

The appearance of  $\epsilon h$  in w modifies the characteristic equation significantly, and also the method for its numerical solution. In general, one will solve the characteristic equation first for  $M = 0$ , i.e.  $w = 1$ , and then increase  $M$  iteratively to its final value, taking solutions for the earlier  $M$  as starting solutions  $zs_i$  in the numerical procedure:

$$zs_1 = \epsilon h(M_{k-3}), \quad zs_2 = \epsilon h(M_{k-2}), \quad zs_3 = \epsilon h(M_{k-1}). \quad (14)$$

One must take very small steps  $\Delta M$ , especially at the beginning of the iteration through  $M$ . A better choice of starting solutions is at the beginning of the iteration:

$$zs_1 = \epsilon h(0), \quad zs_2 = (zs_1 + zs_3)/2, \quad zs_3 = \epsilon h(0) + \Delta M \cdot d(\epsilon h)/dM|_{M=0}, \quad (15)$$

and at later steps:

$$zs_1 = \epsilon h(M_{k-2}), \quad zs_2 = \epsilon h(M_{k-1}), \quad zs_3 = \epsilon h(M_{k-1}) + \Delta M \cdot d(\epsilon h)/dM|_{M(k-1)}. \quad (16)$$

The required derivatives  $d(\epsilon h)/dM$  are for symmetrical modes, for both exponents  $\alpha = 1, 2$ , with the abbreviation  $qw = \sqrt{(\epsilon h)^2 (1 - M^2) - (k_0 h)^2}$  (17)

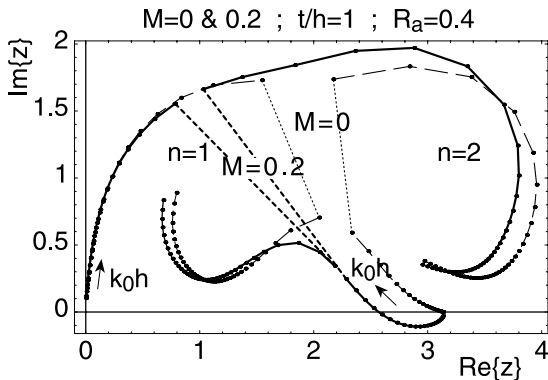
$\alpha = 1$ :

$$\frac{d(\epsilon h)}{dM} = Z_0 G \frac{-(\epsilon h)^2 (1 - M^2) + (k_0 h)^2 (1 + M^2) + 2j k_0 h \cdot M \cdot qw}{qw \cdot (1 - M^2) \left[ M \frac{\epsilon h}{qw} Z_0 G + \frac{\epsilon h}{\cos^2(\epsilon h)} + \tan(\epsilon h) \right]}; \quad (18)$$

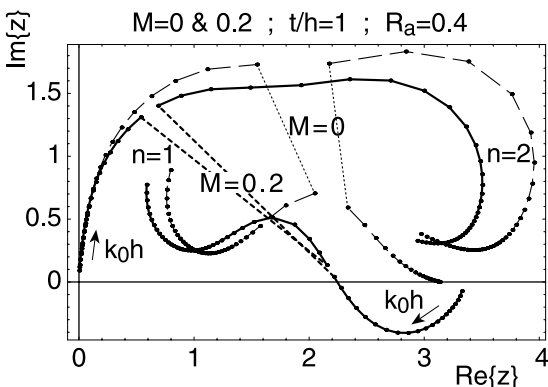
$\alpha = 2$ :

$$\frac{d(\epsilon h)}{dM} = Z_0 G \frac{2(k_0 h + jM \cdot qw) [-(\epsilon h)^2 (1 - M^2) + (k_0 h)^2 (1 + M^2) + 2j k_0 h \cdot M \cdot qw]}{qw \cdot (1 - M^2)^3 \left[ 2j \frac{M^2}{1 - M^2} \frac{\epsilon h}{k_0 h} Z_0 G + 2 \frac{M}{1 - M^2} \frac{\epsilon h}{qw} Z_0 G + \frac{\epsilon h}{\cos^2(\epsilon h)} + \tan(\epsilon h) \right]}. \quad (19)$$

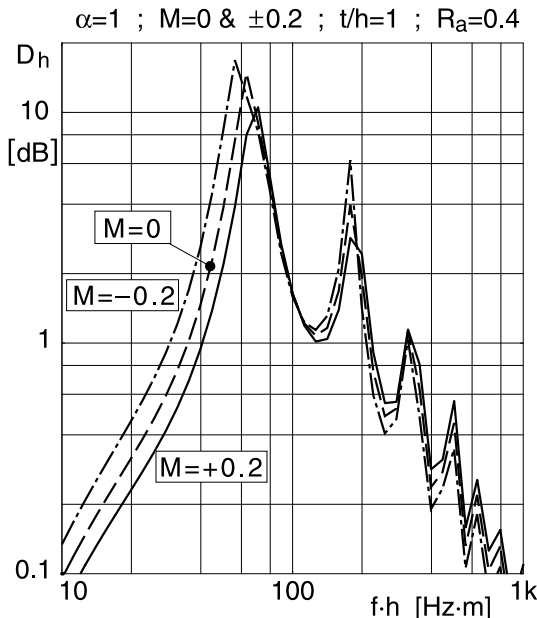
For anti-symmetrical modes replace  $1/\cos^2(\epsilon h) \rightarrow -1/\sin^2(\epsilon h)$ ,  $\tan(\epsilon h) \rightarrow \cot(\epsilon h)$  and  $Z_0 G \rightarrow -Z_0 G$ .



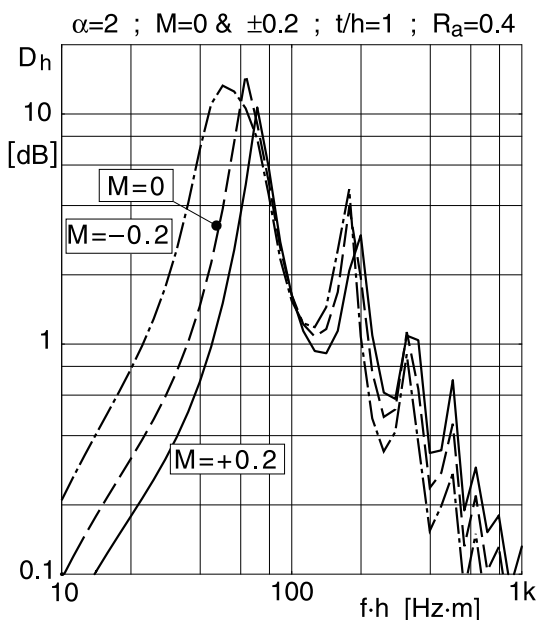
The first two mode solutions  $z = \epsilon h$  in a flat duct with a locally reacting lining, consisting of a simple layer of glass fibres with thickness  $t$  and normalised flow resistance  $R_a = \Xi t / Z_0$ . For Mach numbers  $M = 0$  and  $M = 0.2$  with the boundary condition form  $\alpha = 1$ . The numerical solutions jump at curve sections with *short dashes*



Same as above, but for the boundary condition form  $\alpha = 2$



Attenuation curves  $D_h$  for the least attenuated mode in a duct as above, for Mach numbers  $M = 0$  and  $M = \pm 0.2$  with the boundary condition form  $\alpha = 1$



As above, but for the boundary condition form  $\alpha = 2$

One needs, in a number of applications, the branch points of the complex transformation which is induced by the characteristic equation. We write this equation for symmetrical modes in a flat duct of (half) width  $h$  with a locally reacting lining having a surface admittance  $G$  in the form:

$$f(z; M) = -j \frac{z \cdot \tan z}{w^\alpha} \stackrel{!}{=} U ; \quad \alpha = 1, 2 ; \quad z = \varepsilon h ; \quad U = k_0 h \cdot Z_0 G . \quad (20)$$

The branch points  $z_{b,n}(M)$  are determined as solutions of the equation:

$$\frac{f'(z; 0)}{f(z; 0)} \stackrel{!}{=} \alpha \cdot \frac{w'(z; M)}{w(z; M)} \quad (21)$$

with

$$\begin{aligned} \frac{f'(z; 0)}{f(z; 0)} &= \frac{1}{z} + \frac{1}{\sin z \cdot \cos z}, \\ \frac{w'(z; M)}{w(z; M)} &= j \frac{M(1 - M^2)}{k_0 h} \frac{z}{\sqrt{z^2(1 - M^2) - (k_0 h)^2} \left[ 1 + j \frac{M}{k_0 h} \sqrt{z^2(1 - M^2) - (k_0 h)^2} \right]} . \end{aligned} \quad (22)$$

For small Mach numbers the branch points can be approximated by:

$$z_{b,n}(M) \approx z_{b,n}(0) + M \cdot \left. \frac{dz_b}{dM} \right|_{M=0} \quad (23)$$

with the derivative

$$\begin{aligned} \frac{dz_b}{dM} = & \left\{ (2jM(1 - M^2) + k_0 h(1 - M^2)/qw) \cdot z_b^2 + k_0 h \cdot qw + jM \cdot qw^2 \right. \\ & + \left[ k_0 h \cdot qw + jM(-(k_0 h)^2 + (1 - \alpha)(1 - M^2) \cdot z_b^2) \right] \cdot \cos^2(z_b) \\ & + \left[ 2j(1 - \alpha)(1 - M^2)M \cdot z_b + k_0 h(1 - M^2) \cdot z_b/qw \right] \cdot \cos(z_b) \cdot \sin(z_b) \\ & - \left. \left[ k_0 h \cdot qw + jM(-(k_0 h)^2 + (1 - \alpha)(1 - M^2) \cdot z_b^2) \right] \cdot \sin^2(z_b) \right\} \\ & \cdot \left\{ (2jM^2 + k_0 hM/qw) \cdot z_b^3 - jz_b \cdot qw^2 \right. \\ & + \left[ (2jM^2(1 - \alpha) + k_0 hM/qw) \cdot z_b^2 - j(-(k_0 h)^2 + (1 - \alpha)(1 - M^2) \cdot z_b^2) \right] \\ & \cdot \cos(z_b) \cdot \sin(z_b) \left. \right\}^{-1} , \end{aligned} \quad (24)$$

which for  $M = 0$  becomes (with the abbreviation  $z_b = z_{b,n}(0)$ )

$$\left. \frac{dz_b}{dM} \right|_{M=0} = jk_0 h \frac{4z_b^2 - 2(k_0 h)^2 + 2(z_b^2 - (k_0 h)^2) \cos(2z_b) + z_b \sin(2z_b)}{\sqrt{z_b^2 - (k_0 h)^2} \left[ 2z_b(z_b^2 - (k_0 h)^2) + ((1 - \alpha)z_b^2 - (k_0 h)^2) \sin(2z_b) \right]} . \quad (25)$$

One gets for the first branch point  $n = 1$  with  $z_b = 2.1062 + 1.12536 \cdot j$ :

$$\text{for } k_0 h = 2 ; \alpha = 1: z_{b,1}(M) \approx z_{b,1}(0) + (-1.33228 + j \cdot 0.403591)M , \quad (26)$$

$$\text{for } k_0 h = 2 ; \alpha = 2: z_{b,1}(M) \approx z_{b,1}(0) + (-0.66614 + j \cdot 0.201793)M ,$$

$$\text{for } k_0 h = 1 ; \alpha = 1: z_{b,1}(M) \approx z_{b,1}(0) + (-0.599752 + j \cdot 0.406326)M ,$$

$$\text{for } k_0 h = 1 ; \alpha = 2: z_{b,1}(M) \approx z_{b,1}(0) + (-0.299878 + j \cdot 0.203163)M . \quad (27)$$

The images  $U_{b,n}(M)$  of the branch points  $z_{b,n}(M)$  can be approximated by:

$$U_{b,n}(M) \approx U_{b,n}(0) + M \cdot \frac{dU_b}{dM} \Big|_{M=0} \quad (28)$$

with the derivative

$$\begin{aligned} \frac{dU_b}{dM} \Big|_{M=0} &= \\ &= j \frac{(k_0 h)^2 (2z_b + \sin(2z_b)) (4z_b^2 - 2(k_0 h)^2 + 2(z_b^2 - (k_0 h)^2) \cos(2z_b) + z_b \sin(2z_b))}{2 (2z_b(z_b^2 - (k_0 h)^2) + ((1 - \alpha)z_b^2 - (k_0 h)^2) \sin(2z_b))} . \end{aligned} \quad (29)$$

One gets for the first branch point  $n = 1$  with  $U_b = 2.05998 + j \cdot 1.65061$ :

$$\text{for } k_0 h = 2 ; \alpha = 1: U_{b,1}(M) \approx U_{b,1}(0) + (-7.206913 \cdot 10^{-6} + j \cdot 0.000152866)M ,$$

$$\text{for } k_0 h = 2 ; \alpha = 2: U_{b,1}(M) \approx U_{b,1}(0) + (-3.603788 \cdot 10^{-6} + j \cdot 0.0000764332)M ,$$

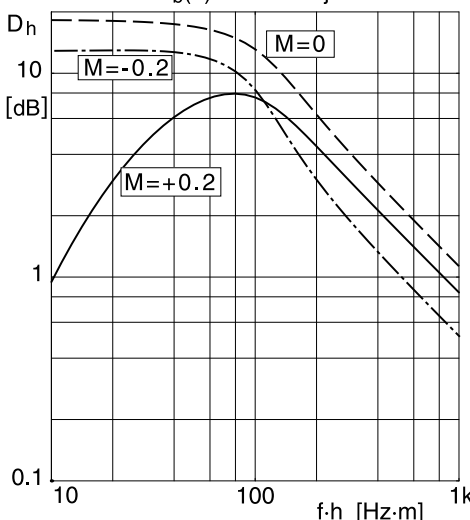
$$\text{for } k_0 h = 1 ; \alpha = 1: U_{b,1}(M) \approx U_{b,1}(0) + (0.0000218572 + j \cdot 0.0000352125)M , \quad (30)$$

$$\text{for } k_0 h = 1 ; \alpha = 2: U_{b,1}(M) \approx U_{b,1}(0) + (0.0000109286 + j \cdot 0.0000176063)M .$$

Influence of the flow on the attenuation for a lining with  $U = U_{b,1}(0)$ :

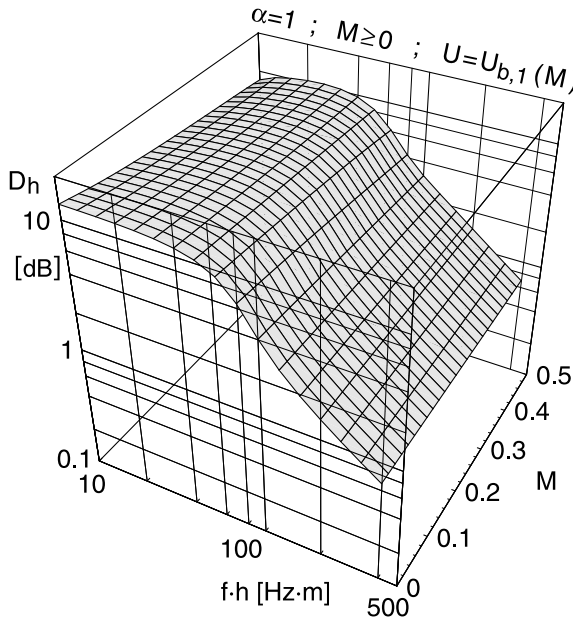
$$\alpha=1 ; M=0 \& \pm 0.2 ;$$

$$U=U_b(0)=2.05998+j \cdot 1.65061$$

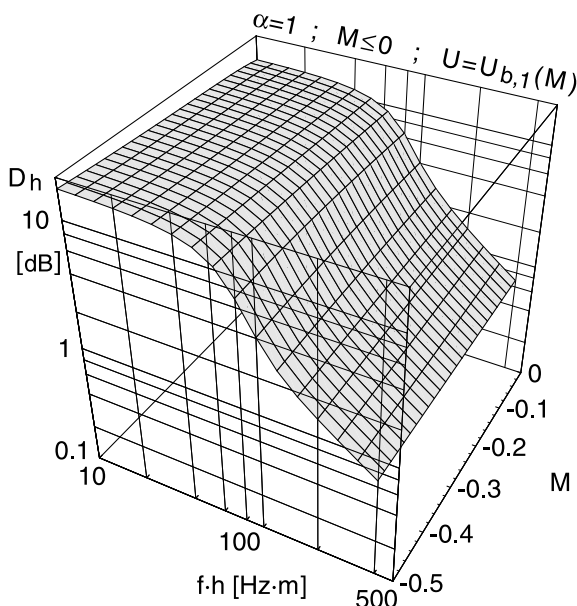


Influence of flow on the attenuation  $D_h$  of the least attenuated mode in a duct whose lining has a  $U$  function  $U = U_{b,1}(0)$  which for  $M = 0$  is in the first branch point

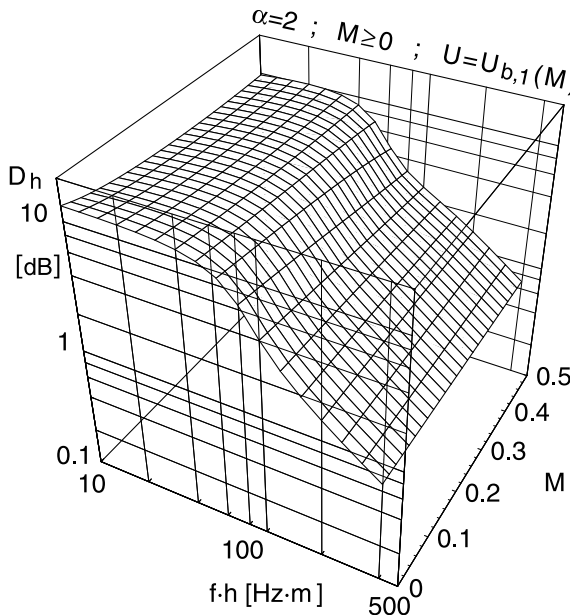
If, however, the lining has a  $U$  function  $U = U_{b,1}(M)$ , the attenuation remains high.



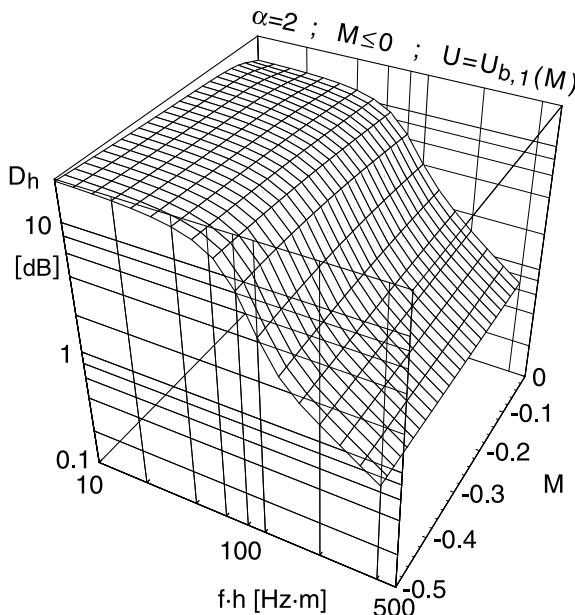
Attenuation  $D_h$  of the least attenuated mode in a flat duct having a locally reacting lining with  $U = U_{b,1}(M)$ , for  $M \geq 0$  and boundary condition form  $\alpha = 1$



As above, i.e. for  $\alpha = 1$ , but with  $M \leq 0$



As above, but for the boundary condition form  $\alpha = 2$  and with  $M \geq 0$



As above, i.e. for  $\alpha = 2$ , but with  $M \leq 0$

## J.36 Influence of Temperature on Attenuation

---

► See also: Mechel, Vol. II, Ch. 42 (1998)

Silencers are used in gas flows with a wide variety of temperatures. The question is how to take the operation temperature into consideration in the design of a silencer.

If the attenuation is evaluated as a non-dimensional quantity (like  $D_h = 8.6858 \cdot \text{Re}[\text{Th}]$ ) using only non-dimensional parameters, and if it is plotted over a non-dimensional variable, then the result is valid for all fluids like air, and also for air at different temperatures. Some different influences of the temperature on the attenuation may be distinguished. Below,  $T$  is the operation temperature (in Kelvin) and  $T_0$  is the standard temperature.

(1) *Influence of representation:*

In a plot of  $D_h$  over  $f \cdot h$  the abscissa comes from  $f \cdot h = c_0/(2\pi) \cdot k_0 h$ . The (linear) abscissa should be multiplied with  $c_0(T)/c_0(T_0)$ .

(2) *Temperature-dependent input parameters:*

Some parameters, like frequency  $f$ , geometrical dimensions, porosities, shape factors etc., are not changed by temperature. Other parameters, like bulk densities of porous materials, surface mass densities  $m$  of foils and plates, remain virtually unchanged. If, however, a non-dimensional parameter  $M = m/(\rho_0 d)$  is used, with air density  $\rho_0$  and some thickness  $d$ ,  $M$  becomes  $M(T) = \rho_0(T_0)/\rho(T) \cdot M_0$ . Often impedances or admittances are made non-dimensional (normalised) with the free field wave impedance  $Z_0 = \rho_0 c_0$ . This reference impedance changes as  $Z_0(T) = \rho_0(T)c_0(T)/(\rho_0 c_0) \cdot Z_0(T_0)$ . If the impedance which is normalised with  $Z_0$  is a mass reactance  $Z_m$  of a solid element (e.g. foil or plate), it is not modified by the temperature; thus the variation in  $Z_m/Z_0$  comes from  $Z_0$ . Commonly used resistances include the flow resistance  $\Xi \cdot d$  of a porous layer ( $d$  its thickness;  $\Xi$  the material flow resistivity) or the flow resistance  $Z_f$  of a porous foil or plate. One can always write  $\Xi \cdot a^2/\eta = f(d)$ , where  $a$  and  $d$  are characteristic lengths (e.g.  $a$  = fibre radius,  $d$  = fibre distance) and  $\eta$  is the dynamic viscosity of air. Thus  $\Xi(T) = \eta(T)/\eta(T_0) \cdot \Xi_0$ . This transformation holds for all other resistances based on the friction of air.

(3) *Temperatur-dependent non-dimensional material data of air:*

Theories for the characteristic propagation constant  $\Gamma_a$  and wave impedance  $Z_a$  of porous materials take into consideration not only the flow resistivity  $\Xi$ , but also material data of air, such as the adiabatic exponent  $\kappa$  and the Prandtl number  $Pr$ . The best procedure is to evaluate  $\Gamma_a$  and  $Z_a$  with a physical model theory and to use material data of air at the operation temperature.

An important parameter is the product  $f_{cr} \cdot d$  of the critical frequency  $f_{cr}$  and thickness  $d$  of an elastic plate. From the relation

$$\frac{f_{cr}d}{fd} = \left( \frac{k_b}{k_0} \right)^2 = c_0 \sqrt{\frac{m}{B}}, \quad (1)$$

and with the assumption that the surface mass density  $m$  and the bending modulus  $B$  do not (or only slightly) change with temperature, the parameter  $f_{cr} \cdot d$  changes as  $c_0(T)$ .

► Section L.2 contains material data for air and relations for their temperature dependence. For some approximations it may be sufficient to use the ideal gas relations:

$$\rho_0(T) = \rho_0(T_0) \cdot T_0/T,$$

$$c_0(T) = \sqrt{\kappa(T)\rho_0(T_0)/\kappa(T_0)\rho_0(T)} \cdot c_0(T_0) \approx c_0(T_0) \cdot \sqrt{T/T_0},$$

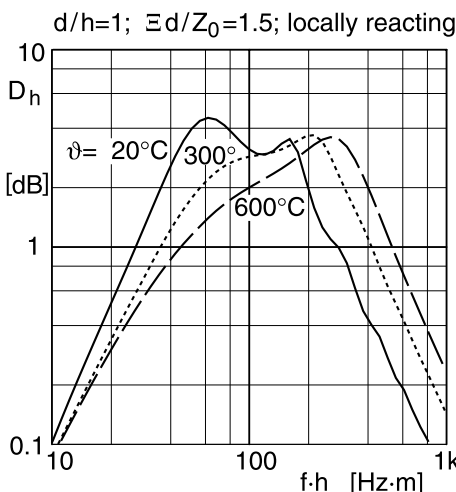
$$\kappa(T) \approx \kappa(T_0), \quad Pr(T) \approx Pr(T_0),$$

$$Z_0(T) = Z_0(T_0) / \sqrt{T/T_0}, \quad k_0(T) = k_0(T_0) / \sqrt{T/T_0}, \quad (2)$$

$$\eta(T) = \eta(T_0) \cdot \sqrt{T/T_0}, \quad \Xi(T) = \Xi(T_0) \cdot \sqrt{T/T_0},$$

$$R(T) = R(T_0) \cdot T/T_0, \quad E(T) = E(T_0) \cdot (T/T_0)^{-3/2},$$

where  $R$  is the gas constant and  $E = \rho_0 f / \Xi$  is a non-dimensional input parameter for some porous material model theories.



Attenuation  $D_h$  of least attenuated mode in a flat duct with a locally reacting glass fibre layer as lining, for three operation temperatures

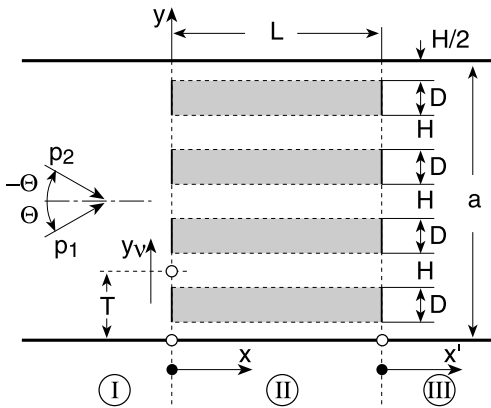
### J.37 Stationary Flow Resistance of Splitter Silencers

► See also: Mechel, Vol. III, Ch. 42 (1998)

The acoustic design of silencers is often in conflict with the static pressure loss of the stationary flow, especially in splitter silencers.

The stationary flow resistance is usually described by the  $\zeta$  value of the silencer:

$$\zeta = \frac{\Delta P_{\text{with}} - \Delta P_{\text{no}}}{\rho_0 \langle V \rangle^2 / 2}, \quad (1)$$



where  $\Delta P_{\text{with}}$  is the static pressure drop over the silencer,  $\Delta P_{\text{no}}$  is the static pressure drop in the empty duct over the same distance and  $\langle V \rangle$  is the average flow velocity in the duct in front of the splitters. If, alternatively, the average flow velocity  $\langle V_s \rangle$  is determined in a splitter duct, the corresponding  $\zeta$  value is:

$$\zeta_s = \zeta / (1 + D/H)^2. \quad (2)$$

Many measurements with splitter silencers (the splitters having rectangular corners) can be summarised by:

$$\zeta_s = 0.53 + 0.66 \cdot \lg \frac{D}{H} + \left( 0.027 - \frac{0.004}{D/H} \right) \cdot \frac{L}{H}. \quad (3)$$

Rounding the splitter heads reduces  $\zeta$  by about  $\Delta \zeta \approx 0.5 - 1.5$ .

### J.38 Non-linearities by Amplitude and/or Flow

► See also: Mechel, Vol. II, Ch. 28 (1995); Ronneberger (1967/68); Cummings (1975)

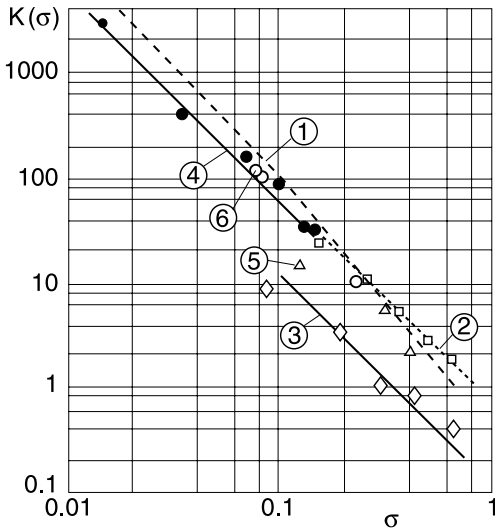
High sound amplitudes and stationary flow produce non-linearities in some absorber components, especially in fences and perforated sheets. The references combine their own measurements with a survey of the literature.

#### I. Amplitude non-linearity of fences:

Let  $\Delta p_s$  be the sound pressure drop across a fence,  $v_s$  the particle velocity in the fence orifice (both averaged over the orifice) and  $\sigma$  the porosity of the fence; then the non-linear contribution to the normalised partition impedance  $Z_s = (\Delta p_s / v_s) / Z_0$  of the fence opening can be written as:

$$\Delta Z_s = \Delta \left( \frac{1}{Z_0} \frac{p_s}{v_s} \right) = \sigma^2 K(\sigma) \frac{v_s}{c_0}. \quad (1)$$

The following diagram gives values of the factor  $K(\sigma)$  over the porosity  $\sigma$ .



Values of factor  $K(\sigma)$  in  $\Delta Z_s$

(1): With the stationary flow resistance coefficient  $\zeta$  defined by  $\Delta P = \zeta \cdot \rho_0 / 2 \cdot U^2$ , where  $\Delta P$  = static pressure drop and  $U/\sigma$  = average flow velocity through the fence opening, the relation is  $K(\sigma) = 0.42 \cdot \zeta$ . (2)

(2): Slit-shaped orifice with sharp corners:  $K(\sigma) = 0.675/\sigma^2$ . (3)

(3): Slit-shaped orifice with rounded corners:  $K(\sigma) = 0.119/\sigma^2$ . (4)

(4): Thin perforated sheet:  $K(\sigma) = 0.58/\sigma^2$ . (5)

(5), (6): Some other values for perforated sheets are taken from the literature.

## II. Non-linearity by flow over orifices:

A flow with velocity  $U$  is past the orifice with diameter  $d = 2a$  of a neck in the duct wall. Experimental results by Cummings for the real part  $Z'$  of the orifice input impedance and for the orifice end correction  $\Delta\ell$  can be represented by the following relations ( $f$  = frequency;  $\ell$  = neck length):

$$\frac{Z'}{\rho_0 f d} = [12.52 \cdot (\ell/d)^{-0.32} - 2.44] \cdot (U^*/f\ell) - 3.2, \quad (6)$$

$$\frac{\Delta\ell}{\Delta\ell_0} = \begin{cases} 1; & U^*/f\ell \leq 0.12d/\ell \\ (1 + 0.6\ell/d) \cdot e^{-(U^*/f\ell + 0.12d/\ell)/(0.25 + \ell/d)} - 0.6\ell/d; & U^*/f\ell > 0.12d/\ell \end{cases},$$

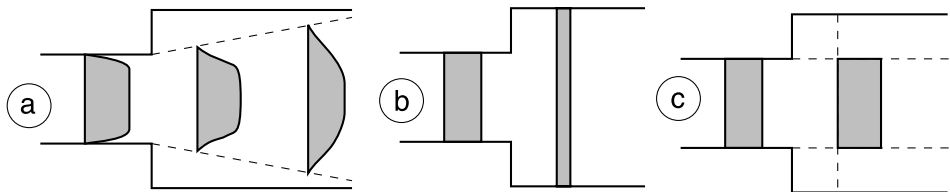
where  $\Delta\ell_0$  is the orifice end correction without flow and  $U^*$  is the flow shear velocity. It is evaluated from  $U^* = \sqrt{\lambda/8} \cdot \langle U \rangle$ ;  $\lambda = 0.306 \cdot Re^{-1/4}$ , (7)

where  $\langle U \rangle$  is the average velocity in the duct,  $\lambda$  is the coefficient of flow resistance by viscous shear and  $Re$  is the Reynold's number of the flow using the duct diameter (the

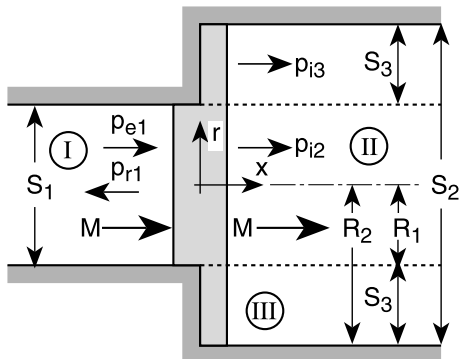
relation between  $\lambda$  and  $Re$  is for square ducts; the corresponding relation in circular ducts with diameter  $2R$  is  $\lambda = 0.316 \cdot Re^{-1/4}$ .

### III. Non-linearity by flow through an orifice:

Consider an orifice generated by a step in a hard duct. The flow velocity profile will have shape (a). Ronneberger in his analysis uses shape (b); Cummings applies shape (c), which is also used in the analysis of [Mechel (1995)] presented below.



The sketch below shows the co-ordinates  $x, r$ , the duct areas  $S_i$ , the field zones I, II, III and the component sound fields.  $M$  is the Mach number with the average flow velocity. The grey area with limits near  $x = 0$  may contain near fields, which will not be considered in detail.



Integrals of conservation of the mass, the impulse and the energy can be assumed to exist in this transition volume:

$$\int_A \rho v \cdot dA = 0 ; \quad \int_A (\rho v)v \cdot dA + \int_A p \cdot dA = 0 ; \quad \int_A \rho Hv \cdot dA = 0 , \quad (8)$$

where  $A$  is the surface of the volume;  $\rho, p, v$  are density, pressure and velocity, respectively; and  $H$  is the stagnation enthalpy. The approximation  $p_{i3} = p_{i1} + p_{r1}$  will be used at the step. The density variations are  $\rho = (p + \delta)/c_0^2$ , where  $\delta$  is the pressure produced by variations of the enthalpy  $S$ :

$$S = \frac{-\delta}{\rho_0 T_0 (\kappa - 1)} \quad (9)$$

( $T_0$  = stationary temperature;  $\kappa$  = adiabatic exponent). The stagnation enthalpy is:

$$H = T \cdot S + \frac{p}{\rho} + \frac{1}{2} |v|^2 . \quad (10)$$

Let the  $x$  factors of the sound fields  $p_{i2}, p_{i3}$  be  $e^{-jk_0x}$  with a correction factor  $K$  for the free field wave number  $k_0$ . The axial particle velocity in zone II is:

$$v_{i2} = \frac{Kp_{i2}}{\rho_0 c_0 (1 - MK)} . \quad (11)$$

At the limit between zones II and III let  $p_{i3} = p_{i2}$ ; let the fields within a zone be (approximately) constant in the radial direction. Then, with the porosity  $\sigma = S_1/S_2$ , the integrals give:

$$\begin{aligned} (1 + M)p_{i1} - (1 - M)p_{r1} &= \left( \frac{KS_3}{S_1} + M + \frac{K}{1 - MK} \right) p_{i2} + M\delta , \\ \left( \frac{1}{\sigma} + 2M + M^2 \right) p_{i1} + \left( \frac{1}{\sigma} - 2M + M^2 \right) p_{r1} &= \left( \frac{1}{\sigma} + M^2 + \frac{2MK}{1 - MK} \right) p_{i2} + M^2\delta , \quad (12) \\ (1 + M)p_{i1} + (1 - M)p_{r1} &= \left( 1 + \frac{MK}{1 - MK} \right) p_{i2} - \frac{\delta}{\kappa - 1} \end{aligned}$$

with the Bessel function  $J_0(z)$  and the Neumann function  $Y_0(z)$ ; as radial functions the amplitude  $A$  follows from the condition of zero radial particle velocity at the outer radius of zone III. The boundary conditions are  $p_{i2}(R_1) = p_{i3}(R_1)$  and

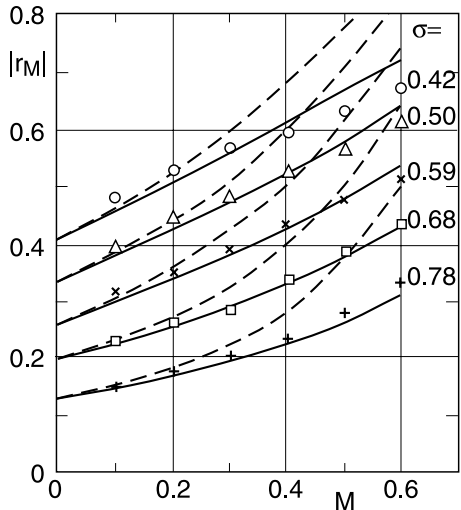
$$\frac{\partial p_{i3}(R_1)}{\partial r} = \frac{1}{(1 - MK)^2} \frac{\partial p_{i2}(R_1)}{\partial r} . \quad (13)$$

They lead to a characteristic equation for  $K$ :

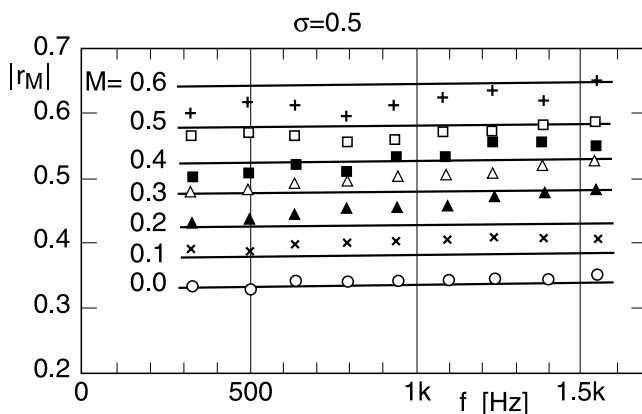
$$\begin{aligned} &\frac{J_1(k_0 R_1 \sqrt{1 - K^2}) \cdot Y_1(k_0 R_2 \sqrt{1 - K^2}) - J_1(k_0 R_2 \sqrt{1 - K^2}) \cdot Y_1(k_0 R_1 \sqrt{1 - K^2})}{J_0(k_0 R_1 \sqrt{1 - K^2}) \cdot Y_1(k_0 R_2 \sqrt{1 - K^2}) - J_1(k_0 R_2 \sqrt{1 - K^2}) \cdot Y_0(k_0 R_1 \sqrt{1 - K^2})} \\ &- \frac{\sqrt{(1 - MK)^2 - K^2} \cdot J_1(k_0 R_1 \sqrt{(1 - MK)^2 - K^2})}{(1 - MK)^2 \sqrt{1 - K^2} \cdot J_0(k_0 R_1 \sqrt{(1 - MK)^2 - K^2})} = 0 . \quad (14) \end{aligned}$$

A start value for its numerical solution is  $K \approx 1/(1 + \sigma M)$ .

The following diagrams show the magnitude of the reflection factor  $r_M = p_{r1}(x = 0)/p_{i1}(x = 0)$ .



Magnitude of reflection factor  $r_M$  over Mach number  $M$  for different porosities  $\sigma = S_1/S_2$ . Points: measured by Ronneberger; Dashed: computed by Ronneberger; Solid: present computation



Magnitude of the reflection factor  $r_M$  over the frequency for porosity  $\sigma = 0.5$  and different Mach numbers  $M$ . Points: measured; Curves: present evaluation

#### IV. Non-linearity by flow along mineral fibre absorbers:

The flow resistivity  $\Xi(U)$  of fibrous absorbers with flow along their surface from measurements with flow velocities up to  $U = 80$  [m/s] can be represented by:

$$\frac{\Xi(U)}{\Xi(0)} = (1 - A_f U)^{-4}; \quad A_{f[s/m]} \approx \frac{0.085}{\sqrt{f_{[Hz]}}}. \quad (15)$$

### V. Non-linearity by flow through porous absorbers:

The following representation of the characteristic propagation constant  $\Gamma_a$  and wave impedance  $Z_a$  with flow through the porous material does not include the possibility that the material is compressed by the flow!

$$\begin{aligned}\Gamma_a &= \sqrt{j\omega\sigma C_{\text{eff}} \left[ F_\eta \Xi + 2\xi_t \cdot |U| + j\omega\rho_0 \frac{\chi}{\sigma} \right]}, \\ Z_a &= \sqrt{\frac{\rho_0 \chi / \sigma^2 + \frac{1}{j\omega\sigma} (F_\eta \Xi + 2\xi_t |U|)}{C_{\text{eff}}}}\end{aligned}\quad (16)$$

with

$$\begin{aligned}C_{\text{eff}} &= \frac{1}{\rho_0 c_0^2} \left[ 1 + (\kappa - 1) \frac{\tan(k_{\alpha 0} h)}{k_{\alpha 0} h} \right], \\ F_\eta &= \frac{1}{3} \frac{\left( \frac{\Theta_p}{\Theta_\alpha} - 1 \right) k_v h \cdot \tan(k_v h)}{1 - \frac{1}{\sqrt{\kappa P_r}} \frac{\Theta_p}{\Theta_\alpha} \tan(k_{\alpha 0} h) + \left( \frac{\Theta_p}{\Theta_\alpha} - 1 \right) \tan(k_v h)},\end{aligned}\quad (17)$$

$$k_{\alpha 0} h = \sqrt{\kappa P_r} \cdot k_v h; \quad k_v h = \sqrt{-j6\pi E}; \quad E = \rho_0 f / \Xi, \quad (18)$$

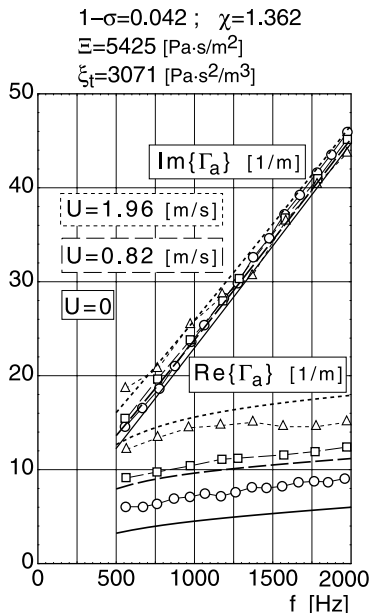
and  $\xi_t$  from a  $\Delta P - U$  record of stationary flow with velocity  $U$  through a material layer with thickness  $\Delta z$  according to:

$$\frac{-\Delta P}{\Delta z \cdot U} = \Xi + \xi_t \cdot U \quad (19)$$

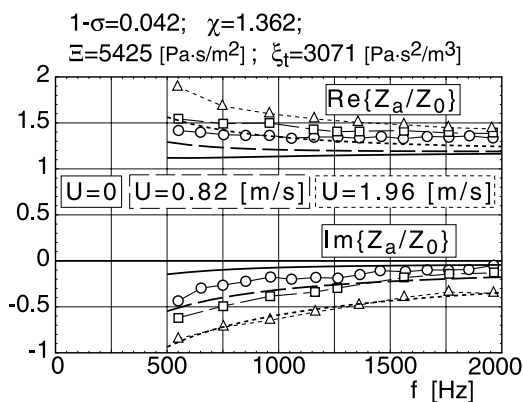
(make a quadratic regression through measured  $\Delta P - U$  values; the coefficient of the linear term in  $U$  gives  $\Xi$ ; the coefficient of the quadratic term gives  $\xi_t$ ).

$f =$	frequency;
$\omega =$	angular frequency;
$\rho_0 =$	air density;
$c_0 =$	sound velocity in air;
$U =$	stationary flow velocity;
$\kappa =$	adiabatic exponent;
$P_r =$	Prandtl number;
$\sigma =$	material porosity;
$\chi =$	1.362 = structure factor;
$\Xi =$	measured flow resistivity;
$\xi_t =$	quadratic term of flow resistivity;
$k_v =$	viscosity wave number;
$k_{\alpha 0} =$	thermal wave number;
$\Theta_p, \Theta_\alpha$	see  Sect. B.1

The following diagrams show measured points and computed curves for the characteristic values  $\Gamma_a$ ,  $Z_a$  in a polyurethane foam for velocities  $U = 0; 0.82; 1.96$  [m/s].



Real and imaginary parts of propagation constant  $\Gamma_a$  in a PU foam with three flow velocities



Real and imaginary parts of normalised wave impedance  $Z_a/Z_0$  in PU foam, with three flow velocities

### J.39 Flow-Induced Non-linearity of Perforated Sheets

► See also: Mechel, Vol. II, Ch. 28 (1995); Coelho (1983)

The following table gives partition impedances  $Z_m = Z'_m + j \cdot Z''_m$  for perforated sheets, which are mostly based on experimental data. The perforations are circular with radius  $a$  at mutual distances  $b$ ; the porosity is  $\sigma = \pi a^2/b^2$ ; the sheet thickness is  $t$ . The Mach number  $M_0$  for high sound levels is  $M_0 = v/c_0$ , with  $v$  the particle velocity in the exit orifice; in the Mach number  $M_\infty = U_\infty/c_0$  the flow velocity  $U_\infty$  belongs to the undisturbed flow parallel to the sheet. Ranges of the sound pressure level  $L_p$  (relative to 20 [ $\mu$ Pa]) are given by  $L_{0l}, L_{0h}$  without flow, and  $L_{Ul}, L_{Uh}$  with flow;  $v$  is the kinematic viscosity. Other symbols are explained in the table below.

**Table 1** Formulas for the partition impedance  $Z_m$  of perforated sheets for different sound pressure levels, with or without parallel flow

		<b>Low level</b>		<b>Medium level</b>		<b>High level</b>	
<b>No flow</b>		$L_p < L_{0l}$		$L_{0l} \leq L_p \leq L_{0h}$		$L_p > L_{0h}$	
$M_\infty < 0.025$		$L_{0l} = 107 + 27 \lg [4(1 - \sigma^2) \omega \rho_0 v (1 + t/2a)^2]$		$L_{0h} = 137 + 27 \lg [4(1 - \sigma^2) \omega \rho_0 v (1 + t/2a)^2]$			
$(U_\infty \lesssim 8 \text{ m/s})$		$Z'_m = R_0 ; \quad Z''_m = X_0(\delta)$		$Z'_m = \sqrt{ R_h^2 - R_0^2 } ; \quad Z''_m = X_0(\delta)$		$Z'_m = R_h ; \quad Z''_m = X_0(\delta)$	
$R_0 = \frac{\rho_0}{\sigma} \sqrt{8v\omega} (1 + t/2a)$		$R_h = \frac{1}{\sigma} \sqrt{2\rho_0(1 - \sigma^2)} \cdot 10^{-2.25+0.185l_p}$		$X_0 = \frac{\omega \rho_0}{\sigma} \left[ \sqrt{8v/\omega} (1 + t/2a) + t + \delta \right]$			
$\delta = \delta_0 = 0.85 \cdot 2a \cdot \Phi_0(\sigma)$		$\delta = \delta_0 \cdot \Phi_1(M_0)$					
$\Phi_0(\sigma) = 1 - 1.47\sqrt{\sigma} + 0.47\sqrt{\sigma^3}$		$M_0 = \frac{10^{-2.25+0.025l_p}}{\sqrt{0.5\rho_0 c_0^2(1 - \sigma^2)}}$		$\Phi_1(M_0) = \frac{1 + 5 \cdot 10^3 M_0^2}{1 + 10^4 M_0^2}$			
<b>With flow</b>		$L_p < L_{Ul}$		$L_{Ul} \leq L_p \leq L_{Uh}$		$L_p > L_{Uh}$	
$M_\infty \geq 0.025$		$L_{Ul} = 175 + 40 \lg M_\infty$		$L_{Uh} = 193 + 40 \lg M_\infty$			
$(U_\infty \gtrsim 10 \text{ m/s})$		$Z'_m = R_M ; \quad Z''_m = X_0(\delta)$		$Z'_m = \sqrt{R_M^2 + R_h^2} ; \quad Z''_m = X_0(\delta)$		$Z'_m = R_h ; \quad Z''_m = X_0(\delta)$	
$R_M = 0.6 \rho_0 c_0 \frac{1 - \sigma^2}{\sigma} (M_\infty - 0.025) - 40 R_0 (M_\infty - 0.05) ; \quad M_\infty \leq 0.05$		$= 0.3 \rho_0 c_0 \frac{1 - \sigma^2}{\sigma} M_\infty ; \quad M_\infty > 0.05$					
$\delta = \delta_0 \cdot \Phi_2(M_\infty)$		$\delta = \delta_0 \cdot \Phi_1(M_0)$					
$\Phi_2(M_\infty) = 1 / (1 + 305 M_\infty^2)$							

## J.40 Reciprocity at Duct Joints

► See also: Cho (1980); Mechel, Vol. III, Ch. 33 (1998)

Consider two ducts,  $\alpha = a, b$ , each with constant width and lining, possibly different in the ducts. The ducts are anechoic and be connected with some transition duct (step, corner, cone etc.). In the ducts there are modes with axial propagation constants  $\gamma_{\alpha n}$  and mode norms  $N_{\alpha n}$ .

In a first “experiment” the  $m$ -th mode of duct  $a$  with amplitude  $P_{im}^a$  is incident on the joint; it produces modes  $n$  in duct  $b$  with amplitudes  $P_{tn}^b(m)$ . In a second “experiment” the  $\mu$ -th mode of duct  $b$  with amplitude  $P_{ip}^b$  is incident on the joint; it produces modes in duct  $a$  with amplitudes  $P_{tm}^a(\mu)$ . A relation of reciprocity holds for the transmitted modes:

$$\frac{P_{tm}^a(\mu)}{P_{ip}^b} = \frac{\gamma_{b\mu}}{\gamma_{am}} \frac{N_{am}}{N_{b\mu}} \frac{P_{tp}^b(m)}{P_{im}^a}. \quad (1)$$

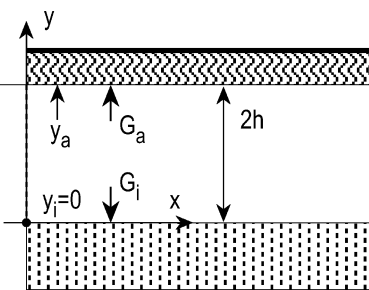
The corresponding relation for the reflected modes in two “experiments” in which modes (e.g. of duct  $a$ ) of orders  $m, n$  are incident on the joint is:

$$\frac{P_{rn}^a(m)}{P_{rm}^a(n)} = \frac{\gamma_{am}}{\gamma_{an}} \frac{N_{an}}{N_{am}} \frac{P_{in}^a}{P_{im}^a}. \quad (2)$$

## J.41 Mode Sets in Flat Ducts with Unsymmetrical, Locally Reacting Lining

► See also: Mechel (2006), Grigoryan (1969)

The object is a flat duct with different locally reacting linings on opposite sides. A similar object is treated in ➤ Sect. J.11, where the least attenuated mode was sought. Complete sets of mode solutions shall be determined here. In contrast to ➤ Sect. J.11, the origin of the co-ordinates here is in a wall (with index I, the opposite wall with index a).



Mode formulation (constant in  $z$  direction) of the mode with index  $\mu$ :

$$\begin{aligned} p_\mu(x, y) &= (\cos(\epsilon_\mu y) + \beta \sin(\epsilon_\mu y)) e^{-\Gamma_\mu x}; \quad \Gamma_\mu^2 = \epsilon_\mu^2 - k_0^2; \\ Z_0 v_{py}(x, y) &= j \frac{\epsilon_\mu}{k_0} \frac{\partial p_\mu}{\partial (\epsilon_\mu y)} = j \frac{\epsilon_\mu}{k_0} \left( \cos'(\epsilon_\mu y) + \beta \sin'(\epsilon_\mu y) \right) e^{-\Gamma_\mu x} \end{aligned} \quad (1)$$

satisfying the transversal Helmholtz equation

$$\left( \frac{\partial^2}{\partial y^2} + k_0^2 + \Gamma_\mu^2 \right) p_\mu(y) = \left( \frac{\partial^2}{\partial y^2} + \epsilon_\mu^2 \right) p_\mu(y) = 0, \quad (2a)$$

and the boundary conditions at  $y = 0$  and  $y = 2h$ :

$$Z_0 v_{\mu y}(x, y_{i,a}) = \mp Z_0 G_{i,a} \cdot p_\mu(x, y_{i,a}). \quad (3a)$$

They assume, with the non-dimensional quantities

$$\epsilon_\mu y \rightarrow \eta ; \quad \epsilon_\mu y_{i,a} \rightarrow \eta_{i,a} ; \quad y_i = 0 ; \quad y_a = 2h ; \quad k_0 h \cdot Z_0 G_{i,a} \rightarrow U_{i,a}, \quad (4)$$

the forms

$$\partial^2 p_\mu(\epsilon y) / \partial (\epsilon y)^2 + p_\mu(\epsilon y) = 0 \rightarrow \partial^2 p_\mu(\eta) / \partial \eta^2 + p_\mu(\eta) = 0, \quad (2b)$$

$$\eta_{i,a} \left( \cos'(\eta_{i,a}) + \beta \sin'(\eta_{i,a}) \right) = \pm 2jU_{i,a} \cdot (\cos(\eta_{i,a}) + \beta \sin(\eta_{i,a})). \quad (3b)$$

The amplitude ratio  $\beta$  of the terms in (1) will be at the walls  $\beta \rightarrow \beta_{i,a}$ :

$$\begin{aligned} \beta_i &= -\frac{2jU_i \cos \eta_i - \eta_a \cos' \eta_i}{2jU_i \sin \eta_i - \eta_a \sin' \eta_i} \xrightarrow{\eta_i=0} \frac{2jU_i}{\eta_a}, \\ \beta_a &= -\frac{2jU_a \cos \eta_a + \eta_a \cos' \eta_a}{2jU_a \sin \eta_a + \eta_a \sin' \eta_a} = -\frac{2jU_a \cos \eta_a - \eta_a \sin \eta_a}{2jU_a \sin \eta_a + \eta_a \cos \eta_a}. \end{aligned} \quad (5)$$

Requiring  $\beta_i = \beta_a$  leads to the characteristic equation for the lateral wave number  $\eta_a$ :

$$\begin{aligned} &\left( 2jU_i \sin \eta_i - \eta_a \sin' \eta_i \right) \cdot \left( 2jU_a \cos \eta_a + \eta_a \cos' \eta_a \right) \\ &- \left( 2jU_i \cos \eta_i - \eta_a \cos' \eta_i \right) \cdot \left( 2jU_a \sin \eta_a + \eta_a \sin' \eta_a \right) = 0. \end{aligned} \quad (6a)$$

*Expansion in continued fractions:*

Insertion of the derivatives in (6a) will give:

$$\begin{aligned} &(4U_i U_a + \eta_a^2) (\sin \eta_i \cos \eta_a - \cos \eta_i \sin \eta_a) \\ &+ 2j\eta_a (U_i + U_a) (\sin \eta_i \sin \eta_a + \cos \eta_i \cos \eta_a) = 0. \end{aligned} \quad (6b)$$

And, after application of the addition theoreme:

$$-(4U_i U_a + \eta_a^2) \sin(\eta_a - \eta_i) + 2j\eta_a (U_i + U_a) \cos(\eta_a - \eta_i) = 0, \quad (6c)$$

and of the special value  $\eta_i = 0$ :

$$-(4U_i U_a + \eta_a^2) \sin \eta_a + 2j\eta_a (U_i + U_a) \cos \eta_a = 0. \quad (6d)$$

Division by  $\sin \eta_a$  (which is possible for  $\eta_a \neq n\pi$ ,  $n = \text{integer}$ ; these values are assumed only in ducts with hard walls) returns:

$$2j(U_i + U_a) \cdot \eta_a \cot \eta_a - (4U_i U_a + \eta_a^2) = 0, \quad (6e)$$

where the continued fraction expansion can be applied on  $z \cdot \cot z$ , resulting in the following form of the characteristic equation for  $\eta_a$ :

$$2j(U_i + U_a) \cdot \left( 1 - \frac{\eta_a^2}{3} - \frac{\eta_a^2}{5} - \frac{\eta_a^2}{7} \dots \right) - (4U_i U_a + \eta_a^2) = 0 . \quad (7)$$

On truncation and putting everything in one fraction, the numerator becomes a polynomial equation in  $(\eta_a)^2$  whose solutions, with  $\text{Im}((\eta_a)^2) \geq 0$  and  $|\text{char.eq}(\eta_a)| < \text{limit}$  (a value of limit  $\approx 80$  may be taken), are approximations to a set of mode solutions. They can be taken as starters for Muller's procedure of a numerical solution (see [Sect. J.4](#)) of the characteristic equation (6d). This is a mode-safe and fast computing procedure for a set of mode eigenvalues  $\eta_a$ .

*Grigoryan's expansion of the characteristic equation:*

Grigoryan has applied his method for the expansion of the characteristic equation in bent ducts, [Grigoryan (1969)]. It can be generalised and then applied on asymmetrical flat ducts as well; see [Mechel (2006)].

Equation (6a) may be written as:

$$\begin{aligned} & 4U_i U_a \begin{vmatrix} \sin \eta_i & \sin \eta_a \\ \cos \eta_i & \cos \eta_a \end{vmatrix} + \eta_a^2 \begin{vmatrix} \sin' \eta_i & \sin' \eta_a \\ \cos' \eta_i & \cos' \eta_a \end{vmatrix} \\ & - 2jU_i \eta_a \begin{vmatrix} \sin \eta_i & \sin' \eta_a \\ \cos \eta_i & \cos \eta_a \end{vmatrix} + 2jU_a \eta_a \begin{vmatrix} \sin' \eta_i & \sin \eta_a \\ \cos' \eta_i & \cos \eta_a \end{vmatrix} = 0 , \end{aligned} \quad (6f)$$

or with the abbreviations for the determinants:

$$D_{n,m}(\eta_i, \eta_a) = \begin{vmatrix} \sin^{(n)} \eta_i & \sin^{(m)} \eta_a \\ \cos^{(n)} \eta_i & \cos^{(m)} \eta_a \end{vmatrix} ; \quad (n), (m) \in (0), (1) , \quad (8)$$

in which  $(n), (m) \in (0), (1)$  are degrees of derivatives, in the form:

$$\begin{aligned} & 4U_i U_a D_{0,0}(\eta_i, \eta_a) + \eta_a^2 D_{1,1}(\eta_i, \eta_a) \\ & - 2jU_i \eta_a D_{0,1}(\eta_i, \eta_a) + 2jU_a \eta_a D_{1,0}(\eta_i, \eta_a) = 0 . \end{aligned} \quad (6g)$$

According to Grigoryan, a Taylor expansion is applied on the second column of  $D_{n,m}(\eta_i, \eta)$  around  $\eta = \eta_i = 0$ , i.e. as a series in  $\chi = (\eta - \eta_i)$ :

$$\begin{aligned} D_{n,m}(\eta_i, \eta) &= \begin{vmatrix} \sin^{(n)} \eta_i & \sum_{k \geq 0} \frac{\chi^k}{k!} \sin^{(m+k)} \eta_i \\ \cos^{(n)} \eta_i & \sum_{k \geq 0} \frac{\chi^k}{k!} \cos^{(m+k)} \eta_i \end{vmatrix} \\ &= \sum_{k \geq 0} \frac{\chi^k}{k!} \begin{vmatrix} \sin^{(n)} \eta_i & \sin^{(m+k)} \eta_i \\ \cos^{(n)} \eta_i & \cos^{(m+k)} \eta_i \end{vmatrix} . \end{aligned} \quad (9)$$

In the special case  $\eta = \eta_a$ , i.e. for  $\chi = \eta_a = 2\epsilon h$ , one gets for the determinants in (6g):

$$D_{n,m}(\eta_i, \eta_a) = \sum_{k \geq 0} \frac{(\eta_a)^k}{k!} \begin{vmatrix} \sin^{(n)} \eta_i & \sin^{(m+k)} \eta_i \\ \cos^{(n)} \eta_i & \cos^{(m+k)} \eta_i \end{vmatrix} := \sum_{k \geq 0} \frac{(\eta_a)^k}{k!} B_{n,m+k}(\eta_i) , \quad (10)$$

which may be interpreted as definitions of the coefficient determinants:

$$B_{n,v}(z) = \begin{vmatrix} \sin^{(n)} z & \sin^{(v)} z \\ \cos^{(n)} z & \cos^{(v)} z \end{vmatrix} = \begin{vmatrix} f^{(n)}(z) & f^{(v)}(z) \\ g^{(n)}(z) & g^{(v)}(z) \end{vmatrix}, \quad (11)$$

where  $f(z), g(z)$  stand for independent solutions of the non-dimensional Helmholtz equation

$$f^{(2)}(z) + f(z) = 0 ; \quad g^{(2)}(z) + g(z) = 0. \quad (12)$$

Evidently, the trivial relations  $B_{v,v} = 0; B_{n,n} = -B_{v,n}$  hold, and therefore a recursive evaluation is possible:

$n = 0 :$

$$B_{0,0}(z) = 0 ; \quad B_{0,1}(z) = W(f(z), g(z)) ; \quad B_{0,v}(z) = -B_{0,v-2}(z); \quad (13a)$$

$n = 1 :$

$$B_{1,0}(z) = -W(f(z), g(z)) ; \quad B_{1,1}(z) = 0 ; \quad B_{1,v}(z) = -B_{1,v-2}(z),$$

where  $W(f(z), g(z))$  is the Wronski determinant of the pair of solutions  $f(z), g(z)$ . In the special case  $f(z) = \sin z; g(z) = \cos z$ , with  $W(f(z), g(z)) = -1$ , follows:

$n = 0 :$

$$B_{0,0}(z) = 0 ; \quad B_{0,1}(z) = -1 ; \quad B_{0,2}(z) = 0 ; \quad B_{0,3}(z) = 1 ; \quad B_{0,4}(z) = 0 ; \\ B_{0,v}(z) = -B_{0,v-2}(z) = -\sin(v\pi/2); \quad (13b)$$

$n = 1 :$

$$B_{1,0}(z) = 1 ; \quad B_{1,1}(z) = 0 ; \quad B_{1,2}(z) = -1 ; \quad B_{1,3}(z) = 0 ; \quad B_{1,4}(z) = 1 ; \\ B_{1,v}(z) = -B_{1,v-2}(z) = \cos(v\pi/2).$$

Thus, the determinants in (10) can be evaluated by:

$$D_{0,m}(\eta_i, \eta_a) = \sum_{k \geq 0} \frac{(\eta_a)^k}{k!} B_{0,m+k}(\eta_i) = - \sum_{k \geq 0} \frac{(\eta_a)^k}{k!} \sin((m+k)\pi/2), \quad (14a)$$

$$D_{1,m}(\eta_i, \eta_a) = \sum_{k \geq 0} \frac{(\eta_a)^k}{k!} B_{1,m+k}(\eta_i) = \sum_{k \geq 0} \frac{(\eta_a)^k}{k!} \cos((m+k)\pi/2),$$

and in special cases of the indices  $n, m$ :

$$D_{1,1}(\eta_i, \eta_a) = \sum_{k_{\text{odd}} \geq 1} \frac{(\eta_a)^k}{k!} \cos((1+k)\pi/2) = \sum_{k_{\text{odd}} \geq 1} (-1)^{(1+k)/2} \frac{(\eta_a)^k}{k!}, \quad (14b)$$

$$D_{1,0}(\eta_i, \eta_a) = \sum_{k_{\text{even}} \geq 0} \frac{(\eta_a)^k}{k!} \cos(k\pi/2) = \sum_{k_{\text{even}} \geq 0} (-1)^{k/2} \frac{(\eta_a)^k}{k!},$$

$$D_{0,0}(\eta_i, \eta_a) = - \sum_{k_{\text{odd}} \geq 1} \frac{(\eta_a)^k}{k!} \sin(k\pi/2) = \sum_{k_{\text{odd}} \geq 1} (-1)^{(1+k)/2} \frac{(\eta_a)^k}{k!}, \quad (14c)$$

$$D_{0,1}(\eta_i, \eta_a) = - \sum_{k_{\text{even}} \geq 0} \frac{(\eta_a)^k}{k!} \sin((1+k)\pi/2) = - \sum_{k_{\text{even}} \geq 0} (-1)^{k/2} \frac{(\eta_a)^k}{k!}.$$

The characteristic equation (6g) will be, after these transformations:

$$(4U_i U_a + \eta_a^2) \sum_{k_{\text{odd}} \geq 1} (-1)^{(1+k)/2} \frac{(\eta_a)^k}{k!} + 2j\eta_a (U_i + U_a) \sum_{k_{\text{even}} \geq 0} (-1)^{k/2} \frac{(\eta_a)^k}{k!} = 0. \quad (15a)$$

On truncation at  $k = k_{hi}$  this returns an odd polynomial in  $\eta_a$  without a constant term (in  $\eta_a$ ). Since  $\eta_a = 0$  can be excluded as solution, one may divide (15a) by  $\eta_a$ , leading to:

$$(4U_i U_a + \eta_a^2) \sum_{k_{\text{odd}} \geq 1} (-1)^{(1+k)/2} \frac{(\eta_a)^{k-1}}{k!} + 2j(U_i + U_a) \sum_{k_{\text{even}} \geq 0} (-1)^{k/2} \frac{(\eta_a)^k}{k!} = 0, \quad (15b)$$

and with the abbreviations  $k_{\text{even}} \rightarrow 2\kappa$ ;  $k_{\text{odd}} \rightarrow 2\kappa + 1$ ;  $\kappa = 0, 1, 2, \dots$ ; to:

$$-(4U_i U_a + \eta_a^2) \sum_{\kappa \geq 0} (-1)^\kappa \frac{(\eta_a)^{2\kappa}}{(2\kappa+1)!} + 2j(U_i + U_a) \sum_{\kappa \geq 0} (-1)^\kappa \frac{(\eta_a)^{2\kappa}}{(2\kappa)!} = 0, \quad (15c)$$

or, with collected sums, finally:

$$\sum_{\kappa \geq 0} (-1)^\kappa \frac{(\eta_a)^{\kappa}}{(2\kappa)!} \left[ 2j(U_i + U_a) - \frac{(4U_i U_a + \eta_a^2)}{(2\kappa+1)} \right] = 0. \quad (15d)$$

The degree of the polynomial in  $(\eta_a^2)$  on truncation at  $k_{hi}$  is  $k_{hi} + 1$ . The polynomial solutions  $\eta_a$  may be taken as approximations to mode solutions and as starters in Muller's procedure, after solutions with  $\text{Im}((\eta_a)^2) < 0$  and/or  $|\text{char.eq}| > \text{limit}$  ( $\text{limit} \approx 80$  is feasible) are rejected. The number of unusable polynomial solutions (for equal limits  $k_{hi}$  of truncation) is higher in Grigoryan's expansion than with the continued-fraction expansion, and the set of usable mode solutions is less "compact" (i. e. more solutions missing) than with the continued-fraction method.

## J.42 Mode Sets in Annular Ducts with Unsymmetrical, Locally Reacting Lining

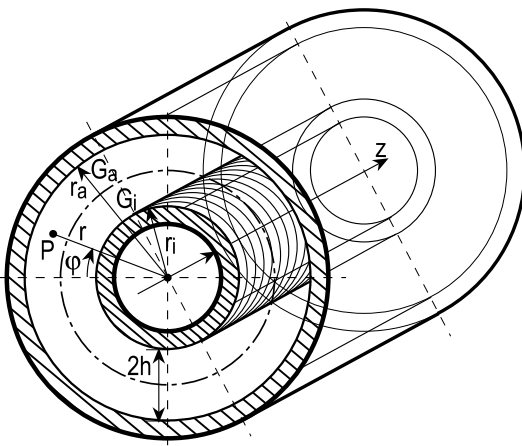
► See also: Mechel (2006); Grigoryan (1969)

The object is a ring-shaped duct with different locally reacting linings on opposite sides. A similar object is treated in ➤ Sect. J.16, where the least attenuated mode was sought. Complete sets of mode solutions shall be determined here.

Some methods will be displayed for the numerical evaluation of mode eigenvalues (*mode solutions*). They all transform the transcendental characteristic equation to a polynomial equation whose solutions shall serve as starters in Muller's procedure of numerical solution of the exact characteristic equation (see ➤ Sect. J.4). (More methods and details can be found in [Mechel (2006)].)

Formulations of modes  $p_\mu(r, \varphi, z)$  in an annular duct preferably use the Bessel and Neumann functions,  $J_\mu(k_r r)$ ,  $Y_\mu(k_r r)$ , for the radial factor, with the unknown radial wave number  $k_r$  ( $k_0$ ,  $Z_0$  = free field wave number and wave impedance); the azimuthal mode index  $\mu$  is mostly given by the angular distribution of the excitation:

$$\begin{aligned} p_\mu(r, \varphi, z) &= (J_\mu(k_r r) + \beta Y_\mu(k_r r)) e^{-j\mu\varphi} e^{-\Gamma z} ; \quad \Gamma^2 = k_r^2 - k_0^2 , \\ Z_0 v_{\mu r}(r, \varphi, z) &= j \frac{k_r}{k_0} \frac{\partial p}{\partial(k_r r)} = j \frac{k_r}{k_0} (J'_\mu(k_r r) + \beta Y'_\mu(k_r r)) e^{-j\mu\varphi} e^{-\Gamma z} . \end{aligned} \quad (1)$$



The boundary conditions at the walls with wall admittances  $G_{i,a}$  at  $r = r_{i,a}$  are:

$$k_r r_{i,a} \left( J'_\mu(k_r r_{i,a}) + \beta Y'_\mu(k_r r_{i,a}) \right) = \pm j k_0 r_{i,a} Z_0 G_{i,a} \left( J_\mu(k_r r_{i,a}) + \beta Y_\mu(k_r r_{i,a}) \right) \quad (2a)$$

(primes indicate derivatives). Introduce non-dimensional quantities:

$$k_r r \rightarrow \rho ; \quad k_r r_{i,a} \rightarrow \rho_{i,a} ; \quad k_0 r_{i,a} \cdot Z_0 G_{i,a} \rightarrow U_{i,a} ; \quad \lambda = r_i/r_a = \rho_i/\rho_a .$$

By elimination of the radial term factor  $\beta$  from both boundary conditions:

$$\rho_{i,a} \left( J'_\mu(\rho_{i,a}) + \beta Y'_\mu(\rho_{i,a}) \right) = \pm j U_{i,a} \left( J_\mu(\rho_{i,a}) + \beta Y_\mu(\rho_{i,a}) \right) , \quad (2b)$$

one gets the characteristic equation for the mode eigenvalues  $\rho_a$ ;  $\rho_i = \lambda \cdot \rho_a$  with given  $\lambda$ :

$$\begin{aligned} & \left( U_i J_\mu(\rho_i) + j \rho_i J'_\mu(\rho_i) \right) \cdot \left( U_a Y_\mu(\rho_a) - j \rho_a Y'_\mu(\rho_a) \right) \\ & - \left( U_i Y_\mu(\rho_i) + j \rho_i Y'_\mu(\rho_i) \right) \cdot \left( U_a J_\mu(\rho_a) - j \rho_a J'_\mu(\rho_a) \right) = 0 , \end{aligned} \quad (3a)$$

or grouped differently with determinants as factors:

$$\begin{aligned} & U_i \cdot U_a \begin{vmatrix} J_\mu(\rho_i) & J_\mu(\rho_a) \\ Y_\mu(\rho_i) & Y_\mu(\rho_a) \end{vmatrix} + \rho_i \cdot \rho_a \begin{vmatrix} J'_\mu(\rho_i) & J'_\mu(\rho_a) \\ Y'_\mu(\rho_i) & Y'_\mu(\rho_a) \end{vmatrix} \\ & - j \rho_a U_i \begin{vmatrix} J_\mu(\rho_i) & J'_\mu(\rho_a) \\ Y_\mu(\rho_i) & Y'_\mu(\rho_a) \end{vmatrix} + j \rho_i U_a \begin{vmatrix} J'_\mu(\rho_i) & J_\mu(\rho_a) \\ Y'_\mu(\rho_i) & Y_\mu(\rho_a) \end{vmatrix} = 0 . \end{aligned} \quad (3b)$$

With the determinant symbols in which (n), (m)  $\in (0), (1)$  are orders of derivatives:

$$D_{n,m}(\mu, \rho_i, \rho_a) := \begin{vmatrix} J_\mu^{(n)}(\rho_i) & J_\mu^{(m)}(\rho_a) \\ Y_\mu^{(n)}(\rho_i) & Y_\mu^{(m)}(\rho_a) \end{vmatrix} ; \quad (n), (m) \in (0), (1) , \quad (4)$$

the characteristic equation reads:

$$\begin{aligned} & \rho_i \rho_a D_{1,1}(\mu, \rho_i, \rho_a) - j \rho_a U_i D_{0,1}(\mu, \rho_i, \rho_a) \\ & + j \rho_i U_a D_{1,0}(\mu, \rho_i, \rho_a) + U_i \cdot U_a D_{0,0}(\mu, \rho_i, \rho_a) = 0 . \end{aligned} \quad (3c)$$

### **Expansion of characteristic equation with Grigoryan's method:**

We generalise the mode formulation (1) by symbolic writing  $f_\mu(k_r r)$ ,  $g_\mu(k_r r)$  for the radial functions, instead of Bessel and Neumann functions as in (1). These functions may also be the Hankel functions of both kinds or Bessel functions with positive and negative non-integer orders  $\mu$ :

$$\begin{aligned} p_\mu(r, \varphi, z) &= (f_\mu(k_r r) + \beta g_\mu(k_r r)) e^{-j\mu\varphi} e^{-\Gamma z} ; \quad \Gamma^2 = k_r^2 - k_0^2 , \\ Z_0 v_{\mu r}(r, \varphi, z) &= j \frac{k_r}{k_0} \frac{\partial p}{\partial(k_r r)} = j \frac{k_r}{k_0} (f'_\mu(k_r r) + \beta g'_\mu(k_r r)) e^{-j\mu\varphi} e^{-\Gamma z} . \end{aligned} \quad (5)$$

The radial functions  $f_\mu(k_r r) = f_\mu(\rho)$  and  $g_\mu(k_r r) = g_\mu(\rho)$  satisfy the Bessel differential equations:

$$\begin{aligned} \rho^2 f''_\mu + \rho f'_\mu + (\rho^2 - \mu^2) f_\mu &\equiv 0 , \\ \rho^2 g''_\mu + \rho g'_\mu + (\rho^2 - \mu^2) g_\mu &\equiv 0 , \end{aligned} \quad (6)$$

and have a non-zero Wronski determinant  $W(f_\mu, g_\mu) = f_\mu g'_\mu - f'_\mu g_\mu$ . The boundary conditions at the locally absorbing walls at  $r = r_{i,a}$ :

$$\frac{Z_0 v_{\mu r}(r_{i,a}, \varphi, z)}{p_\mu(r_{i,a}, \varphi, z)} = j \frac{f'_\mu(k_r r_{i,a}) + \beta g'_\mu(k_r r_{i,a})}{f_\mu(k_r r_{i,a}) + g_\mu(k_r r_{i,a})} = \mp \frac{k_0}{k_r} Z_0 G_{i,a} \quad (7)$$

lead with the abbreviations  $k_r r_{i,a} = \rho_{i,a}$ ;  $k_0 r_{i,a} Z_0 G_{i,a} = U_{i,a}$ ;  $\lambda = r_i/r_a$  to the characteristic equation (3c) in which the determinants are now:

$$D_{n,m}(\mu, \rho_i, \rho_a) := \begin{vmatrix} f_\mu^{(n)}(\rho_i) & f_\mu^{(m)}(\rho_a) \\ g_\mu^{(n)}(\rho_i) & g_\mu^{(m)}(\rho_a) \end{vmatrix} ; \quad (n), (m) \in (0), (1) . \quad (8)$$

We perform a Taylor series expansion of the first column around  $\rho_a$  in the variable  $\xi = (\rho - \rho_a)$  having the special value  $x = (\rho_a - \rho_i) = \rho_a(1 - \lambda)$ :

$$\begin{aligned} D_{n,m}(\mu, \rho_i, \rho_a) &= \begin{vmatrix} \sum_{k \geq 0} \frac{(-1)^k}{k!} f_\mu^{(n+k)}(\rho_a) \cdot x^k & f_\mu^{(m)}(\rho_a) \\ \sum_{k \geq 0} \frac{(-1)^k}{k!} g_\mu^{(n+k)}(\rho_a) \cdot x^k & g_\mu^{(m)}(\rho_a) \end{vmatrix} \\ &= \sum_{k \geq 0} \frac{(-1)^k}{k!} \begin{vmatrix} f_\mu^{(n+k)}(\rho_a) & f_\mu^{(m)}(\rho_a) \\ g_\mu^{(n+k)}(\rho_a) & g_\mu^{(m)}(\rho_a) \end{vmatrix} \cdot x^k \\ &= \sum_{k \geq 0} \frac{(-1)^k}{k!} B_{n+k,m}(\mu, \rho_a) \cdot x^k . \end{aligned} \quad (9)$$

This defines the coefficient determinants  $B_{v,m}$ :

$$B_{v,m}(\mu, \rho) = \begin{vmatrix} f_\mu^{(v)}(\rho) & f_\mu^{(m)}(\rho) \\ g_\mu^{(v)}(\rho) & g_\mu^{(m)}(\rho) \end{vmatrix} . \quad (10)$$

For their evaluation, one writes down the  $v$ -th derivative of the Bessel differential equation (6), e.g. for  $f(\rho)$ :

$$\begin{aligned}
 & \partial^v (\rho^2 f'' + \rho f' + (\rho^2 - \mu^2) f) / \partial \rho^v \\
 &= v \cdot (v-1) f^{(v-2)}(\rho) + 2v\rho f^{(v-1)}(\rho) + (v^2 - \mu^2 + \rho^2) f^{(v)}(\rho) \\
 &\quad + (2v+1)\rho f^{(v+1)}(\rho) + \rho^2 f^{(v+2)}(\rho) \\
 &\xrightarrow[v=0]{} (-\mu^2 + \rho^2) f^{(0)}(\rho) + \rho f^{(1)}(\rho) + \rho^2 f^{(2)}(\rho) \\
 &\xrightarrow[v=1]{} 2\rho f^{(0)}(\rho) + (1 - \mu^2 + \rho^2) f^{(1)}(\rho) + 3\rho f^{(2)}(\rho) + \rho^2 f^{(3)}(\rho) \\
 &\xrightarrow[v=2]{} 2 f^{(0)}(\rho) + 4\rho f^{(1)}(\rho) + (4 - \mu^2 + \rho^2) f^{(2)}(\rho) + 5\rho f^{(3)}(\rho) + \rho^2 f^{(4)}(\rho) \\
 &\xrightarrow[v=3]{} 6 f^{(1)}(\rho) + 6\rho f^{(2)}(\rho) + (9 - \mu^2 + \rho^2) f^{(3)}(\rho) + 7\rho f^{(4)}(\rho) + \rho^2 f^{(5)}(\rho) \\
 &\xrightarrow[v=4]{} 12 f^{(2)}(\rho) + 8\rho f^{(3)}(\rho) + (16 - \mu^2 + \rho^2) f^{(4)}(\rho) + 9\rho f^{(5)}(\rho) + \rho^2 f^{(6)}(\rho).
 \end{aligned} \tag{11}$$

These expressions are used for the cross-product:

$$g^{(m)} \cdot \partial^v (\rho^2 f'' + \rho f' + (\rho^2 - \mu^2) f) / \partial \rho^v - f^{(m)} \cdot \partial^v (\rho^2 g'' + \rho g' + (\rho^2 - \mu^2) g) / \partial \rho^v \tag{12a}$$

together with the coefficient determinants  $B_{v,m}(\mu, \rho)$ :

$$\begin{aligned}
 & g^{(m)} \cdot \partial^v (\rho^2 f'' + \rho f' + (\rho^2 - \mu^2) f) / \partial \rho^v - f^{(m)} \cdot \partial^v (\rho^2 g'' + \rho g' + (\rho^2 - \mu^2) g) / \partial \rho^v \\
 &= v \cdot (v-1) B_{v-2,m}(\mu, \rho) + 2v\rho B_{v-1,m}(\mu, \rho) + (v^2 - \mu^2 + \rho^2) B_{v,m}(\mu, \rho) \\
 &\quad + (2v+1)\rho B_{v+1,m}(\mu, \rho) + \rho^2 B_{v+2,m}(\mu, \rho).
 \end{aligned} \tag{12b}$$

For  $v = 0$  both leading terms vanish; for  $v = 1$  the first term is zero. The sum (12b) must vanish identically; therefore (12b) represents an iteration for  $B_{v,m}(\mu, \rho)$ ;  $v = 2, 3, 4, \dots$ :

$$\begin{aligned}
 B_{v,m}(\mu, \rho) &= - \left[ \frac{2v-3}{\rho} B_{v-1,m} + \frac{(v-2)^2 + \rho^2 - \mu^2}{\rho^2} B_{v-2,m} \right. \\
 &\quad \left. + \frac{2(v-2)}{\rho} B_{v-3,m} + \frac{(v-2)(v-3)}{\rho^2} B_{v-4,m} \right]; \quad \begin{cases} v = 2, 3, \dots \\ m = 0, 1 \end{cases} \\
 &\xrightarrow[v=2]{} B_{2,m}(\mu, \rho) = - \left[ \frac{1}{z} B_{1,m} + \frac{\rho^2 - \mu^2}{\rho^2} B_{0,m} \right] \\
 &\xrightarrow[v=3]{} B_{3,m}(\mu, \rho) = - \left[ \frac{3}{z} B_{2,m} + \frac{1 + \rho^2 - \mu^2}{\rho^2} B_{1,m} + \frac{2}{\rho} B_{0,m} \right] \\
 &\xrightarrow[v=4]{} B_{4,m}(\mu, \rho) = - \left[ \frac{5}{\rho} B_{3,m} + \frac{4 + \rho^2 - \mu^2}{\rho^2} B_{2,m} + \frac{4}{\rho} B_{1,m} + \frac{2}{\rho^2} B_{0,m} \right]
 \end{aligned} \tag{13}$$

and so on. The required starting values  $B_{0,m}$ ,  $B_{1,m}$  of the recursion follow from the identities  $B_{v,v} = 0$ ;  $B_{v,m} = -B_{m,v}$  and from the Wronski determinant  $W(f_\mu(\rho), g_\mu(\rho))$ :

$$\begin{aligned}
 B_{0,m}(\mu, \rho) &= \begin{cases} 0; & m = 0 \\ W(f_\mu(\rho), g_\mu(\rho)) & ; \quad m = 1 \end{cases}; \\
 B_{1,m}(\mu, \rho) &= \begin{cases} -W(f_\mu(\rho), g_\mu(\rho)) & ; \quad m = 0 \\ 0 & ; \quad m = 1 \end{cases}.
 \end{aligned} \tag{14}$$

The Wronski determinant is the point where the choice of the pair of functions  $f(\rho)$ ,  $g(\rho)$  enters into the evaluation:

$$W(J_\mu(\rho), Y_\mu(\rho)) = \frac{2}{\pi\rho} ; \quad W(H_\mu^{(1)}(\rho), H_\mu^{(2)}(\rho)) = -\frac{4j}{\pi\rho}. \quad (15)$$

In case of the function pair  $f_\mu(\rho) = J_\mu(\rho)$ ;  $g_\mu(\rho) = Y_\mu(\rho)$ : the initial terms of the iteration are:

$m = 0 :$

$$\begin{aligned} B_{00} &= 0 ; \quad B_{10} = -\frac{2}{\pi\rho} ; \quad B_{20} = \frac{2}{\pi\rho^2} ; \\ B_{30} &= \frac{2}{\pi\rho} \left( 1 - \frac{2 + \mu^2}{\rho^2} \right) ; \quad B_{40} = \frac{4}{\pi\rho^2} \left( -1 + \frac{3 + 3\mu^2}{\rho^2} \right) ; \end{aligned} \quad (16a)$$

$m = 1 :$

$$\begin{aligned} B_{01} &= \frac{2}{\pi\rho} ; \quad B_{11} = 0 ; \quad B_{21} = \frac{2}{\pi\rho} \left( -1 + \frac{\mu^2}{\rho^2} \right) ; \\ B_{31} &= \frac{2}{\pi\rho^2} \left( 1 - \frac{3\mu^2}{\rho^2} \right) ; \quad B_{41} = \frac{2}{\pi\rho} \left( 1 - \frac{3 + 2\mu^2}{\rho^2} + \frac{q^4 + 11\mu^2}{\rho^4} \right) . \end{aligned} \quad (16b)$$

Although the coefficients  $B_{v,m}(\mu, \rho_a)$  also contain odd powers of  $\rho_a$ , the characteristic equation is made up of even powers  $(\rho_a^2)^k$ ; so it is advisable to solve for  $(\rho_a^2)$ . Then polynomial solutions with  $\text{Im}(\rho_a^2) < 0$  can be rejected. Some of the polynomial solutions may produce large magnitudes  $|\text{char.eq}| > \text{lim}$  of the characteristic equation. They should be rejected if a limit of about  $\text{lim} \approx 80$  is exceeded if the polynomial solutions are used as starters for Muller's procedure (see Sect. J.4) when solving the characteristic equation; a direct use of polynomial solutions as mode solutions in further field evaluations may be possible for  $\text{lim} \leq 0.001$ . In the latter case the summation limit  $k_{hi}$  must be sufficiently high: about  $k_{hi} \approx (3 \text{ to } 4) \cdot k_0 r_a$  with larger values of  $k_0 r_a (> 4)$ , and  $k_{hi} \approx (12 \text{ to } 20)$  with small values of  $k_0 r_a$ . It is a principal disadvantage of Grigoryan's method that it is based on a Taylor series approximation (in (9)) which assumes small values of  $x = (\rho_a - \rho_i)$ . This drawback is avoided with the next method.

#### *Expansion of characteristic equation with theorem of multiplication of cylindrical functions:*

Let the couple of radial functions again be  $f_\mu(\rho) = J_\mu(\rho)$ ;  $g_\mu(\rho) = Y_\mu(\rho)$ . We start with the characteristic equation (3c) with the determinants in (4).

For any of the basic cylindrical functions  $C_\mu(\rho)$  (Bessel, Neumann, Hankel functions) and a factor  $\lambda$  in the argument with  $|\lambda^2 - 1| < 1$  the theorem of multiplication reads:

$$C_\mu(\lambda\rho) = \lambda^\mu \sum_{k \geq 0} (-1)^k \frac{(\lambda^2 - 1)^k \rho^k}{2^k k!} C_{\mu+k}(\rho), \quad (17)$$

and from this the derivative  $\partial/\partial(\lambda\rho) = (1/\lambda) \cdot \partial/\partial\rho$ :

$$C'_\mu(\lambda\rho) = \lambda^{\mu-1} \sum_{k \geq 0} (-1)^k \frac{(\lambda^2 - 1)^k}{2^k k!} \left[ k\rho^{k-1} C_{\mu+k}(\rho) + \rho^k C'_{\mu+k}(\rho) \right]. \quad (18)$$

This, when inserted in the determinant (4), gives:

$$\begin{aligned}
 D_{0,m}(\mu, \rho_i, \rho_a) &:= \begin{vmatrix} J_\mu(\lambda\rho_a) & J_\mu^{(m)}(\rho_a) \\ Y_\mu(\lambda\rho_a) & Y_\mu^{(m)}(\rho_a) \end{vmatrix} \\
 &= \lambda^\mu \sum_{k \geq 0} (-1)^k \frac{(\lambda^2 - 1)^k \rho_a^k}{2^k k!} \begin{vmatrix} J_{\mu+k}(\rho_a) & J_\mu^{(m)}(\rho_a) \\ Y_{\mu+k}(\rho_a) & Y_\mu^{(m)}(\rho_a) \end{vmatrix}; \\
 D_{1,m}(\mu, \rho_i, \rho_a) &:= \begin{vmatrix} J_\mu^{(1)}(\lambda\rho_a) & J_\mu^{(m)}(\rho_a) \\ Y_\mu^{(1)}(\lambda\rho_a) & Y_\mu^{(m)}(\rho_a) \end{vmatrix} \\
 &= \lambda^{\mu-1} \sum_{k \geq 0} (-1)^k \frac{(\lambda^2 - 1)^k}{2^k k!} \left[ k \rho_a^{k-1} \begin{vmatrix} J_{\mu+k}(\rho_a) & J_\mu^{(m)}(\rho_a) \\ Y_{\mu+k}(\rho_a) & Y_\mu^{(m)}(\rho_a) \end{vmatrix} \right. \\
 &\quad \left. + \rho_a^k \begin{vmatrix} J'_{\mu+k}(\rho_a) & J_\mu^{(m)}(\rho_a) \\ Y'_{\mu+k}(\rho_a) & Y_\mu^{(m)}(\rho_a) \end{vmatrix} \right].
 \end{aligned} \tag{19a,b}$$

We introduce the “subdeterminants”

$$\begin{vmatrix} J_{\mu+k}^{(n)}(\rho) & J_\mu^{(m)}(\rho) \\ Y_{\mu+k}^{(n)}(\rho) & Y_\mu^{(m)}(\rho) \end{vmatrix} =: d_{n,m}(\mu, k, \rho), \tag{20}$$

and obtain for the special cases (with the Wronski determinant  $W(J_\mu(\rho), Y_\mu(\rho))$ ):

$$n = 0; \quad k = 0 :$$

$$d_{0,m}(\mu, 0, \rho) = \begin{cases} 0; & m = 0 \\ W(J_\mu(\rho), Y_\mu(\rho)); & m = 1 \end{cases}; \tag{21a}$$

$$n = 1; \quad k = 0 :$$

$$d_{1,m}(\mu, 0, \rho) = \begin{cases} -W(J_\mu(\rho), Y_\mu(\rho)); & m = 0 \\ 0; & m = 1 \end{cases}. \tag{21b}$$

From there one gets, with the recursions for derivatives of cylindrical functions  $C_\mu(\rho)$ :

$$n = 0; \quad k = 1 :$$

$$C_{\mu+1}(\rho) = \frac{\mu}{z} C_\mu(\rho) - C'_\mu(\rho); \tag{21c}$$

$$d_{0,m}(\mu, 1, \rho) = \frac{\mu}{\rho} d_{0,m}(\mu, 0, \rho) - d_{1,m}(\mu, 0, \rho);$$

$$n = 1; \quad k = 1 :$$

$$C'_{\mu+1}(\rho) = C_\mu(\rho) - \frac{\mu+1}{\rho} C_{\mu+1}(\rho); \tag{21d}$$

$$d_{1,m}(\mu, 1, \rho) = d_{0,m}(\mu, 0, \rho) - \frac{\mu+1}{\rho} d_{0,m}(\mu, 1, \rho);$$

$$n = 0; \quad k + 1 :$$

$$C_{\mu+k+1}(\rho) = \frac{\mu+k}{\rho} C_{\mu+k}(\rho) - C'_{\mu+k}(\rho); \tag{21e}$$

$$d_{0,m}(\mu, k+1, \rho) = \frac{\mu+k}{\rho} d_{0,m}(\mu, k, \rho) - d_{1,m}(\mu, k, \rho);$$

$$n = 1 ; \quad k + 1 :$$

$$\begin{aligned} C'_{\mu+k+1}(\rho) &= C_{\mu+k}(\rho) - \frac{\mu+k+1}{\rho} C_{\mu+k+1}(\rho); \\ d_{1,m}(\mu, k+1, \rho) &= d_{0,m}(\mu, k, \rho) - \frac{\mu+k+1}{\rho} d_{0,m}(\mu, k+1, \rho). \end{aligned} \quad (21f)$$

Relations (21) show that the subdeterminants  $d_{n,m}(\mu, k, \rho)$  can be evaluated by recursion.

$$d_{n,m}(\mu, k+1, \rho) = \begin{cases} \frac{\mu+k}{\rho} d_{0,m}(\mu, k, \rho) - d_{1,m}(\mu, k, \rho) & ; \quad n = 0 \\ d_{0,m}(\mu, k, \rho) - \frac{\mu+k+1}{\rho} d_{0,m}(\mu, k+1, \rho) & ; \quad n = 1 \\ k = 0, 1, 2, 3, \dots \end{cases}; \quad (22)$$

beginning at  $k = 1$  with:

$$d_{n,m}(\mu, 1, \rho) = \begin{cases} \frac{\mu}{\rho} d_{0,m}(\mu, 0, \rho) - d_{1,m}(\mu, 0, \rho) & ; \quad n = 0 \\ d_{0,m}(\mu, 0, \rho) - \frac{\mu+1}{\rho} d_{0,m}(\mu, 1, \rho) & ; \quad n = 1 \end{cases}; \quad (23)$$

and at  $k = 0$  with:

$$\begin{aligned} d_{n,m}(\mu, 0, \rho) &= \begin{cases} 0 & ; \quad m = 0 \\ W(J_\mu(\rho), Y_\mu(\rho)) & ; \quad m = 1 \quad ; \quad n = 0 \\ -W(J_\mu(\rho), Y_\mu(\rho)) & ; \quad m = 0 \quad ; \quad n = 1 \\ 0 & ; \quad m = 1 \end{cases} \\ &= \begin{cases} 0 & ; \quad m = 0 \\ 2/(\pi\rho) & ; \quad m = 1 \quad ; \quad n = 0 \\ -2/(\pi\rho) & ; \quad m = 0 \quad ; \quad n = 1 \\ 0 & ; \quad m = 1 \end{cases}. \end{aligned} \quad (24)$$

The main determinants (19a,b) then become:

$$\begin{aligned} D_{0,m}(\mu, \rho_i, \rho_a) &= \lambda^\mu \sum_{k \geq 0} (-1)^k \frac{(\lambda^2 - 1)^k \rho_a^k}{2^k k!} d_{0,m}(\mu, k, \rho_a); \\ D_{1,m}(\mu, \rho_i, \rho_a) &= \lambda^{\mu-1} \sum_{k \geq 0} (-1)^k \frac{(\lambda^2 - 1)^k}{2^k k!} \left[ k \rho_a^{k-1} d_{0,m}(\mu, k, \rho_a) \right. \\ &\quad \left. + \rho_a^k d_{1,m}(\mu, k, \rho_a) \right]. \end{aligned} \quad (25a,b)$$

With these the characteristic equation finally is:

$$\begin{aligned} \lambda^\mu \sum_{k \geq 0} (-1)^k \frac{(\lambda^2 - 1)^k \rho_a^k}{2^k k!} \{ [U_i \cdot U_a + j U_a k] d_{0,0}(\mu, k, \rho_a) \\ + \rho_a [k - j U_i] d_{0,1}(\mu, k, \rho_a) + j U_a \rho_a d_{1,0}(\mu, k, \rho_a) + \rho_a^2 d_{1,1}(\mu, k, \rho_a) \} = 0. \end{aligned} \quad (26)$$

The summation over  $k$  and the iteration of the  $d_{n,m}(\mu, k, \rho)$  in  $k$  may run in parallel. Special cases for different summation limits  $k_{hi}$  are:

$k_{hi} = 0$  :

$$-j\frac{2}{\pi} \{U_i + U_a\} = 0; \quad (27a)$$

$k_{hi} = 1$  :

$$\begin{aligned} -j\frac{2}{\pi} \{U_i + U_a\} \\ + \frac{(1 - \lambda^2)}{\pi} \{U_i \cdot U_a + jU_a + \mu(1 - jU_i) + \rho_a^2 - jU_a(\mu + 1) - \mu(\mu + 1)\} = 0; \end{aligned} \quad (27b)$$

$k_{hi} = 4$  :

$$-\frac{a}{\pi} \cdot \rho_a^4 + \frac{b}{\pi} \cdot \rho_a^2 - \frac{c}{\pi} = 0 \quad (27c)$$

with factor terms:

$$a = \frac{(1 - \lambda^2)^3}{24} + \frac{(1 - \lambda^2)^4}{192} (4 + 4\mu + j(U_i + U_a)), \quad (28a)$$

$$\begin{aligned} b = (1 - \lambda^2) + \frac{(1 - \lambda^2)^2}{4} (2\mu + j(U_i + U_a)) \\ + \frac{(1 - \lambda^2)^3}{24} (5\mu^2 + 4jU_i - U_a(U_i - 2j) + 3j\mu(U_a + U_i - 2j)) \\ + \frac{(1 - \lambda^2)^4}{48} (2 + \mu) (3\mu^2 + 3jU_i - U_a(U_i - j) + 2j\mu(U_a + U_i - 2j)), \end{aligned} \quad (28b)$$

$$\begin{aligned} c = 2j(U_i + U_a) + (1 - \lambda^2)(\mu + jU_i)(\mu + jU_a) \\ + \frac{(1 - \lambda^2)^2}{2} (1 + \mu)(\mu + jU_i)(\mu + jU_a) \\ + \frac{(1 - \lambda^2)^3}{6} (2 + 3\mu + \mu^2)(\mu + jU_i)(\mu + jU_a) \\ + \frac{(1 - \lambda^2)^4}{24} (6 + 11\mu + 6\mu^2 + \mu^3)(\mu + jU_i)(\mu + jU_a). \end{aligned} \quad (28c)$$

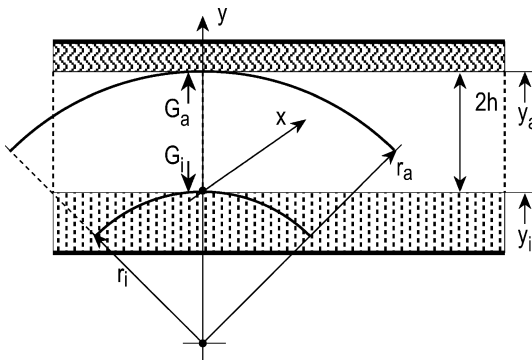
One obtains even-order polynomials in  $(\rho_a^2)$ ; the rank is  $(\rho_a^2)^{khi/2}$ . The odd powers which appear in the subdeterminants cancel each other during the combination to the characteristic equation.

This procedure requires no transcendental functions. The coefficients of the powers of  $(\rho_a^2)$  in the polynomial approximation of the characteristic equation are of moderate magnitudes. The polynomial solutions can be used as starters for *Muller's procedure* up to about  $\text{Re}(\rho_a) = k_{hi}$ . This procedure computes slower than *Grigoryan's procedure*; however, it returns for equal  $k_{hi}$  more useable approximations, and it is not so sensitive to large  $\rho_a$  as *Grigoryan's procedure*. A reasonable point of transition from *Grigoryan's procedure* to the present procedure may be at about  $|\rho_a| \approx 2$ .

### J.43 Mode Sets in Annular Ducts via Mode Sets in Flat Ducts with Unsymmetrical Lining

► See also: Mechel (2006)

The problem in the numerical evaluation of mode sets in annular ducts consists in finding reliable starters for Muller's procedure in solving the characteristic equation. Under the conditions of narrow ring width, i. e.  $\lambda = r_i/r_a > 0.75$ , and not too small  $k_0 r_a$ , i. e.  $k_0 r_a > 10$ , a fast computing method for finding reliable starters makes use of the similarity of transversal mode profiles in "equivalent" annular and flat ducts.



This sketch makes plausible that an annular duct defines an equivalent flat duct; however, several annular ducts (with different radii) may have the same equivalent flat duct. Therefore the equivalence will be best for large radii and small gap widths.

Geometrical equivalences are, with the notations from the previous sections for annular ducts:

$$h = (r_a - r_i)/2 = r_a(1 - \lambda)/2 ; \quad k_0 h = k_0 r_a(1 - \lambda)/2 ; \quad k_0 r_a = \frac{2k_0 h}{(1 - \lambda)}, \quad (1)$$

from which follow the correspondences of modal quantities in annular ducts and in unsymmetrical flat ducts:

$$k_r r_a - k_r r_i = k_r(r_a - r_i) = \rho_a - \rho_i = \rho_a(1 - \lambda) \stackrel{\wedge}{=} \varepsilon(r_a - r_i) = \varepsilon 2h = \eta_a , \quad (2)$$

$$\rho_a \stackrel{\wedge}{=} \frac{\eta_a}{1 - \lambda} .$$

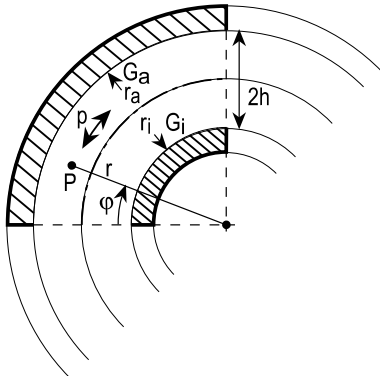
The procedure works well under the mentioned conditions.

### J.44 Bent, Flat Ducts with Locally Reacting Lining

► See also: Mechel (2006); Grigoryan (1969)

The objects of this section are modes in circularly bent, lined ducts running in the azimuthal direction (*bow modes*). The free duct cross-section is between the inner and outer radii  $r_i, r_a$ ; it is unlimited in the  $z$  direction (or the mode fields are constant in the

$z$  direction). The linings at the duct walls are defined by (radial) wall admittances  $G_i$ ,  $G_a$ . Generally the admittances are different from each other (due to the different radii), though the construction of the linings may be similar. The duct is anechoic in the  $\varphi$  direction.



A general formulation of a mode in the cylindrical co-ordinate system  $\{r, \varphi, z\}$  is composed of factor functions:

$$p(r, \varphi, z, t) = R(r) \cdot Z(z) \cdot \Phi(\varphi) \cdot e^{+j\omega t} \quad (1)$$

with radial functions like:

$$\begin{aligned} R(r) &= H_\mu^{(1)}(k_r r) + \beta H_\mu^{(2)}(k_r r) \\ &= J_\mu(k_r r) + \beta Y_\mu(k_r r) \quad \text{solutions of } \frac{\partial^2 R}{\partial r^2} + \frac{1}{r} \frac{\partial R}{\partial r} + \left( k_r^2 - \frac{\mu^2}{r^2} \right) R = 0, \\ &= J_\mu(k_r r) + \beta J_{-\mu}(k_r r) \end{aligned} \quad (2)$$

and lateral functions like:

$$\begin{aligned} Z(z) &= \gamma_1 e^{jk_z z} + \gamma_2 e^{-jk_z z} \\ &= \gamma_1 \cos(k_z z) + \gamma_2 \sin(k_z z) \quad \text{solutions of } \frac{\partial^2 Z}{\partial z^2} + k_z^2 Z = 0. \end{aligned} \quad (3)$$

$$\text{Both parts are connected by the secular equation: } k_0^2 = k_r^2 + k_z^2. \quad (4)$$

The mode also has azimuthal functions like:

$$\begin{aligned} \Phi(\varphi) &= \varepsilon_1 e^{+j\mu\varphi} + \varepsilon_2 e^{-j\mu\varphi} \\ &= \varepsilon_1 \sin(\mu\varphi) + \varepsilon_2 \cos(\mu\varphi) \quad \text{solutions of } \frac{\partial^2 \Phi}{\partial \varphi^2} + \mu^2 \Phi = 0. \end{aligned} \quad (5)$$

The assumedly constant profile in the  $z$  direction is obtained in the special case  $k_z = 0$ ;  $\gamma_1 = 1$ ;  $\gamma_2 = 0$  in (3), and the anechoic terminations in the  $\varphi$  direction may be represented by  $\varepsilon_1 = 0$ ;  $\varepsilon_2 = 1$  in (5), and with  $\operatorname{Re}(\mu) \geq 0$ ,  $\operatorname{Im}(\mu) \leq 0$  the mode, propagating in  $+ \varphi$  direction, obeys the far field condition. The modes  $p_\mu(r, \varphi)$  considered further have the form:

$$\begin{aligned} p_\mu(r, \varphi) &= R(r) \cdot \Phi(\varphi) = (J_\mu(k_r r) + \beta Y_\mu(k_r r)) e^{-j\mu\varphi}, \\ Z_0 v_{\mu r}(r, \varphi) &= j \frac{k_r}{k_0} \frac{\partial p}{\partial (k_r r)} = j \frac{k_r}{k_0} (J'_\mu(k_r r) + \beta Y'_\mu(k_r r)) e^{-j\mu\varphi}. \end{aligned} \quad (6)$$

The boundary conditions at the walls at  $r_i, r_a$  are for given (radial) admittance values  $G_i, G_a$  of the locally reacting walls:

$$\frac{Z_0 v_{\mu r}(r_{i,a}, \varphi, z)}{p_{\mu}(r_{i,a}, \varphi, z)} = j \frac{J'_{\mu}(k_r r_{i,a}) + \beta Y'_{\mu}(k_r r_{i,a})}{J_{\mu}(k_r r_{i,a}) + \beta Y_{\mu}(k_r r_{i,a})} \stackrel{!}{=} \mp \frac{k_0}{k_r} Z_0 G_{i,a}. \quad (7)$$

The coefficient  $\beta$  must be identical in both of them; thus, eliminating  $\beta$  gives the following characteristic equation for the indices  $\mu$  of the modes:

$$\begin{aligned} & \left( \frac{k_0}{k_r} Z_0 G_i J_{\mu}(k_r r_i) + j J'_{\mu}(k_r r_i) \right) \cdot \left( \frac{k_0}{k_r} Z_0 G_a Y_{\mu}(k_r r_a) - j Y'_{\mu}(k_r r_a) \right) \\ & - \left( \frac{k_0}{k_r} Z_0 G_i Y_{\mu}(k_r r_i) + j Y'_{\mu}(k_r r_i) \right) \cdot \left( \frac{k_0}{k_r} Z_0 G_a J_{\mu}(k_r r_a) - j J'_{\mu}(k_r r_a) \right) = 0. \end{aligned} \quad (8a)$$

It has a formal similarity with the characteristic equation for modes propagating in the  $z$  direction in annular ducts (see previous sections), so some transformations may be similar also, but the unknown mode number here is  $\mu$ , whereas it is  $k_r$  in annular ducts.

Define the non-dimensional quantities:  $k_r r_{i,a} \rightarrow \rho_{i,a}$ ;  $k_0 r_{i,a} \cdot Z_0 G_{i,a} \rightarrow U_{i,a}$ ;  $\lambda = r_i/r_a < 1$  with  $\rho_i = \lambda \cdot \rho_a$ .

The characteristic equation (8a) can be transformed into:

$$\begin{aligned} & \rho_i \cdot \rho_a \begin{vmatrix} J'_{\mu}(\rho_i) & J'_{\mu}(\rho_a) \\ Y'_{\mu}(\rho_i) & Y'_{\mu}(\rho_a) \end{vmatrix} - j \rho_a U_i \begin{vmatrix} J_{\mu}(\rho_i) & J'_{\mu}(\rho_a) \\ Y_{\mu}(\rho_i) & Y'_{\mu}(\rho_a) \end{vmatrix} \\ & + j \rho_i U_a \begin{vmatrix} J'_{\mu}(\rho_i) & J_{\mu}(\rho_a) \\ Y'_{\mu}(\rho_i) & Y_{\mu}(\rho_a) \end{vmatrix} + U_i \cdot U_a \begin{vmatrix} J_{\mu}(\rho_i) & J_{\mu}(\rho_a) \\ Y_{\mu}(\rho_i) & Y_{\mu}(\rho_a) \end{vmatrix} = 0, \end{aligned} \quad (8b)$$

or, with the determinants in it, written:

$$D_{n,m}(\mu, \rho_i, \rho_a) := \begin{vmatrix} J_{\mu}^{(n)}(\rho_i) & J_{\mu}^{(m)}(\rho_a) \\ Y_{\mu}^{(n)}(\rho_i) & Y_{\mu}^{(m)}(\rho_a) \end{vmatrix}; \quad (n), (m) \in (0), (1), \quad (9)$$

in which  $(n), (m) \in (0), (1)$  are orders of derivatives; the characteristic equation may then be written as

$$\begin{aligned} & \rho_i \rho_a D_{1,1}(\mu, \rho_i, \rho_a) - j \rho_a U_i D_{0,1}(\mu, \rho_i, \rho_a) \\ & + j \rho_i U_a D_{1,0}(\mu, \rho_i, \rho_a) + U_i \cdot U_a D_{0,0}(\mu, \rho_i, \rho_a) = 0. \end{aligned} \quad (8c)$$

The coefficient determinants in this equation, when nullified individually, represent the characteristic equations for the special cases of the bow duct with ideally reflecting walls:

- first determinant = 0: inner and outer walls hard; denoted h-h;
- second determinant = 0: inner wall soft, outer wall hard; denoted w-h;
- third determinant = 0: inner wall hard, outer wall soft; denoted h-w;
- fourth determinant = 0: inner and outer walls soft; denoted w-w.

Thus, these special cases are singularities of the general equation. This may become important in solution methods which start with known solutions in hard bow ducts and then proceed iteratively to absorbing walls because the evaluation may approach such singularities during the iteration.

Of some practical interest may be cases of bow ducts with one wall hard and the other wall absorbing. If the *outer wall at  $r_a$  is hard*, i.e.,  $U_a = 0$ , then the characteristic equation is:

$$\begin{aligned} \rho_i \cdot \rho_a & \left( J'_\mu(\rho_i) \cdot Y'_\mu(\rho_a) - Y'_\mu(\rho_i) \cdot J'_\mu(\rho_a) \right) \\ & - j\rho_a U_i \left( J_\mu(\rho_i) \cdot Y'_\mu(\rho_a) - Y_\mu(\rho_i) \cdot J'_\mu(\rho_a) \right) = 0. \end{aligned} \quad (9a)$$

If the *inner wall at  $r_i$  is hard*, i.e.,  $U_i = 0$ , then:

$$\begin{aligned} \rho_i \cdot \rho_a & \left( J'_\mu(\rho_i) \cdot Y'_\mu(\rho_a) - Y'_\mu(\rho_i) \cdot J'_\mu(\rho_a) \right) \\ & + j\rho_i U_a \left( J'_\mu(\rho_i) \cdot Y_\mu(\rho_a) - Y'_\mu(\rho_i) \cdot J_\mu(\rho_a) \right) = 0. \end{aligned} \quad (9b)$$

One sees that a procedure for arriving at a solution of these equations which starts an iteration with real or imaginary solutions  $\mu$  in a double-sided hard duct will produce dramatic changes in  $\mu$  in its first step. So the procedure may fail.

Because, on the other hand, one may expect that the eigenvalues  $\mu$  of the "ideal" cases will bracket the eigenvalues of the lined bow duct anyway, and because some published approximations for mode solutions  $\mu$  in hard-walled or soft-walled ducts proved to be erroneous, we first consider some "ideal cases".

**Special case h-h:** hard walls at  $r_i$  and  $r_a$ :

With  $U_i = U_a = 0$  and  $\lambda = r_i/r_a < 1$ ;  $\rho_i = \lambda \cdot \rho_a$ , the equation for the eigenvalues  $\mu$  is:

$$J'_\mu(\lambda\rho_a)Y'_\mu(\rho_a) - J'_\mu(\rho_a)Y'_\mu(\lambda\rho_a) = 0, \quad (10a)$$

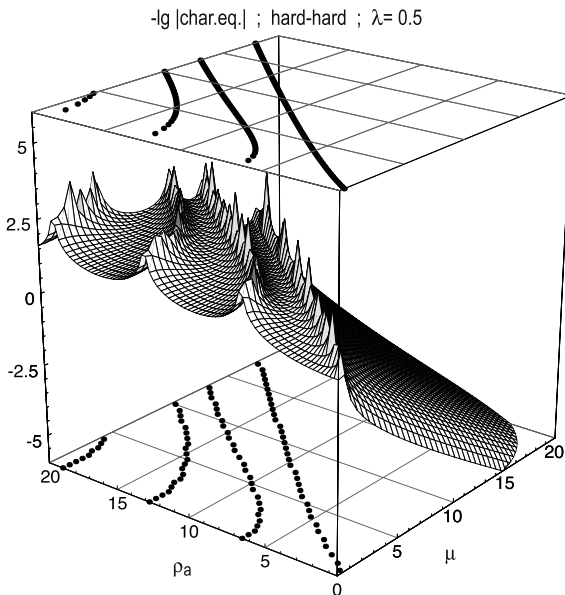
or, with the recursions for the derivatives of Bessel and Neumann functions:

$$\begin{aligned} & \left( \frac{\mu}{\lambda\rho_a} J_\mu(\lambda\rho_a) - J_{1+\mu}(\lambda\rho_a) \right) \left( \frac{\mu}{\rho_a} Y_\mu(\rho_a) - Y_{1+\mu}(\rho_a) \right) \\ & - \left( \frac{\mu}{\rho_a} J_\mu(\rho_a) - J_{1+\mu}(\rho_a) \right) \left( \frac{\mu}{\lambda\rho_a} Y_\mu(\lambda\rho_a) - Y_{1+\mu}(\lambda\rho_a) \right) = 0, \end{aligned} \quad (10b)$$

and the terms sorted for  $\mu$  and  $\mu^2$  are:

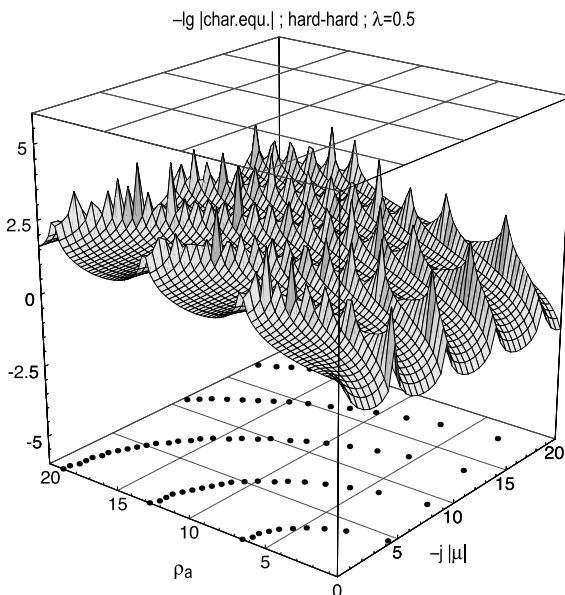
$$\begin{aligned} & \mu^2 [J_\mu(\rho_a) Y_\mu(\lambda\rho_a) - J_\mu(\lambda\rho_a) Y_\mu(\rho_a)] \\ & + \mu\rho_a [J_\mu(\lambda\rho_a) Y_{1+\mu}(\rho_a) - J_{1+\mu}(\rho_a) Y_\mu(\lambda\rho_a)] \\ & + \lambda [J_{1+\mu}(\lambda\rho_a) Y_\mu(\rho_a) - J_\mu(\rho_a) Y_{1+\mu}(\lambda\rho_a)] \\ & + \lambda\rho_a^2 [J_{1+\mu}(\rho_a) Y_{1+\mu}(\lambda\rho_a) - J_{1+\mu}(\lambda\rho_a) Y_{1+\mu}(\rho_a)] = 0. \end{aligned} \quad (10c)$$

The bracketed factor of  $\mu^2$  is just the characteristic equation for the double-sided soft-walled bow duct (w-w); thus, the solutions of the case w-w are pole positions of the characteristic equation for the hard-hard duct (h-h). An unambiguous survey of the positions of solutions may be obtained by plotting in a 3D plot the values of  $-\lg |\text{char.eq.}|$  over  $\rho_a$  and  $\mu$ , where  $\mu$  is either real or imaginary (both possibilities exist for solutions).



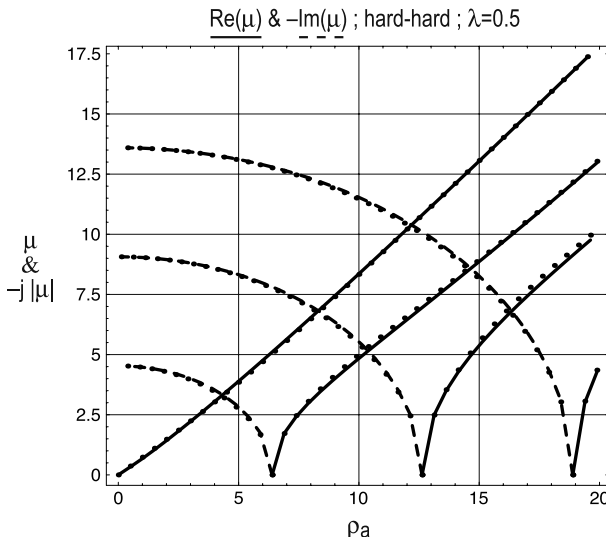
3D plot of  $-\lg |\text{char.eq.}|$  of characteristic equation for a bow duct with hard walls on both sides over  $p_a$  and real  $\mu$  for  $\lambda = r_i/r_a = 0.5$ . The positions of the maxima, which belong to solutions, are collected from the plot list in the floor surface of the enclosing cube; the ceiling surface contains the points after improvement by *Muller's procedure*

The next graph is similar to the plot above, but now for negative-imaginary  $\mu = -j|\mu|$ .



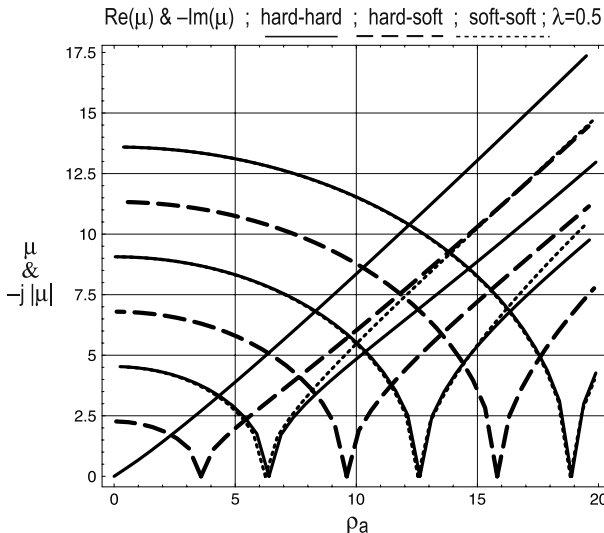
Similar plot as above, but now over negative imaginary values of  $\mu$

The next diagram combines both branches of solutions for real and negative imaginary values of  $\mu$ . The curves are from approximations (see below), the points are solutions after improvement by Muller's procedure.



Real and negative imaginary mode solutions  $\mu$  in a bow duct with hard walls on both sides, for  $\lambda = r_i/r_a = 0.5$ . Solid lines: real  $\mu$ ; dashed: negative imaginary  $\mu$ . Curves: from approximations; points: after improvement with Muller's procedure

The next graph is similar to the previous graph, but it combines, for  $\lambda = 0, 5$ , mode solutions  $\mu$  for bow ducts with two hard walls (h-h; solid lines), inner hard wall and outer soft wall (h-w; long dashes), and both walls soft (w-w; short dashes). The solutions for the w-w duct partly coincide with solutions for other configurations.



Real and negative imaginary mode solutions  $\mu$  in a bow duct with hard walls on both sides (solid), hard inner and soft outer wall (long dashes), soft walls on both sides (short dashes), for  $\lambda = r_i/r_a = 0.5$ . The lowest-order solution in the h-h duct has only a real branch

The parabolic branches of real solutions  $\mu$  in the above diagram belong to propagating modes; they will be numbered with a mode order index  $s = (0), 1, 2, \dots$  (left to right). The branch aiming at  $(\rho_a, \mu) = (0, 0)$  with the mode order  $s = 0$  exists only in the duct h-h with two hard walls; it represents there the fundamental mode. The elliptic branches of imaginary solutions  $\mu = -j|\mu|$  are numbered  $s = -1, -2, \dots$  (left to right); they belong to cut-off modes. The parameters  $\rho_a, \lambda$  must exceed some limit values (the values at the dips at  $\mu \rightarrow 0$  in the diagram) for the existence of higher propagating modes.

*Approximations to mode solutions  $\mu$  in bow ducts with ideally reflecting walls:*

*Duct h-h, both walls hard:*

Characteristic equation (10). Suitable Muller starters  $\mu \approx \{z_1, z_2, z_3\}$  for the real (parabolic) branches are:

$$\begin{aligned} s = 0: \{z_1, z_2, z_3\} &= \{\rho_x, 2\rho_x/(1 + \lambda) + 0.001, 2\rho_x/(1 + \lambda)\}; \quad \rho_x = 0.00001, \\ s > 0: \{z_1, z_2, z_3\} &= \{\rho_x + 0.1, \rho_x + 0.05, \rho_x\}; \quad \rho_x = \pi s/(1 - \lambda). \end{aligned} \quad (11)$$

The imaginary (elliptic) branches are approximated by quarter ellipses. The axes  $|\mu_0| = |\mu|(\rho_a \rightarrow 0, \lambda; s)$  are obtained from the development of the characteristic equation at  $\rho_a \rightarrow 0$ :

$$\begin{aligned} \text{char.eq.} \xrightarrow{\rho_a \rightarrow 0} \frac{-j|\mu|^2(\lambda^{2j|\mu|} - 1)}{\lambda^{1+j|\mu|} \sinh(|\mu|\pi) \Gamma(1 + j|\mu|) \Gamma(1 - j|\mu|)} \\ = \frac{2|\mu|}{\pi\lambda} \sin(|\mu| \ln(\lambda)). \end{aligned} \quad (12)$$

Solutions thereof with  $|\mu_0| \neq 0$  are  $|\mu_0| = -s\pi/\ln(\lambda)$  ;  $s = 1, 2, \dots$  . (13)

The other axes  $\rho_{a0}$  at  $\mu \rightarrow 0$  are the solutions  $\rho$  of  $J_1(\lambda\rho)Y_1(\rho) - J_1(\rho)Y_1(\lambda\rho) = 0$  from the literature or from mathematical computer programs, or they may be approximated by:

$$\rho_{a0} \approx \begin{cases} \frac{\delta}{1+\lambda} ; & \delta \approx 10^{-3} ; \\ \frac{\pi s}{1-\lambda} + \frac{3(1-\lambda)}{8\pi s \lambda} ; & s > 0 \end{cases} . \quad (14)$$

Thus, the quarter elliptic arcs for  $\mu = -j \cdot |\mu|$  are given by:

$$|\mu| = |\mu_0| \sqrt{1 - (\rho_a/\rho_{a0})^2} \quad \begin{cases} |\mu_0| = |\mu_0|(\lambda, s) = -s\pi/\ln(\lambda) \\ \rho_{a0} = \rho_{a0}(\lambda, s) \end{cases} ;$$

$$\begin{cases} s = 1, 2, 3, \dots \\ 0 < \lambda < 1; \quad 0 < \rho_a \leq \rho_{a0} \end{cases} . \quad (15)$$

For small  $\rho_a$  ( $< 4$ ) and not too small  $\lambda = \rho_i/\rho_a = r_i/r_a$  the parabolic branches can be approximated with the positive real approximations:

$$\mu^2 \approx \left\{ (77 - 10\rho_a^2) - \lambda(137 - 26\rho_a^2) + \lambda^2(97 - 22\rho_a^2) - \lambda^3(25 - 6\rho_a^2) \right. \\ \left. - \left[ 4(1-\lambda)^2(7-5\lambda)\rho_a^2 \right. \right. \\ \left. \cdot ((30-3\rho_a^2) - \lambda(36-7\rho_a^2) + \lambda^2(24-5\rho_a^2) - \lambda^3(6-\rho_a^2)) \right. \\ \left. + ((77-10\rho_a^2) - \lambda(137-26\rho_a^2) + \lambda^2(97-22\rho_a^2) - \lambda^3(25-6\rho_a^2))^2 \right]^{1/2} \right\} \\ / (2(5\lambda-7)(\lambda-1)^2) . \quad (16)$$

The approximations should be used as "Muller starters" for the numerical solution of the characteristic equation (10).

*Duct h-w, inner wall hard, outer wall soft:*

Characteristic equation:

$$J'_\mu(\lambda\rho_a)Y_\mu(\rho_a) - J_\mu(\rho_a)Y'_\mu(\lambda\rho_a) = 0 ; \quad \lambda < 1 . \quad (17)$$

The limit values  $\rho_{a0} = \rho_a(\mu \rightarrow 0; \lambda, s)$  (for the dip points on the  $\rho_a$  axis) may be approximated by:

$$\rho_{a0} \approx \frac{\pi(s-1/2)}{1-\lambda} + \frac{3+\lambda}{4\pi\lambda(2s-1)} ; \quad s = 1, 2, \dots , \quad (18)$$

and the limit values  $|\mu_0| = |\mu|(\rho_a \rightarrow 0, \lambda; s)$  (on the  $\mu$  axis) for the branches of cut-off modes are obtained by series expansion in  $\rho_a$  of Eq. (17) and nullifying the  $\rho_a$ -free term:

$$\text{char. eq.} \approx \frac{(1 + \lambda^{2j}|\mu|)}{\pi\lambda^{j|\mu|}} = \frac{(\lambda^{j|\mu|} + \lambda^{-j|\mu|})}{\pi} \\ = \frac{2}{\pi} \cos\left(\frac{|\mu| \ln(\lambda^2)}{2}\right) = \frac{2}{\pi} \cos(|\mu| \ln(\lambda)) \stackrel{!}{\approx} 0 \quad (19)$$

$$\text{with solutions } |\mu_0| = \frac{-(2s-1)\pi/2}{\ln(\lambda)} ; \quad s = 1, 2, 3, \dots . \quad (20)$$

The branches of the cut-off modes with imaginary  $\mu$  are approximated by quarter ellipses:

$$|\mu| = |\mu_0| \sqrt{1 - (\rho_a/\rho_{a0})^2} ; \quad \begin{cases} s = 1, 2, 3, \dots \\ 0 < \lambda < 1 ; \quad 0 < \rho_a \leq \rho_{a0} \end{cases} . \quad (21)$$

The parabolic branches of the propagating modes may be approximated for low  $\rho_a$  ( $< 5$ ) and not too small  $\lambda$  by positive real values of:

$$\begin{aligned} \mu^2 \approx & \left\{ (580 - 28\rho_a^2) - \lambda(1145 - 74\rho_a^2) + \lambda^2(850 - 64\rho_a^2) - 9\lambda^3(25 - 2\rho_a^2) \right. \\ & - [16(17425 - 1190\rho_a^2 + 9\rho_a^4) - 8\lambda(142625 - 12035\rho_a^2 + 108\rho_a^4) \\ & + 15\lambda^2(133135 - 13400\rho_a^2 + 144\rho_a^4) - 20\lambda^3(95975 - 11092\rho_a^2 + 144\rho_a^4) \\ & + 10\lambda^4(107215 - 13672\rho_a^2 + 216\rho_a^4) - 12\lambda^5(27475 - 3730\rho_a^2 + 72\rho_a^4) \\ & \left. + 9\lambda^6(4825 - 680\rho_a^2 + 16\rho_a^4) \right]^{1/2} \Big\} / (10(3\lambda - 4)(\lambda - 1)^2) . \end{aligned} \quad (22)$$

### Duct w-w, both walls soft:

The characteristic equation is:

$$J_\mu(\lambda\rho_a)Y_\mu(\rho_a) - J_\mu(\rho_a)Y_\mu(\lambda\rho_a) = 0 ; \quad \lambda < 1 . \quad (23)$$

The limit values  $\rho_{a0} = \rho_a(\mu \rightarrow 0, \lambda; s)$  on the  $\rho_a$  axis may be obtained from published solutions of Eq. (23) in the special case  $\mu = 0$ , or from the approximation (they get better the larger are  $s$  and  $\lambda$ ):

$$\rho_{a0}(s) \approx \begin{cases} \frac{s\pi}{1-\lambda} ; & \lambda \leq 0.05 \\ \frac{s\pi}{1-\lambda} - \frac{1-\lambda}{8s\pi\lambda} & ; \quad s = 1, 2, \dots . \end{cases} \quad (24)$$

The limit solutions  $\mu_0$  for  $\rho_a \rightarrow 0$  are obtained from the  $\rho_a$ -free term of the series expansion of Eq. (23):

$$\text{char.eq.} \approx j \frac{-1 + \lambda^{2j|\mu|}}{|\mu|\pi\lambda^{j|\mu|}} = j \frac{\lambda^{j|\mu|} - \lambda^{-j|\mu|}}{|\mu|\pi} = -2 \frac{\sin(|\mu|\ln\lambda)}{|\mu|\pi} \stackrel{!}{=} 0 \quad (25)$$

with solutions

$$|\mu_0| = -s\pi/\ln\lambda ; \quad s = 1, 2, \dots ; \quad 0 < \lambda < 1 . \quad (26)$$

The elliptic branches of the cut-off modes with imaginary  $\mu$  can be approximated with elliptic arcs (21) using (24) and (26). The parabolic branches for propagating modes can be approximated for small  $\rho_a$  ( $< 6$ ) and not too small  $\lambda$  by positive real values of:

$$\begin{aligned} \mu^2 \approx & \left\{ (245 - 10\rho_a^2) - \lambda(425 - 26\rho_a^2) + \lambda^2(295 - 22\rho_a^2) - \lambda^3(75 - 6\rho_a^2) \right. \\ & - [(43561 - 2520\rho_a^2 + 16\rho_a^4) - 2\lambda(86317 - 6256\rho_a^2 + 48\rho_a^4) \\ & + \lambda^2(281591 - 25528\rho_a^2 + 240\rho_a^4) - 4\lambda^3(62571 - 6848\rho_a^2 + 80\rho_a^4) \\ & + \lambda^4(130791 - 16328\rho_a^2 + 240\rho_a^4) - \lambda^5(38170 - 5152\rho_a^2 + 96\rho_a^4) \\ & \left. + \lambda^6(4825 - 680\rho_a^2 + 16\rho_a^4) \right\}^{1/2} / (2(5\lambda - 7)(\lambda - 1)^2). \end{aligned} \quad (27)$$

*Sets of mode solutions  $\mu$  in bow ducts with locally reacting wall linings:*

#### *Grigoryan's method:*

The modes are formulated as in Eq. (6). They satisfy the boundary conditions at the walls in (7). We still use the non-dimensional quantities  $k_r r_{i,a} \rightarrow \rho_{i,a}$ ;  $k_0 r_{i,a} \cdot Z_0 G_{i,a} \rightarrow U_{i,a}$ ;  $\lambda = r_i/r_a < 1$  with  $\rho_i = \lambda \cdot \rho_a$ . The characteristic equation for mode eigenvalues  $\mu$  then assumes the form of (8c) with the determinants  $D_{n,m}(\mu, \rho_i, \rho_a)$  defined in (9), where  $(n, m) \in (0, 1)$  are orders of derivatives.

A Taylor series expansion with the centre at  $\rho_a$  and the new variable  $x = \rho_a - \rho_i = \rho_a(1-\lambda)$  is applied on the first column (with variable  $\rho_i$ ) of the  $D_{n,m}(\mu, \rho_i, \rho_a)$ , which defines coefficient determinants  $B_{v,m}(\mu, \rho_a)$ ;  $v = n + k$ :

$$\begin{aligned} D_{n,m}(\mu, \rho_i, \rho_a) &= \sum_{k \geq 0} \frac{(-1)^k}{k!} \begin{vmatrix} J_\mu^{(n+k)}(\rho_a) & J_\mu^{(m)}(\rho_a) \\ Y_\mu^{(n+k)}(\rho_a) & Y_\mu^{(m)}(\rho_a) \end{vmatrix} \cdot x^k \\ &= \sum_{k \geq 0} \frac{(-1)^k}{k!} B_{n+k,m}(\mu, \rho_a) \cdot x^k. \end{aligned} \quad (28)$$

The coefficient determinants can be evaluated by recursion, starting with  $B_{0,m}$  and  $B_{1,m}$ . One of the starters,  $B_{0,0} = 0$  or  $B_{1,1} = 0$ , is an identity; the other starters  $B_{0,1}$  or  $B_{1,0}$  are obtained from the Wronski determinant. The recursion is (with  $v = n + k$ ;  $k = 0, 1, 2, \dots$ ):

$$\begin{aligned} B_{v,m}(\mu, \rho_a) &= - \left[ \frac{2v-3}{\rho_a} B_{v-1,m} + \frac{(v-2)^2 + \rho_a^2 - \mu^2}{\rho_a^2} B_{v-2,m} \right. \\ &\quad \left. + \frac{2(v-2)}{\rho_a} B_{v-3,m} + \frac{(v-2)(v-3)}{\rho_a^2} B_{v-4,m} \right] \quad (29) \\ \xrightarrow{v=2} B_{2,m}(\mu, \rho_a) &= - \left[ \frac{1}{\rho_a} B_{1,m} + \frac{\rho_a^2 - \mu^2}{\rho_a^2} B_{0,m} \right] \\ \xrightarrow{v=3} B_{3,m}(\mu, \rho_a) &= - \left[ \frac{3}{\rho_a} B_{2,m} + \frac{1 + \rho_a^2 - \mu^2}{\rho_a^2} B_{1,m} + \frac{2}{\rho_a} B_{0,m} \right] \\ \xrightarrow{v=4} B_{4,m}(\mu, \rho_a) &= - \left[ \frac{5}{\rho_a} B_{3,m} + \frac{4 + \rho_a^2 - \mu^2}{\rho_a^2} B_{2,m} + \frac{4}{\rho_a} B_{1,m} + \frac{2}{\rho_a^2} B_{0,m} \right]. \end{aligned}$$

The initial members of the recursions are as follows:

for  $m = 0$ :

$$B_{00} = 0 ; \quad B_{10} = -\frac{2}{\pi\rho_a} ; \quad B_{20} = \frac{2}{\pi\rho_a^2} ; \quad B_{30} = \frac{2}{\pi\rho_a} \left( 1 - \frac{2 + \mu^2}{\rho_a^2} \right) ; \quad (30a)$$

$$B_{40} = \frac{4}{\pi\rho_a^2} \left( -1 + \frac{3 + 3\mu^2}{\rho_a^2} \right) ;$$

for  $m = 1$ :

$$B_{01} = \frac{2}{\pi\rho_a} ; \quad B_{11} = 0 ; \quad B_{21} = \frac{2}{\pi\rho_a} \left( -1 + \frac{\mu^2}{\rho_a^2} \right) ; \quad (30b)$$

$$B_{31} = \frac{2}{\pi\rho_a^2} \left( 1 - \frac{3\mu^2}{\rho_a^2} \right) ; \quad B_{41} = \frac{2}{\pi\rho_a} \left( 1 - \frac{3 + 2\mu^2}{\rho_a^2} + \frac{\mu^4 + 11\mu^2}{\rho_a^4} \right) .$$

After truncation of the sum in Eq. (28) at  $k_{hi}$  the characteristic equation (8c) becomes a polynomial equation in  $\mu^2$ . Numerical tests show that the summation limit should be  $k_{hi} > \rho_a$ , more precisely  $k_{hi} \approx 3\rho_a/2$  for large  $\rho_a$  but not smaller than about  $k_{hi} \approx 12$ . The degree of the polynomial in  $\mu^2$  will be near  $k_{hi}/2$ . If the limit  $k_{hi}$  is too low, solutions will be missed in the mode set; if  $k_{hi}$  is unnecessarily high, Muller's procedure will furnish duplicates. Polynomial approximations with  $\text{Re}(\mu) < 0$  and/or  $\text{Im}(\mu) > 0$  should be rejected. A principal drawback of the method comes from the Taylor series expansion with the variable  $x = \rho_a - \rho_i = \rho_a(1 - \lambda)$ , which prefers narrow ducts and/or low frequencies. This will be avoided in the next method of transformation into a polynomial equation which applies asymptotic expansions of the cylindrical functions.

### **Transformation with Hankel asymptotics:**

The mode form is again:

$$p_\mu(r, \varphi) = (J_\mu(k_r r) + \beta Y_\mu(k_r r)) e^{-j\mu\varphi}. \quad (31)$$

Abbreviations:  $\rho = k_r r$ ;  $k_r r_{i,a} = \rho_{i,a}$ ;  $k_0 r_{i,a} \cdot Z_0 G_{i,a} = U_{i,a}$ ;  $\lambda = r_i/r_a = \rho_i/\rho_a$ . The modes satisfy two boundary conditions:

$$\rho_{i,a} \left( J'_\mu(\rho_{i,a}) + \beta Y'_\mu(\rho_{i,a}) \right) = \pm j U_{i,a} \left( J_\mu(\rho_{i,a}) + \beta Y_\mu(\rho_{i,a}) \right) , \quad (32)$$

four recursions for derivatives of cylindrical functions:

$$J'_\mu(\rho_{i,a}) = J_{\mu-1}(\rho_{i,a}) - \frac{\mu}{\rho_{i,a}} J_\mu(\rho_{i,a}) ; \quad Y'_\mu(\rho_{i,a}) = -Y_{\mu+1}(\rho_{i,a}) + \frac{\mu}{\rho_{i,a}} Y_\mu(\rho_{i,a}) , \quad (33)$$

and two Wronski determinants:

$$J_\mu(\rho_{i,a}) Y'_\mu(\rho_{i,a}) - J'_\mu(\rho_{i,a}) Y_\mu(\rho_{i,a}) = 2/(\pi\rho_{i,a}) . \quad (34)$$

Eliminate from this system of eight equations the seven quantities:

$$\beta ; \quad J'_\mu(\rho_i) ; \quad J'_\mu(\rho_a) ; \quad Y'_\mu(\rho_i) ; \quad Y'_\mu(\rho_a) ; \quad Y_{\mu+1}(\rho_i) ; \quad Y_{\mu+1}(\rho_a) .$$

This gives the characteristic equation in the form:

$$\begin{aligned} J_\mu(\rho_a) & \left( \rho_a J_{\mu-1}(\rho_a) - (\mu - jU_a) J_\mu(\rho_a) \right) - J_\mu(\rho_i) \left( \rho_i J_{\mu-1}(\rho_i) \right. \\ & \left. - (\mu + jU_i) J_\mu(\rho_i) \right) + \frac{\pi}{2} \left( J_\mu(\rho_a) Y_\mu(\rho_i) - J_\mu(\rho_i) Y_\mu(\rho_a) \right) \\ & \cdot \left( \rho_i J_{\mu-1}(\rho_i) - (\mu + jU_i) J_\mu(\rho_i) \right) \left( \rho_a J_{\mu-1}(\rho_a) - (\mu - jU_a) J_\mu(\rho_a) \right) = 0. \end{aligned} \quad (35a)$$

Divide with  $J_\mu^2(\rho_a) \neq 0$  and introduce the well convergent continued fractions for ratios of Bessel functions:

$$\begin{aligned} F_\mu(z) &= z \frac{J_{\mu-1}(z)}{J_\mu(z)} \\ &= 2\mu - \frac{z^2}{2(\mu+1)-} \frac{z^2}{2(\mu+2)-} \frac{z^2}{2(\mu+3)-} \cdots \frac{z^2}{2(\mu+i_{hi})-} \end{aligned} \quad (36)$$

resulting in the form of the characteristic equation:

$$\begin{aligned} & (F_\mu(\rho_a) - (\mu - jU_a)) - \left( J_\mu(\rho_i)/J_\mu(\rho_a) \right)^2 (F_\mu(\rho_i) - (\mu + jU_i)) \\ & + \frac{\pi}{2} \left( J_\mu(\rho_i)/J_\mu(\rho_a) \right) \cdot \left( J_\mu(\rho_a) Y_\mu(\rho_i) - J_\mu(\rho_i) Y_\mu(\rho_a) \right) \\ & \cdot (F_\mu(\rho_a) - (\mu - jU_a)) (F_\mu(\rho_i) - (\mu + jU_i)) = 0. \end{aligned} \quad (35b)$$

The remaining Bessel and Neumann functions are substituted by their asymptotic series:

$$\begin{aligned} J_\mu(z) &= \sqrt{2/(\pi z)} [P_\mu(z) \cdot \cos(z - (\mu/2 + 1/4)\pi) - Q_\mu(z) \cdot \sin(z - (\mu/2 + 1/4)\pi)], \\ Y_\mu(z) &= \sqrt{2/(\pi z)} [P_\mu(z) \cdot \sin(z - (\mu/2 + 1/4)\pi) + Q_\mu(z) \cdot \cos(z - (\mu/2 + 1/4)\pi)] \end{aligned} \quad (37)$$

with the component series  $P(\mu, z) = P_\mu(z)$ ;  $Q(\mu, z) = Q_\mu(z)$ :

$$\begin{aligned} P(\mu, z) &= \sum_{k=0}^K (-1)^k \frac{(\mu, 2k)}{(2z)^{2k}} = \sum_{k_{\text{even}}=0}^K (-1)^{k/2} \cdot t_k, \\ Q(\mu, z) &= \sum_{k=0}^K (-1)^k \frac{(\mu, 2k+1)}{(2z)^{2k+1}} = \sum_{k_{\text{odd}}=1}^K (-1)^{(k-1)/2} \cdot t_k, \end{aligned} \quad (38)$$

where the Hankel symbols  $(\mu, v)$  and the terms  $t_k$  can be evaluated recursively:

$$\begin{aligned} (\mu, 0) &= 1; \quad (\mu, k) = \frac{4\mu^2 - (2k-1)^2}{4k} \cdot (\mu, k-1); \\ t_0 &= 1; \quad t_k = \frac{4\mu^2 - (2k-1)^2}{8k z} \cdot t_{k-1}. \end{aligned} \quad (39)$$

The fraction of Bessel functions in Eq. (35b) can be written (if  $\mu \neq$  odd integer) as:

$$\begin{aligned} \left( J_\mu(\rho_i)/J_\mu(\rho_a) \right) &= \frac{1}{\sqrt{\lambda}} \frac{[Q(\mu, \rho_i) (\cos \rho_i - \sin \rho_i) + P(\mu, \rho_i) (\cos \rho_i + \sin \rho_i)] + \dots}{[Q(\mu, \rho_a) (\cos \rho_a - \sin \rho_a) + P(\mu, \rho_a) (\cos \rho_a + \sin \rho_a)] + \dots} \\ & \dots + \tan(\mu\pi/2) [Q(\mu, \rho_i) (\cos \rho_i + \sin \rho_i) - P(\mu, \rho_i) (\cos \rho_i - \sin \rho_i)] \\ & \dots + \tan(\mu\pi/2) [Q(\mu, \rho_a) (\cos \rho_a + \sin \rho_a) - P(\mu, \rho_a) (\cos \rho_a - \sin \rho_a)]. \end{aligned} \quad (40)$$

Multiply  $\tan(\mu\pi/2)$  by the identity  $(\mu\pi/2)/(\mu\pi/2)$  and use for  $(\mu\pi/2) \cdot \tan(\mu\pi/2)$  the well convergent continued fraction:

$$z \cdot \tan z = \frac{z^2}{1 - \frac{z^2}{3 - \frac{z^2}{5 - \dots}}}. \quad (41)$$

In total, the terms  $(J_\mu(\rho_i)/J_\mu(\rho_a))$  in Eq. (35b) can be written as a fraction with polynomials of  $\mu$  in the numerator and denominator. Next one expands the cross product  $(J_\mu(\rho_a)Y_\mu(\rho_i) - J_\mu(\rho_i)Y_\mu(\rho_a))$  in Eq. (35b) to

$$\begin{aligned} & (J_\mu(\rho_a)Y_\mu(\rho_i) - J_\mu(\rho_i)Y_\mu(\rho_a)) \\ &= \frac{-2}{\pi\rho_a\sqrt{\lambda}} [P(\mu, \rho_i)(Q(\mu, \rho_a)\cos(\rho_a - \rho_i) + P(\mu, \rho_a)\sin(\rho_a - \rho_i)) \\ &\quad + Q(\mu, \rho_i)(Q(\mu, \rho_a)\sin(\rho_a - \rho_i) - P(\mu, \rho_a)\cos(\rho_a - \rho_i))]. \end{aligned} \quad (42)$$

This too can be expanded as a polynomial in  $\mu$ . Thus the characteristic equation can be substituted by a polynomial equation in  $\mu$ . This transformation here is more complicated than for the Grigoryan method; however, its advantage is an extension of range of  $\rho_a$  to large values.

#### *Transformation with Hankel asymptotics for modes with Hankel functions:*

Part of the complexity of the previous transformation can be avoided when the bow modes are formulated with Hankel functions:

$$p_\mu(r, \varphi) = \left( H_\mu^{(1)}(k_r r) + \beta H_\mu^{(2)}(k_r r) \right) e^{-j\mu\varphi}, \quad (43)$$

$$Z_0 v_{\mu r}(r, \varphi) = j \frac{k_r}{k_0} \frac{\partial p}{\partial(k_r r)} = j \frac{k_r}{k_0} \left( H_\mu'^{(1)}(k_r r) + \beta H_\mu'^{(2)}(k_r r) \right) e^{-j\mu\varphi}.$$

The boundary conditions

$$\frac{Z_0 v_{\mu r}(r_{i,a}, \varphi)}{p_\mu(r_{i,a}, \varphi)} = j \frac{k_r r_{i,a} \left( H_\mu'^{(1)}(k_r r_{i,a}) + \beta H_\mu'^{(2)}(k_r r_{i,a}) \right)}{H_\mu^{(1)}(k_r r_{i,a}) + \beta H_\mu^{(2)}(k_r r_{i,a})} \stackrel{!}{=} \mp k_0 r_{i,a} Z_0 G_{i,a} \quad (44)$$

lead to the characteristic equation for mode eigenvalues  $\mu$  in the form:

$$\begin{aligned} & \left( (\mu - jU_i)H_\mu^{(1)}(\rho_i) - \rho_i H_{1+\mu}^{(1)}(\rho_i) \right) \left( (\mu + jU_a)H_\mu^{(2)}(\rho_a) - \rho_a H_{1+\mu}^{(2)}(\rho_a) \right) \\ & - \left( (\mu + jU_a)H_\mu^{(1)}(\rho_a) - \rho_a H_{1+\mu}^{(1)}(\rho_a) \right) \left( (\mu - jU_i)H_\mu^{(2)}(\rho_i) - \rho_i H_{1+\mu}^{(2)}(\rho_i) \right) = 0. \end{aligned} \quad (45)$$

Apply the asymptotic expansions to the Hankel functions:

$$H_\mu^{(1,2)}(z) = \sqrt{2/(\pi z)} \cdot [P(\mu, z) \pm jQ(\mu, z)] \cdot e^{\pm j(z - (\mu/2 + 1/4)\pi)} \quad (46)$$

with the component series  $P(\mu, z) = P_\mu(z)$ ;  $Q(\mu, z) = Q_\mu(z)$  from Eq. (38). Because only mixed products with both kinds of Hankel function as factors will appear in Eq. (45), these products produce as common factors  $e^{\pm j(\rho_a - \rho_i)}$  and the exponential factors  $e^{\pm j\mu/2}$  will cancel. Thus, Eq. (45) becomes a polynomial in  $\mu$  if the asymptotic series Eq. (38) is truncated at  $k_{hi}$ . Tests for  $\text{Re}(\mu) \geq 0$  and  $\text{Im}(\mu) \leq 0$ , and for  $|\text{char.eq.}| < \text{lim}$  (with  $\text{lim} \approx$

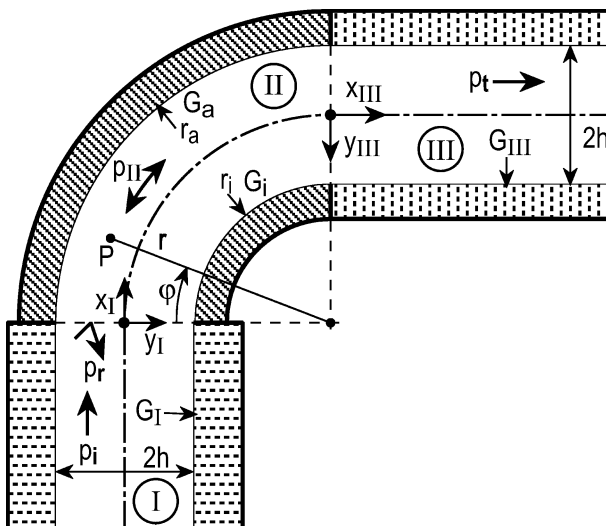
80) should be made with the polynomial solutions before they are applied as Muller starters. The numerical coefficients in the polynomials are of moderate magnitude [in contrast to the modes in the form of Eq. (31) and the previous transformation, where the coefficients may become extremely large].

## J.45 Lined Bow Duct Between Lined Straight Ducts

► See also: Mechel (2006)

Turning-vane splitters in the corners of wind tunnels may have locally reacting absorber surfaces; such *turning-vane splitter silencers* may be designed so that they have a broad-band middle and high-frequency attenuation. The elementary ducts between the turning-vane splitters can be considered as a sequence in the direction of sound propagation of a circular bow duct between straight entrance and exit ducts.

The three zones (I), (II), (III), with their co-ordinate systems, wall lining admittances, and component sound waves, are depicted in the sketch. The linings and their admittances  $G_i$ ,  $G_a$  may be different on both sides in (II); the admittances  $G_I$ ,  $G_{III}$  are assumed (for simplicity) to be the same on both sides in (I) and (III). The incident wave  $p_i$  is supposed to be the  $v$ -th mode of the entrance duct (I) (more complicated excitations can be synthesised with such modes). The exit duct (III) is anechoic (for simplicity also) for the transmitted wave  $p_t$ , which is a sum of modes of (III), analogously to the reflected wave  $p_r$  in (I), which is synthesised with modes of (I). The sound field  $p_{II}$  in the bow duct is composed as a mode sum of forward and backward ( $\varphi$  direction) running bow modes.



The sound fields in general are unsymmetrical with respect to the central planes of the straight sections and to  $r = (r_i + r_a)/2$  in the bow duct, even if the excitation is symmetrical in (I) and if the linings are the same on both sides. Therefore the mode sums in (I) and (III) must include both symmetrical and anti-symmetrical modes of

those sections. For ease of writing we attribute even mode indices  $n = n_s = 0, 2, 4, \dots$  to symmetrical modes, and odd mode indices  $n = n_a = 1, 3, 5, \dots$  to anti-symmetrical modes. The index  $n = 0$  is attributed to the least attenuated mode.

*Field formulation in (I):*

Cross profiles of modes:

$$q_n(\epsilon_n y) = \begin{cases} \cos(\epsilon_n y); & \text{symmetrical mode;} \\ \sin(\epsilon_n y); & \text{anti-symmetrical mode;} \end{cases} \quad n = 0, 2, 4, \dots \quad (1)$$

Incident mode:

$$\begin{aligned} p_i(x_I, y_I) &= P_i \cdot q_v(\epsilon_v y) \cdot e^{-\Gamma_v x_I}; \quad \Gamma_v^2 - \epsilon_v^2 + k_0^2 = 0, \\ Z_0 v_{ix}(x_I, y_I) &= \frac{j}{k_0} \frac{\partial p_i(x_I, y_I)}{\partial x_I} = \frac{-j\Gamma_v}{k_0} p_i(x_I, y_I). \end{aligned} \quad (2)$$

Wave reflected at  $x_I = 0$  (summation and mode index  $n \geq 0$ ):

$$\begin{aligned} p_r(x_I, y_I) &= \sum_n A_n q_n(\epsilon_n y) \cdot e^{+\Gamma_n x_I}; \quad \Gamma_n^2 - \epsilon_n^2 + k_0^2 = 0, \\ Z_0 v_{rx}(x_I, y_I) &= j \sum_n A_n \frac{\Gamma_n}{k_0} q_n(\epsilon_n y) \cdot e^{+\Gamma_n x_I}. \end{aligned} \quad (3)$$

The wave numbers  $\epsilon_{n_s}, \epsilon_{n_a}$  of the symmetrical and anti-symmetrical modes are solutions of the characteristic equations:

$$\epsilon_{n_s} h \cdot \tan(\epsilon_{n_s} h) = j k_0 h \cdot Z_0 G_I; \quad \epsilon_{n_a} h / \tan(\epsilon_{n_a} h) = -j k_0 h \cdot Z_0 G_I. \quad (4)$$

See earlier sections in this chapter for the evaluation of sets of modes. The range of the summation and mode index  $n$  must include, at least, the order  $v$  of the incident mode.

*Field formulation in (III):*

Cross profiles of modes:

$$q_n(\eta_n y) = \begin{cases} \cos(\eta_n y); & \text{symmetrical mode;} \\ \sin(\eta_n y); & \text{anti-symmetrical mode;} \end{cases} \quad n = 0, 2, 4, \dots \quad (5)$$

Transmitted wave (summation and mode index  $n \geq 0$ ):

$$\begin{aligned} p_t(x_{III}, y_{III}) &= \sum_n D_n \cdot q_n(\eta_n y_{III}) \cdot e^{-\gamma_n x_{III}}; \quad \gamma_n^2 - \eta_n^2 + k_0^2 = 0, \\ Z_0 v_{tx}(x_{III}, y_{III}) &= -j \sum_n D_n \frac{\gamma_n}{k_0} q_n(\eta_n y_{III}) \cdot e^{-\gamma_n x_{III}}. \end{aligned} \quad (6)$$

The wave numbers  $\eta_{n_s}, \eta_{n_a}$  of the symmetrical and anti-symmetrical modes are solutions of the characteristic equations:

$$\eta_{n_s} h \cdot \tan(\eta_{n_s} h) = j k_0 h \cdot Z_0 G_{III}; \quad \eta_{n_a} h / \tan(\eta_{n_a} h) = -j k_0 h \cdot Z_0 G_{III}. \quad (7)$$

*Field formulation in (II):*

$$\begin{aligned} p_{II+}(r, \varphi) &= \sum_{\mu} B_{\mu} (J_{\mu}(k_0 r) + \beta_{\mu} \cdot Y_{\mu}(k_0 r)) e^{-j\mu\varphi}, \\ p_{II-}(r, \varphi) &= \sum_{\mu} C_{\mu} (J_{\mu}(k_0 r) + \beta_{\mu} \cdot Y_{\mu}(k_0 r)) e^{+j\mu\varphi}. \end{aligned} \quad (8)$$

If the same manifold of modes is assumed in both directions of propagation (reasonable, but not necessary), the sound field in (II) is:

$$\begin{aligned} p_{II}(r, \varphi) &= p_{II+}(r, \varphi) + p_{II-}(r, \varphi) \\ &= \sum_{\mu} (J_{\mu}(k_0 r) + \beta_{\mu} \cdot Y_{\mu}(k_0 r)) (B_{\mu} e^{-j\mu\varphi} + C_{\mu} e^{+j\mu\varphi}), \\ Z_0 v_{II\varphi}(r, \varphi) &= \frac{j}{k_0} \text{grad}_{\varphi} p_{II}(r, \varphi) = \frac{j}{k_0 r} \frac{\partial p_{II}(r, \varphi)}{\partial \varphi} \\ &= \frac{1}{k_0 r} \sum_{\mu} \mu (J_{\mu}(k_0 r) + \beta_{\mu} \cdot Y_{\mu}(k_0 r)) (B_{\mu} e^{-j\mu\varphi} - C_{\mu} e^{+j\mu\varphi}). \end{aligned} \quad (9)$$

Abbreviation:  $U_{i,a} := k_0 r_{i,a} Z_0 G_{i,a}$ . (10)

The mode eigenvalues  $\mu$  are solutions of the characteristic equation; see ► Sect. J.44:

$$\begin{aligned} &(k_0 r_i J_{1+\mu}(k_0 r_i) - (\mu - jU_i) J_{\mu}(k_0 r_i)) \cdot (k_0 r_a Y_{1+\mu}(k_0 r_a) - (\mu + jU_a) Y_{\mu}(k_0 r_a)) \\ &- (k_0 r_a J_{1+\mu}(k_0 r_a) - (\mu + jU_a) J_{\mu}(k_0 r_a)) \cdot (k_0 r_i Y_{1+\mu}(k_0 r_i) - (\mu - jU_i) Y_{\mu}(k_0 r_i)) = 0. \end{aligned} \quad (11)$$

The ratios of the radial component waves are:

$$\begin{aligned} \beta_{\mu} &= -\frac{((\mu - jU_i) J_{\mu}(k_0 r_i) - k_0 r_i J_{1+\mu}(k_0 r_i))}{((\mu - jU_i) Y_{\mu}(k_0 r_i) - k_0 r_i Y_{1+\mu}(k_0 r_i))} \\ &= -\frac{((\mu + jU_a) J_{\mu}(k_0 r_a) - k_0 r_a J_{1+\mu}(k_0 r_a))}{((\mu + jU_a) Y_{\mu}(k_0 r_a) - k_0 r_a Y_{1+\mu}(k_0 r_a))}. \end{aligned} \quad (12)$$

*Matching of sound pressures at  $\varphi = 0$   $\hat{=} x_I = 0$ :*

$$p_i(0, y_I) + p_r(0, y_I) \stackrel{!}{=} p_{II}(r, 0), \quad (13a)$$

$$P_i \cdot q_v(\epsilon_v y_I) + \sum_n A_n q_n(\epsilon_n y_I) = \sum_{\mu} (J_{\mu}(k_0 r) + D_{\mu} \cdot Y_{\mu}(k_0 r)) (B_{\mu} + C_{\mu}). \quad (13b)$$

Make use of the mutual orthogonality of the modes in (I), i.e. perform on both sides the integral

$$\frac{1}{2h} \int_{-h}^h q_m(\epsilon_m y) \dots dy, \quad (14)$$

giving on the left-hand side of Eq. (13b) (with  $\delta_{m,n}$  = Kronecker symbol):

$$\frac{1}{2h} \int_{-h}^h q_m(\epsilon_m y) \cdot q_n(\epsilon_n y) dy = \begin{cases} 0 & \text{symm. and anti-symm} \\ \delta_{m,n} \cdot N_n & \text{symm. or anti-symm} \end{cases} \quad (15)$$

the *mode norms*  $N_n$ :

$$N_n = \frac{1}{2} \left[ 1 \pm \frac{\sin 2(\epsilon_n h)}{2\epsilon_n h} \right]; \quad \begin{cases} n = n_s & \text{symm} \\ n = n_a & \text{anti-symm} \end{cases} \quad (16)$$

Integral Eq. (14), with a fixed index  $m$  from within the range of  $n$ , applied on both sides of Eq. (13b) will result in:

$$P_i \cdot \delta_{m,v} \cdot N_v + \sum_n A_n \delta_{m,n} \cdot N_n = \sum_\mu (I J_{m,\mu} + \beta_\mu \cdot I Y_{m,\mu}) (B_\mu + C_\mu), \quad (17a)$$

or, with the left-hand side simplified, one obtains the linear system of equations with running  $m$  for the mode amplitudes  $A_n, B_\mu, C_\mu$ :

$$P_i \cdot \delta_{m,v} \cdot N_v + A_m N_m = \sum_\mu (I J_{m,\mu} + \beta_\mu \cdot I Y_{m,\mu}) (B_\mu + C_\mu). \quad (17b)$$

There appear the *mode coupling integrals*:

$$\begin{aligned} I J_{m,\mu} &= \frac{1}{2h} \int_{-h}^h q_m(\epsilon_m y) \cdot J_\mu(k_0 r) dy \\ &\xrightarrow{y \rightarrow (r_a + r_i)/2 - r} \frac{-1}{2h} \int_{r_i}^{r_a} q_m(\epsilon_m (r_a + r_i)/2 - \epsilon_m r) \cdot J_\mu(k_0 r) dr \\ &= \frac{-1}{2k_0 h} \int_{k_0 r_i}^{k_0 r_a} q_m\left(\frac{\epsilon_m}{k_0} (k_0 r_a + k_0 r_i)/2 - \frac{\epsilon_m}{k_0} (k_0 r)\right) \cdot J_\mu(k_0 r) d(k_0 r), \end{aligned} \quad (18a)$$

$$\begin{aligned} I Y_{m,\mu} &= \frac{1}{2h} \int_{-h}^h q_m(\epsilon_m y) \cdot Y_\mu(k_0 r) dy \\ &\xrightarrow{y \rightarrow (r_a + r_i)/2 - r} \frac{-1}{2h} \int_{r_i}^{r_a} q_m(\epsilon_m (r_a + r_i)/2 - \epsilon_m r) \cdot Y_\mu(k_0 r) dr \\ &= \frac{-1}{2k_0 h} \int_{k_0 r_i}^{k_0 r_a} q_m\left(\frac{\epsilon_m}{k_0} (k_0 r_a + k_0 r_i)/2 - \frac{\epsilon_m}{k_0} (k_0 r)\right) \cdot Y_\mu(k_0 r) d(k_0 r). \end{aligned} \quad (18b)$$

*Matching of axial particle velocities at  $\varphi = 0$*   $\stackrel{\wedge}{=} x_I = 0$ :

$$Z_0 v_{ix}(0, y_I) + Z_0 v_{rx}(0, y_I) \stackrel{!}{=} Z_0 v_{II\varphi}(r, 0), \quad (19a)$$

$$\begin{aligned} \frac{\Gamma_v}{k_0} P_i \cdot q_v(\epsilon_v y) - \sum_n A_n \frac{\Gamma_n}{k_0} q_n(\epsilon_n y) \\ = j \sum_{\mu} \mu (J_{\mu}(k_0 r)/k_0 r + \beta_{\mu} \cdot Y_{\mu}(k_0 r)/k_0 r) (B_{\mu} - C_{\mu}). \end{aligned} \quad (19b)$$

Perform again integral (14) on both sides taking  $m \in \{n\}$ , with the following result:

$$\frac{\Gamma_v}{k_0} P_i \cdot \delta_{m,v} \cdot N_v - \sum_n A_n \frac{\Gamma_n}{k_0} \delta_{m,n} \cdot N_n = j \sum_{\mu} \mu (KJ_{m,\mu} + \beta_{\mu} \cdot KY_{m,\mu}) \cdot (B_{\mu} - C_{\mu}). \quad (20a)$$

With the left-hand side simplified, one gets the linear system of equations for the mode amplitudes  $A_n, B_{\mu}, C_{\mu}$ :

$$\frac{\Gamma_v}{k_0} P_i \cdot \delta_{m,v} \cdot N_v - A_m \frac{\Gamma_m}{k_0} N_m = j \sum_{\mu} \mu (KJ_{m,\mu} + \beta_{\mu} \cdot KY_{m,\mu}) (B_{\mu} - C_{\mu}). \quad (20b)$$

The mode-coupling integrals here differ from those in (18a) and (18b) by a division with  $k_0 r$  in the integrands:

$$\begin{aligned} KJ_{m,\mu} &= \frac{1}{2h} \int_{-h}^h q_m(\epsilon_m y) \cdot J_{\mu}(k_0 r)/k_0 r dy \\ &\xrightarrow{y \rightarrow (r_a + r_i)/2 - r} \frac{-1}{2h} \int_{r_i}^{r_a} q_m(\epsilon_m (r_a + r_i)/2 - \epsilon_m r) \cdot J_{\mu}(k_0 r)/k_0 r dr \\ &= \frac{-1}{2k_0 h} \int_{k_0 r_i}^{k_0 r_a} q_m\left(\frac{\epsilon_m}{k_0} (k_0 r_a + k_0 r_i)/2 - \frac{\epsilon_m}{k_0} (k_0 r)\right) \cdot J_{\mu}(k_0 r)/k_0 r d(k_0 r), \end{aligned} \quad (21a)$$

$$\begin{aligned} KY_{m,\mu} &= \frac{1}{2h} \int_{-h}^h q_m(\epsilon_m y) \cdot Y_{\mu}(k_0 r)/k_0 r dy \\ &\xrightarrow{y \rightarrow (r_a + r_i)/2 - r} \frac{-1}{2h} \int_{r_i}^{r_a} q_m(\epsilon_m (r_a + r_i)/2 - \epsilon_m r) \cdot Y_{\mu}(k_0 r)/k_0 r dr \\ &= \frac{-1}{2k_0 h} \int_{k_0 r_i}^{k_0 r_a} q_m\left(\frac{\epsilon_m}{k_0} (k_0 r_a + k_0 r_i)/2 - \frac{\epsilon_m}{k_0} (k_0 r)\right) \cdot Y_{\mu}(k_0 r)/k_0 r d(k_0 r). \end{aligned} \quad (21b)$$

Matching of sound pressure at  $\varphi = \Theta \stackrel{\wedge}{=} x_{III} = 0$ :

$$p_t(0, y_{III}) \stackrel{!}{=} p_{II}(r, \Theta), \quad (22a)$$

$$\sum_n D_n \cdot q_n(\eta_n y_{III}) = \sum_{\mu} (J_{\mu}(k_0 r) + \beta_{\mu} \cdot Y_{\mu}(k_0 r)) (B_{\mu} e^{-j\mu\Theta} + C_{\mu} e^{+j\mu\Theta}). \quad (22b)$$

Use the orthogonality of modes in section (III) and perform the integral on both sides, with  $m$  from the applied mode range in (III):

$$\frac{1}{2h} \int_{-h}^h q_m(\eta_m y) \cdot \dots dy, \quad (23)$$

defining on the left-hand side the mode norms  $M_n$ :

$$\frac{1}{2h} \int_{-h}^h q_m(\eta_m y) \cdot q_n(\eta_n y) dy = \begin{cases} 0 & \text{symm. and anti-symm} \\ \delta_{m,n} \cdot M_n & \text{symm. or anti-symm} \end{cases} \quad (24)$$

$$\text{with values } M_n = \frac{1}{2} \left[ 1 \pm \frac{\sin(2\eta_n h)}{2\eta_n h} \right]; \quad \begin{cases} n = n_s & \text{symm.} \\ n = n_a & \text{anti-symm.} \end{cases}, \quad (25)$$

and on the right-hand side the mode coupling integrals:

$$RJ_{m,\mu} = \frac{1}{2h} \int_{-h}^h q_m(\eta_m y) \cdot J_\mu(k_0 r) dy; \quad RY_{m,\mu} = \frac{1}{2h} \int_{-h}^h q_m(\eta_m y) \cdot Y_\mu(k_0 r) dy. \quad (26a,b)$$

They differ from the mode-coupling integrals in Eq.(18a,b) by the substitution  $\epsilon_m \rightarrow \eta_m$  and may therefore be evaluated analogously to those integrals. Thus one gets a linear system of equations for the amplitudes  $D_m, B_\mu, C_\mu$ :

$$D_m M_m = \sum_{\mu} (RJ_{m,\mu} + \beta_\mu \cdot RY_{m,\mu}) (B_\mu e^{-j\mu\Theta} + C_\mu e^{+j\mu\Theta}). \quad (27)$$

*Matching of axial particle velocities at  $\varphi = \Theta \stackrel{\wedge}{=} x_{III} = 0$ :*

$$Z_0 v_{tx}(0, y_{III}) \stackrel{!}{=} Z_0 v_{II\varphi}(r, \Theta), \quad (28)$$

$$-j \sum_n D_n \frac{Y_n}{k_0} q_n(\eta_n y_{III}) = \frac{1}{k_0 r} \sum_{\mu} \mu (J_\mu(k_0 r) + \beta_\mu \cdot Y_\mu(k_0 r)) \cdot (B_\mu e^{-j\mu\Theta} - C_\mu e^{+j\mu\Theta}). \quad (29)$$

With the integral of Eq.(28) applied on both sides one gets the linear system of equations for the amplitudes  $D_m, B_\mu, C_\mu$ :

$$D_m \frac{Y_m}{k_0} M_m = j \sum_{\mu} \mu (S J_{m,\mu} + \beta_\mu \cdot S Y_{m,\mu}) (B_\mu e^{-j\mu\Theta} - C_\mu e^{+j\mu\Theta}), \quad (30)$$

where the mode-coupling integrals are:

$$\begin{aligned} SJ_{m,\mu} &= \frac{1}{2h} \int_{-h}^h q_m(\eta_m y) \cdot J_\mu(k_0 r) / k_0 r dy; \\ SY_{m,\mu} &= \frac{1}{2h} \int_{-h}^h q_m(\eta_m y) \cdot Y_\mu(k_0 r) / k_0 r dy. \end{aligned} \quad (31)$$

In total one has four linear systems of equations (17b), (20b), (27), (30) for four sets of mode amplitudes  $A_n, D_n, B_\mu, C_\mu$ ; systems (17b) and (20b) are inhomogeneous (the value of  $P_i$  can be chosen arbitrarily, e.g.  $P_i = 1$ ). In both first systems (17b) and (20b) the index  $m$  sweeps through the range of mode indices in (I); in (27) and (30)  $m$  passes through the mode orders in (III). It is plausible to eliminate the  $A_m$  by the operation (20b) + (17b) ·  $\Gamma_m/k_0$ , giving:

$$\sum_\mu B_\mu \left[ \frac{\Gamma_{m_1}}{k_0} (IJ_{m_1,\mu} + \beta_\mu \cdot IY_{m_1,\mu}) + j\mu (KJ_{m_1,\mu} + \beta_\mu \cdot KY_{m_1,\mu}) \right] + C_\mu \left[ \frac{\Gamma_{m_1}}{k_0} (IJ_{m_1,\mu} + \beta_\mu \cdot IY_{m_1,\mu}) - j\mu (KJ_{m_1,\mu} + \beta_\mu \cdot KY_{m_1,\mu}) \right] = 2 \frac{\Gamma_v}{k_0} P_i \cdot \delta_{m_1,v} \cdot N_v, \quad (32)$$

and analogously to eliminate the  $D_m$  by the operation (30) -  $\gamma_m/k_0 \cdot (27)$ :

$$\sum_\mu B_\mu e^{-j\mu\Theta} \left[ j\mu (SJ_{m_3,\mu} + \beta_\mu \cdot SY_{m_3,\mu}) - \frac{Y_{m_3}}{k_0} (RJ_{m_3,\mu} + \beta_\mu \cdot RY_{m_3,\mu}) \right] - C_\mu e^{+j\mu\Theta} \left[ j\mu (SJ_{m_3,\mu} + \beta_\mu \cdot SY_{m_3,\mu}) + \frac{Y_{m_3}}{k_0} (RJ_{m_3,\mu} + \beta_\mu \cdot RY_{m_3,\mu}) \right] = 0. \quad (33)$$

Both systems together form a combined, inhomogeneous, linear system of equations for the amplitude sets  $B_\mu, C_\mu$ . With them,  $A_n$  and  $D_n$  follow from (27) and (30). Evidently, the task of sound field evaluation in a sequence of a bent lined duct between straight lined ducts consists of the principal steps:

- determination of wall admittances;
- evaluation of sets of mode eigenvalues in the ducts;
- evaluation of the mode-coupling integrals (here by numerical integration);
- solution of the linear systems of equations for the mode amplitudes;
- insertion of mode amplitudes and mode wave numbers in the field formulations.

## J.46 Zero-Order and First-Order Transmission Loss of Turning-Vane Splitter Silencers

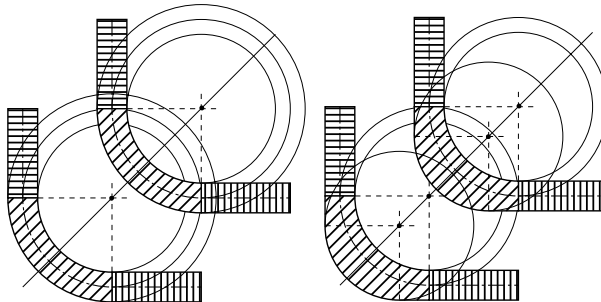
---

► See also: Mechel (2006)

Turning-vane splitter silencers rarely satisfy the requirement of the sketch and the analysis in the previous  Sect. J.45 that both walls of the elementary bent duct section must occupy concentric arcs. The silencers often are formed by juxtaposition of bent splitters with about constant thickness (left-hand sketch). A better approach to the requirement may be achieved with curved splitters of variable thickness (right-hand sketch), and a more broad-band attenuation is possible with such constructs.

Regarding these and other visible deviations from the theoretical assumptions, it may be sufficient to evaluate the transmission loss of the silencer in an approximation of either zero order or first order. For this it is assumed that the straight duct sections have the lengths  $L_1, L_3$  and the bent duct section is bent with an angle  $\Theta$  ( $\Theta = \pi/2$  in the sketches).

The *zero-order transmission loss* is the sum of the sound pressure level reductions of the least attenuated modes in the sections over the lengths  $L_1, L_2$  and the bend angle  $\Theta$ , respectively. Additional losses by reflections at the section limits are then neglected.



The *first-order transmission loss* again uses only the least attenuated modes of the sections (instead of sums of modes as in the previous [Sect. J.45](#)), but the additional reduction by reflections of these modes at the section limits are considered. The symbols of the previous section will be used below.

The linear systems of equations (17b), (20b), (27), (30) of the previous [Sect. J.45](#) for the four amplitudes of the least attenuated modes  $A_0, D_0, B_\mu, C_\mu$  simplify to:

$$P_i \cdot N_0 + A_0 N_0 = (IJ_{0,\mu} + \beta_\mu \cdot IY_{0,\mu}) (B_\mu + C_\mu), \quad (1)$$

$$\frac{\Gamma_0}{k_0} P_i \cdot N_0 - A_0 \frac{\Gamma_0}{k_0} N_0 = j\mu (KJ_{0,\mu} + \beta_\mu \cdot KY_{0,\mu}) (B_\mu - C_\mu), \quad (2)$$

$$D_0 M_0 = (RJ_{0,\mu} + \beta_\mu \cdot RY_{0,\mu}) (B_\mu e^{-j\mu\Theta} + C_\mu e^{+j\mu\Theta}), \quad (3)$$

$$D_0 \frac{Y_0}{k_0} M_0 = j\mu (SJ_{0,\mu} + \beta_\mu \cdot SY_{0,\mu}) (B_\mu e^{-j\mu\Theta} - C_\mu e^{+j\mu\Theta}), \quad (4)$$

and after elimination of  $A_0, D_0$  as in (32) and (33):

$$\begin{aligned} B_\mu & \left[ \frac{\Gamma_0}{k_0} (IJ_{0,\mu} + \beta_\mu \cdot IY_{0,\mu}) + j\mu (KJ_{0,\mu} + \beta_\mu \cdot KY_{0,\mu}) \right] \\ & + C_\mu \left[ \frac{\Gamma_0}{k_0} (IJ_{0,\mu} + \beta_\mu \cdot IY_{0,\mu}) - j\mu (KJ_{0,\mu} + \beta_\mu \cdot KY_{0,\mu}) \right] = 2 \frac{\Gamma_0}{k_0} P_i \cdot N_0, \end{aligned} \quad (5)$$

$$\begin{aligned} B_\mu e^{-j\mu\Theta} & \left[ j\mu (SJ_{0,\mu} + \beta_\mu \cdot SY_{0,\mu}) - \frac{Y_0}{k_0} (RJ_{0,\mu} + \beta_\mu \cdot RY_{0,\mu}) \right] \\ & - C_\mu e^{+j\mu\Theta} \left[ j\mu (SJ_{0,\mu} + \beta_\mu \cdot SY_{0,\mu}) + \frac{Y_0}{k_0} (RJ_{0,\mu} + \beta_\mu \cdot RY_{0,\mu}) \right] = 0. \end{aligned} \quad (6)$$

Combining the mode-coupling integrals like:

$$\begin{aligned} IJ_{0,\mu} &= (IJ_{0,\mu} + \beta_\mu \cdot IY_{0,\mu}) ; \quad KJ_{0,\mu} = (KJ_{0,\mu} + \beta_\mu \cdot KY_{0,\mu}), \\ RJ_{0,\mu} &= (RJ_{0,\mu} + \beta_\mu \cdot RY_{0,\mu}) ; \quad SJ_{0,\mu} = (SJ_{0,\mu} + \beta_\mu \cdot SY_{0,\mu}), \end{aligned} \quad (7)$$

one gets explicit solutions for  $B_\mu$ ,  $C_\mu$ :

$$\begin{aligned} B_\mu &= 2P_i \frac{\Gamma_0}{k_0} N_0 (\gamma_0/k_0 \cdot R J Y_{0,\mu} + j\mu \cdot S J Y_{0,\mu}) \\ &\quad \cdot \{j\mu \cdot K J Y_{0,\mu} [\gamma_0/k_0 (1 + e^{-2j\mu\Theta}) R J Y_{0,\mu} + j\mu (1 - e^{-2j\mu\Theta}) S J Y_{0,\mu}] \\ &\quad + \Gamma_0/k_0 \cdot I J Y_{0,\mu} [\gamma_0/k_0 (1 - e^{-2j\mu\Theta}) R J Y_{0,\mu} + j\mu (1 + e^{-2j\mu\Theta}) S J Y_{0,\mu}]\}^{-1}, \end{aligned} \quad (8)$$

$$\begin{aligned} C_\mu &= -2P_i \frac{\Gamma_0}{k_0} N_0 e^{-2j\mu\Theta} (\gamma_0/k_0 \cdot R J Y_{0,\mu} - j\mu \cdot S J Y_{0,\mu}) \\ &\quad \cdot \{j\mu \cdot K J Y_{0,\mu} [\gamma_0/k_0 (1 + e^{-2j\mu\Theta}) R J Y_{0,\mu} + j\mu (1 - e^{-2j\mu\Theta}) S J Y_{0,\mu}] \\ &\quad + \Gamma_0/k_0 \cdot I J Y_{0,\mu} [\gamma_0/k_0 (1 - e^{-2j\mu\Theta}) R J Y_{0,\mu} + j\mu (1 + e^{-2j\mu\Theta}) S J Y_{0,\mu}]\}^{-1}. \end{aligned} \quad (9)$$

With these the amplitudes  $A_0$ ,  $D_0$  are obtained from:

$$A_0 = -P_i + I J Y_{0,\mu}/N_0 \cdot (B_\mu + C_\mu); \quad D_0 = R J Y_{0,\mu}/M_0 \cdot (B_\mu e^{-j\mu\Theta} + C_\mu e^{+j\mu\Theta}). \quad (10a,b)$$

If the attenuation in the bent duct section is high, i.e.  $|e^{-2j\mu\Theta}| \ll 1$ , one may further simplify:

$$B_\mu \approx 2P_i \frac{\Gamma_0}{k_0} N_0 \frac{1}{\Gamma_0/k_0 \cdot I J Y_{0,\mu} + j\mu \cdot K J Y_{0,\mu}}, \quad (11)$$

$$\begin{aligned} C_\mu &\approx -2P_i \frac{\Gamma_0}{k_0} N_0 e^{-2j\mu\Theta} \frac{\gamma_0/k_0 \cdot R J Y_{0,\mu} - j\mu \cdot S J Y_{0,\mu}}{\gamma_0/k_0 \cdot R J Y_{0,\mu} + j\mu \cdot S J Y_{0,\mu}} \\ &\quad \cdot \frac{1}{\Gamma_0/k_0 \cdot I J Y_{0,\mu} + j\mu \cdot K J Y_{0,\mu}}. \end{aligned} \quad (12)$$

And even the reflected wave in the bow duct with the amplitude  $C_\mu$  may be neglected if the attenuation in the bow is sufficiently high.

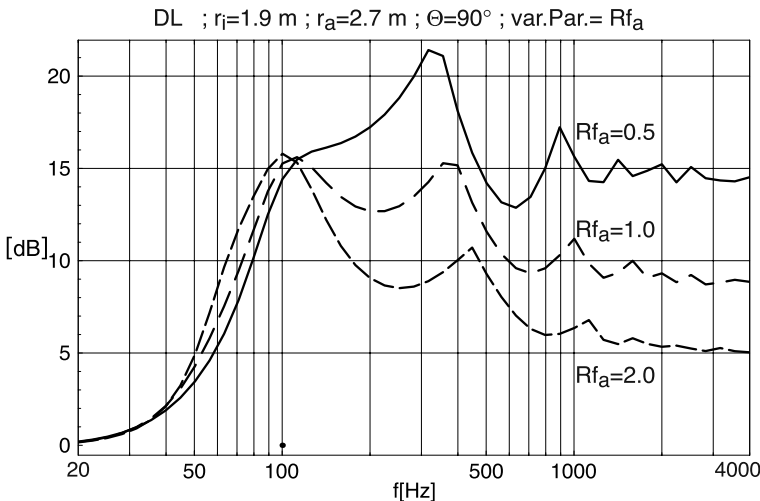
The resulting sound pressure ratio (on the duct axis) of the transmitted wave  $p_t(L_3, 0)$  to the incident wave  $p_i(-L_1, 0)$  is:

$$p_t(L_3, 0)/p_i(-L_1, 0) = D_0 e^{-\gamma_0 L_3} = e^{-\gamma_0 L_3} R J Y_{0,\mu}/M_0 \cdot (B_\mu e^{-j\mu\Theta} + C_\mu e^{+j\mu\Theta}). \quad (13)$$

The transmission loss  $D$  in dB becomes in the first-order approximation:

$$\begin{aligned} D &= -20 \cdot \lg |p_t(L_3, 0)/p_i(-L_1, 0)| \\ &= 8.686 \cdot (\operatorname{Re}(\Gamma_0)L_1 + \operatorname{Re}(\gamma_0)L_3 - \operatorname{Im}(\mu)\Theta) \\ &\quad - 20 \cdot \lg \left| 2 \frac{N_0}{M_0} \frac{\Gamma_0/k_0 \cdot R J Y_{0,\mu}}{\Gamma_0/k_0 \cdot I J Y_{0,\mu} + j\mu \cdot K J Y_{0,\mu}} \left( 1 - \frac{\gamma_0/k_0 \cdot R J Y_{0,\mu} - j\mu \cdot S J Y_{0,\mu}}{\gamma_0/k_0 \cdot R J Y_{0,\mu} + j\mu \cdot S J Y_{0,\mu}} \right) \right| \\ &= 8.686 \cdot (\operatorname{Re}(\Gamma_0)L_1 + \operatorname{Re}(\gamma_0)L_3 - \operatorname{Im}(\mu)\Theta) \\ &\quad - 20 \cdot \lg \left| 4 \frac{N_0}{M_0} \frac{\Gamma_0/k_0 \cdot R J Y_{0,\mu}}{\Gamma_0/k_0 \cdot I J Y_{0,\mu} + j\mu \cdot K J Y_{0,\mu}} \frac{j\mu \cdot S J Y_{0,\mu}}{\gamma_0/k_0 \cdot R J Y_{0,\mu} + j\mu \cdot S J Y_{0,\mu}} \right| \\ &= 8.686 \cdot (\operatorname{Re}(\Gamma_0)L_1 + \operatorname{Re}(\gamma_0)L_3 - \operatorname{Im}(\mu)\Theta) \\ &\quad + 20 \cdot \lg \left| \frac{M_0}{4N_0} \left( 1 + \frac{j\mu \cdot K J Y_{0,\mu}}{\Gamma_0/k_0 \cdot R J Y_{0,\mu}} \right) \left( 1 + \frac{\gamma_0/k_0 \cdot R J Y_{0,\mu}}{j\mu \cdot S J Y_{0,\mu}} \right) \right|. \end{aligned} \quad (14)$$

The first lines of Eq. (14) represent the transmission loss in the zero-order approximation; the second lines represent the additional terms of the first-order transmission loss due to reflections at the section limits.



Sound transmission loss  $DL$  of the least attenuated mode in a bow duct with bending angle  $\Theta = 90^\circ$ ; the linings consist of glass fibre boards, covered with porous limp foils and perforated metal sheet. The foil on the outer lining has three values of flow resistance ratio  $Rf_a$

An important contribution to the sum of transmission losses of the sections may come from the bent section, as the above diagram illustrates, showing the transmission loss  $DL$  of the least attenuated mode in a single bow duct section with bending angle  $\Theta = 90^\circ$ , radii  $r_i = 1.9$  [m],  $r_a = 2.7$  [m], linings consisting of  $t_i = t_a = 0.2$  [m]-thick glass fibre boards with flow resistivities  $\Xi_i = \Xi_a = 7000$  [Pa · s/m<sup>2</sup>], covered with porous, limp foils having surface mass densities  $mf_i = 0.4$  [kg/m<sup>2</sup>],  $mf_a = 1.0$  [kg/m<sup>2</sup>], the inner foil with a fixed flow resistance ratio (relative to  $Z_0$ )  $Rf_i = 2.0$ , and the outer foil with one of the alternative resistance ratio values  $Rf_a = \{0.5, 1.0, 2.0\}$ . The linings are covered (towards the duct) with perforated metal sheet,  $d_{i,a} = 1.5$  [mm] thick, with holes of  $dia_{i,a} = 5$  [mm] and a porosity of  $\sigma_{i,a} = 0.4$ .

It is conspicuous that, assuming a proper layout of the linings is chosen, the usual high-frequency decrease in the attenuation in straight ducts, as a consequence of ray formation in straight ducts, can be avoided. It is remarkable that such extraordinary frequency curves of attenuation must not be a consequence of multimode compensations but can be obtained also with single-mode fields of the least attenuated mode in the bend.

## J.47 Bent and Straight Ducts with Unsymmetrical Linings

► See also: Mechel (2006)

The duct arrangement and the naming of symbols is similar to those in ► Sect. J.45. Unlike in that section, the linings in the straight duct sections (I) and/or (III) now are unsymmetrical.

As a special case of unsymmetry the straight ducts (I) and/or (III) first are assumed to be one-sided hard, the other side absorbing with local reaction. The origin  $y = 0$  of the Cartesian co-ordinates is placed in the hard wall; the width of the duct is  $h$  (in contrast to ► Sect. J.45, where it is  $2h$ ). Only symmetrical modes relative to  $y = 0$  will appear in the field sums in sections (I) and (III). The mode formulations in these sections are:

$$\begin{aligned} p_n(x_I, y_I) &= q_n(\epsilon_n y_I) \cdot e^{-\Gamma_n x_I}; \quad \Gamma_n^2 - \epsilon_n^2 + k_0^2 = 0; \quad q_n(\epsilon_n y) = \cos(\epsilon_n y), \\ Z_0 v_{nx}(x_I, y_I) &= \frac{j}{k_0} \frac{\partial p_n(x_I, y_I)}{\partial x_I} = \frac{-j\Gamma_n}{k_0} p_n(x_I, y_I). \end{aligned} \quad (1)$$

The principal distinctions with respect to ► Sect. J.45 arise by the modification of the mode-coupling integrals and the mode norms (► Sect. J.45 here):

*Outer wall hard:  $y = 0$  at  $r = r_a$ :  $r = r_a - y$ ;  $0 \leq y \leq h$  ;  $h = r_a - r_i$*

$$\begin{aligned} \frac{1}{2h} \int_{-h}^h q_m(\epsilon_m y) \dots dy &\Rightarrow \frac{1}{h} \int_0^h q_m(\epsilon_m y) \dots dy, \\ N_n = \frac{1}{2} \left[ 1 \pm \frac{\sin(2\epsilon_n h)}{2\epsilon_n h} \right] &\Rightarrow N_n = \frac{1}{h} \int_0^h \cos^2(\epsilon_n y) dy = \frac{1}{2} \left[ 1 + \frac{\sin(2\epsilon_n h)}{2\epsilon_n h} \right]. \end{aligned} \quad (2)$$

*Inner wall hard:  $y = 0$  at  $r = r_i$ :  $r = r_i - y$  ;  $-h \leq y \leq 0$ ;  $h = r_a - r_i$*

$$\begin{aligned} \frac{1}{2h} \int_{-h}^h q_m(\epsilon_m y) \dots dy &\Rightarrow \frac{1}{h} \int_{-h}^0 q_m(\epsilon_m y) \dots dy, \\ N_n = \frac{1}{2} \left[ 1 \pm \frac{\sin(2\epsilon_n h)}{2\epsilon_n h} \right] &\Rightarrow N_n = \frac{1}{h} \int_{-h}^0 \cos^2(\epsilon_n y) dy = \frac{1}{2} \left[ 1 + \frac{\sin(2\epsilon_n h)}{2\epsilon_n h} \right]. \end{aligned} \quad (3)$$

Substitute  $\epsilon_n \rightarrow \eta_n$  if the exit duct section (III) is one-sided hard.

The one-sided hard ducts are limit cases  $G_1 = 0, G_2 = 0$  of straight ducts with unsymmetrical locally reacting linings.

*Straight duct sections with unsymmetrical locally reacting linings  $G_1 \neq G_2$ :*

Only formulas for the case of unsymmetrical linings of duct section (I) will be given; unsymmetrical linings in section (III) would be treated analogously.

The co-ordinate origin  $y = 0$  is again in the duct centre; the duct width is  $2h$ . Define the symmetrical  $U_s$  and anti-symmetrical  $U_a$  parts of the lining functions  $U$ :

$$\begin{aligned} U_1 &= k_0 h \cdot Z_0 G_1; \quad U_2 = k_0 h \cdot Z_0 G_2, \\ U_s &= (U_1 + U_2)/2; \quad U_a = (U_1 - U_2)/2 \end{aligned} \quad (4)$$

(if  $\operatorname{Re}(U_a) < 0$  with this choice, take  $U_a = (U_2 - U_1) / 2$ ). The mode formulation is:

$$\begin{aligned} p(x, y) &= (\cos(\epsilon y) + b \cdot \sin(\epsilon y)) \cdot e^{-\Gamma x} ; \quad \Gamma^2 - \epsilon^2 + k_0^2 = 0, \\ Z_0 v_y(x, y) &= -\frac{j\epsilon}{k_0} (\sin(\epsilon y) - b \cdot \cos(\epsilon y)) \cdot e^{-\Gamma x} \end{aligned} \quad (5)$$

$$\text{with the mode cross profile: } q_n(\epsilon_n y) = (\cos(\epsilon_n y) + b_n \cdot \sin(\epsilon_n y)). \quad (6)$$

The amplitude ratio of the cross-profile components is:

$$b = -\cot(\epsilon h) \frac{\epsilon h \cdot \tan(\epsilon h) - j k_0 h \cdot Z_0 G_2}{\epsilon h \cdot \cot(\epsilon h) + j k_0 h \cdot Z_0 G_2} = \cot(\epsilon h) \frac{\epsilon h \cdot \tan(\epsilon h) - j k_0 h \cdot Z_0 G_1}{\epsilon h \cdot \cot(\epsilon h) + j k_0 h \cdot Z_0 G_1}, \quad (7)$$

and the characteristic equation for mode wave numbers  $\epsilon h$  is:

$$[\epsilon h \cdot \tan(\epsilon h) - j U_s] \cdot [\epsilon h \cdot \cot(\epsilon h) + j U_s] = U_a^2 \quad (8a)$$

or

$$U_1 U_2 + (\epsilon h)^2 + j(U_1 + U_2)/2 \cdot (\epsilon h \cdot \tan(\epsilon h) - \epsilon h \cdot \cot(\epsilon h)) = 0. \quad (8b)$$

The mode norms are:

$$\begin{aligned} \frac{1}{2h} \int_{-h}^h q_m(\epsilon_m y) \cdot q_n(\epsilon_n y) dy &= \delta_{m,n} \cdot N_n, \\ N_n &= \frac{1}{2} \left( (b_n^2 + 1) + (b_n^2 - 1) \frac{\sin(2\epsilon_n h)}{2\epsilon_n h} \right). \end{aligned} \quad (9)$$

*Matching of sound pressures at  $\varphi = 0 \hat{x}_I = 0$ :*

$$p_i(0, y_I) + p_r(0, y_I) \stackrel{!}{=} p_{II}(r, 0), \quad (10a)$$

$$P_i \cdot q_v(\epsilon_v y_I) + \sum_n A_n q_n(\epsilon_n y_I) = \sum_\mu (J_\mu(k_0 r) + \beta_\mu \cdot Y_\mu(k_0 r)) (B_\mu + C_\mu). \quad (10b)$$

The mode-coupling integrals with the modes in the bow duct (II):

$$IJ_{m,\mu} = \frac{1}{2h} \int_{-h}^h q_m(\epsilon_m y) \cdot J_\mu(k_0 r) dy ; \quad IY_{m,\mu} = \frac{1}{2h} \int_{-h}^h q_m(\epsilon_m y) \cdot Y_\mu(k_0 r) dy \quad (11)$$

with substitution in the arguments of the cylindrical functions  $r = (r_i + r_a)/2 - y$ .

The first linear, inhomogeneous system of equations (running index  $m$ ) for mode amplitudes  $A_m, B_\mu, C_\mu$  will become:

$$P_i \cdot \delta_{m,v} \cdot N_v + A_m N_m = \sum_\mu (IJ_{m,\mu} + \beta_\mu \cdot IY_{m,\mu}) (B_\mu + C_\mu). \quad (12)$$

*Matching of axial particle velocities at  $\varphi = 0 \hat{x}_I = 0$ :*

$$Z_0 v_{ix}(0, y_I) + Z_0 v_{rx}(0, y_I) \stackrel{!}{=} Z_0 v_{II\varphi}(r, 0), \quad (13a)$$

$$\frac{\Gamma_v}{k_0} P_i \cdot q_v(\epsilon_v y) - \sum_n A_n \frac{\Gamma_n}{k_0} q_n(\epsilon_n y) = j \sum_{\mu} \mu \left( J_{\mu}(k_0 r)/k_0 r + \beta_{\mu} \cdot Y_{\mu}(k_0 r)/k_0 r \right) (B_{\mu} - C_{\mu}) \quad (13b)$$

leads to the second inhomogeneous linear system of equations with  $m \in \{n\}$  for the mode amplitudes  $A_m, B_{\mu}, C_{\mu}$ :

$$\frac{\Gamma_v}{k_0} P_i \cdot \delta_{m,v} \cdot N_v - A_m \frac{\Gamma_m}{k_0} N_m = j \sum_{\mu} \mu \left( KJ_{m,\mu} + \beta_{\mu} \cdot KY_{m,\mu} \right) (B_{\mu} - C_{\mu}), \quad (14)$$

where the integrals of mode coupling between sections (I) and (III) are:

$$\begin{aligned} KJ_{m,\mu} &= \frac{1}{2h} \int_{-h}^h q_m(\epsilon_m y) \cdot J_{\mu}(k_0 r)/k_0 r dy, \\ KY_{m,\mu} &= \frac{1}{2h} \int_{-h}^h q_m(\epsilon_m y) \cdot Y_{\mu}(k_0 r)/k_0 r dy. \end{aligned} \quad (15)$$

If only the straight duct section (I) has an unsymmetrical lining, the lining of section (III) still is symmetrical, the other systems of equations remain as in [Sect. J.45](#). If the duct section (III) also has an unsymmetrical lining, the mode formulations there will be:

$$\begin{aligned} p_n(x, y) &= (\cos(\eta_n y) + c \cdot \sin(\eta_n y)) \cdot e^{-Y_n x}; \quad \gamma_n^2 - \eta_n^2 + k_0^2 = 0, \\ Z_0 v_{yn}(x, y) &= \frac{j\eta_n}{k_0} (-\sin(\eta_n y) + c_n \cdot \cos(\eta_n y)) \cdot e^{-Y_n x}, \end{aligned} \quad (16)$$

$$\begin{aligned} c_n &= -\cot(\eta_n h) \frac{\eta_n h \cdot \tan(\eta_n h) - jk_0 h \cdot Z_0 G_2}{\eta_n h \cdot \cot(\eta_n h) + jk_0 h \cdot Z_0 G_2} \\ &= \cot(\eta_n h) \frac{\eta_n h \cdot \tan(\eta_n h) - jk_0 h \cdot Z_0 G_1}{\eta_n h \cdot \cot(\eta_n h) + jk_0 h \cdot Z_0 G_1}. \end{aligned} \quad (17)$$

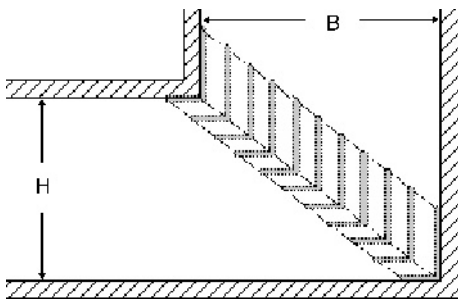
The other systems of equations for mode amplitudes will transform analogously.

## **J.48 Silencer with Rectangular Turning-Vane Splitters**

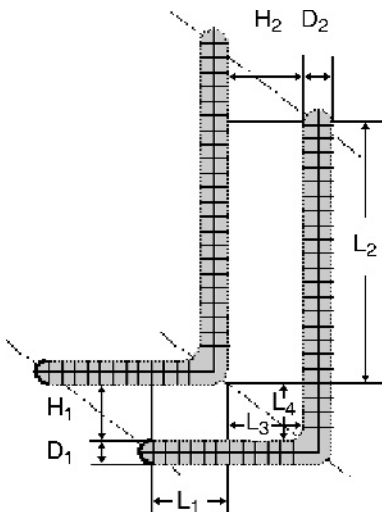
This section describes a task which can be solved with results from earlier sections of this chapter, and shows some results. In some sense, this section at the end of the chapter illustrates the application of earlier sections for the solution of a practical task.

*The task:*

One needs a silencer with a broad-band transmission loss, also at high frequencies. The duct has a corner or bent (e.g. a horizontal duct, with a width  $H$ , enters a vertical stack for an exhaust silencer, with a width  $B$ ). It is advisable to attribute the high-frequency end of the insertion loss to a turning-vane splitter silencer and to design the silencer in the exhaust stack for the remaining transmission loss, if any.



Details of the splitters are shown in the sketch below. The splitters are assumed to be locally reacting in the numerical example given below, which is indicated by internal partitions; it is also assumed that the splitters have a hard central sheet.



The splitters are treated as a combination of two lined ducts, one with a length  $L_1$  and width  $H_1$ , the other with  $L_2$  and  $H_2$ , plus a lined duct corner with dimensions  $L_3 = H_2$  and  $L_4 = H_1$ .

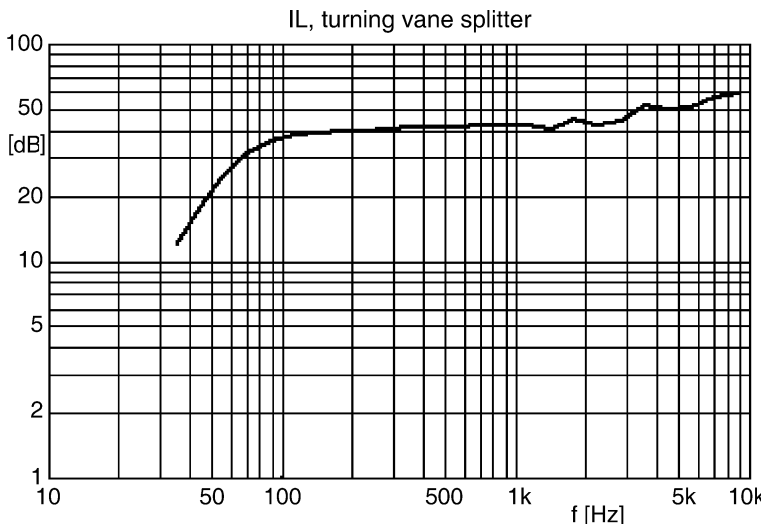
(The possible additional transmission loss due to the additional lengths  $L_3$  and  $L_4$  is neglected below.)

Such objects are treated in Sect. J.26, "Lined duct corners".

The insertion loss of the turning-vane splitter silencer is the sum of the transmission losses of the two straight ducts plus the insertion loss of the corner which is evaluated as in [Sect. J.26](#). The design makes use of the possibility of avoiding by lined duct corners the high-frequency decrease of attenuation due to ray formation in the ducts.

The dimensions of the ducts in the example shown are  $H = 10$  [m], and  $B = 17$  [m] (in a gas turbine test cell, with a meanflow Mach number in the empty stack of  $M = 0.0424$ , and in the silencer ducts of  $M = 0.106$ ). In the parameter list of the example is  $H_1 = 2 \cdot h_1$ ;  $D_1 = 2 \cdot d_1$ ;  $H_2 = 2 \cdot h_2$ ;  $D_2 = 2 \cdot d_2$ . The splitter branches consist of layers of glass fibre (made locally reacting) with flow resistivity values  $\Xi_1, \Xi_2$ , covered with porous steel foils of thickness  $df_1, df_2$  with normalised flow resistances  $Rf_1, Rf_2$ , respectively. It is assumed that a plane wave is incident.

The lengths  $L_i$ ;  $i = 1, 2$ ; should be  $L_i \geq 2H_i$ .



#### Parameters:

IL with flow, turning-vane splitter silencer with locally reacting lined duct corner  $M(B) = 0.0424$  empty, mode index limit  $m_{hi} = 8$ .

Width of ducts:  $B$  [m] = 17.,  $H$  [m] = 10.

Duct (1):

$L_1$  [m] = 3 .

$h_1$  [m] = 0.2,  $d_1$  [m] = 0.3

$\Xi_1$  [Pa s/m^2] = 2000 .

$rof_1$  [kg/m^3] = 7800 .,  $df_1$  [m] = 0.0005,  $Rf_1$  = 3 .

Duct (2):

$L_2$  [m] = 3 .

$h_2$  [m] = 0.34,  $d_2$  [m] = 0.51

$\Xi_2$  [Pa s/m^2] = 2000 .

$rof_2$  [kg/m^3] = 7800 .,  $df_2$  [m] = 0.0005,  $Rf_2$  = 1 .

**Corner (3):**

$$h_3 \text{ [m]} = 0.2, d_3 \text{ [m]} = 0.3 \\ \Xi_3 \text{ [Pa s/m}^2\text{]} = 2000 \\ rof_3 \text{ [kg/m}^3\text{]} = 7800, df_3 \text{ [m]} = 0.0005, Rf_3 = 3.$$

**Corner (4):**

$$h_4 \text{ [m]} = 0.34, d_4 \text{ [m]} = 0.51 \\ \Xi_4 \text{ [Pa s/m}^2\text{]} = 2000 \\ rof_4 \text{ [kg/m}^3\text{]} = 7800, df_4 \text{ [m]} = 0.0005, Rf_4 = 1.$$

## References

---

Cremer, L.: Theorie der Luftschalldämpfung mit schluckender Wand und das sich dabei ergebende höchste Dämpfungsmaß. *Acustica, Akust. Beihefte* 3, 249–263 (1953)

Coelho, J.L.B.: Acoustic Characteristics of Perforate Liners in Expansion Chambers. Thesis, Fac. Engineer., Inst. Sound Vibr., Southampton (1983)

Cummings, A.J.: Sound transmission at sudden area expansions in circular ducts with superimposed mean flow. *Sound Vibr.* 38, 149–155 (1975)

Félix, S., Pagneux, V.: Multimodal analysis of acoustic propagation in three-dimensional bends. *Wave Motion* 36, 157–158 (2002)

Félix, S., Pagneux, V.; Sound attenuation in lined bends. *J. Acoust. Soc. Am.* 116, 1921–1931 (2004)

Grigoryan, E.E.: Theory of sound wave propagation in curvilinear waveguides. *Soviet Phys.-Acoust.* 14, 315–321 (1969)

Ko, S.-H., Ho, L.T.: Sound attenuation in acoustically lined curved ducts in the absence of fluid flow. *J. Sound Vibr.* 53, 189–201 (1977)

Ko, S.-H.: Three-dimensional acoustic wave propagation in acoustically lined cylindrically curved ducts without fluid flow. *J. Sound Vibr.* 66, 165–179 (1979)

Mechel, F.P.: Schallabsorber, Vol. II, Ch. 10: Sound in capillaries. Hirzel, Stuttgart (1995)

Mechel, F.P.: Schallabsorber, Vol. II, Ch. 28: Non-linearities by amplitude and flow. Hirzel, Stuttgart (1995)

Mechel, F.P.: Mathieu Functions; Formulas, Generation, Use. Hirzel, Stuttgart (1997)

Mechel, F.P.: Schallabsorber, Vol. III, Ch. 25.4: Superposition of flow. Hirzel, Stuttgart (1998)

Mechel, F.P.: Schallabsorber, Vol. III, Ch. 26: Rectangular duct with local lining. Hirzel, Stuttgart (1998)

Mechel, F.P.: Schallabsorber, Vol. III, Ch. 27: Rectangular duct with lateral lining. Hirzel, Stuttgart (1998)

Mechel, F.P.: Schallabsorber, Vol. III, Ch. 28: Rectangular duct with unsymmetrical lining. Hirzel, Stuttgart (1998)

Mechel, F.P.: Schallabsorber, Vol. III, Ch. 29: Silencers with circular ducts. Hirzel, Stuttgart (1998)

Mechel, F.P.: Schallabsorber, Vol. III, Ch. 30: Silencers with annular ducts. Hirzel, Stuttgart (1998)

Mechel, F.P.: Schallabsorber, Vol. III, Ch. 32: Ducts with cross-layered lining and pine tree silencers. Hirzel, Stuttgart (1998)

Mechel, F.P.: Schallabsorber, Vol. III, Ch. 33: Duct with steps. Hirzel, Stuttgart (1998)

Mechel, F.P.: Schallabsorber, Vol. III, Ch. 34: Silencer of finite length and silencer cascade. Hirzel, Stuttgart (1998)

Mechel, F.P.: Schallabsorber, Vol. III, Ch. 35: Locally concentrated absorbers in a duct lining. Hirzel, Stuttgart (1998)

Mechel, F.P.: Schallabsorber, Vol. III, Ch. 36: Splitter type silencer with local lining. Hirzel, Stuttgart (1998)

Mechel, F.P.: Schallabsorber, Vol. III, Ch. 37: Splitter type silencer with lateral lining. Hirzel, Stuttgart (1998)

Mechel, F.P.: Schallabsorber, Vol. III, Ch. 38: Lined duct junctions. Hirzel, Stuttgart (1998)

- Mechel, F.P.: Schallabsorber, Vol. III, Ch. 39: Sound radiation of exits of ducts and silencers. Hirzel, Stuttgart (1998)
- Mechel, F.P.: Schallabsorber, Vol. III, Ch. 40: Application of modes. Hirzel, Stuttgart (1998)
- Mechel, F.P.: Schallabsorber, Vol. III, Ch. 41: Cremer admittance and hybrid absorbers. Hirzel, Stuttgart (1998)
- Mechel, F.P.: Schallabsorber, Vol. III, Ch. 42: Influence of flow and temperature on attenuation. Hirzel, Stuttgart (1998)
- Mechel, F.P.: Modes in lined wedge-shaped ducts. *J. Sound Vibr.* **216**, 649–671 (1998)
- Mechel, F.P.: Modal analysis in lined wedge-shaped ducts. *J. Sound Vibr.* **216**, 673–696 (1998)
- Mechel, F.P.: The scattering at a corner with absorbing flanks and absorbing cylinder. *J. Sound Vibr.* **219**, 581–601 (1999)
- Mechel, F.P.: Modal-Analyse im Bogen- oder Ring-Kanal; Teil I: Bogen-Kanal; Teil II: Ring-Kanal. *Acta acustica* **94**, 173–206 (2008)
- Press, W.H., Flannery, B.P., Teukolsky, S.A., Vetterling, W.T.: Numerical Recipes. Cambridge University Press, New York (1989)
- Ronneberger, D.: Experimentelle Untersuchungen zum akustischen Reflexionsfaktor von unstetigen Querschnittsänderungen in einem luftdurchströmten Rohr. *Acustica* **19**, 222–235 (1967/68)
- Young-Chung Cho J.; Reciprocity principle in duct acoustics. *Acoust. Soc. Am.* **67**, 1421–1426 (1980)
- Zwicker, C., Kosten, C.W.: Soundabsorbing materials. Elsevier, London (1949)